

MODIFICATION OF SUPPORTED METAL CATALYSTS WITH THIOL SELF-  
ASSEMBLED MONOLAYERS

by

KARL RUDOLPH KAHSAR

B.S., University of Virginia, 2010

A thesis submitted to the  
Faculty of the Graduate School of the  
University of Colorado in partial fulfillment  
of the requirement for the degree of  
Doctor of Philosophy  
Department of Chemical and Biological Engineering

2014

This thesis entitled:  
Modification of Supported Metal Catalysts with Thiol Self-Assembled Monolayers  
written by Karl Rudolph Kahsar  
has been approved for the Department of Chemical and Biological Engineering

---

J. Will Medlin

---

Daniel K. Schwartz

Date\_\_\_\_\_

The final copy of this thesis has been examined by the signatories, and we find that both the content and the form meet acceptable presentation standards of scholarly work in the above mentioned discipline.

## ABSTRACT

Kahsar, Karl Rudolph (Ph.D, Chemical and Biological Engineering)

Modification of Supported Metal Catalysts with Thiol Self-Assembled Monolayers

Thesis directed by Professor J. Will Medlin & Professor Daniel K. Schwartz

The study of catalysis is of fundamental importance to the petrochemical industry where the fast, precise production of desired products is prized for its ability to conserve energy and save money. Here we created selective catalysts by modifying Pt/Al<sub>2</sub>O<sub>3</sub> and Pd/Al<sub>2</sub>O<sub>3</sub> with thiol self-assembled monolayers (SAMs), modifiers with the capacity to influence the near surface environment of the catalyst.

SAM coatings were first explored for liquid phase hydrogenation of epoxybutene (EPB) in an extension to the liquid phase of previous work performed in the gas phase. These studies indicated that while general improvements in selectivity for this reaction still occurred in the liquid phase, there were other important parameters that affected the selectivity and activity of the reaction. For example, an octadecanethiol coating did not improve the selectivity of the reaction whereas a thioglycerol coating improved the selectivity from 40% to 75% when solvated in heptane. Ethanol solvated reactions were shown to have consistently lower selectivities than reactions solvated in heptane, possibly due to increased desorption of the monolayer.

The use of alkanethiols as catalyst modifiers for liquid phase reactions was next extended to larger reactants, fatty acids, which inherently require liquid phase study due to their high boiling points. The partial hydrogenation of unsaturated fatty acids is difficult to control, but an

alkanethiol coated catalyst increased selectivity of the sequential reaction pathway to monounsaturated fatty acids, a desirable result for the production of biodiesel. This effect was attributed to the ability of alkanethiol tails non-specifically restricting access to the surface for monounsaturated fatty acids.

Finally, the use of functional SAMs was explored for the liquid phase hydrogenation of  $\alpha,\beta$ -unsaturated aldehydes over Pt/Al<sub>2</sub>O<sub>3</sub> catalysts. Here, the tail ligands of the thiol modifiers were specifically chosen to selectively orient the reactant cinnamaldehyde with the catalyst surface in a manner that serves as a functional handle for controlling selectivity. The work was extended to modification of Pd/Al<sub>2</sub>O<sub>3</sub> catalysts, which showed an increase in selectivity after thiol modification, but without ligand-specific control seen for modification of Pt catalysts. Repeated recycling of these catalysts showed a decrease in efficacy, which was subsequently stabilized by adding a coating regeneration step between recycles.

## ACKNOWLEDGEMENTS

First of all I would like to thank my family. It is easy to look at this thesis and see only science, but it would be insincere not to acknowledge the people and experiences early in my life which allowed me to get to this point. There are too many examples to list, but my parents were influential in my development, dragging me on cultural outings, signing me up for activities, pushing me to succeed, and giving me space to learn. I am extremely fortunate to have grown up in a country, a community, a family where I had such opportunity to succeed.

Here at The University of Colorado, the greatest influences on my development as a scientist have been my advisors Will Medlin and Dan Schwartz. Their guidance along the way has been the most important force for turning me into a PhD chemical engineer. As an undergraduate at The University of Virginia I can remember aimlessly forging my way through years of classes until mid-way through my 4<sup>th</sup> year, while working on my senior design project, heat exchangers finally became useful and relevant. For the first time I understood what it meant to be a chemical engineer. In many ways, my experience under Will and Dan has been the same. In the last 4 years I have forged through experiments and manuscripts until finally I began writing my thesis. It was at this point that I realized what it meant to be a PhD. Along the way, my entire thought process has changed to where I now think about problems differently, see research differently, and have gained skills to pursue answers differently. My brain has been molded to processes information in new ways and the tutelage of Will and Dan has been paramount in the transformation.

Along with their help I would also like to thank the many other people who have played a role in helping me with my PhD. First, the other members of my thesis committee John

Falconer, Rex Skodje, and Jen Cha for their input and support. Second, I have been blessed to work with two fantastic research groups, the Medlin Group and the Schwartz Group. The work presented in this thesis contains fragments of input from almost all members of these groups stemming from informal discussions to group meetings, journal clubs, and happy hours. In particular I would like to thank Carolyn Schoennbaum who, being on the same project, has helped me more than anyone, especially when I first joined the lab groups and didn't know how to do much of anything.

Outside of the lab groups I would like to thank all of the undergraduates who have worked with me over the years running reactions. REU students Stephanie Johnson & Lukas Campolo, and CU students Nigel Wang, Charlie Hartman, Sarah Waldner, and Jacob Dysart for their help running reactions of the liquid phase system. Their work contributed greatly to the sums of data I collected and was invaluable for replicating tedious data sets and experiments. I would also like to thank Hans Funke for his constant source of conversation around the lab and help with catalyst analysis.

In addition to thanking all of the people involved in my thesis and the funding sources which made the research possible, I would also like to briefly mention the important role triathlon has played in the course of my PhD. When I moved to Colorado, I had become a top amateur triathlete and was ecstatic to be moving to a place where the top athletes trained. My first year as a graduate student, school was very difficult, but I took the time to stay consistent with my training, constantly improving and eventually racing for 3 years as a professional. School has always been my top priority, and looking back, there were many times when I felt I didn't have the time or energy to train, but I stayed true to my commitment and credit it with much of my success in graduate school. My best ideas have all come while training, and

likewise, the daily regimen of training and the constraints on my time have kept me efficient and productive in the lab. As I move on to a new career and plan to retire from triathlon, I hope to remember the importance that balance serves in life. For any new scientists just beginning research, it is important to remember the best ideas come from having an open mind, and that such a state is fostered by living a healthy and balanced life.

Finally, this work would not have been possible without our funding sources. This research was primarily supported by the Department of Energy, Office of Science, Basic Energy Sciences Program, Chemical Sciences, Geosciences, and Biosciences Division under grant number DE-FG02-10ER16206. I also obtained funding through the RASEI Renewable Energy Graduate Certificate Program Fellowship as well as the GAANN Energy Fellowship.

## CONTENTS

### CHAPTER

1: INTRODUCTION.....	1
1.1 Fundamentals of Catalysis.....	2
1.1.1 Concepts of reactions.....	3
1.1.2 Reaction rates.....	4
1.1.3 Reaction selectivity.....	6
1.1.4 Transition state theory.....	7
1.1.5 Metals as catalysts.....	11
1.2 Self-Assembled Monolayers.....	13
1.2.1 Metal structures.....	14
1.2.2 Formation of SAMs .....	17
1.3 Hydrogenation of olefins and aldehydes .....	21
1.3.1 Hydrogenation of olefins .....	22
1.3.2 Hydrogenation of aldehydes .....	23
1.4 Description of Common Techniques.....	25
1.4.1 Preparation of thiol coated catalysts .....	25
1.4.2 Surface area and particle size measurements of the catalysts.....	27
1.4.3 The reactor system .....	29
1.4.4 Selectivity and rate calculations.....	34
1.4.5 Infrared spectroscopy techniques.....	35
1.5 Thesis Goal .....	39
1.6 Thesis Scope .....	40
1.7 References .....	44
2: LIQUID- AND VAPOR-PHASE HYDROGENATION OF 1-EPOXY-3-BUTENE USING SELF-ASSEMBLED MONOLAYER COATED PALLADIUM AND PLATINUM CATALYSTS.....	53
2.1 Abstract.....	53
2.2 Background.....	53
2.3 Methods .....	55
2.3.1 Catalyst preparation .....	56
2.3.2 Catalyst characterization.....	56

2.3.3 Reaction system .....	58
2.4 Results .....	59
2.4.1 Vapor-phase hydrogenation using supported Pd and Pt catalysts .....	59
2.4.2 Liquid-phase hydrogenation of EpB .....	60
2.4.3 Effect of SAM quality on liquid-phase hydrogenation.....	65
2.5 Conclusion .....	66
2.6 References .....	67
<b>3: SELECTIVE HYDROGENATION OF POLYUNSATURATED FATTY ACIDS USING ALKANETHIOL SELF-ASSEMBLED MONOLAYER COATED Pd/Al<sub>2</sub>O<sub>3</sub> CATALYSTS</b>	<b>70</b>
3.1 Abstract.....	70
3.2 Background.....	70
3.3 Methods .....	73
3.3.1 Materials .....	73
3.3.2 Reaction system .....	74
3.3.3 Catalyst characterization.....	74
3.3.4 Rate calculations .....	75
3.3.5 Catalyst characterization.....	76
3.4 Results .....	77
3.4.1 Hydrogenation of linoleic acid.....	78
3.4.2 Hydrogenation of linolenic acid.....	81
3.4.3 Discussion of ligand effects .....	82
3.5 Conclusion .....	85
3.6 References .....	86
<b>4: CONTROL OF METAL CATALYST SELECTIVITY THROUGH SPECIFIC NON- COVALENT MOLECULAR INTERACTIONS</b> .....	<b>89</b>
4.1 Abstract.....	89
4.2 Introduction .....	89
4.3 Materials and Methods .....	91
4.3.1 Materials .....	91
4.3.2 Preparation of catalysts .....	92
4.3.3 Reaction system .....	92

4.3.4 Thin film PM-RAIRS .....	93
4.4 Results and discussion .....	94
4.4.1 Non-covalent control of selectivity.....	94
4.4.2 Hydrogenation of prenal .....	102
4.4.3 PM-RAIRS study of reactant binding geometry.....	105
4.4.4 Rates of intermediate consumption.....	111
4.4.5 Solvent effects on ligand specific interactions.....	113
4.5 Conclusions .....	115
4.6 References .....	116
<b>5: HYDROGENATION OF CINNAMALDEHYDE OVER Pd/Al<sub>2</sub>O<sub>3</sub> CATALYSTS MODIFIED WITH THIOL MONOLAYERS .....</b>	<b>119</b>
5.1 Abstract.....	119
5.2 Introduction .....	119
5.3 Methods .....	122
5.3.1 Materials .....	122
5.3.2 Reaction system .....	122
5.4 Results and discussion.....	123
5.5 Conclusions .....	130
5.6 References .....	131
<b>6: STABILITY OF SELF-ASSEMBLED MONOLAYER COATED Pt/Al<sub>2</sub>O<sub>3</sub> CATALYSTS FOR LIQUID PHASE HYDROGENATION OF CINNAMALDEHYDE.....</b>	<b>133</b>
6.1 Abstract.....	133
6.2 Introduction .....	133
6.3 Materials and Methods .....	136
6.3.1 Materials .....	136
6.3.2 Catalyst Preparation.....	136
6.3.3 Reaction system .....	137
6.3.4 Diffuse Reflectance Infrared Fourier Transform Spectroscopy (DRIFTS) .....	137
6.3.5 Inductively Coupled Plasma/Optical Emission Spectroscopy (ICP/OES) .....	138
6.3.6 CO chemisorption of recycled catalysts .....	138
6.4 Results and Discussion .....	138

6.4.1	Recyclability of thiol SAM coated catalysts.....	139
6.4.2	Characterization of recycled catalysts .....	145
6.4.3	Effects of SAM aging in air .....	157
6.5	Conclusions .....	160
6.6	References .....	160
7:	CONCLUSIONS AND FUTURE DIRECTIONS.....	164
7.1	Introduction .....	164
7.2	Thesis Conclusions .....	164
7.3	Future Paths .....	166
7.3.1	Competitive reaction.....	168
7.3.2	Imprinting .....	170
7.3.3	Solvent effects.....	175
7.3.4	Desorption of thiols in solution.....	175
7.3.5	Active site characterization.....	176
7.4	References .....	177
8:	BIBLIOGRAPHY.....	180

## LIST OF TABLES

Table 2-1: Selectivity and rate data for EpB hydrogenation over Pt/Al <sub>2</sub> O <sub>3</sub> .....	60
Table 2-2: Selectivity and rate with thiol added to the reaction solution .....	63
Table 2-3: Selectivity and rate data for heptane solvated EpB hydrogenation.....	64
Table 3-1: Rates of elaidic acid hydrogenation showing first-order reaction dependence.....	75
Table 4-1: Rates of benzaldehyde hydrogenation.....	99
Table 4-2: Peak assignments for PM-RAIRS .....	108
Table 6-1: Recycle procedures .....	140
Table 6-2: CO chemisorption of recycled catalysts.....	153

## LIST OF FIGURES

Figure 1-1: Extraction of reaction rate from first order kinetic data .....	5
Figure 1-2: Reaction coordinate diagram .....	9
Figure 1-3: Epoxybutene hydrogenation on Pd .....	9
Figure 1-4: The Sabatier Principle .....	12
Figure 1-5: Facets of the FCC lattice .....	16
Figure 1-6: Formation of an octadecanethiol self-assembled monolayer .....	18
Figure 1-7: Periodic $\sqrt{3}\times\sqrt{3}$ structure of a SAM .....	19
Figure 1-8: Hydrogenation pathways of olefins .....	22
Figure 1-9: Hydrogenation of $\alpha,\beta$ -unsaturated aldehydes .....	24
Figure 1-10: SEM of Pd/Al <sub>2</sub> O <sub>3</sub> catalyst .....	29
Figure 1-11: Schematic of the liquid phase semi-batch reactor sample procedure .....	31
Figure 1-12: Sample GC Chromatogram .....	32
Figure 1-13: Sample IR spectrum .....	37
Figure 1-14: PM-RAIRS spectroscopy technique .....	39
Figure 1-15: Liquid and vapor phase hydrogenation of epoxybutene—chapter 2 .....	41
Figure 1-16: Selective Hydrogenation of Polyunsaturated Fatty Acids —chapter 3 .....	41
Figure 1-17: Specific Non-Covalent Molecular Interactions—chapter 4 .....	42
Figure 1-18: Selective hydrogenation of cinnamaldehyde over Pd —chapter 5 .....	43
Figure 1-19: Stability of thiol coated catalysts for liquid phase hydrogenation —chapter 6 .....	43
Figure 2-1: Covalent binding process of alkanethiols on Pd/Al <sub>2</sub> O <sub>3</sub> .....	54
Figure 2-2: ATR of pure thioglycerol and DRIFTS of thioglycerol deposited on Pd/Al <sub>2</sub> O <sub>3</sub> .....	57
Figure 2-3: Reaction pathway for EpB hydrogenation .....	59
Figure 2-4: Selective hydrogenation of EpB to epoxybutane in the liquid phase .....	61
Figure 2-5: Rate, selectivity, and DRIFTS data for well-ordered SAMs and disordered SAMs .....	65
Figure 3-1: Reaction pathway for linoleic acid hydrogenation .....	73
Figure 3-2: Contact angle measurements of fatty acids .....	77
Figure 3-3: Kinetic data for linoleic acid hydrogenation over uncoated Pd/Al <sub>2</sub> O <sub>3</sub> .....	78
Figure 3-4: Linoleic acid selectivity and fatty acid hydrogenation rates .....	80
Figure 3-5: Kinetic data linolenic acid hydrogenation .....	81
Figure 3-6: Proposed fatty acid-SAM interaction mechanism .....	84
Figure 4-1: Hydrogenation pathway of cinnamaldehyde .....	91

Figure 4-2: Kinetic plots of cinnamaldehyde hydrogenation .....	95
Figure 4-3: Thiol SAMs and reactants.....	96
Figure 4-4: Contact angles on phenylated surfaces .....	97
Figure 4-5: Selectivity v. conversion for cinnamaldehyde .....	98
Figure 4-6: Selectivity v. conversion for ALD nanocatalysts .....	100
Figure 4-7: Selectivity v. conversion alkanethiol coatings.....	101
Figure 4-8: Selectivity of cinnamaldehyde and prenal hydrogenation .....	103
Figure 4-9: ICP-AES data of thiol catalysts .....	104
Figure 4-10: Orientation effect of 3-phenyl-1-propanethiol.....	105
Figure 4-11: PM-RAIRS analysis of adsorption geometry .....	106
Figure 4-12: PM-RAIRS hydrocinnamaldehyde .....	109
Figure 4-12: Rate v selectivity for cinnamaldehyde and prenal .....	111
Figure 4-13: Hydrogenation of cinnamyl alcohol and hydrocinnamaldehyde .....	112
Figure 4-14: Solvent studies of cinnamaldehyde hydrogenation.....	114
Figure 5-1: Thiol SAMs used in Chapter 5.....	120
Figure 5-2: Cinnamaldehyde hydrogenation pathway .....	121
Figure 5-3: Kinetic plots for the hydrogenation of cinnamaldehyde.....	124
Figure 5-4: Selectivity to cinnamyl alcohol.....	125
Figure 5-5: Selectivity to hydrocinnamaldehyde.....	128
Figure 5-6: Rates of cinnamaldehyde consumption .....	129
Figure 6-1: Recycle reactions without regeneration .....	139
Figure 6-2: Recycle reactions with regeneration .....	141
Figure 6-3: Recycle reactions with thiol in solution.....	142
Figure 6-4: Rates of recycle reactions .....	144
Figure 6-5: DRIFTS spectra of recycled catalysts .....	146
Figure 6-6: DRIFTS spectra of recycled regenerated catalysts .....	149
Figure 6-7: CO-DRIFTS of recycled regenerated C18 catalysts .....	150
Figure 6-8: CO-DRIFTS of recycled regenerated C18 catalysts .....	152
Figure 6-9: ICP-AES analysis of only re-deposited catalysts.....	155
Figure 6-10: ICP-AES analysis of recycle regeneration catalysts .....	156
Figure 6-11: Effects of aging coated catalysts in air .....	158
Figure 6-12: DRIFTS spectra of aged coated catalysts .....	159
Figure 7-1: Competitive reaction scheme .....	168
Figure 7-2: Preliminary competitive reaction data .....	169

Figure 7-3: Imprinting a Pd surface with thioglycerol .....	172
Figure 7-4: Reaction of trans-stilbene on imprinted Pd.....	173

## CHAPTER 1

### Introduction

“I am the wisest man alive, for I know one thing, and that is that I know nothing.” -Socrates

As the world moves well into the 21<sup>st</sup> century, the demand for energy and resources is projected to grow at an increasing rate as developing countries require more refined goods, and developed countries look increasingly for ways to make refined goods more efficiently<sup>1</sup>. The petrochemical industry is fundamental to meeting these demands through selective conversion of crude hydrocarbon and biomass inputs to desirable outputs. Underlying this entire industry is the field of catalysis, concerned fundamentally with the study of catalytic materials, typically metals, which can convert raw inputs quickly and precisely to useful products<sup>2-9</sup>.

A primary concern in the production of fine chemicals is the ability to direct reactions as efficiently as possible to the desired product of a reaction pathway<sup>10</sup>. Catalytic efficiency requires a combination of desirable traits, particularly a high rate of reaction accompanied by high selectivity to the desired product. Unfortunately for the petrochemical industry, controlling the selectivity of a multifunctional reaction pathway is difficult because natural energetics and thermodynamics lead to side reactions and undesirable products. Selectivity control is therefore among the most important parameters when considering useful modern catalysts<sup>7,11,12</sup>. Methods for improving selectivity include choosing different reaction pressures<sup>13,14</sup>, temperatures, metals<sup>15</sup>, bimetallics<sup>16,17</sup>, catalyst promoters<sup>18-20</sup>, changing the catalyst support<sup>21</sup> and recently, modification of the catalyst surface with thiol self-assembled monolayers (SAMs) as will be discussed in this thesis<sup>8,22-27</sup>.

## 1.1 Fundamentals of Catalysis

One of the earliest recorded instances of a catalyzed reaction was made by Humphry Davy in 1817. While working with fine platinum wires, Davy recorded a “new and curious series of phenomena” where coal gas (methane) and a supply of oxygen would cause the platinum wire to glow red-hot. Unbeknownst to Davy, this was a simple case of heterogeneous catalytic oxidation, and the two metals that he identified as capable of exhibiting this phenomenon, platinum and palladium, would turn out to be two of the most valuable catalytic materials today. The culmination of Davy’s work and other early observations was the defining of the “catalytic force” by Swedish chemist J.J. Berzelius of the Stockholm Academy of Sciences in the 1836 annual chemistry review<sup>28</sup>. As research and interest increased, the term catalysis came to be ubiquitous in modern English, used not only to describe chemical phenomena, but also to describe instigators, people or things that facilitate action, sparks that change the status quo.

This rise of the colloquial use of the word “catalyst” is strongly correlated with its use in industry. As the industrial revolution progressed into the early 20<sup>th</sup> century, the use of oil and petrochemical derivatives took flight as demand for fuels, industrial chemicals, and household items became increasingly important<sup>29</sup>. Inventors and investors took notice of the tremendous potential of catalysts<sup>30</sup>, and in 1913 the first large scale reactor began production of ammonia over iron catalysts via the Haber process, a process still responsible for much of the world’s supply of fertilizer<sup>31-33</sup>. Platinum and palladium, the exceptional metals studied by Davy and discussed here in this thesis, became famous in the 1970s for their use in the modern catalytic converter which since its inception has dramatically reduced automobile pollution<sup>31</sup>. Today, 80-90% of all industrial chemicals interact with a catalyst at some point during processing, in an industry worth trillions of dollars worldwide<sup>34</sup>.

Clearly catalysts are an important technology for providing the inputs to our everyday lives, and are of similarly great importance to a chemical engineer. Chemical kinetics and the study of catalysis are basic curricula in the chemical engineering education. Important concepts include the study of rate order, catalyst design, synthesis, and deactivation, each vital to the toolbox of a chemical engineer<sup>35</sup>. In this introduction Chapter, I will describe some of the most relevant concepts for understanding the subsequent Chapters of this thesis.

1.1.1 Concepts of reactions: In the late 1700s, the French scientist Antoine Lavoisier completed a series of fundamental experiments that would lay the framework for modern reaction chemistry. With a fine balance, Lavoisier determined that when a metal was oxidized inside a sealed container, the mass of the container did not change<sup>36</sup>. In addition, he noted that reactions always take place in fixed proportions based on the amount of starting material<sup>37</sup>. These two observations laid the foundations for the laws of the conservation of mass and the rules of reaction stoichiometry, pillars of reaction chemistry. We now know that atoms must always be conserved and that they will only react in discrete amounts. With this simple understanding of chemical reactions, we can describe a reaction system by its conversion as a function of initial and final concentrations, an important metric for describing the extent of reaction.

$$Conversion = \frac{[initial] - [final]}{[initial]} \times 100\%$$

As the field of reaction chemistry developed, so did different classes of reactions. Some reactions took place in the gas phase, some on a solid surface, and some were a combination of phases. Reactions that took place between two distinct phases are termed heterogeneous reactions and reactions that take place in the same phase are termed homogenous reactions<sup>31,38</sup>.

These terms are also applied to modern catalysts, that is, catalysts that exist in the same phase as the reactant are homogenous catalysts, and reactants that exist in a different phase are heterogeneous catalysts<sup>31,36,38</sup>. Many fine chemical reactions take place over homogenous catalysts<sup>39</sup>, whereas the majority of all industrial catalysis is heterogeneous, typically between a solid metal surface and a liquid or gas phase reactant. The reactions discussed in this thesis are all heterogeneous—liquid phase reactants and solid metal catalysts.

1.1.2 Reaction rates: Inherent to reaction chemistry is the study of rates. Friedrich Wilhelm Ostwald was a German chemist who spent considerable time studying sugar inversions in the presence of acid catalysts. He coupled his studies with all the present literature of reaction rates in a large meta-analysis and eventually came up with the modern rate equation<sup>36</sup>. Here,  $n$  is the order of the reaction,  $k$  is the fitting constant and  $C_A$  is the concentration of reactant A in the system.

$$r_A = -k_n(C_A)^n$$

From this equation, reactions with  $n=1$  are called ‘first-order’ reactions, those with  $n=2$  are called second-order and so on. Simplifying this equation, first order reactions can therefore be represented as follows.

$$r_A = \frac{dC_A}{dt} = -k_n C_A$$

This equation indicates that a first order reaction can be expected to show an exponential decay in the concentration of reactant similar to the data plotted in Figure 1-1. Because the rate of reaction is defined as the change in concentration over time, the initial slope of this plot should be proportional to the initial rate of reaction, that is, the maximum rate of reaction in the

absence of mass transfer limitations. This simple analysis is typically very accurate provided there are enough data points at short times in the data set. It is for this reason that throughout this thesis, data points are taken at exponentially increasing time intervals, so as to capture as much data from early on in the reaction as possible.

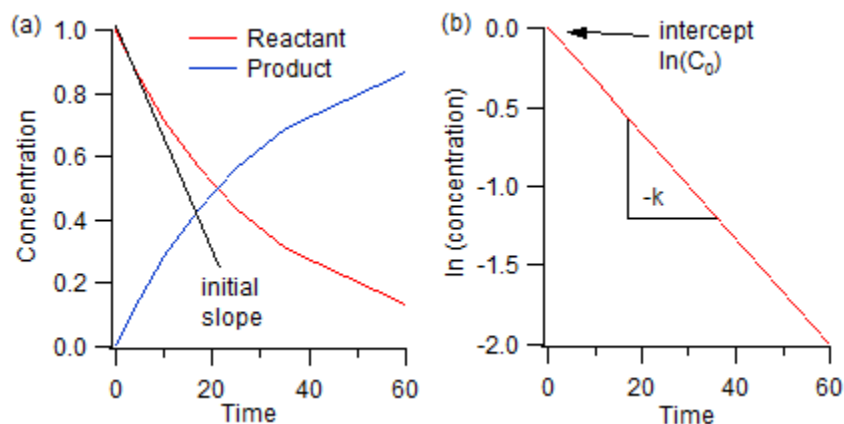


Figure 1-1: Extraction of reaction rate from first-order kinetic data for the simple reaction  $A \rightarrow B$  (a) kinetic plot where the rate of reaction can be estimated from the slope of the concentration (b) linearized form of the same data where the slope can be used to determine the reaction constant  $k$  and therefore the rate of the reaction

Data that exhibit first order kinetics can be linearized, as shown in Figure 1-1 (b) by taking the natural log of the concentration data set and plotting these data against time<sup>31,36</sup>. This linear version of the data has an intercept equal to the natural log of the initial concentration and a slope equal to the negative of the rate constant. The linear analysis of the rate provides a more robust measurement by taking into account the entire data set and can therefore be a powerful method for extracting rate information.

The study of reaction rates is at the heart of the catalysis industry and catalysis research where, historically, scientists sought to make unfavorable reactions proceed more quickly and with less of a thermal barrier<sup>33</sup>. As the field has progressed, researchers now spend more time developing lower cost catalysts, more environmentally benign catalyst materials, or studying how the selectivity of reactions can be enhanced<sup>22,40,41</sup>. Still, at the heart of these new pursuits is the notion of rate, and how to improve other catalyst properties while preserving a high rate of reaction<sup>42</sup>.

1.1.3 Reaction selectivity: The selectivity of chemical reactions is important in many families of reaction systems and particularly pertinent to the content of this thesis<sup>25,41,43</sup>. As chemical processing industries have become more advanced, demand has increased for catalysts that can produce a pure product stream without adding separation steps. For highly specialized industries like pharmaceutical processes the demand for very pure products is obvious, but for large petrochemical processes, high selectivity is also desirable<sup>7,30,44-46</sup>. In both cases, some purification is likely to follow any reaction steps to ensure a product stream of the proper composition<sup>47</sup>. For most chemical processes the construction and operation of separations processes accounts for 40-70% of all costs; as such, economics is a major factor for reducing this percentage<sup>47-49</sup>. A catalyst which can produce the desired product at high selectivity and reduces these costs is highly valued<sup>50</sup>.

The selectivity of a reaction can be defined a few different ways depending on the text, so it is important to note which version of selectivity is being referenced<sup>31,36,51</sup>. Throughout this thesis, I will refer to selectivity  $S_i$  as the total amount of desired product *species i*, divided by the total amount of all products, including *species i*.

$$S_i = \frac{\text{total amount of species } i}{\text{total amount of products of interest}} \times 100\%$$

This definition of selectivity easily allows for the analysis of the efficacy of the reaction in terms of a percentage where 100% selectivity means a reaction that proceeds entirely to the desired product. A similarly important term which will be referenced throughout this thesis is the yield  $Y_i$  which refers to the total amount of *species i* formed in relation to the amount of reactant fed to the reactor<sup>51</sup>.

$$Y_i = \frac{\text{total amount of product } i \text{ formed}}{\text{initial amount of reactant fed}} \times 100\%$$

Chapter 3 will highlight the usefulness of yield when examining the selective hydrogenation of polyunsaturated fatty acids. A reaction system can have a high selectivity but if that selectivity is present only at low conversion, then the yield of useful product will not be very high<sup>51</sup>. In contrast, a reaction with high yield will produce a larger amount of product relative to the amount of reactant fed, thus indicating a reaction where high selectivity is maintained to high conversion. High yield is a desirable catalytic condition similar to high selectivity in that it results in a greater production of desired product. A higher selectivity means less purification steps and a higher yield means that the process can be run at a higher conversion, thus minimizing recycling of the reactant<sup>47,51</sup>.

1.1.4 Transition state theory: The fundamental concepts of activity and selectivity presented in 1.1.3 and 1.1.4 are important macroscopic deliverables of the catalyst system, but the fundamental drivers of these processes are the microscopic changes that occur on the catalyst surface as a chemical reaction takes place<sup>31,36</sup>.

During any chemical reaction, atoms of reactant molecules are arranged via a transition state into product molecules<sup>36</sup>. Statistical mechanics tells us that this process naturally occurs in both the forward and reverse directions, without a catalyst, and even after equilibrium is reached in a state of dynamic equilibrium; however, the probability of the reaction occurring can be very small without a catalyst. Therefore, the use of a catalyst can be essential for enabling a reaction to reach an acceptable conversion in a reasonable time frame. For example, reduction with hydrogen requires the breaking of an H-H bond, a process which in the gas phase would require a high energy collision to overcome the high potential energy barrier of pulling two hydrogen atoms apart. Catalysts that can stabilize hydrogen and disassociate it into hydrogen adatoms are therefore vital for achieving hydrogenation reactions with reasonable rates.

The way a catalyst works is by changing a series of high energy steps between reactant and product to a new set of steps with lower barriers. Considering the hydrogenation example, exchanging the high energy barrier of splitting hydrogen in the gas phase with a stabilization and splitting step on the surface of a catalyst. A model reaction coordinate is shown in Figure 1-2 for the conversion of reactant A  $\rightarrow$  product B where the transition state is the peak of the potential energy curve.

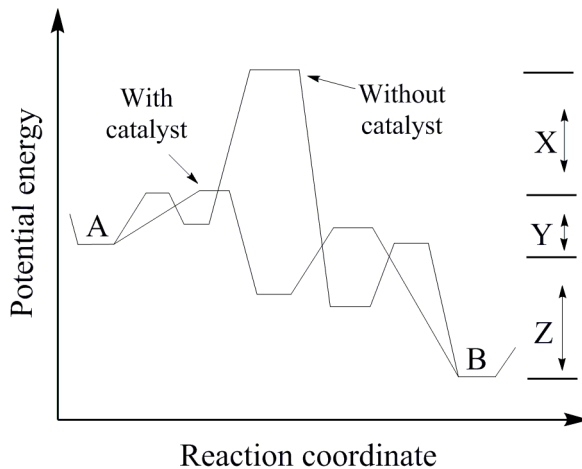


Figure 1-2: Reaction coordinate of a simple reaction  $A \rightarrow B$ . The potential energy barrier for this reaction  $X+Y$  is reduced to only  $Y$  with the use of a catalyst. The  $\Delta H_{rxn}$  is  $Z$  for both cases.

For an uncatalyzed reaction to proceed, it must overcome the potential barrier of  $X + Y$  in order to reach the transition state and fall to the potential energy well of product  $B$ <sup>31,36,52</sup>. As shown in Figure 1-2, the use of a catalyst does not affect the energy of the products ( $B$ ) or reactants ( $A$ ), but merely reduces the potential energy barrier that must be overcome by creating a transition state which is stable at lower energy<sup>31</sup>. Out of this falls one of the fundamental definitions of a catalyst: a material which stabilizes the transition state of a reaction<sup>31,53</sup>.

The predominant reactions studied throughout this thesis are the reduction of olefins and aldehydes, discussed in detail in section 1.3, each of which are composed of a double bond, rich in electrons. These groups can bind to a metal catalyst surface, such as the case shown in Figure 1-3 for epoxybutene, a molecule discussed in Chapter 2<sup>25,54,55</sup>.

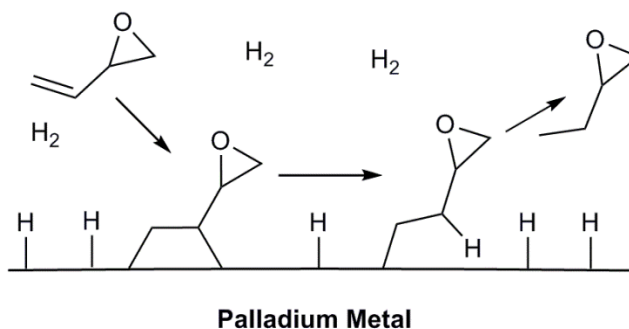


Figure 1-3: Hydrogenation of epoxybutene over a palladium catalyst. Palladium stabilizes the olefin as well as hydrogen atoms that can add sequentially to the olefinic carbons to yield epoxybutane product

The hydrogenation of epoxybutene proceeds rapidly on the surface of a palladium catalyst, but without a catalyst to stabilize the olefin and the hydrogen adatoms and allow them to interact, it is highly unlikely that hydrogenation would occur. Pt and Pd, the two metals studied throughout the content of this thesis, are particularly effective at stabilizing hydrogen ( $H_2$ ) on their surface by disassociating it into elemental hydrogen adatoms<sup>56</sup>. Although functionalized reactants such as epoxybutene can interact with many types of metal catalysts, hydrogen is not very reactive on many materials, making Pt and Pd catalysts highly valuable<sup>12,56,57</sup>.

With hydrogen adatoms on the surface of the catalyst, hydrocarbon reactants can more easily interact and reach a transition state associated with hydrogenation—in the case of Figure 1-3, the point at which a hydrogen atom is added to each olefinic carbon. It is important to note that the transition state is not a reaction intermediate, as are shown in Figure 1-3, but rather a high-energy amalgam of the initial and final state. As such, there are transition states associated with each of the steps shown in Figure 1-3<sup>31</sup>.

The addition of a thiol coating to the catalyst surface, the novel modification made in this thesis, further changes the potential energy diagram of the reaction. For example, the sulfur head group of a thiol modifier is strongly electronegative and can change the electronic properties of a metal catalyst surface, which in turn affects how strongly the reactants and products can bind to the catalyst surface<sup>55,58</sup>. This ability to further adjust the potential energy diagram via the presence of sulfur is one of the most important properties of thiol SAM catalyst modifiers and is associated with much of the selectivity improvement presented in his thesis<sup>22,25,41,43</sup>. Still, SAMs

provide other mechanisms of selectivity improvement, such as orientation effects described in Chapters 4, 5, and 6 which also affect the potential energy diagram by stabilizing certain conformations of reactants, adsorbed intermediates, and even products through non-covalent interactions.

1.1.5 Metals as catalysts: The background provided in this introduction has focused on explaining the usefulness of catalysts, how their efficacy is measured, and general concepts of how they work. Particular focus has been given to platinum and palladium, the metals studied extensively throughout this thesis; however, platinum and palladium are two of the most expensive and rare of all the metals in the periodic table<sup>12</sup>. What is it that makes these two metals so useful as catalysts, and for that matter, why do we use metals in the first place?

Typical metals studied in catalysis are those in the d-block of the periodic table that have incomplete filling of their d-orbital. These metals have an electronic band structure which is narrowly concentrated near the Fermi level. In contrast, s-orbital and p-orbital electrons have a band structure which spreads much wider above and below the Fermi level. The result is that d-band metals can easily “loan” and “receive” electrons from contacting molecules, stabilizing them, and allowing them to react<sup>36</sup>. This is especially true for a reactant rich in electrons such as an olefin or an aldehyde. As discussed in Chapter 1.1.4, the ability to stabilize reactive intermediates and reduce the transition state of a reaction is vital to the efficacy of a catalyst.

Each of the metals in the d-block of the periodic table have differing structure of their d-band due to a combination of atom-specific electronic properties including, most fundamentally, different numbers of electrons in their d-orbitals<sup>36,59</sup>. It is easy to think that the filling of electrons is representative of how well reactants can bind to the surface, but this is not a

complete picture. Thermodynamically, Ni has similar filling of its d-orbitals and similar binding energies for potential reactant groups, but because of its smaller atomic size has different catalytic properties. A widely held hypothesis is that Pt and Pd have the right d-band symmetry around the Fermi Level to allow for the formation of the most important reaction intermediates such as those for C-H bond scission and formation<sup>36</sup>.

When all of these subtle parameters are considered simultaneously, the important outcome is the ability of a metal catalyst to bind reactive intermediates to its surface. Out of this falls a fundamental theory of catalysis, the Sabatier Principle, which states that in order for a catalytic process to proceed effectively, it must bind a reactant strongly enough to stabilize it for reaction, yet weakly enough so that when the reaction is completed, the molecule can detach from the surface<sup>36,59</sup>. This concept is shown in Figure 1-4, adapted from Heterogeneous Catalysis and Solid Catalysts<sup>59</sup>.

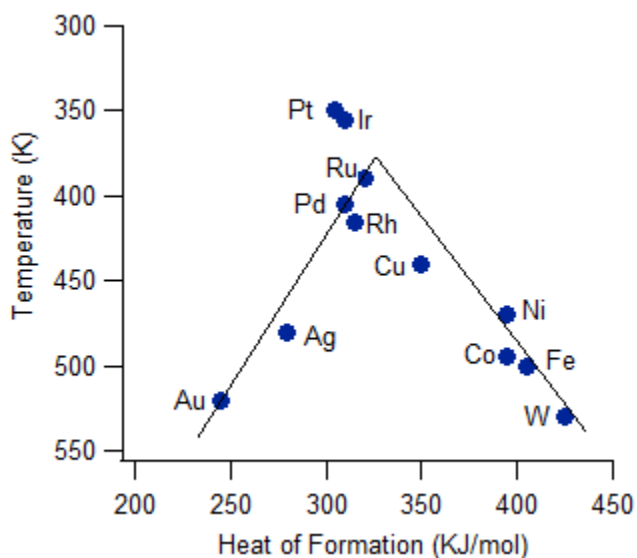


Figure 1-4: The Sabatier Principle shown for aldehyde hydrogenation over a variety of metal catalysts. The metals on the left of the chart bind the reactants too weakly to

achieve reactivity, and the metals on the right bind the product too strongly such that it cannot desorb and therefore clogs the surface<sup>59</sup>

Typically, metal catalyzed reactions proceed through a series of steps discussed in section 1.1.4 where the reactants adsorb on the surface of the metal, undergo surface reactions, and finally desorb from the surface as products. Shown in Figure 1-4, metals on the left of the plot such as gold and silver tend to bind reactants too weakly to achieve reaction, whereas metals on the right of the plot such as tungsten or iron bind reactants too strongly such that products cannot desorb from the surface. Not surprisingly, platinum group metals are in the center of this plot indicating that they bind reactants just strongly enough to react but weakly enough so that products can desorb<sup>12,36</sup>. Although Pt and Pd are expensive and rare metals, they are highly effective as catalysts and therefore are studied extensively in catalysis literature<sup>12-14,22,24,25,43,60-64</sup>. Still, there is room for improving the catalytic properties of these metals by slightly altering their electronic properties or near surface environment. In this thesis, these effects are achieved with the addition of thiol self-assembled monolayers.

## **1.2 Self-Assembled Monolayers**

Self-assembled monolayers (SAMs) are large ordered domains of organic molecules that form spontaneously on a substrate. SAMs have been studied since the 1940's when Zisman et al. first published findings of the formation of oleophobic octadecylamine monolayers on polished Pt surfaces<sup>65</sup>. At the time, the work found no large-scale application and therefore generated little interest. Then in 1983, Nuzzo and Allara published the first work on the formation of

alkanethiol SAMs on gold surfaces, and it was after this point that the characterization and use of SAMs began to increase dramatically<sup>66,67</sup>.

Today, SAMs made from silanes, amines, fatty acids, and thiols have been studied and used for applications as sensors, etch resists, capping nanoparticles, and recently for their use as catalyst modifiers<sup>22,25,27,41,43,66,68-70</sup>. For catalytic reactions, modifiers or promoters are an important industrial means of improving catalytic activity, suppressing undesirable side reactions, and improving selectivity<sup>36</sup>. While each of the aforementioned types of SAMs could potentially be used as a catalyst modifier, current interest is focused on those formed from thiols due to their ability to form a covalent bond with a late transition metal surface. The hypothesis is that these modifiers can form a robust coating on the catalyst surface, which can be used to direct reactions on the surface.

1.2.1 Metal structures: Before discussing the formation of thiol SAMs, it is useful to discuss the underlying metal crystal structure on which the monolayer will form. For metal crystals, there are four basic crystal structures: simple cubic, face centered cubic (FCC), body centered cubic (BCC), and hexagonal close packed (HPC)<sup>36,71</sup>. Each of these structures forms a unique unit cell, the smallest repeatable structure in the lattice. Platinum group metals form in the FCC structure, which we will consider in detail here.

Although the underlying structure of a metal crystal is repeatable and identical, the exposed face of a crystal is different depending on which side of the lattice is exposed. For example, the exposed face of an FCC crystal looks different when cut in different directions. Some of the earliest descriptions of a lattice structure were provided by Miller and Whewell who in 1829 identified different faces of rocks while studying crystallography of minerals<sup>72,73</sup>.

During this time, there was great interest in the periodic arrangement of crystals, and the idea that a crystal's geometry will look the same when viewed from any equivalent lattice point. Eventually in 1850, Auguste Bravais showed that there are 14 possible symmetry groups, or unit cell arrangements, in three-dimensional space; these are known today as the 14 Bravais Lattices<sup>72,74</sup>. With this basis in theoretical geometry, scientists began to look for the structures of real crystals. The famous J. Willard Gibbs proposed that a system of atoms or droplets will rearrange itself in a manner to minimize its surface energy thereby minimizing its Gibbs free energy<sup>75,76</sup>. This was demonstrated by Georg Wulff who in 1901 used a combination of Gibbs' and Bravais' theory to determine the equilibrium shape of a selection of droplets or atoms in a crystal<sup>72,77-79</sup>. As predicted, a collection of particles would adopt a common material-specific underlying packing structure (BCC, FCC, cubic, or HPC) with distinct lattice faces (111, 110, 100, etc.) each of which would have a different surface energy<sup>75,76,80</sup>. For a lattice comprised of Pt or Pd, there are many theoretical faces such as (211) or (755), but the most common are the (111), (110), and (100) facets, shown in Figure 1-5.

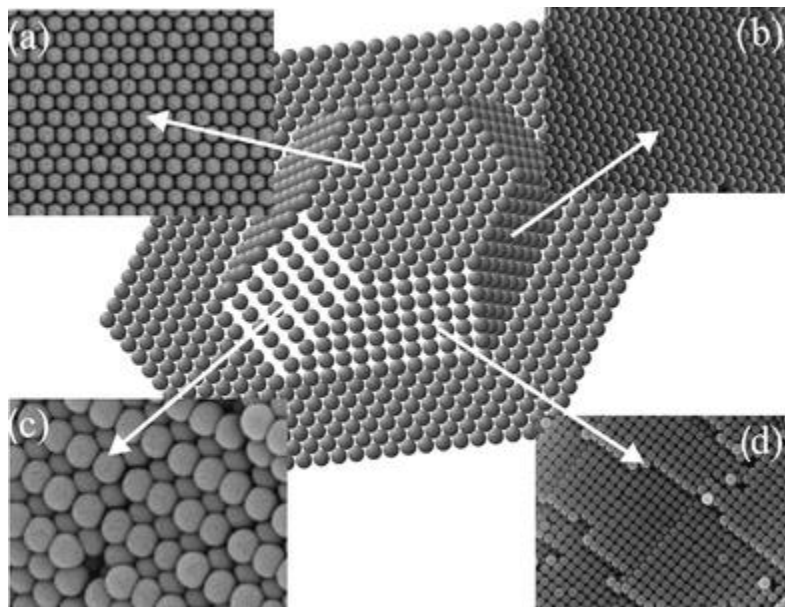


Figure 1-5: The 4 facets of the FCC lattice shown by SEM of spherical colloids<sup>81,82</sup>. A model crystal is shown in the center. (a-b) The (111) lattice (c) the (110) lattice (d) the (100) lattice

The most stable surface face, defined by Miller Indices, is the so called (111) face. Atoms on the (111) face can each bind to 9 nearest-neighbor atoms, 6 around it and 3 beneath it whereas the (110) surface allows only 6 nearest neighbor interactions and the (100) surface only 8 nearest neighbor interactions (noting that the overlap of electron orbitals in these nearest-neighbor interactions are also different such that the 100 surface is the least stable)<sup>54,55,83,84</sup>. This can be seen in Figure 1-5 (a, b) where the atoms are closer packed than in Figure 1-5 (c, d). As predicted by Gibbs, since the (111) face is the most stable, it is also the most commonly occurring face and as such, is one of the most important metal surfaces for catalytic reactions. Not surprisingly, it receives a great deal of attention in the literature, especially for ultra-high vacuum and theoretical studies<sup>54,55,61,84-86</sup>.

The (111) face makes for a useful basis of study, but real catalysts, such as the supported nanoparticles studied in this thesis, are particles and therefore contain additional faces such as the (110) and (100) shown in Figure 1-5 (c, d). Some reactions, such as the hydrogenation of benzene show higher activity and lower activation energy on (100) surfaces<sup>87</sup>. In general, olefin hydrogenation on Pt and Pd is also faster on defect sites where the rate trends as (110) > (100) > (111)<sup>88,89</sup>. Again, since the (111) surface is the most stable, atoms will preferentially rearrange themselves to maximize their surface area in this form, but where the (110) and (100) facets can become especially important for nanoparticle catalysts is at the interface of two terrace surfaces,

points where one face ends and another begins<sup>82-80</sup>. For example, a step edge between two (111) terraces creates a (100) plane in that single step<sup>80</sup>. The smaller a nanoparticle catalyst becomes, the more curvature it contains, and therefore, more edge sites and defects. All of these features make the study of catalysts a challenging undertaking. Next we will consider an additional level of complexity by adding thiol SAMs to these surfaces.

1.2.2 Formation of SAMs: The formation of alkanethiol SAMs on the (111) face of gold surfaces has been extensively characterized, and such studies have in recent years been extended to other coinage metals as well<sup>68,69,84,90-95</sup>. In a standard SAM deposition, thiols are introduced to the metal surface from a dilute thiol solution, typically 1-100 mM in ethanol or n-alkane<sup>22,68,69,93</sup>. The sulfur head groups have a strong affinity for metal surfaces and quickly adsorb through bulk diffusion to form a disordered initial coverage. During the adsorption step, the sulfur covalently binds to the catalyst surface, resulting in a strong bond, and releasing hydrogen gas<sup>22,83,93</sup>. Over time, thermal motion facilitates ordering of the adsorbed thiols on the metal surface, which subsequently allows additional thiols to access and adsorb on the surface. When allowed sufficient time, this slow two-dimensional organization step yields a well-ordered monolayer bound to the active metal surface by a metal-sulfur bond<sup>68,69,92</sup>. This process is depicted in Figure 1-6.

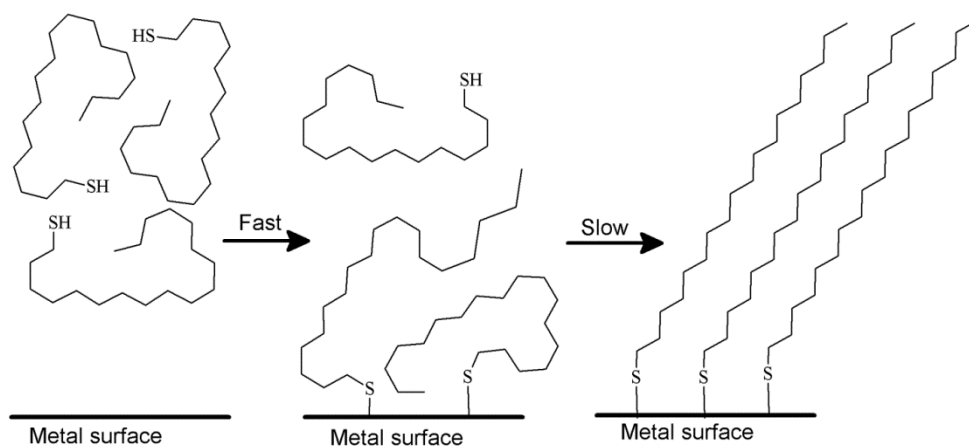


Figure 1-6: Formation of octadecanethiol self-assembled monolayer on a metal surface. Initially, there is a fast step of disordered surface coverage followed by a slow re-ordering step facilitated by thermal motion

As thiols bind to a metal surface, they arrange themselves to form a monolayer that is organized not just in the one dimension but in two dimensions. Looking at the formation of an alkanethiol monolayer on a (111) surface from the top view, alkanethiols form a periodic  $\sqrt{3} \times \sqrt{3}$  structure on the underlying metal crystal surface with a nearest neighbor distance of approximately 5 Å on Au, Pd, and Pt<sup>68,93,94</sup>. This is referred to as a 1/3 monolayer coverage and the structure is depicted in Figure 1-7.

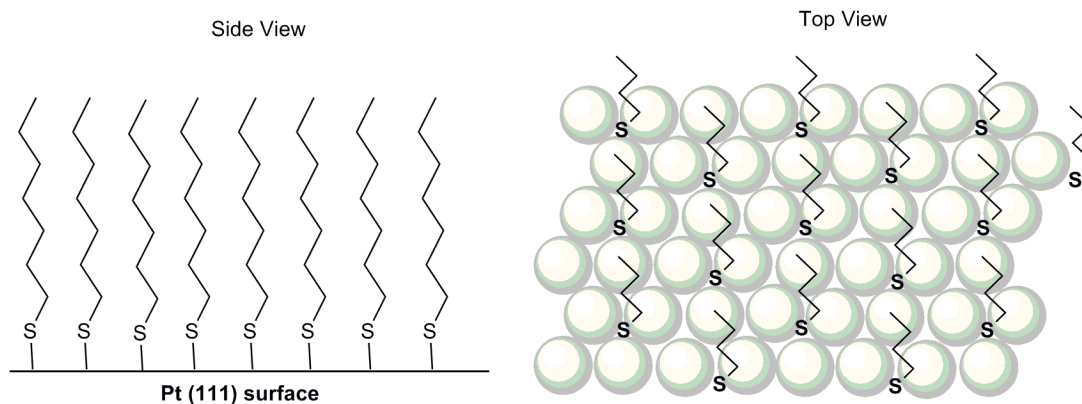


Figure 1-7: Alkanethiols form a periodic  $\sqrt{3}\times\sqrt{3}$  structure on the surface of a metal (111) crystal

Nearly all of the thiol SAMs discussed in this thesis form a  $\sqrt{3}\times\sqrt{3}$  structure on (111) surfaces; however, some types of thiol SAMs form different overlayers on metal crystals. For example, 1-adamantanethiol has a bulky tail which forms a (7 x 7) structure on the (111) facet and has a nearest neighbor distance of 7 Å due to steric interactions of its large organic ligand<sup>27,93,96</sup>. Even with exceptional cases such as adamantanethiol, a major advantage of using thiols as catalyst modifiers is that they will reproducibly form the same structure on an underlying metal surface.

Beginning with their inception, thiol SAMs on Au have received much attention, and as such, these studies comprise the foundation of knowledge on the structure and properties of thiol modifiers<sup>68,97</sup>. The entirety of work in this thesis is on Pt and Pd surfaces, so it is useful that many of the studies carried out on Au can be used to understand what is occurring on Pt and Pd surfaces as well<sup>93,94</sup>. For example, thiols have been shown to form the same  $\sqrt{3}\times\sqrt{3}$  coverage structure on Pt and Pd (111) metal surfaces<sup>93,94</sup>. The wetting behaviors of alkanethiol SAMs on

palladium are similar to those observed for the same SAMs on gold, silver, and copper substrates<sup>93</sup>. Similarly, alkanethiols on platinum have been shown using XPS not to undergo C-S bond scission or to contain weakly adsorbed species<sup>94</sup>. There are however relevant differences between SAM formation on different metals. For example, the aliphatic chains of alkanethiol SAMs have been shown to orient at an angle normal to the surface on platinum<sup>94</sup> whereas they form an angle of approximately 38° with respect to the surface normal on gold and 14-18° on palladium<sup>93,97</sup>. Subtle differences such these can be very important, especially for design of the catalyst near surface environment.

One of the biggest challenges for extending the use of thiol modifiers to supported metal catalysts is understanding how the thiols assemble on edge sites, including the (110) and the (100) facets of the metal crystal. As discussed in section 1.2.1 and here for the formation of thiol SAMs, much research has been conducted on the (111) facet but relatively less work has been done on other sites. One of the challenges of studying alternative facets of these crystals is that they will spontaneously re-organize into the more stable (111) structure. In fact, the cases that have received the greatest study are metals that are more thermodynamically stable in these alternative lattice structures. For example, alkanethiol modified Cu(100), and GaAs surfaces have been studied for their ability to increase resistance to acidic corrosion<sup>98,99</sup>. On Au(100) surfaces, a butanethiol modifier was shown to exhibit a striped structure with interatomic sulfur spacing of about 5.2Å<sup>100</sup> which is approximately the same as the 4.7Å spacing observed for alkanethiols on an Au(111) surface<sup>97</sup>. More importantly, it has been shown that thiol mobility is much lower on edge sites than on terrace sites indicating that once a thiol becomes present on a step edge, it is unlikely to be removed during reaction<sup>84,90,94,97</sup>. Although no systematic study has been carried out on the (110) or the (100) facets of a Pd or Pt crystal, these studies indicate that

thiols will likely form some periodic structure on their surfaces, perhaps with greater binding strength and less mobility than on the (111) facet.

Because alkanethiol SAMs are readily fabricated in a controlled, reproducible manner, they offer an excellent way to control the near-surface environment. Regioselectivity studies have been pursued previously using organic monolayers to create favorable geometries for directing organic photoreactions<sup>101</sup>, and various types of organic modifiers have been successfully used to non-specifically tune the surface of heterogeneous catalysts<sup>22-24,26,102,103</sup>. One of the main goals of this thesis is to develop an understanding of thiol SAMs sufficient to rationally and precisely tune chemoselectivity of a catalyst through non-covalent interactions in the near surface environment.

### **1.3 Hydrogenation of olefins and aldehydes**

Throughout this thesis, a number of different reaction pathways were used to probe the chemistry of interaction between the thiol SAM modifier, the reactant, and the catalyst surface. The relevance of each of these reactants to the petrochemical processing industry will be discussed specifically in each chapter, but here it is important to provide a basic background for these reactions, focusing specifically on hydrogenation chemistry.

All of the reactions discussed in this thesis are hydrogenation reactions, meaning reactions where a certain moiety, or functional group of the reactant, is reduced by elemental hydrogen<sup>57</sup>. The predominant moieties studied throughout this thesis are olefins (C=C) and aldehydes (C=O), which are also two of the most commonly studied groups in catalysis

literature<sup>12,18,25,43,56,57,104</sup>. In fact, one of the most important types of molecules studied in this thesis are  $\alpha,\beta$ -unsaturated aldehydes, molecules that contain both of these moieties.

1.3.1 Hydrogenation of olefins: Catalytic hydrogenation of olefins was first conducted by Sabatier and Senderens in 1897, and since then has become one of the most studied reactions in the field of catalysis<sup>105-108</sup>. Although the reaction is relatively simple, there is still not complete consensus on how olefins are hydrogenated on the surface of a catalyst<sup>108,109</sup>. The ongoing debate centers on whether the hydrogen atoms are added to the olefin in a stepwise procedure<sup>108</sup>, in a concerted step<sup>110</sup>, or via transfer of hydrogen from a neighboring hydrocarbon species<sup>12,108,111</sup>. These alternative pathways are shown in Figure 1-8.

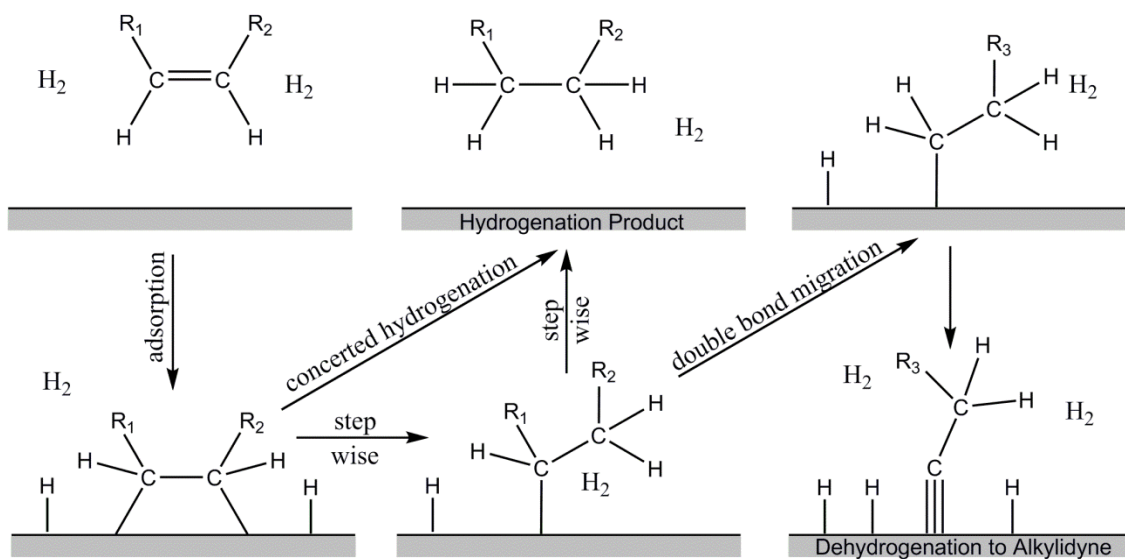


Figure 1-8: Hydrogenation pathways for olefins on Pt and Pd surfaces. The olefin can be reduced by a concerted step, individual steps, or can be converted to carbonaceous deposits through dehydrogenation which participate in subsequent hydrogenations<sup>108</sup>

In the past 10 years, the literature on olefin hydrogenation has converged on the idea that no reaction occurs on a clean surface, but instead on a surface covered with strongly adsorbed carbonaceous species, organic fragments of other reactants<sup>108,109</sup>. This effect is due to the strong binding energies of organic hydrocarbons to Pd and Pt surfaces which results in rapid decomposition of the adsorbed species to form stable ethylidyne species on the surface of the catalyst<sup>105,107,109,112</sup>. The strongly bound ethylidyne intermediates are thought to exert important effects on the kinetics of hydrogenation, influencing both how additional hydrocarbon reactants access the surface and how the surface atomic hydrogen forms and is incorporated to the reducing group<sup>105,108,109</sup>. This might seem tangential to the study of SAM coated catalysts, but in fact, thiol coatings can cover a catalyst in a similar manner as would be expected to occur by coking under reaction conditions<sup>22,25,27,43,109,112</sup>. In this way, thiol SAMs might not change the surface of the catalyst as dramatically as expected for olefin hydrogenation.

For example, Chapter 6 will demonstrate how thiol SAMs might in effect “pre-coke” the surface with thiolates thereby preventing further coking by the reactants. Supported by infrared spectroscopy of the catalyst surface, these studies indicate thiol modifiers may in fact keep the surface more free of coking products than it would be without a SAM. Olefin hydrogenation has been studied for over 100 years without a consensus on its mechanism, and even though here we introduce a completely new aspect, a thiol SAM coating, it is possible that the coated catalyst surface is not entirely different from the surface produced under ordinary hydrogenation conditions.

1.3.2 Hydrogenation of aldehydes: Aldehyde hydrogenation is similar to olefin hydrogenation, in that aldehydes can undergo reduction on Pt and Pd surfaces with similar reaction conditions<sup>18,20,24,61,85,113</sup>. The mechanism of hydrogenation is proposed to begin with

formation of a C-H bond to produce an alkoxy intermediate followed by addition of another hydrogen atom to form the adsorbed alcohol<sup>114-116</sup>.

Much of the work on aldehyde hydrogenation is focused on the study of  $\alpha,\beta$ -unsaturated aldehydes, molecules that contain both an olefin and aldehyde moiety<sup>18,20,24,61,85,113</sup>. In studying the adsorption energies and geometries of  $\alpha,\beta$ -unsaturated aldehydes, the field is concerned with developing catalysts that can improve the selectivity of this reaction towards production of unsaturated alcohol as shown in Figure 1-9 (a).

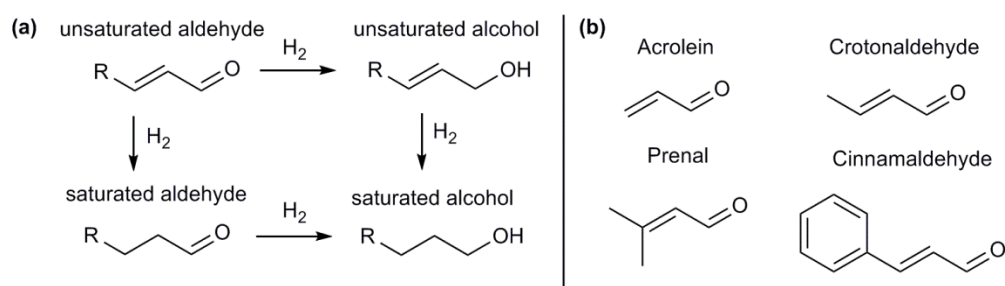


Figure 1-9: Hydrogenation of  $\alpha,\beta$ -unsaturated aldehydes. (a) pathway for sequential hydrogenation. (b) common  $\alpha,\beta$ -unsaturated aldehydes

In the liquid phase, selectivity to the unsaturated alcohol is approximately 30% over a platinum catalyst and as low as 0% over palladium catalysts<sup>14,18,41,113</sup>. In addition to differences in the metal used for hydrogenation, as the tail segment of  $\alpha,\beta$ -unsaturated aldehydes becomes larger, the average adsorption energy decreases due to the substitution effect on the  $\beta$ -carbon<sup>19</sup>. This leads to more selective hydrogenation for larger molecules like cinnamaldehyde shown in Figure 1-9 (b). For each of these unsaturated aldehydes, reduction of the olefin is thermodynamically favorable over reduction of the aldehyde by approximately 35 kJ/mol, a

point made repeatedly and often misleadingly in the  $\alpha,\beta$ -unsaturated aldehyde literature to justify the naturally higher selectivity of these reactions towards olefin hydrogenation<sup>104,117</sup>. The kinetic barrier of the transition state is what ultimately leads to the differences in the observed rate and selectivity in practice—the root of the thermodynamic argument can be traced back to a study by Jenck et al. which showed that in general, for aldehydes, ketones, and olefins, the thermodynamic barriers of reaction are a good predictor of selectivity<sup>118</sup>.

This chapter on the hydrogenation of olefins and aldehydes is important for understanding the reaction chemistry underlying the hydrogenation process, but it is necessary to remember that for this thesis, these hydrogenation reactions serve mainly as a probe. The ultimate goal is to identify the underlying effects that the thiol SAM imparts on the catalyst surface so that future catalysts can be rationally designed.

## **1.4 Description of Common Techniques**

Across this thesis, many of the same techniques were used to prepare the catalysts and to test them, including the SAM deposition procedure, the procedure used to run catalytic reactions, and some of the basic Fourier Transform Infrared Spectroscopy (FTIR) techniques used to analyze the catalysts. Below is a brief summary of the techniques used. Each of the individual chapters will address specific technique concerns.

1.4.1 Preparation of thiol coated catalysts: Each of the catalysts discussed in this thesis is either platinum or palladium metal supported on alumina or carbon, and was purchased from Sigma Aldrich. The defining characteristic of the catalysts is the addition of a thiol self-assembled monolayer (SAM) to the surface of the metal. Consistent with standard catalytic

practice, the early chapters of this thesis discuss an oxidation and reduction step for the catalysts before the SAM deposition; however, it was later determined that this step does not significantly affect the functionality of the thiol coating. That is, for the reactions presented here, the oxidation and reduction step did not result in a discernable difference for the uncoated catalyst or the coated catalysts. Infrared spectroscopy also did not show any discernable differences between coated catalysts that had been oxidized and reduced beforehand. This result is not surprising since studies were limited to platinum and palladium, noble transition metals, which stay relatively clean under ambient conditions. If studies were extended to less noble metals, the pretreatment step may become more important<sup>119</sup>. For this reason, it would be prudent to test this control before trying other reaction systems and catalysts in the future.

SAM-coated catalysts were prepared by immersing the catalyst in an ethanolic solution of 10 mM for thiols that were liquid at room temperature and 1 mM for thiols that were solid at room temperature, as has been done in many previous studies of SAM catalysis and SAM characterization<sup>22,25,27,43,70,93,94</sup>. A concentration of 1-10 mM is effective because it is 10-50x the total amount of thiols required to completely cover the surface. As will be shown in Chapter 6, using too low a deposition concentration results in formation of an incomplete monolayer whereas too high a concentration can result in poor ordering of thiols in the self-assembly process, including the formation of multilayers.

The thiols were deposited overnight for use the next day, a deposition time of 12-16 hr. The following day, the thiol solution was poured off and the catalyst was rinsed for 3 hr in ethanol to remove any weakly adsorbed thiols. Ethanol was typically the solvent used to perform these steps, but other solvents might be considered for varying abilities to solvate the thiols. As discussed in section 1.2 on the chemistry of self-assembled monolayers, the rinse step is

important to remove any potentially physisorbed thiols from the surface of the catalyst. Such thiols do not have much effect on reactions run in the gas phase since they would not participate in the reaction happening on the surface of the catalyst, but for reactions in the liquid phase, these thiols, if not rinsed off will be solvated in the reaction solution if transferred with the catalyst. The effect of such a transfer is discussed briefly in Chapter 2 and more extensively in Chapter 6 when thiols are intentionally dosed into the reactor. For systems where thiols are not especially soluble in the deposition solution, care should be taken to prevent accidentally transferring physisorbed thiols to the liquid phase reaction.

Finally, after the rinse procedure, the ethanol supernatant was again poured off and the catalyst was dried under vacuum for 20 min in a vacuum desiccator. As discussed in section 1.2.2 and in Chapter 6, thiols are susceptible to autoxidation in air, so storing them under vacuum is not only an effective method for drying the catalysts, it is also a good way to reduce oxidative degradation. Throughout chapters 2 and 3, the thiol-modified catalysts were used within a few days of preparation with little noted effect on the results, but from Chapter 4 on, it was noted that ligand specific effects between the thiol and the reactant were susceptible to degradation in air and henceforth all catalysts were used immediately following their deposition.

1.4.2 Surface area and particle size measurements of the catalysts: Surface area and particle size measurements of the catalysts are important parameters for understanding the results of kinetic studies and making rate calculations. Chemisorption, gas phase titration of the catalyst metal surface is one of the most common techniques for gaining this information. During chemisorption, a catalyst is first cleaned by oxidizing it to burn off any carbonaceous species and then reducing it under hydrogen to return the metal to its ground state and remove any metal oxides that may have formed during the oxidation step. Next, a chemical such as CO or H<sub>2</sub> is

dosed on to the surface from an inert or vacuum environment. The total metal sites present on the catalyst surface can then be determined by measuring either the amount of dosant that is adsorbed from a known input stream, or by evacuating the chamber and heating the catalyst to measure the amount of dosant that subsequently comes off the surface. In either case, the chemical dosant is used to measure how many metal sites are present on a known mass of catalyst, thereby allowing a measurement of the total metal sites per gram of catalyst. Knowledge of the weight loading of the catalyst allows for the further calculation of the catalyst dispersion, or the percentage of exposed metal atoms vs metal atoms submerged in the bulk of a nanoparticle.

The commercial uncoated 5wt% Pt/Al<sub>2</sub>O<sub>3</sub> and the commercial uncoated 5wt% Pd/Al<sub>2</sub>O<sub>3</sub> used throughout this thesis were both characterized by chemisorption of CO on a Quantachrome Autosorb-1 to determine their active surface area. For measurements of the uncoated catalysts, the powder was first reduced in situ at 473K for 16 hours. The active surface area of the 5wt% Pd/Al<sub>2</sub>O<sub>3</sub> was determined as 3.7 m<sup>2</sup>/g with a dispersion of 17%. The 5wt% Pt/Al<sub>2</sub>O<sub>3</sub> had an active surface area of 2.9 m<sup>2</sup>/g and a dispersion of 27%. One of the key benefits of using the commercial Pt and Pd catalysts was that these same catalysts were used for the majority of the studies discussed in this thesis and the values for surface were considered to remain constant. This assumption was, however, verified at various time intervals by re-running the chemisorption with hydrogen and also characterizing the particle size using SEM. Shown in Figure 1-10 is an example SEM image showing the large porous poly-disperse alumina support (1-50 μm) with the small white palladium atoms on the surface (average particle size 7 ± 1 nm). Particle size of the Pt/Al<sub>2</sub>O<sub>3</sub> was also measured by SEM as 4 ± 1 nm.

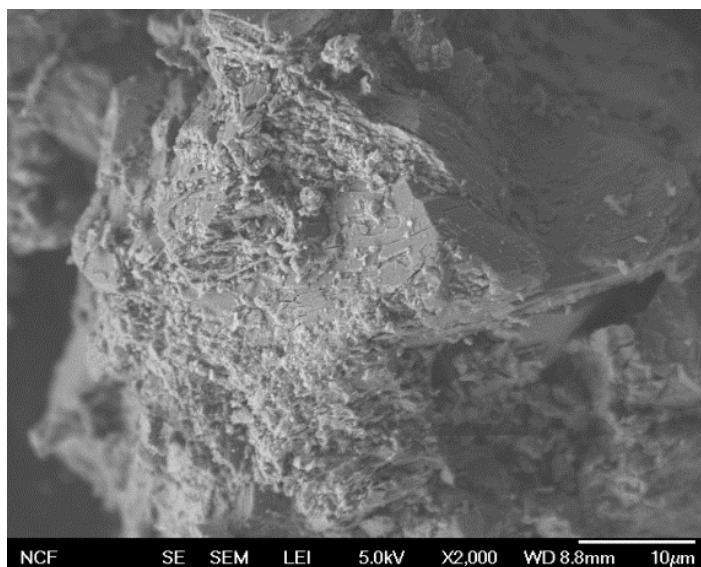


Figure 1-10: SEM of Pd/Al<sub>2</sub>O<sub>3</sub> catalyst

1.4.3 The reactor system: Reactions were run in a 100 mL Parr semi-batch reactor. For many of the systems described in this thesis, the temperature was held at 50°C and the reactor was pressurized to 40 bar with hydrogen gas. Both higher and lower temperatures and pressures are discussed. For different reaction pressures a low pressure regulator can be used between 1.2 bar and 5.5 bar whereas a high pressure regulator can go up to 200 bar. For safety reasons, no reactions run here were any higher than 40 bar hydrogen, which is still considered high pressure and results in highly effective hydrogenation over Pd and Pt catalysts. For sampling reasons, no pressures lower than 1.2 bar were used because at lower pressures, the procedure for taking samples does not have enough internal reactor pressure to expel a sample.

Reactor contents were prepared as 48 mL solvent, 5 mL internal standard for the GC analysis, and 1 mL of reactant giving the system a reactant concentration of approximately 0.15 M. For most of the reactions discussed, ethanol was chosen as the reaction solvent as light alcohols have been shown previously to give the highest rates<sup>18,113</sup>. Chapter 4 provides a

discussion of solvent choice and shows that ethanol does in fact yield higher rates and selectivity for cinnamaldehyde hydrogenation than benzene, heptane, or cyclohexane. It is important to note that higher reaction temperatures would require solvents with higher boiling points to maintain liquid phase reaction—even if reactor pressure keeps the solvent liquid, there is potential for it to flash to vapor upon sampling causing loss of solvent or internal standard.

All reactions discussed in this thesis were run for either 90 min or 60 min during which eight 1.5 mL liquid samples were taken at exponentially increasing time intervals. As discussed in section 1.1.2, data points at low conversion are especially important for extrapolating rate information, so more samples were taken at short times in order to capture this effect. Longer reaction times were avoided because the reactor itself showed the ability to induce hydrogenation, a confounding effect on measurements of activity. Shorter reaction times can outcompete the reactor but are more susceptible to experimental differences. Therefore, a moderate reaction time is optimal for capturing the intrinsic kinetics of the reaction.

The ability of the reactor to self-catalyze reactions is worth its own discussion because it is a constant source of frustration. Over time, Parr reactors are known to undergo “seasoning” where nanoparticles of metal catalyst from previous reactions can become deposited on the interior of the reactor and the glass liner, and lead to the unaccounted for activity of the reactor. This effect is one of the most elusive and confounding of the entire SAM catalysis project. Thorough and frequent cleaning of the interior of the reactor can help to moderate this effect, but future researchers should be aware of this effect and periodically run control reactions with no catalyst to test the inherent activity of the reactor walls. In addition, the glass liner is an effective way of reducing the effect of “ghost reactions”, but it too can become “seasoned” with deposition of displaced metal nanoparticles from previous reactions. As such the glass liner

should be replaced with a new liner or cleaned in an aqua regia solution to dissolve any transplanted metal. The reactor should be frequently sonicated, scrubbed, and periodically polished.

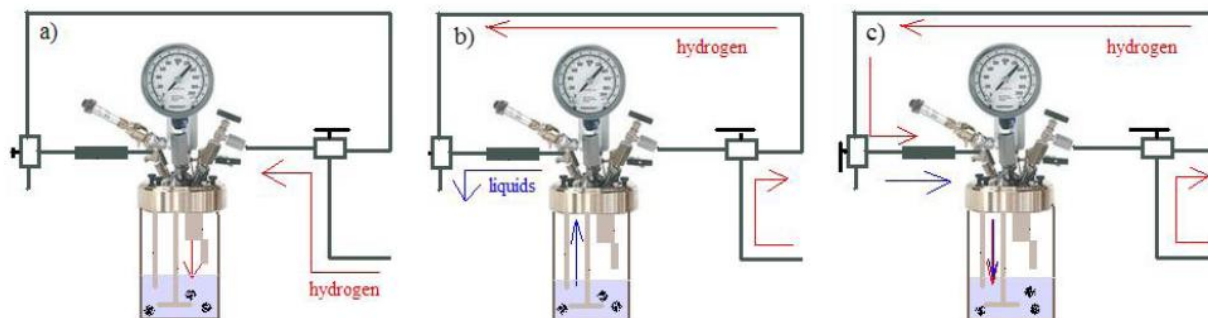


Figure 1-11: Parr liquid phase batch reactor sampling mechanism. (a) hydrogen pressurizes the reactor (b) pressure in the reactor is used to expel liquid through the sample loop (c) the reactor is re-pressurized through the sample loop forcing any excess liquid from the previous sample back into the reactor

For taking samples, hydrogen pressure on the interior of the reactor was used to push liquid samples out of the sample tube and through a disposable filter which was replaced after each sample, as shown in Figure 1-11. By sampling the liquid catalyst mixture and filtering out the catalyst, the reactor setup allows the ratio of catalyst to reactant to remain constant within the reactor independent on how much liquid was sampled.

The final step in the reaction procedure was to analyze the sample vials to determine the concentration of reactants and products—this was done using a gas chromatograph (GC). In its most simple form, a GC is simply an oven that is used to heat a collection of molecules while

pushing them through a long narrow capillary column such that molecules with different sizes, shapes, and functional groups take differing amounts of time to elute from the column<sup>120</sup>. At the end of the column, a detector measures a signal based on the quantity of molecules eluting at any given time. For most GC analysis, the temperature of the oven can be controlled on a set program to ramp from low to high temperature in a time specific method. When a sample of molecules is injected to the GC and the same method is run, each molecule will elute at its characteristic time. As shown in Figure 1-12, numerous different products can be identified from their characteristic elution time.

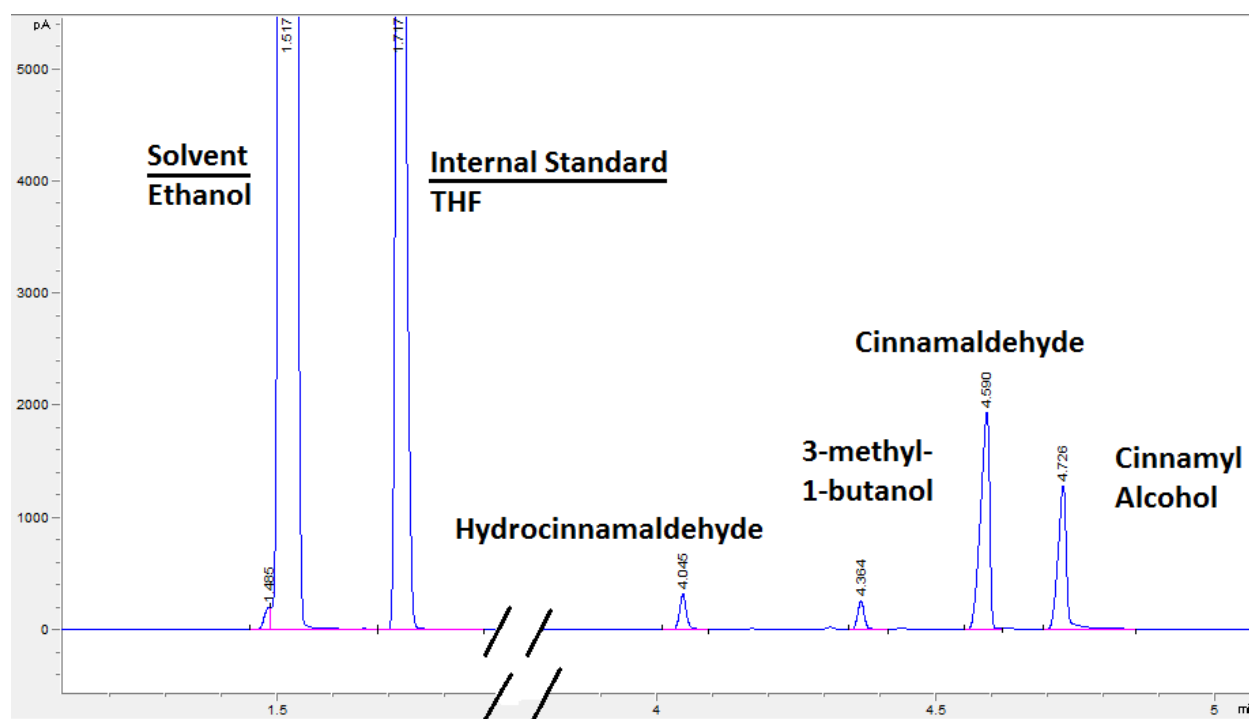


Figure 1-12: GC chromatogram obtained from the analysis of a cinnamaldehyde hydrogenation. Important peaks are labeled including the reactant, products, internal standard, and solvent.

Measurement of the quantity of products eluting can be done with a selection of detectors including thermal conductivity detectors (TCD) which measure the thermal conductivity of the eluting stream or flame ionization detectors (FID) which burn the eluting stream in a small hydrogen flame and measure the intensity of the ionization. Of course, FID requires that a sample can be burned, so molecules like water and CO<sub>2</sub> cannot be measured this way. An FID was used for all of the analysis in this thesis. The response measured by the detector can be calibrated so that the area of the peak measured can be related to the concentration of molecule in the sample. In total, the GC thus gives information on what products are present, as well as how much are present, in a sample. All of the collected liquid samples in this thesis were taken in 2 mL vials and analyzed in an Agilent 5890A gas chromatograph. The two capillary columns used in this thesis for separating the samples were an Agilent DB-FFAP capillary column with dimensions of 30 m x 0.32 mm x 0.50 μm and an Agilent HP-5 capillary column with dimensions of 30 m x 0.32 mm x 0.25 μm. The use of each of these columns will be discussed in each chapter specifically.

A final discussion of the reactor system is necessary to describe the role of the internal standard. The internal standard is used to calibrate the samples when injected into the GC. When a sample is injected in the GC for analysis, it is possible that a different volume of sample can be injected from run to run. The auto sampler used on the Agilent 5890 used throughout this thesis is typically very good about making precise repeatable injections, but still has periodic variance. Consider the situation where you have 1 sample vial of component A and you inject it in the GC two times. Assume that the second time, the GC sample injector injects twice as much volume as the first time. Analysis would indicate a doubling of the volume of component A, a condition you know is not true. To fix the analysis problem you now add to the vial a known

concentration of B, your internal standard. Now, if the GC injects twice as much volume in the second run, it will inject twice as much A but also twice as much B. In this case the ratio of A/B will always be constant no matter how much volume is injected to the GC. An internal standard is a powerful method for converting a highly variable and error prone extrinsic measurement into a more precise repeatable intrinsic measurement.

The choice of an internal standard is important for obtaining consistent rate and selectivity data from liquid phase reactions. First and foremost, the internal standard should be completely inert in the reaction and should not be a product, reactant, or solvent. To work effectively, the internal standard cannot be produced, consumed, or otherwise altered during reaction; it serves as the one molecule in the system which has a precisely known concentration, so any conditions that might compromise its integrity will also compromise the quality of the results. Throughout this thesis, tetrahydrofuran (THF), a cyclic ether, was commonly used as the internal standard because it met these conditions.

1.4.4 Selectivity and rate calculations: For the SAM coated catalysis discussed in this thesis, reaction rates for both the coated and uncoated catalysts were calculated as the moles of reactant consumed per mole of surface metal per second. In conventional catalysis literature, this would reduce to the turn over frequency (TOF) reported as inverse seconds ( $s^{-1}$ ) where the moles of reactant consumed would be cancelled with the moles of surface metal<sup>121</sup>. For SAM catalysis, the moles of surface metal are not well known due to the partial coverage of the catalyst surface by the thiol adsorbates. It is still unclear to what extent the SAMs block surface sites, and what differences in coverage arise from different coatings<sup>27</sup>. An additional confounding effect is the surface site requirements of reactants. Therefore, in order to make fair comparisons between

coated and uncoated catalysts as well as between different types of SAM coatings, all rates are reported relative to the total surface sites available on the uncoated catalyst. Most of the rates reported in this thesis use the initial slope of the consumption of reactant per time at short time intervals where the slope could be approximated as linear (see section 1.1.2). All of the reactions studied in this thesis are first order in nature and in some cases it was possible to linearize the reaction data to determine the rate data more accurately.

Reaction selectivity, reported throughout the thesis was calculated as the conversion to a particular product divided by the total conversion to all products (see section 1.1.3). Therefore, selectivity always totaled 100%. Error bars in selectivity were calculated from repeat measurements.

1.4.5 Infrared spectroscopy techniques: Throughout this thesis, various infrared spectroscopy experiments were employed to characterize the formation of thiols on the surface of a coated catalyst as well as the molecular interactions of reactants with the surface of a catalyst.

Infrared spectroscopy (IR) is fundamentally based on the idea that infrared light, light longer in wavelength and lower in frequency than the visible spectrum, is of the proper wavelength to interact with molecular bonds<sup>122</sup>. All chemical bonds exhibit some form of vibrations associated with their molecular arrangement including stretching (stretching the bond length), bending (changing the bond angle), rocking, wagging, twisting, and scissoring to name a few<sup>122,123</sup>. Each of the vibrational modes in a molecule has the ability to absorb infrared frequencies of light characteristic of their structure, so a spectroscopic technique can be designed to monitor either the absorption of light or the emission of light from a sample, which thereby

yields information about what structure is present<sup>123</sup>. For example, organic chemists use infrared spectroscopy extensively to analyze samples of organics and to identify unknown structures. Historically, scientists had the tedious task of exciting a sample with individual frequencies one at a time to test for absorption, but the advent of computers made possible the use of Fourier Transform Infrared Spectroscopy (FTIR) so that an entire spectrum could be collected and analyzed at once<sup>122-124</sup>. Given that the only requirement of IR is to expose a sample to infrared light and then collect it, many different methods can be used including transmission through a sample, reflection off of a sample, or more complicated techniques like Diffuse Reflectance Infrared Spectroscopy (DRIFTS), Attenuated Total Reflection (ATR), or Polarization-Modulation Reflection Absorption Infrared Spectroscopy (PM-RAIRS) used here.

In this thesis, the most common form of IR employed was DRIFTS, a technique that is optimal for analyzing powders like supported metal catalysts. In this technique, incident light can be absorbed and diffusely reflected from the catalyst sample, collected, and focused for analysis<sup>125</sup>. This procedure can be used to analyze thiols deposited on the catalyst surface as well as coking products, carbon species left over after reactions. The basic DRIFTS spectrum is shown in Figure 1-13.

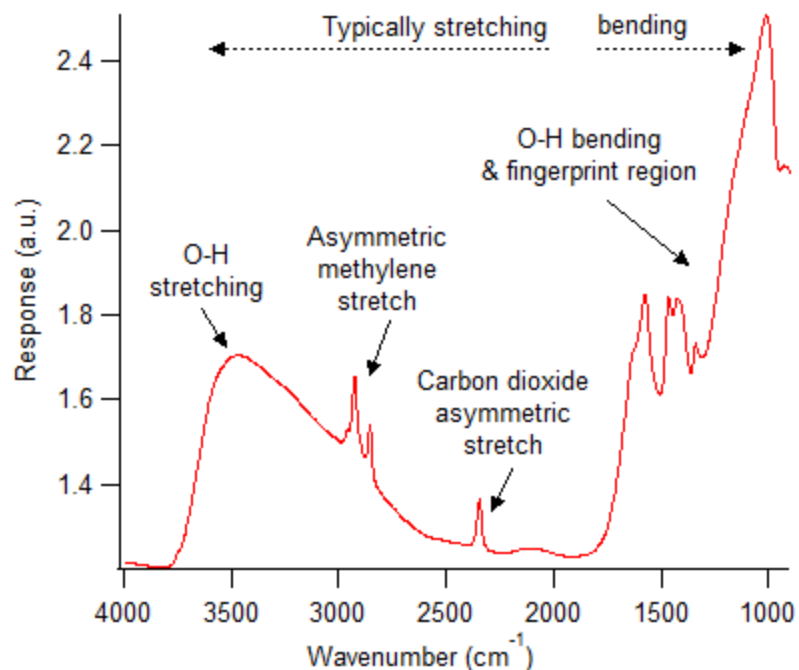


Figure 1-13: IR spectrum for DRIFTS of an octadecanethiol coated Pd/Al<sub>2</sub>O<sub>3</sub> catalyst

Looking at Figure 1-13, we can see that vibrational modes associated with stretching are typically found at higher wavenumbers whereas lower wavenumbers are associated more commonly with bending<sup>122-124</sup>. Other modes such as twisting and wagging can also be excited in this low wavenumber region. For the octadecanethiol coated catalyst shown, the most relevant peak to this thesis is the asymmetric methylene stretch ( $\nu_a$ ), which refers to asymmetric stretching of methylene (CH<sub>2</sub>) groups in the backbone of an alkanethiol tail. As will be discussed extensively in subsequent chapters, the position of the asymmetric methylene stretch is indicative of the order of a thiol monolayer where a lower wavenumber corresponds to a more ordered SAM<sup>22,25,43,68,93,94</sup>. For alkanethiols, this stretch can be found at a range of frequencies as low as 2918 cm<sup>-1</sup> corresponding to a fully crystalline structure to as high as 2936 cm<sup>-1</sup> for a very disordered liquid phase structure<sup>68</sup>.

A second type of IR used in this thesis is ATR, a technique optimal for looking at a flat surface<sup>126</sup>. ATR works by totally internally reflecting the incident beam of infrared light on the inside of a germanium crystal, opposite of which is the sample of interest. When total internal reflection occurs, an evanescently decreasing field occurs on the outside of the prism<sup>126</sup>. This wave can be used to excite bonds and measure their vibrations to a penetration depth of about 1  $\mu\text{m}$ . In this thesis, this technique was used to analyze pure mixtures of liquid reactants and thiols that can be placed on the germanium crystal.

The final important IR technique used in this thesis was PM-RAIRS, a technique used for its ability to analyze vibrational frequencies of molecules on a reflective surface. This technique was essential to identifying and supporting the orientation effects presented in Chapter 4. Pioneered in 1966 by Robert Greenler, PM-RAIRS polarizes incident light at a grazing angle to a reflective sample creating two forms of radiation, s-polarized light which is parallel to the surface and destructively interferes with itself, and p-polarized light which is perpendicular to the surface, is phase shifted and IR active at the surface<sup>127,128</sup>. The benefit of this technique is that away from the reflective surface, both types of polarized light are absorbed by randomly oriented molecules, whereas at the surface, only the p-polarized light is absorbed—the s-polarized light destructively interferes with itself and is canceled out<sup>128</sup>. Using some simple calculations, these two signals can be used to deduce what molecular vibrations are happening at the surface and subtract what is occurring in the bulk. This process is depicted in Figure 1-14.

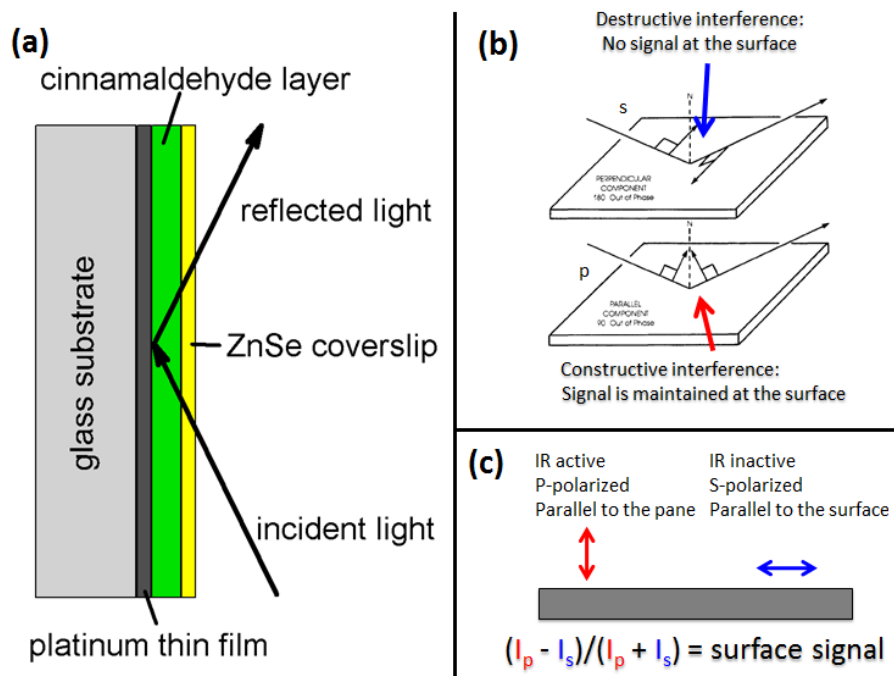


Figure 1-14: PM-RAIRS spectroscopy technique. (a) setup used to analyze liquid samples of cinnamaldehyde adsorption on a metal surface described in Chapter 4 (b) p-polarized and s-polarized light reflecting from a surface (c) how p-polarized and s-polarized light are used to deduce a response on the surface of a sample

As shown in Figure 1-14 (a), the key use of this technique will be discussed in Chapter 4 for analyzing the absorption of cinnamaldehyde on a Pt surface. Although only a thin layer of cinnamaldehyde is present on the surface of the metal, PM-RAIRS can identify cinnamaldehyde molecules specifically at the surface, the region of greatest interest.

Throughout this thesis, FTIR analysis was performed with a Thermo Scientific Nicolet 6700. A Harrick closed cell attachment was used for (DRIFTS) and a Thermo Scientific TOM optical box was used for PM-RAIRS measurements.

### 1.5 Thesis Goal

As the field of catalysis continues to develop, demand is increasingly focused on designing catalysts that not only help a reaction precede in a manageable time frame, but that also achieve high conversion with high selectivity. The overarching goal of this thesis is to explore the ways in which thiol SAMs can improve the selectivity of chemical pathways without compromising rate. These effects will be explored specifically through ligand non-specific and ligand specific interactions.

In the case of the ligand non-specific reaction environment, the effect of the sulfur head group and the steric effect of the tail of the thiol will be examined. The second step will be to explore the modes of ligand specific interaction between a functional group on the thiol and a corresponding group on the reactant.

## **1.6 Thesis Scope**

Here is a brief description of each of the remaining chapters of this thesis:

### **Chapter 2: Liquid- and Vapor-Phase Hydrogenation of 1-Epoxy-3-butene Using Self-Assembled Monolayer Coated Palladium and Platinum Catalysts**

Thiol self-assembled monolayers were previously shown to be effective catalyst modifiers for the gas phase selective hydrogenation of epoxybutene over Pd/Al<sub>2</sub>O<sub>3</sub> catalysts. Here, this work is extended to the liquid phase and to Pt/Al<sub>2</sub>O<sub>3</sub> catalysts where disordered thiols were shown to have reduced rate of reaction.

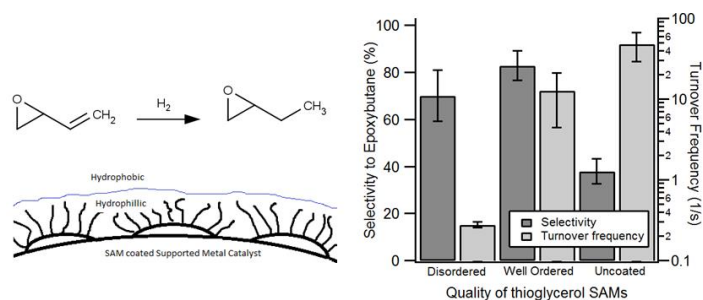


Figure 1-15: Liquid and vapor phase hydrogenation of epoxybutene—chapter 2

### Chapter 3: Selective Hydrogenation of Polyunsaturated Fatty Acids Using Alkanethiol Self-Assembled Monolayer Coated Pd/Al<sub>2</sub>O<sub>3</sub> Catalysts

Pd/Al<sub>2</sub>O<sub>3</sub> catalysts coated with various thiolate self-assembled monolayers (SAMs) were used to direct the partial hydrogenation of eighteen-carbon polyunsaturated fatty acids, yielding a product stream enriched in monounsaturated fatty acids (with low saturated fatty acid content), a favorable result for increasing the oxidative stability of biodiesel.

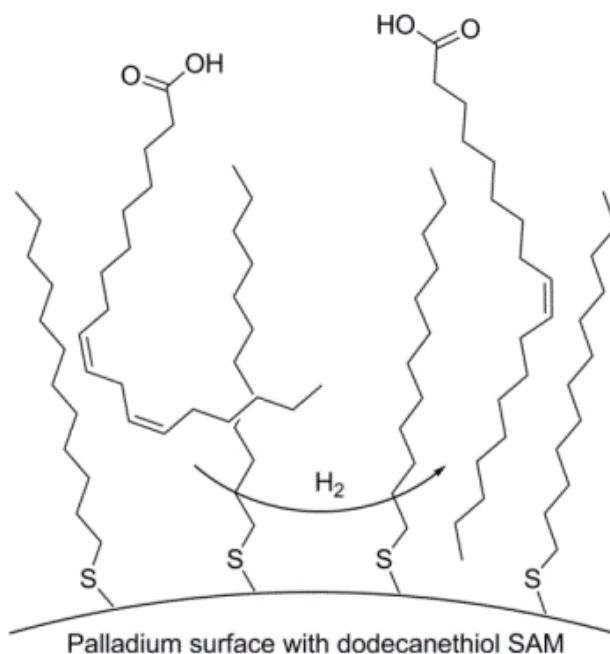


Figure 1-16: Selective Hydrogenation of Polyunsaturated Fatty Acids—chapter 3

## Chapter 4: Control of Metal Catalyst Selectivity through Specific Non-Covalent Molecular Interactions

Alkanethiol self-assembled monolayers with terminal phenyl rings were tuned to direct reactant orientation of cinnamaldehyde approaching a catalyst surface via non-covalent aromatic stacking interactions in order to control reaction selectivity to cinnamyl alcohol.

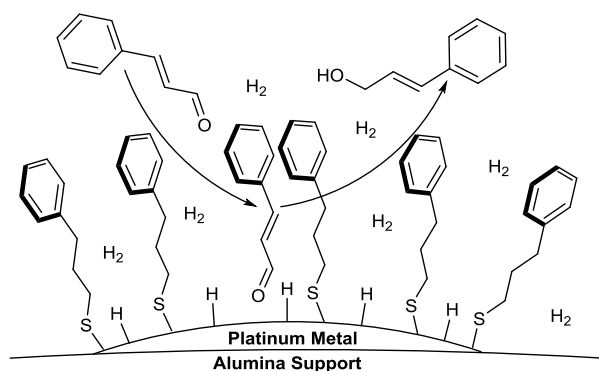


Figure 1-17: Specific Non-Covalent Molecular Interactions—chapter 4

## Chapter 5: Hydrogenation of cinnamaldehyde over Pd/Al<sub>2</sub>O<sub>3</sub> catalysts modified with thiol monolayers

Alkanethiol SAMs used for controlling  $\alpha,\beta$ -unsaturated aldehyde selectivity in Chapter 4 were applied to Pd/Al<sub>2</sub>O<sub>3</sub> catalysts. The coating improves selectivity to unsaturated alcohol but without specific control seen on Pt/Al<sub>2</sub>O<sub>3</sub>.

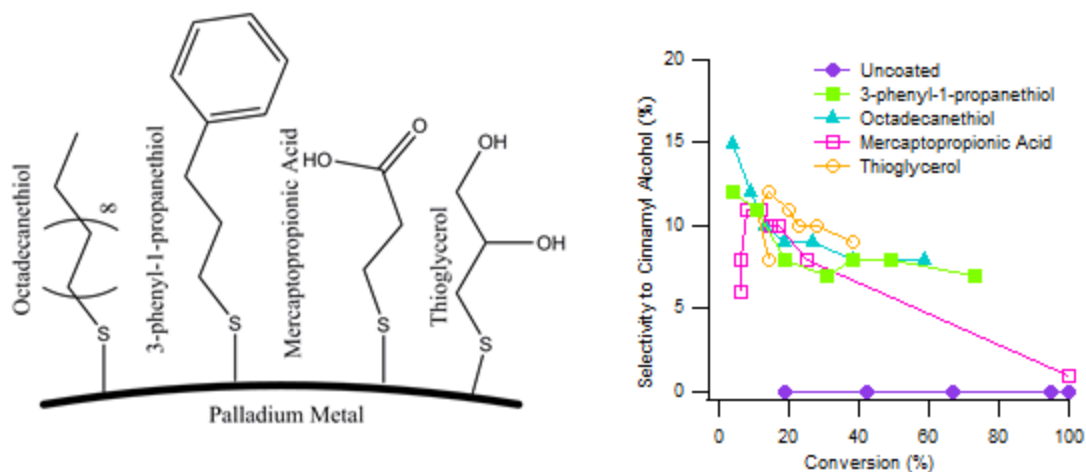


Figure 1-18: Selective hydrogenation of cinnamaldehyde over Pd —chapter 5

## Chapter 6: Stability of Self-Assembled Monolayer Coated Pt/Al<sub>2</sub>O<sub>3</sub> Catalysts for Liquid Phase Hydrogenation of Cinnamaldehyde

Ligand specific selectivity improvements from thiols are not very durable under liquid phase hydrogenation but can be stabilized by regeneration procedures between reactions. Coated metal catalysts also degrade in 2 days in air, affecting their catalytic properties.

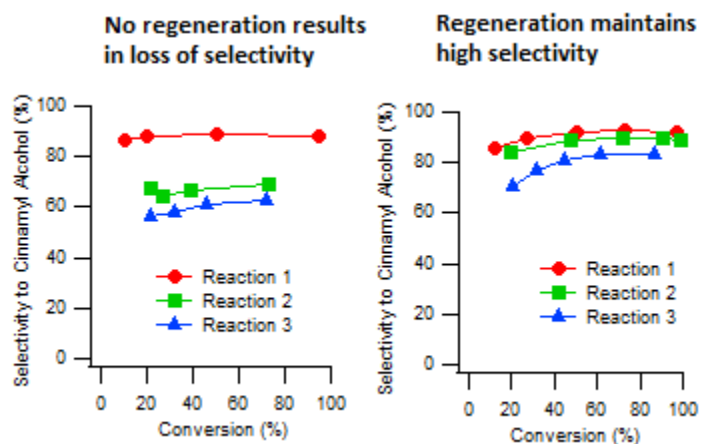


Figure 1-19: Stability of thiol coated catalysts for liquid phase hydrogenation —chapter 6

## 1.7 References

- (1) Hoffert, M. I.; Caldeira, K.; Benford, G.; Criswell, D. R.; Green, C.; Herzog, H.; Jain, A. K.; Kheshgi, H. S.; Lackner, K. S.; Lewis, J. S.; Lightfoot, H. D.; Manheimer, W.; Mankins, J. C.; Mauel, M. E.; Perkins, L. J.; Schlesinger, M. E.; Volk, T.; Wigley, T. M. L. *Science* **2002**, 298, 981.
- (2) Wachs, I. E. *Catalysis Today* **2005**, 100, 79.
- (3) Kaufmann, T.; Kaldor, A.; Stuntz, G.; Kerby, M.; Ansell, L. *Catalysis Today* **2000**, 62, 77.
- (4) MacMillan, D. W. *Nature* **2008**, 455, 304.
- (5) Behrens, M. *Angewandte Chemie International Edition* **2010**, 49, 2095.
- (6) Chen, B.; Dingerdissen, U.; Krauter, J. G. E.; Lansink Rotgerink, H. G. J.; Möbus, K.; Ostgard, D. J.; Panster, P.; Riermeier, T. H.; Seebald, S.; Tacke, T.; Trauthwein, H. *Applied Catalysis A: General* **2005**, 280, 17.
- (7) de Jong, K. P. *Synthesis of solid catalysts*; Wiley-VCH: Darmstadt, 2009.
- (8) Torborg, C.; Beller, M. *Adv. Synth. Catal.* **2009**, 351, 3027.
- (9) Veldsink, J. W.; Bouma, M. J.; Schoon, N. H.; Beenackers, A. *Catal. Rev.-Sci. Eng.* **1997**, 39, 253.
- (10) Zope, B. N.; Hibbitts, D. D.; Neurock, M.; Davis, R. J. *Science* **2010**, 330, 74.
- (11) Besson, M.; Gallezot, P. *Catalysis Today* **2000**, 57, 127.
- (12) Rylander, P. *Catalytic Hydrogenation over Platinum Metals*; Elsevier Science, 2012.
- (13) Barbier, J.; Churin, E.; Marecot, P.; Menezo, J. C. *Applied Catalysis* **1988**, 36, 277.

- (14) Shirai, M.; Tanaka, T.; Arai, M. *Journal of Molecular Catalysis A: Chemical* **2001**, *168*, 99.
- (15) Singh, U. K.; Vannice, M. A. *Applied Catalysis A: General* **2001**, *213*, 1.
- (16) Ruban, A. V.; Skriver, H. L. *Computational Materials Science* **1999**, *15*, 119.
- (17) Xin, H.; Holewinski, A.; Lincic, S. *ACS Catalysis* **2011**, *2*, 12.
- (18) Gallezot, P.; Richard, D. *Catalysis Reviews* **1998**, *40*, 81.
- (19) Haubrich, J.; Loffreda, D.; Delbecq, F.; Sautet, P.; Jugnet, Y.; Krupski, A.; Becker, C.; Wandelt, K. *The Journal of Physical Chemistry C* **2008**, *112*, 3701.
- (20) Ponec, V. *Applied Catalysis A: General* **1997**, *149*, 27.
- (21) Pham-Huu, C.; Keller, N.; Ehret, G.; Charbonniere, L. c. J.; Ziessel, R.; Ledoux, M. J. *Journal of Molecular Catalysis A: Chemical* **2001**, *170*, 155.
- (22) Marshall, S. T.; O'Brien, M.; Oetter, B.; Corpuz, A.; Richards, R. M.; Schwartz, D. K.; Medlin, J. W. *Nat. Mater.* **2010**, *9*, 853.
- (23) Kwon, S. G.; Krylova, G.; Sumer, A.; Schwartz, M. M.; Bunel, E. E.; Marshall, C. L.; Chattopadhyay, S.; Lee, B.; Jellinek, J.; Shevchenko, E. V. *Nano Lett.* **2012**, *12*, 5382.
- (24) Wu, B.; Huang, H.; Yang, J.; Zheng, N.; Fu, G. *Angewandte Chemie International Edition* **2012**, *51*, 3440.
- (25) Kahsar, K. R.; Schwartz, D. K.; Medlin, J. W. *Applied Catalysis A: General* **2012**, *445–446*, 102.
- (26) Taguchi, T.; Isozaki, K.; Miki, K. *Adv. Mater.* **2012**, *24*, 6462.
- (27) Schoenbaum, C. A.; Schwartz, D. K.; Medlin, J. W. *Journal of Catalysis* **2013**, *303*, 92.
- (28) Robertson, A. *Platinum Metals Rev* **1975**, *19*, 64.

- (29) Yergin, D. *The prize: The epic quest for oil, money & power*; Simon and Schuster, 2011.
- (30) Armor, J. N. *Catalysis Today* **2011**, 163, 3.
- (31) Davis, M. E.; Davis, R. J. *Fundamentals of chemical reaction engineering*; Courier Dover Publications, 2012.
- (32) Trewavas, A. *Nature* **2002**, 418, 668.
- (33) Smil, V. *Enriching the earth: Fritz Haber, Carl Bosch, and the transformation of world food production*; MIT press, 2004.
- (34) Kieboom, A.; Moulijn, J.; Leeuwen, v. P.; Santen, v. R. *Catalysis: an integrated approach/Ed. RA van Santen, PWNM van Leeuwen, JA Moulijn* **1999**, 123, 3.
- (35) Rothenberg, G. *Catalysis: Concepts and Green Applications* **2008**, 39.
- (36) Masel, R. I. *Chemical kinetics and catalysis*; Wiley-Interscience New York, 2001.
- (37) Holmes, F. L. *Lavoisier and the chemistry of life: an exploration of scientific creativity*; Univ of Wisconsin Press, 1987.
- (38) Widegren, J. A.; Finke, R. G. *Journal of Molecular Catalysis A: Chemical* **2003**, 198, 317.
- (39) Zapf, A.; Beller, M. *Topics in Catalysis* **2002**, 19, 101.
- (40) Patel, A. U. *Environmentally Benign Catalysts: For Clean Organic Reactions*; Springer London, Limited, 2013.
- (41) Kahsar, K. R.; Schwartz, D. K.; Medlin, J. W. *Journal of the American Chemical Society* **2013**, 136, 520.
- (42) Sharma, Y. C.; Singh, B.; Korstad, J. *Fuel* **2011**, 90, 1309.
- (43) Kahsar, K. R.; Schwartz, D. K.; Medlin, J. W. *ACS Catalysis* **2013**, 3, 2041.

- (44) Hughes, M. D.; Xu, Y.-J.; Jenkins, P.; McMorn, P.; Landon, P.; Enache, D. I.; Carley, A. F.; Attard, G. A.; Hutchings, G. J.; King, F. *Nature* **2005**, *437*, 1132.
- (45) Dick, A. R.; Hull, K. L.; Sanford, M. S. *Journal of the American Chemical Society* **2004**, *126*, 2300.
- (46) Hackett, S. F.; Brydson, R. M.; Gass, M. H.; Harvey, I.; Newman, A. D.; Wilson, K.; Lee, A. F. *Angewandte Chemie* **2007**, *119*, 8747.
- (47) Seader, J. D.; Henley, E. J.; Roper, D. K. *Separation Process Principles, 3rd Edition*; John Wiley & Sons, 2010.
- (48) Wankat, P. C. *Separation Process Engineering*; Pearson Education, 2006.
- (49) Abatzoglou, N.; Boivin, S. *Biofuels, Bioproducts and Biorefining* **2009**, *3*, 42.
- (50) Seddon, D. *Petrochemical Economics: Technology Selection in a Carbon Constrained World*; Imperial College Press, 2010.
- (51) Felder, R. M.; Rousseau, R. W. *Elementary Principles of Chemical Processes, Student Workbook*; Wiley, 2005.
- (52) Houston, P. L. *Chemical Kinetics and Reaction Dynamics*; Dover Publications, 2012.
- (53) Spivey, J. J.; Dooley, K. M. *Catalysis*; Royal Society of Chemistry, 2011.
- (54) Marshall, S. T.; Horiuchi, C. M.; Zhang, W. Y.; Medlin, J. W. *Journal of Physical Chemistry C* **2008**, *112*, 20406.
- (55) Marshall, S. T.; Schwartz, D. K.; Medlin, J. W. *Langmuir* **2011**, *27*, 6731.
- (56) Nishimura, S. *Handbook of heterogeneous catalytic hydrogenation for organic synthesis*; J. Wiley, 2001.
- (57) Cervený, L. *Catalytic Hydrogenation*; Elsevier Science, 1986.

- (58) Parker, J. F.; Kacprzak, K. A.; Lopez-Acevedo, O.; Häkkinen, H.; Murray, R. W. *The Journal of Physical Chemistry C* **2010**, *114*, 8276.
- (59) Deutschmann, O.; Knözinger, H.; Kochloefl, K.; Turek, T. In *Ullmann's Encyclopedia of Industrial Chemistry*; Wiley-VCH Verlag GmbH & Co. KGaA: 2000.
- (60) da Silva, A. B.; Jordão, E.; Mendes, M. J.; Fouilloux, P. *Applied Catalysis A: General* **1997**, *148*, 253.
- (61) Pradier, C. M.; Birchem, T.; Berthier, Y.; Cordier, G. *Catal Lett* **1994**, *29*, 371.
- (62) Toukoniitty, E.; Maki-Arvela, P.; Kuzma, M.; Vilella, A.; Neyestanaki, A. K.; Salmi, T.; Sjöholm, R.; Leino, R.; Laine, E.; Murzin, D. Y. *Journal of Catalysis* **2001**, *204*, 281.
- (63) Vannice, M. A.; Sen, B. *Journal of Catalysis* **1989**, *115*, 65.
- (64) Yee, C.; Scotti, M.; Ulman, A.; White, H.; Rafailovich, M.; Sokolov, J. *Langmuir* **1999**, *15*, 4314.
- (65) Bigelow, W.; Pickett, D.; Zisman, W. *Journal of Colloid Science* **1946**, *1*, 513.
- (66) Allara, D. L.; Nuzzo, R. G. *Langmuir* **1985**, *1*, 45.
- (67) Nuzzo, R. G.; Allara, D. L. *Journal of the American Chemical Society* **1983**, *105*, 4481.
- (68) Ulman, A. *Chem. Rev.* **1996**, *96*, 1533.
- (69) Schwartz, D. K. *Annual Review of Physical Chemistry* **2001**, *52*, 107.
- (70) Pang, S. H.; Schoenbaum, C. A.; Schwartz, D. K.; Medlin, J. W. *Nature communications* **2013**, *4*.
- (71) Hammond, C.; Hammond, C. *Basics of crystallography and diffraction*; Oxford, 2001; Vol. 214.
- (72) Spek, A. L. *Acta Crystallographica Section D: Biological Crystallography* **2009**, *65*, 148.

- (73) Ziman, J. M. *Principles of the Theory of Solids*; Cambridge University Press, 1972.
- (74) Donnay, J.; Harker, D. *Am. Mineral* **1937**, 22, 446.
- (75) Gibbs, J. W. *The collected works of J. Willard Gibbs*; Yale University Press, 1948; Vol. 1.
- (76) GiBBS, J. W.; Longmans, New York: 1931.
- (77) Wulff, G. *Z. kristallogr* **1901**, 34, 449.
- (78) Dobrushin, R. L.; Kotecký, R.; Shlosman, S. *Wulff Construction: A Global Shape from Local Interaction*; American Mathematical Society, 1992.
- (79) Dill, K. A.; Bromberg, S. *Molecular Driving Forces: Statistical Thermodynamics in Chemistry and Biology*; Garland Science, 2003.
- (80) Oura, K.; Zotov, A.; Lifshits, V.; Saranin, A.; Katayama, M. *Surface science*; Springer, 2003.
- (81) Dziomkina, N. V.; Vancso, G. J. *Soft Matter* **2005**, 1, 265.
- (82) Zhang, G.; Wang, D.; Gu, Z.-Z.; Möhwald, H. *Langmuir* **2005**, 21, 9143.
- (83) Kodama, C.; Hayashi, T.; Nozoye, H. *Applied Surface Science* **2001**, 169–170, 264.
- (84) Vericat, C.; Vela, M. E.; Salvarezza, R. C. *Physical Chemistry Chemical Physics* **2005**, 7, 3258.
- (85) de Jesús, J. C.; Zaera, F. *Surface science* **1999**, 430, 99.
- (86) Haubrich, J.; Loffreda, D.; Delbecq, F.; Sautet, P.; Jugnet, Y.; Becker, C.; Wandelt, K. *The Journal of Physical Chemistry C* **2009**, 114, 1073.
- (87) Bratlie, K. M.; Lee, H.; Komvopoulos, K.; Yang, P.; Somorjai, G. A. *Nano Lett.* **2007**, 7, 3097.

- (88) Pradier, C.-M.; Margot, E.; Berthier, Y.; Oudar, J. *Applied Catalysis* **1988**, *43*, 177.
- (89) Shekhar, R.; Barteau, M. A. *Surface science* **1994**, *319*, 298.
- (90) Addato, M. A. F.; Rubert, A. A.; Benitez, G. A.; Fonticelli, M. H.; Carrasco, J.; Carro, P.; Salvarezza, R. C. *Journal of Physical Chemistry C* **2011**, *115*, 17788.
- (91) Kim, Y. T.; McCarley, R. L.; Bard, A. J. *Langmuir* **1993**, *9*, 1941.
- (92) Love, J. C.; Estroff, L. A.; Kriebel, J. K.; Nuzzo, R. G.; Whitesides, G. M. *Chem. Rev.* **2005**, *105*, 1103.
- (93) Love, J. C.; Wolfe, D. B.; Haasch, R.; Chabynyc, M. L.; Paul, K. E.; Whitesides, G. M.; Nuzzo, R. G. *Journal of the American Chemical Society* **2003**, *125*, 2597.
- (94) Petrovykh, D. Y.; Kimura-Suda, H.; Opdahl, A.; Richter, L. J.; Tarlov, M. J.; Whitman, L. J. *Langmuir* **2006**, *22*, 2578.
- (95) Vericat, C.; Vela, M.; Benitez, G.; Carro, P.; Salvarezza, R. *Chemical Society Reviews* **2010**, *39*, 1805.
- (96) Dameron, A. A.; Charles, L. F.; Weiss, P. S. *Journal of the American Chemical Society* **2005**, *127*, 8697.
- (97) Ulman, A.; Eilers, J. E.; Tillman, N. *Langmuir* **1989**, *5*, 1147.
- (98) Scherer, J.; Vogt, M.; Magnussen, O.; Behm, R. *Langmuir* **1997**, *13*, 7045.
- (99) Sheen, C. W.; Shi, J. X.; Maartensson, J.; Parikh, A. N.; Allara, D. L. *Journal of the American Chemical Society* **1992**, *114*, 1514.
- (100) Loglio, F.; Schweizer, M.; Kolb, D. *Langmuir* **2003**, *19*, 830.
- (101) Kim, M.; Hohman, J. N.; Cao, Y.; Houk, K. N.; Ma, H.; Jen, A. K.-Y.; Weiss, P. S. *Science* **2011**, *331*, 1312.

- (102) Snelders, D. J. M.; Yan, N.; Gan, W.; Laurencyzy, G.; Dyson, P. J. *ACS Catalysis* **2011**, *2*, 201.
- (103) Makosch, M.; Lin, W.-I.; Bumbálek, V.; Sá, J.; Medlin, J. W.; Hungerbühler, K.; van Bokhoven, J. A. *ACS Catalysis* **2012**, *2*, 2079.
- (104) Kliewer, C. J.; Bieri, M.; Somorjai, G. A. *Journal of the American Chemical Society* **2009**, *131*, 9958.
- (105) Zaera, F. *Langmuir* **1996**, *12*, 88.
- (106) Bond, G.; Webb, G.; Wells, P.; Winterbottom, J. *Journal of Catalysis* **1962**, *1*, 74.
- (107) Zaera, F.; Somorjai, G. *Journal of the American Chemical Society* **1984**, *106*, 2288.
- (108) Zaera, F. *Physical Chemistry Chemical Physics* **2013**, *15*, 11988.
- (109) Tilekaratne, A.; Simonovis, J. P.; López Fagúndez, M. F.; Ebrahimi, M.; Zaera, F. *ACS Catalysis* **2012**, *2*, 2259.
- (110) Gardner, N. C.; Hansen, R. S. *The Journal of Physical Chemistry* **1970**, *74*, 3298.
- (111) Thomson, S. J.; Webb, G. *Journal of the Chemical Society, Chemical Communications* **1976**, 526.
- (112) Aleksandrov, H. A.; Moskaleva, L. V.; Zhao, Z.-J.; Basaran, D.; Chen, Z.-X.; Mei, D.; Rösch, N. *Journal of Catalysis* **2012**, *285*, 187.
- (113) Coq, B.; Kumbhar, P. S.; Moreau, C.; Moreau, P.; Warawdekar, M. G. *Journal of Molecular Catalysis* **1993**, *85*, 215.
- (114) Alcalá, R.; Greeley, J.; Mavrikakis, M.; Dumesic, J. A. *The Journal of chemical physics* **2002**, *116*, 8973.
- (115) Van Druten, G.; Ponec, V. *Applied Catalysis A: General* **2000**, *191*, 153.

- (116) Van Druten, G.; Ponec, V. *Applied Catalysis A: General* **2000**, *191*, 163.
- (117) Mäki-Arvela, P.; Hajek, J.; Salmi, T.; Murzin, D. Y. *Applied Catalysis A: General* **2005**, *292*, 1.
- (118) Jenck, J.; Germain, J.-E. *Journal of Catalysis* **1980**, *65*, 141.
- (119) Kung, H. H. *Transition metal oxides: surface chemistry and catalysis*; Elsevier, 1989.
- (120) Conder, J. R.; Young, C. L. *Physicochemical measurement by gas chromatography*; Wiley New York, 1979; Vol. 632.
- (121) Briand, L. E.; Jehng, J.-M.; Cornaglia, L.; Hirt, A. M.; Wachs, I. E. *Catalysis Today* **2003**, *78*, 257.
- (122) Hair, M. L. *Infrared spectroscopy in surface chemistry*; M. Dekker New York, 1967.
- (123) Stuart, B. *Infrared spectroscopy*; Wiley Online Library, 2004.
- (124) Rao, C. N. R. **1963**.
- (125) Fuller, M. P.; Griffiths, P. R. *Analytical Chemistry* **1978**, *50*, 1906.
- (126) Fahrenfort, J. *Spectrochimica Acta* **1961**, *17*, 698.
- (127) Greenler, R. G. *The Journal of chemical physics* **1966**, *44*, 310.
- (128) Golden, W. G.; Saperstein, D. D.; Severson, M. W.; Overend, J. *The Journal of Physical Chemistry* **1984**, *88*, 574.

## CHAPTER 2

### Liquid- and Vapor-Phase Hydrogenation of 1-Epoxy-3-butene Using Self-Assembled

### Monolayer Coated Palladium and Platinum Catalysts

#### 2.1 Abstract

Alkanethiol self-assembled monolayers (SAMs) have previously been shown to be effective catalyst modifiers for increasing the selectivity of the hydrogenation of 1-epoxy-3-butene (EpB) to 1-epoxybutane in the gas phase over a Pd/Al<sub>2</sub>O<sub>3</sub> catalyst. Here, we demonstrate that SAM coatings can similarly be applied to other supported metals (Pt) and in liquid-phase reaction environments. Coating a Pt/Al<sub>2</sub>O<sub>3</sub> catalyst with n-octadecanethiol resulted in a large improvement in selectivity during vapor-phase EpB hydrogenation, similar to that observed for supported Pd. The liquid phase hydrogenation of EpB using SAM-coated catalysts showed similar selectivity trends in some cases, but interactions of the solvent with the SAM were also important in controlling selectivity. In particular, using a heptane solvent, epoxybutane selectivity increased from 36% with an uncoated Pd/Al<sub>2</sub>O<sub>3</sub> catalyst to 74% with a thioglycerol SAM-coated catalyst. SAM quality was shown to have a strong impact on the rate of reaction but little effect on selectivity. The results generally indicated that selectivity modification with thiol SAMs is extendable to other supported metals and a variety of reaction environments.

#### 2.2 Background

Methods for controlling the chemoselectivity of reactions are desirable for industrial catalysts because they reduce separations costs and increase productivity<sup>1,2</sup>. Recently, it was shown that the coating of a Pd/Al<sub>2</sub>O<sub>3</sub> catalyst with alkanethiol self-assembled monolayers (SAMs) increased the selectivity for vapor-phase hydrogenation of 1-epoxy-3-butene (EpB) to 1-

epoxybutane from <20% on an uncoated catalyst to >90% on a SAM-coated catalyst under equivalent conditions<sup>3</sup>. For this reaction, the deposition of SAMs to the Pd/Al<sub>2</sub>O<sub>3</sub> surface increases the kinetic barrier to epoxide ring opening while the binding of the olefin functionality is not significantly changed<sup>4</sup>. A similar thiol SAM coating technique was also shown to increase the selectivity for the isomerization of allyl alcohols to the corresponding carbonyl compounds using a Pd nanoparticle catalyst<sup>5</sup>. SAM films produced from amines have been applied to catalysts for the selective hydrogenation of  $\alpha,\beta$ -unsaturated aldehydes such as cinnamaldehyde and citral<sup>6</sup>. More generally, chiral catalyst modifiers such as cinchonidine have been used over platinum catalysts to steer enantioselectivity for the selective hydrogenation of ethyl pyruvate<sup>7</sup>.

In previous work, the improved selectivity of EpB hydrogenation was largely attributed to the sulfur head group of the alkanethiol, which covalently binds to the Pd catalyst surface and exerts an electronic effect on the metal catalyst<sup>3,4</sup>. This effect is related in part to the strong electronegativity of sulfur, but as depicted in Scheme 1, all thiols are covalently bound at the palladium-sulfide interface<sup>8</sup>. The thiols were found in surface science experiments to strongly suppress epoxide C-O scission while still permitting adsorption of the olefin function in a reactive pi-bound state<sup>4</sup>.

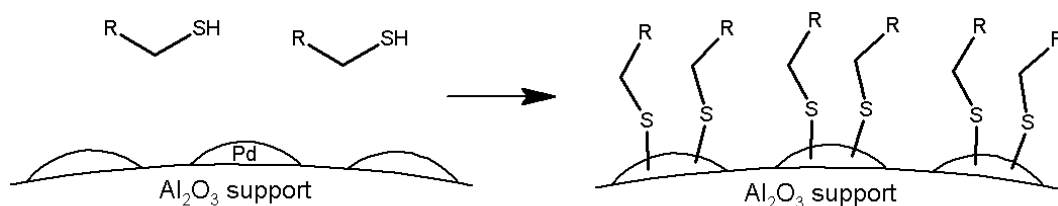


Figure 2-1: Covalent binding process of alkanethiols to the Pd/Al<sub>2</sub>O<sub>3</sub> catalyst surface.

Various “tail group” ligands were found to have little effect on selectivity; however, they played an important role in controlling activity, with longer alkyl tails being associated with higher rates. It is known that SAMs comprised of precursors with longer tail functions generally

result in more ordered (e.g. “crystalline”) films as indicated by infrared spectroscopy measurements<sup>3,8-10</sup>.

Compared to gas phase reactions, EpB hydrogenation in the liquid phase presents new possibilities for tail group effects on selectivity. For example, in some previous work, the solvent has been shown to play a significant role in catalytic hydrogenation reactions by affecting hydrogen solubility, thermodynamic interactions of the solvent and reactant, and the adsorbed structures of reagents, thus affecting the reaction pathways<sup>11-13</sup>. The hydrophobicity of the solvent, as measured by the dielectric constant, has also been shown to affect the enantioselectivity of 1-phenyl-1,2-propanedione hydrogenation<sup>14</sup>. However, not all hydrogenation reactions exhibit solvent effects. The hydrogenation of  $\alpha,\beta$ -unsaturated aldehydes has been extensively studied in the liquid phase, where solvent composition was shown to have an insignificant effect on the rate and the selectivity of the reaction<sup>15-17</sup>.

SAMs may significantly alter solvent-adsorbate surface interactions based on the fact that the presence of tail groups is expected to modify the nature of the near-surface environment. In fact, by selecting appropriate tail functionalities it may be possible to control the degree of solvent exposure near the active catalytic sites. For example, hydrophilic SAMs may be useful in excluding hydrophobic solvents to promote selectivity. This chapter will extend the analysis of EpB hydrogenation over alkanethiol coated catalysts to include Pt/Al<sub>2</sub>O<sub>3</sub> and reactions conducted in the liquid phase.

## 2.3 Methods

2.3.1 Catalyst preparation: The 5wt% Pd/Al<sub>2</sub>O<sub>3</sub> or Pt/Al<sub>2</sub>O<sub>3</sub> catalyst (Sigma Aldrich) was loaded into a glass reactor tube. A mass of 500 mg of catalyst was oxidized under flow conditions of 100 sccm of 20:80 O<sub>2</sub>:He at 573 K for 3 hr, followed by reduction under 100 sccm of 20:80 H<sub>2</sub>:He at 473 K for 2 hr. As discussed in the introduction section, this oxidization and reduction procedure was conducted to maintain consistency with catalysis literature. It was later determined that this reduction procedure did not affect the efficacy of the SAM coating. After the reduction step, the catalyst was cooled and added to a stirred beaker containing 40 mL of ethanolic solution concentrated to 1 mM for octadecanethiol and 10 mM for other thiol SAM precursors. All thiols were obtained from Sigma Aldrich and were >97% purity. Thiols were solvated in 200 proof anhydrous ethanol obtained from Sigma Aldrich. The catalyst was incubated in the solution for 12-36 hr and allowed to settle out of the solution, which was subsequently poured off. The catalyst was rinsed once in ethanol, again allowing the catalyst to settle out of solution (3-4 hr) before pouring off the supernatant ethanol. The remaining catalyst slurry was dried in a desiccator under vacuum. All catalysts were stored under desiccant and used within two days of preparation.

Poor quality SAMs were obtained by allowing the alkanethiol-coated catalysts to sit for longer than two weeks prior to use. During this time, oxidation of the Pd-S bonds is known to result in weakly bound sulfur species that are readily removed<sup>18</sup>. This process deteriorated the quality of the SAM by creating defects in the alkanethiol monolayer<sup>9,19</sup>. This process results in a relatively disordered monolayer described here and by others as a poor or disordered SAM<sup>9,18,20</sup>.

2.3.2 Catalyst characterization: As discussed in the introduction chapter, CO chemisorption was performed on a Quantachrome Autosorb-1 to determine the active surface

area of the Pd/Al<sub>2</sub>O<sub>3</sub> catalysts. Recall that the uncoated commercial 5wt% Pd/Al<sub>2</sub>O<sub>3</sub> was determined to have an active surface area of 3.7 m<sup>2</sup>/g. Specific to this study, the surface area measured by CO chemisorption decreased 94% to 0.22 m<sup>2</sup>/g for a thioglycerol modified catalyst, similar to the decrease previously reported by Marshall et al.<sup>3</sup>. Measured for this study, the uncoated commercial 5wt% Pt/Al<sub>2</sub>O<sub>3</sub> was determined to have an active surface area of 2.9 m<sup>2</sup>/g. Catalysts were also characterized using a Thermo Scientific Nicolet 6700 FT-IR with an attachment for Diffuse Reflectance Infrared Fourier Transform Spectroscopy (DRIFTS) of the dry powder catalyst. The C-H stretching region of 2800-3000 cm<sup>-1</sup> was used to characterize the degree of order of the aliphatic chains as well as thioglycerol adsorption to the catalyst surface.

Unlike *n*-alkanethiols, thioglycerol has not been extensively characterized on metal surfaces. As shown in Figure 2-2, thioglycerol was analyzed by ATR and then compared to a thioglycerol coated Pd/Al<sub>2</sub>O<sub>3</sub> sample by DRIFTS.

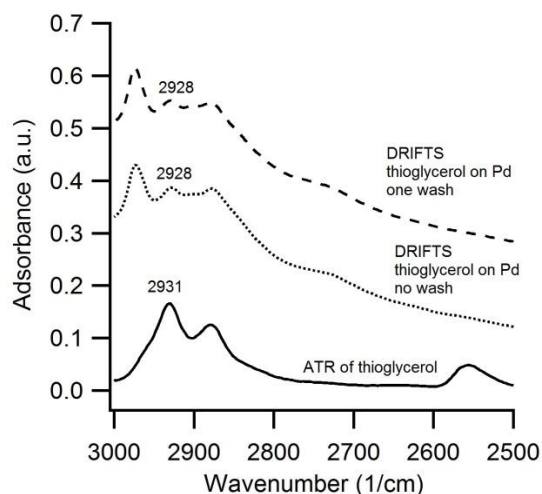


Figure 2-2: ATR-FTIR of pure thioglycerol and DRIFTS of thioglycerol deposited on Pd/Al<sub>2</sub>O<sub>3</sub> for the 2500-3000 cm<sup>-1</sup> range

The methylene stretching mode was observed to shift from  $2931\text{ cm}^{-1}$  to  $2928\text{ cm}^{-1}$  upon adsorption. One wash of ethanol to remove physisorbed thiols was found to have no effect on the positions or the intensities of the DRIFTS spectra. ATR of pure thioglycerol exhibited an SH stretch at  $2550\text{ cm}^{-1}$  which disappeared upon deposition of the thiol indicating that thioglycerol was bound to the surface.

2.3.3 Reaction system: Liquid phase hydrogenation was carried out at  $30\text{ }^{\circ}\text{C}$  using the 100 mL Parr batch reactor discussed in the introduction section. Liquid components of the system were prepared with 48mL of solvent, 5 mL of THF internal standard, and 1mL of reactant. Prepared catalyst, 1 mg to 200 mg, was added to the reactor which was sealed and preheated to the desired reaction temperature. The sampling procedure is discussed in the introduction section. For the experiments presented in this chapter, samples were taken at increasing intervals from zero to 90 min to allow the system to reach 100% conversion. Catalyst recycling was performed by filtering the final reaction mixture and allowing the remaining catalyst to dry in air before being reused.

Gas phase hydrogenation was performed in a flow reactor. EpB was vaporized in the feed stream by bubbling it with 10 sccm helium at  $25\text{ }^{\circ}\text{C}$ . The feed stream was supplemented with hydrogen at a ratio of 10:1 hydrogen to EpB. The reaction was carried out at  $40\text{ }^{\circ}\text{C}$ . Selectivity was measured at 5% conversion as was done previously<sup>3,21</sup>.

Both liquid and gas phase reaction samples were analyzed with an Agilent 5890A gas chromatograph and quantified with a flame ionization detector and Agilent software. The column used in this chapter was the Agilent DB-FFAP capillary column with dimensions of 30 m x 0.32 mm x 0.50  $\mu\text{m}$ .

Epoxybutene (EpB, >98%) was purchased from Alfa Aesar. Heptane (anhydrous >99%) and ethanol (>99.5%) solvents as well as THF were obtained from Sigma Aldrich. All gases used for catalyst preparation and reaction were Airgas ultra-high purity.

## 2.4 Results

2.4.1 Vapor-phase hydrogenation using supported Pd and Pt catalysts: Under hydrogenation conditions, EpB has been shown to undergo both hydrogenation and isomerization through the pathway shown in Figure 2-3. Epoxide ring opening is thermodynamically favorable over hydrogenation of the olefin<sup>22</sup>.

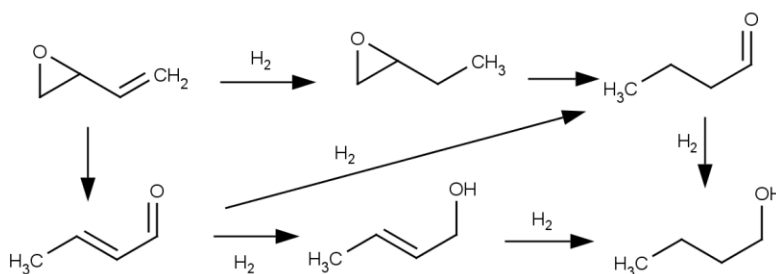


Figure 2-3: Reaction pathway for EpB hydrogenation

Table 2-1 shows the measured rates and epoxybutene selectivity for EpB hydrogenation in the vapor phase using uncoated and SAM-coated Pt and Pd catalysts. Consistent with previous reports, the selectivity on uncoated Pt catalysts (40%) was noticeably higher than on uncoated Pd catalysts (20%) under equivalent conditions<sup>23</sup>. The measured reaction rate was much lower on Pt, however. The addition of an alkanethiol SAM was found to reduce catalyst activity while markedly increasing selectivity on both the Pd and Pt catalysts<sup>3</sup>. Interestingly, the

selectivity improvement on Pt catalysts was somewhat less than on Pd, though the rate of reaction was reduced to a lesser extent on Pt by the SAM. The reasons for these relatively subtle differences are not yet clear. Overall, however, it appears that the qualitative effects of SAM coating are quite similar on Pd and Pt catalysts, suggesting that SAMs can be used as selectivity modifiers across a range of metals.

Table 2-1: Reaction of EpB over Pd and Pt catalysts in the gas phase under identical conditions at 5% conversion. Selectivity to epoxybutane and rate measured as EpB consumed.

	Selectivity (%)		Turnover frequency (1/s)	
	Pd	Pt	Pd	Pt
Uncoated	21	40	9.17	0.17
Octadecanethiol Coated	91	81	0.31	0.037

2.4.2 Liquid-phase hydrogenation of EpB: Liquid phase hydrogenation of EpB was carried out the batch reactor system and a typical experiment was run to nearly full conversion over 90 min with kinetic data similar to that shown in Figure 2-4. The epoxybutane selectivity was observed to depend weakly on conversion regardless of the solvent or SAM used, indicating that epoxybutane is a non-reactive product in the liquid-phase. This was confirmed in separate experiments (not shown) where epoxybutane was fed as a reactant under identical conditions to those used in Figure 2-4, with no detectable conversion. This contrasts with the gas-phase reaction studies where selectivity decreased with increasing conversion<sup>3</sup>. Side products included crotonaldehyde, butyraldehyde, crotyl alcohol, and butanol and are shown in Figure 2-4.

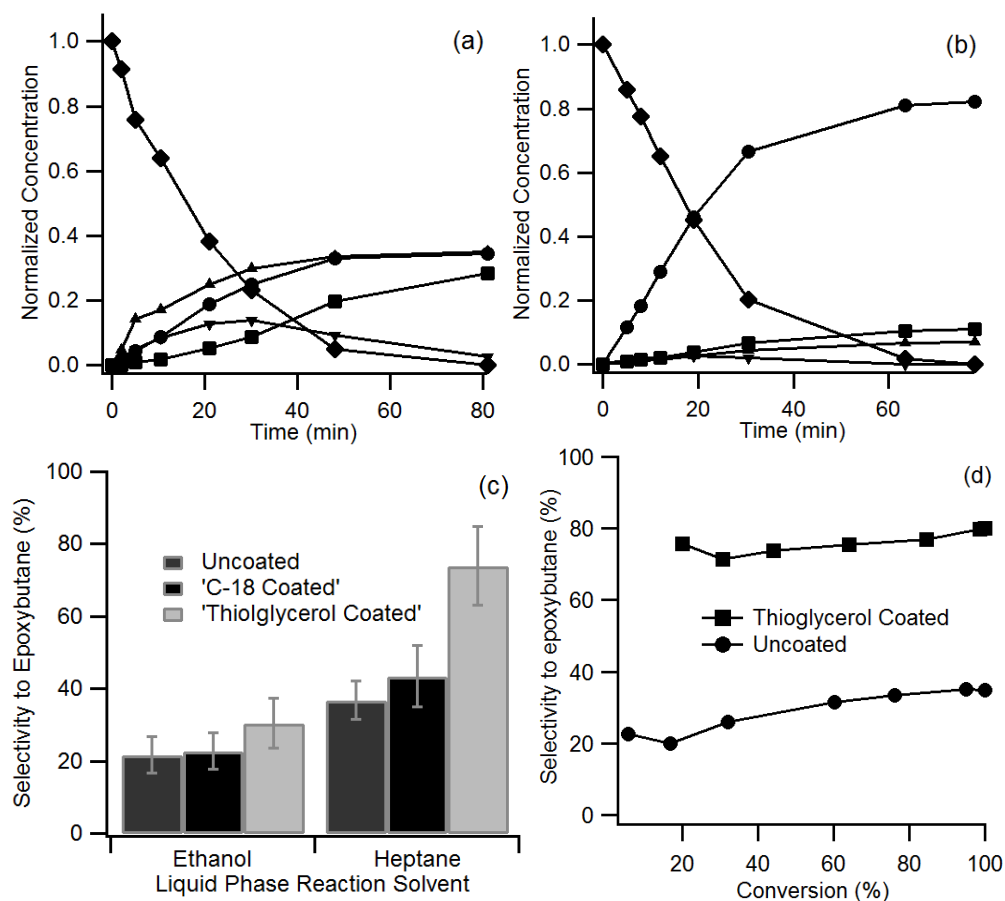


Figure 2-4: Selective hydrogenation of EpB to epoxybutane in the liquid phase. (◆) EpB, (●) epoxybutane, (■) butyraldehyde, (▼) crotonaldehyde, (▲) C4 alcohols. Total molar concentrations are normalized to one. (a) hydrogenation in heptane solvent using 3.8 mg of uncoated Pd/Al<sub>2</sub>O<sub>3</sub> catalyst (b) hydrogenation in heptane solvent over 12.4 mg of thioglycerol coated Pd/Al<sub>2</sub>O<sub>3</sub> catalyst (c) selectivity measured at 10% conversion of different reaction systems (d) selectivity to epoxybutane versus conversion of EpB for the uncoated and thioglycerol coated cases shown in (a) and (b)

Epoxybutane selectivity was found to be dependent on the solvent for both uncoated and SAM-coated catalysts. Using an uncoated Pd/Al<sub>2</sub>O<sub>3</sub> catalyst, the selectivity to epoxybutane was

36% in heptane but only 21% in ethanol. Thus interactions between the surface and solvent appeared to result in a significant change in selectivity while the rate was relatively unaffected. For ethanol solvated reactions, the deposition of thioglycerol monolayers on the catalyst surface resulted in only a moderate increase in selectivity. However, for the heptane-solvated reaction system, the thioglycerol coated catalyst was shown to increase the selectivity to 74%, indicating the presence of a solvent-SAM interaction mechanism. Interestingly, an octadecanethiol-coated catalyst did not result in significant selectivity improvement in either solvent. This result is in sharp contrast to vapor-phase studies, where selectivity was high for a wide range of SAMs, including those comprised of thioglycerol or octadecanethiol.

One hypothesis to explain the dependence of selectivity on the solvent and SAM coating is that the solubility of the thiol precursor in the solvent controls the stability of the SAM layer; i.e., competing hydrophobic (solvent) and hydrophilic (thioglycerol) environments may stabilize the SAM on the catalyst surface. Ethanol is known to be a good solvent for the thiol precursors used in these studies. Schlenoff et al. have previously shown that alkanethiol SAMs desorb at a faster rate in ethanol than in hexane or other typical solvents and that this spontaneous desorption leads to an equilibrium surface coverage which is both solvent and temperature dependent<sup>21</sup>. Equilibrium coverage of SAM coated Pt in hexane was 80% the initial thiol coverage while equilibrium coverage of SAM coated Pt in ethanol was 70% the initial thiol coverage; however, their work monitored 125 hr experiments and showed that any thiol desorption would be well under 10% in both cases over the course of a one hour reaction<sup>21</sup>. Small amounts of SAM desorption could be significant at longer reaction times, or a faster SAM desorption rate would be expected to leave vacant sites on the catalyst surface and could account for the lack of selectivity improvement for some of the alkanethiol coated reaction cases such as those run in

ethanol. In addition, alkanethiols are even more susceptible to desorption from the surface in the presence of hydrogen, as under the hydrogenation conditions in these experiments<sup>8,21</sup>.

One hypothetical method of maintaining thiol surface coverage is to introduce alkanethiols into the reaction mixture itself to account for potential desorption. Accordingly, a hydrogenation reaction was performed under all the same reaction conditions described in the experimental section using an octadecanethiol coated catalyst in ethanol solvent but where different concentrations of octadecanethiol up to 1 mM were added to the bulk phase reaction vessel. As shown in Table 2-2, the octadecanethiol coated catalyst did not exhibit a significant increase in selectivity over the uncoated catalyst in ethanol. However, the rate of reaction was reduced strongly by the addition of the thiol to the reaction vessel suggesting the formation of multilayers. Such octadecanethiol multilayer formation has been previously observed to occur on gold at concentrations of 1 mM<sup>24</sup>. The results in Table 2-2 show that while desorption of SAMs may be an issue in certain solvents, it is not possible to improve selectivity to epoxybutane by simply increasing the reaction concentration of alkanethiols. This suggests that alkanethiol desorption was not responsible for the low selectivity observed for octadecanethiol coated Pd/Al<sub>2</sub>O<sub>3</sub> in comparison to thioglycerol coated Pd/Al<sub>2</sub>O<sub>3</sub>.

Table 2-2: Activity and selectivity for hydrogenation reactions with varying concentrations of octadecanethiol added in the reaction mixture. Hydrogenation was run in ethanol solvent at 30°C and 6bar H<sub>2</sub>. Octadecanethiol was originally deposited on the Pd/Al<sub>2</sub>O<sub>3</sub> catalyst in 1mM ethanol.

Concentration (mM)	Turnover frequency (1/s)	Selectivity %
1	0	-
0.1	0.4	32
0.05	1.7	32

0.01	5.4	28
0	24.6	24
Vapor phase	0.31	91

Based on this result, the efficacy of the thioglycerol SAM for increasing hydrogenation selectivity may depend more on solvent-SAM interactions near the surface than the effect of the solvent in removing SAMs. This effect was verified by testing a range of alkanethiol coatings, which are shown in Table 2-3. Although the thioglycerol coated catalyst still led to the greatest gain in selectivity over the uncoated case, the octadecanethiol coated catalyst exhibited a much lower gain in selectivity compared to its shorter alkanethiol counterparts.

Table 2-3: Selectivity and initial activity for heptane solvated EpB hydrogenation over thiol coated Pd/Al<sub>2</sub>O<sub>3</sub> catalysts.

Coating	Selectivity to EpBane (%)	Turnover frequency (1/s)
None	36	48.4
Thioglycerol	74	12.7
Octadecanethiol	43	11.9
Dodecanethiol	66	13.3
Hexanethiol	60	12.1
Propanethiol	69	9.8

The lower increase in selectivity for the octadecanethiol coated catalyst could be explained by penetration of the reaction solvent heptane into the octadecanethiol monolayer. It has been previously shown that an n-alkane solvent such as decane can penetrate into an alkanethiol monolayer of longer length such as docosanethiol; interactions between the solvent, reactant, and SAM in such cases may have an effect on selectivity, though it is unclear what the nature of this effect would be<sup>21,25</sup>. There is also evidence that the structure of an octadecanethiol monolayer is highly dependent on the adjacent environment where both polar and non-polar

liquids shifted the asymmetric methylene peak stretch from 2918  $\text{cm}^{-1}$  in air to 2921  $\text{cm}^{-1}$  in liquid, consistent with a modest reduction in conformational order in the alkyl chain<sup>26</sup>.

**2.4.3 Effect of SAM quality on liquid-phase hydrogenation:** To further explore the effects of alkanethiol tail disorder in the liquid-phase hydrogenation reaction, we studied catalysts coated with “good” and “poor” quality SAMs<sup>9</sup>. As a measure of SAM quality, we used DRIFTS (discussed in the introduction section) to measure the asymmetric methylene stretching frequency on SAM-coated Pd/Al<sub>2</sub>O<sub>3</sub> catalysts prepared in different ways. It has been shown previously that the asymmetric methylene stretch shifts from its disordered solution phase peak of 2930  $\text{cm}^{-1}$  toward its solid phase well-ordered peak at 2920  $\text{cm}^{-1}$  as the alkanethiol chain length increases<sup>3,8</sup>. This shift to lower frequencies is due to a lower fraction of gauche defects and a higher degree of order<sup>8</sup>. In our liquid phase hydrogenation system, we were able to detect this characteristic SAM quality by changes in the rate of reaction during the hydrogenation of EpB. Shown in Figure 2-5 (a), well-ordered SAM coated Pd/Al<sub>2</sub>O<sub>3</sub> led to a higher rate of reaction than disordered SAM coating.

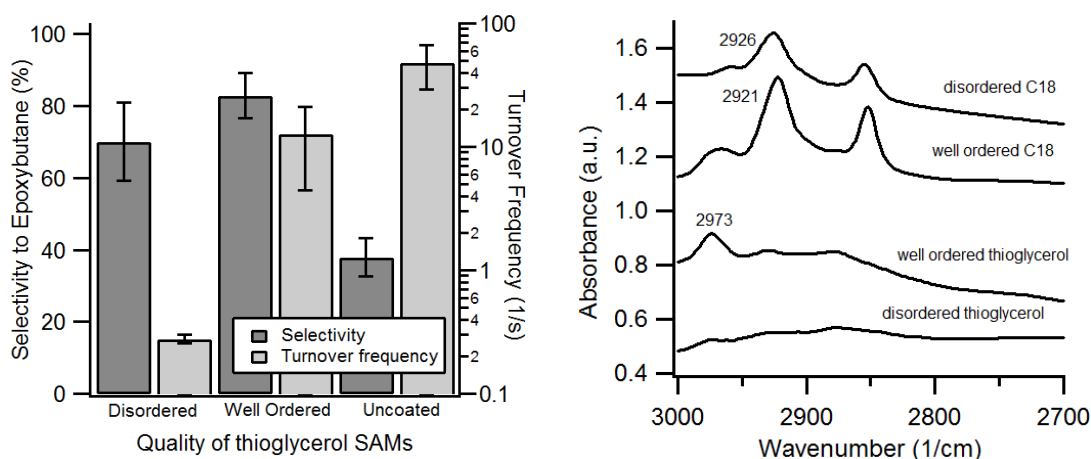


Figure 2-5: Hydrogenation of epoxybutene over thioglycerol coated Pd/Al<sub>2</sub>O<sub>3</sub> catalyst. (a) Rate (turnover frequency) and selectivity (%) for different

preparation methods. Turnover frequency data was calculated as the rate of epoxybutene consumed. (b) Methylene stretching region of octadecanethiol and thioglycerol coated Pd/Al<sub>2</sub>O<sub>3</sub> for well-ordered and disordered SAMs

Similar to thioglycerol, the octadecanethiol coated Pd/Al<sub>2</sub>O<sub>3</sub> also exhibited a decrease in catalytic activity from 11.9 s<sup>-1</sup> to 1.6 s<sup>-1</sup> as SAM order decreased as indicated by a shift in the asymmetric methylene stretching mode from 2921 cm<sup>-1</sup> to 2926 cm<sup>-1</sup>. The DRIFTS data shown in Figure 2-5 (b) include characterization of well-ordered and disordered octadecanethiol coated Pd/Al<sub>2</sub>O<sub>3</sub> to illustrate the characteristic shift in the asymmetric methylene stretch that occurs when SAMs become disordered. This shift is not manifested in the thioglycerol spectrum, which instead loses peak sharpness and intensity upon SAM disorder. Although the activity of the SAM coated Pd/Al<sub>2</sub>O<sub>3</sub> decreased dramatically as SAMs became more disordered, the selectivity of EpB hydrogenation to epoxybutane was not greatly affected. This trend was previously observed by Marshall et al. in the gas phase hydrogenation of EpB where shorter alkanethiol SAMs, with intrinsically more disorder, also had lower rates but had similar selectivity<sup>3</sup>.

## 2.5 Conclusion

Hydrogenation of epoxybutene in the liquid phase showed that the same trends in selectivity observed in gas phase hydrogenation can be induced by depositing self-assembled monolayers on a Pd/Al<sub>2</sub>O<sub>3</sub> catalyst and running under the proper liquid phase reaction conditions. In the liquid phase, solvent and SAM interactions were shown to be more important to the selectivity of the reaction although other factors such as hydrogen solubility play significant roles as well. The quality of the SAMs was shown to be specific to the deposition

technique where poor SAMs had a negative effect on the rate of the reaction but had little effect on selectivity. The most effective catalyst system measured was the contrasting polarity of a nonpolar solvent heptane with the polar SAM thioglycerol, which increased the selectivity of epoxybutene hydrogenation from 36% to 74% between the uncoated and coated cases respectively.

## 2.6 References

- (1) Torborg, C.; Beller, M. *Adv. Synth. Catal.* **2009**, *351*, 3027.
- (2) Behrens, M. *Angewandte Chemie International Edition* **2010**, *49*, 2095.
- (3) Marshall, S. T.; O'Brien, M.; Oetter, B.; Corpuz, A.; Richards, R. M.; Schwartz, D. K.; Medlin, J. W. *Nat. Mater.* **2010**, *9*, 853.
- (4) Marshall, S. T.; Schwartz, D. K.; Medlin, J. W. *Langmuir* **2011**, *27*, 6731.
- (5) Sadeghmoghaddam, E.; Gaieb, K.; Shon, Y. S. *Applied Catalysis a-General* **2011**, *405*, 137.
- (6) Wu, B.; Huang, H.; Yang, J.; Zheng, N.; Fu, G. *Angewandte Chemie International Edition* **2012**, *51*, 3440.
- (7) Vargas, A.; Ferri, D.; Bonalumi, N.; Mallat, T.; Baiker, A. *Angewandte Chemie-International Edition* **2007**, *46*, 3905.
- (8) Love, J. C.; Wolfe, D. B.; Haasch, R.; Chabinyk, M. L.; Paul, K. E.; Whitesides, G. M.; Nuzzo, R. G. *Journal of the American Chemical Society* **2003**, *125*, 2597.
- (9) Addato, M. A. F.; Rubert, A. A.; Benitez, G. A.; Fonticelli, M. H.; Carrasco, J.; Carro, P.; Salvarezza, R. C. *Journal of Physical Chemistry C* **2011**, *115*, 17788.

- (10) Schwartz, D. K. *Annual Review of Physical Chemistry* **2001**, 52, 107.
- (11) Rajadhyaksha, R. A.; Karwa, S. L. *Chemical Engineering Science* **1986**, 41, 1765.
- (12) Taylor, C. D.; Neurock, M. *Current Opinion in Solid State and Materials Science* **2005**, 9, 49.
- (13) Zope, B. N.; Hibbitts, D. D.; Neurock, M.; Davis, R. J. *Science* **2010**, 330, 74.
- (14) Toukoniitty, E.; Maki-Arvela, P.; Kuzma, M.; Vilella, A.; Neyestanaki, A. K.; Salmi, T.; Sjoholm, R.; Leino, R.; Laine, E.; Murzin, D. Y. *Journal of Catalysis* **2001**, 204, 281.
- (15) Englisch, M.; Ranade, V. S.; Lercher, J. A. *Applied Catalysis a-General* **1997**, 163, 111.
- (16) Mukherjee, S.; Vannice, M. A. *Journal of Catalysis* **2006**, 243, 108.
- (17) Singh, U. K.; Vannice, M. A. *Journal of Catalysis* **2000**, 191, 165.
- (18) Lewis, M.; Tarlov, M.; Carron, K. *Journal of the American Chemical Society* **1995**, 117, 9574.
- (19) Schoenfish, M. H.; Pemberton, J. E. *Journal of the American Chemical Society* **1998**, 120, 4502.
- (20) Vericat, C.; Vela, M. E.; Salvarezza, R. C. *Physical Chemistry Chemical Physics* **2005**, 7, 3258.
- (21) Schlenoff, J. B.; Li, M.; Ly, H. *Journal of the American Chemical Society* **1995**, 117, 12528.
- (22) Monnier, J. R. *Applied Catalysis a-General* **2001**, 221, 73.
- (23) Schaal, M. T.; Pickerell, A. C.; Williams, C. T.; Monnier, J. R. *Journal of Catalysis* **2008**, 254, 131.
- (24) Kim, Y. T.; McCarley, R. L.; Bard, A. J. *Langmuir* **1993**, 9, 1941.

(25) Bain, C. D.; Whitesides, G. M. *Angewandte Chemie International Edition in English* **1989**, 28, 506.

(26) Anderson, M. R.; Evaniak, M. N.; Zhang, M. *Langmuir* **1996**, 12, 2327.

## CHAPTER 3

### Selective Hydrogenation Of Polyunsaturated Fatty Acids Using Alkanethiol Self-Assembled Monolayer Coated Pd/Al<sub>2</sub>O<sub>3</sub> Catalysts

#### 3.1 Abstract

Pd/Al<sub>2</sub>O<sub>3</sub> catalysts coated with various thiolate self-assembled monolayers (SAMs) were used to direct the partial hydrogenation of eighteen-carbon polyunsaturated fatty acids, yielding a product stream enriched in monounsaturated fatty acids (with low saturated fatty acid content), a favorable result for increasing the oxidative stability of biodiesel. The uncoated Pd/Al<sub>2</sub>O<sub>3</sub> catalyst quickly saturated all fatty acid reactants under hydrogenation conditions, but the addition of alkanethiol SAMs markedly increased the reaction selectivity to the monounsaturated product oleic acid, to a level of 80–90% even at conversions >70%. This effect, which is attributed to steric effects between the SAMs and reactants, was consistent with the relative consumption rates of linoleic and oleic acid using alkanethiol coated and uncoated Pd/Al<sub>2</sub>O<sub>3</sub> catalysts. With an uncoated Pd/Al<sub>2</sub>O<sub>3</sub> catalyst, each fatty acid, regardless of its degree of saturation had a reaction rate of approximately 0.2 mol reactant consumed per mol surface palladium per second. Using alkanethiol coated Pd/Al<sub>2</sub>O<sub>3</sub> catalysts, the activity was reduced by a factor of 4 for polyunsaturated reactants and by a factor of 100 for the monounsaturated reactants. In contrast to the hydrophobic alkanethiol modifiers, hydrophilic thioglycerol SAM modifiers were found to strongly inhibit reaction kinetics.

#### 3.2 Background

As was presented in Chapter 2, tuning the near-surface environment of heterogeneous catalysts offers a promising route for controlling selectivity in reactions of complex chemicals. The ability to control chemoselectivity of the reaction of multi-functional feedstocks is desirable for industrial reaction processes because it reduces separations costs and maximizes yield<sup>1,2</sup>. Fatty acid oils are one example of an important multi-functional biorenewable feedstock that can be produced from a variety of terrestrial and marine plants, and are associated with low environmental toxicity<sup>3-5</sup>. Fatty acids have many industrial uses, ranging from chemicals and fuels to biological applications, personal care products, plastics and other household commodities<sup>4,5</sup>. Naturally-occurring fatty acids contain a large fraction of unsaturated eighteen carbon components including linolenic acid (cis-9,cis-12,cis-15-octadecatrienoic, C<sub>18:3</sub>) linoleic acid (cis-9,cis-12-octadecadienoic acid, C<sub>18:2</sub>) and oleic acid (cis-9-octadecenoic, C<sub>18:1</sub>), which are especially important in the production of biodiesel<sup>6</sup>.

Since biodiesel is an important bio-renewable fuel, its production from fatty acids has been extensively studied<sup>3,7-10</sup>. Critically, controlling the oxidative stability of fatty acids is vital to the quality of biodiesel that can be produced<sup>11-13</sup>. Polyunsaturated molecules such as linoleic acid are susceptible to auto-oxidative degradation which can produce polymers and other undesirable side products that prevent fuel from meeting regulatory standards<sup>14</sup>. Fortunately, reducing the degree of unsaturation can increase the oxidative stability. The oxygen adsorption rate in fatty acids decreases dramatically with a decrease in the degree of unsaturation where linolenic acid, linoleic acid, and oleic acid have oxygen adsorption rates of 800:100:1 respectively<sup>3</sup>. Soybean oil, a major biodiesel precursor, has a reported 50-60% composition of unsaturated fatty acids, so selectively reducing its degree of unsaturation is highly desirable<sup>11,13-16</sup>. The main challenge with decreasing fatty acid unsaturation is that complete saturation of the

alkane tail would result in a dramatic increase of the melting temperature and viscosity of the fuel<sup>14</sup>. Therefore, a selective reaction environment is desired to partially saturate polyunsaturated fatty acids.

Previous strategies aimed at the selective hydrogenation of polyunsaturated fatty acids have included varying the composition of metal catalyst, temperature, and hydrogenation pressure<sup>11,17-19</sup>. The addition of amines to the reaction mixture has also been shown to affect the activity of Pd catalysts towards polyunsaturated fatty acid ethyl esters in sunflower oil; in some cases providing a modest improvement in the yield of a particular monounsaturated product and inhibiting isomerization<sup>3</sup>.

Selective poisoning of catalysts is an alternative method for affecting reaction selectivity<sup>20-24</sup>. The use of alkanethiol self-assembled monolayers (SAMs) to direct the selectivity of reaction systems is one such example of selective catalyst poisoning. Chapter 2 discussed how alkanethiol monolayers have been used to improve the selectivity of the hydrogenation of 1-epoxy-3-butene (EpB) to 1-epoxybutane as well as to affect the selectivity of allyl alcohol isomerization<sup>20,22,25</sup>. In the case of 1-epoxybutene hydrogenation, modification of the Pd surface by the sulfur headgroup was found to be largely responsible for the increase in selectivity observed in these systems while the tail group was shown to affect the activity<sup>25</sup>. However, these studies examined reactant molecules that are too small to have adsorbed states where the reactant is chemisorbed to the metal while still interacting with more remote regions of the organic ligands<sup>26,27</sup>. We hypothesized that larger reactant molecules, such as fatty acids, would interact more extensively with the organic tail-group ligands of the SAM coating.

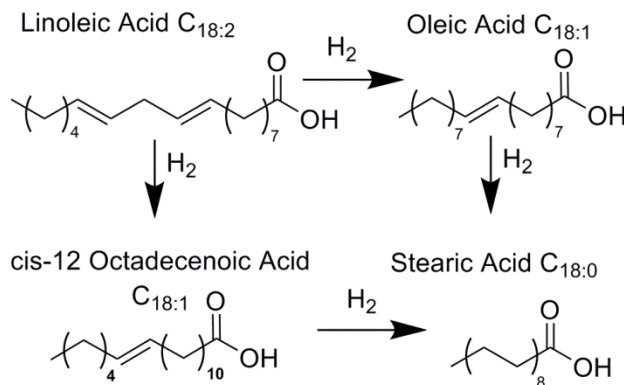


Figure 3-1: Reaction pathway for linoleic acid hydrogenation

Hydrogenation of polyunsaturated fatty acids can yield a wide range of products and isomers. The molecules of greatest interest here were the family of 18-carbon fatty acids including C<sub>18:3</sub> (linolenic acid), C<sub>18:2</sub> (linoleic acid), *cis*-C<sub>18:1</sub> (oleic acid), and C<sub>18:0</sub> (stearic acid). In addition to the differing degrees of unsaturation, each degree of saturation may be present as *trans* and *cis* isomers as well as positional isomers for a wide range of slightly different molecular configurations. For example, the hydrogenation of linoleic acid, shown in Figure 3-1, provides both positional and *cis-trans* isomerization products for each step in the unsaturation sequence.

### 3.3 Methods

3.3.1: Materials The 5wt% Pd/Al<sub>2</sub>O<sub>3</sub> catalyst used throughout this study was purchased from Sigma Aldrich. 1-Propanethiol, 1-hexanethiol, 1-dodecanethiol, 1-octadecanethiol, thioglycerol were all obtained from Sigma Aldrich, as was the ethanol (>99.5%) which was used as a solvent during SAM deposition. Anhydrous dodecane solvent (>99%), tetrahydrofuran (>99.5%) internal standard, and all fatty acids including linolenic acid, linoleic acid, oleic acid,

stearic acid, elaidic acid, and 9-decenoic acid were also obtained from Sigma Aldrich. All gases ( $\text{H}_2$ ,  $\text{O}_2$ , and He) used for catalyst preparation and reaction were Airgas ultra-high purity.

3.3.2 Reaction system: Similar to the catalyst preparation in Chapter 2, the 5wt% Pd/ $\text{Al}_2\text{O}_3$  was loaded in a glass reactor tube then oxidized by flowing 20%  $\text{O}_2$  at 573 K for 3 hr, followed by reduced by flowing  $\text{H}_2$  at 473 K for 2 hr. As discussed in the introduction in Chapter 1, this step was shown not to influence how SAMs affect the catalyst surface; however, this step was nevertheless performed for consistency with the catalyst literature. The rest of the catalyst preparation procedure is consistent with that discussed in the introduction, as is the characterization of the catalyst by chemisorption of CO.

3.3.3 Catalyst characterization: Liquid phase hydrogenation was studied at 30 °C using the 100 mL Parr batch reactor with the procedure discussed in depth in the introduction Chapter 1.4. For most reactants\*, the system was loaded with 48mL of n-dodecane solvent, 5 mL of THF internal standard, and 1 mL of fatty acid reactant giving a concentration of approximately 0.06M. Prepared catalyst was added to the solvent mixture and sealed in the reactor which was then preheated to the desired reaction temperature of 30 °C. For uncoated Pd/ $\text{Al}_2\text{O}_3$  approximately 20-30 mg of catalyst was used, while up to 300 mg of alkanethiol-coated catalyst (typically 120-150 mg) was used for coated catalyst reactions. Samples were taken using the standard reactor sampling procedure discussed in Chapter 1.4 and the column used here in Chapter 3 was the Agilent DB-FFAP capillary column with dimensions of 30 m x 0.32 mm x 0.50  $\mu\text{m}$ . While not all cis-trans and positional isomers were completely resolved, resolution was easily achieved between different degrees of unsaturation (i.e. saturated vs. monounsaturated vs. polyunsaturated). Note that in liquid-phase hydrogenation experiments in hydrophobic solvents,

leaching of thiols from the surface is expected to occur. This leaching requires periods of days, and we restricted our studies to reaction times of approximately an hour or less<sup>28</sup>.

\*Due to its limited solubility, elaidic acid (trans-9-octadecenoic acid) was prepared at a concentration of ~0.015 M for reaction studies. The amount of catalyst was decreased for the rate measurement experiments so that a reasonable conversion versus time profile was obtained over 90 minutes. Rates of hydrogenation were shown to be first order with respect to fatty acid reactant, and the rates of elaidic acid hydrogenation shown in Figure 3-5 (b) were scaled according to their initial concentration. The rate of hydrogenation was shown to be first order by varying the initial concentration of elaidic acid in the reactor within the solubility limits and seeing the initial rate of reaction change proportionally. These data are shown in Table 3-1.

Table 3-1: Rates of elaidic acid hydrogenation showing first-order dependence on reactant concentration. The specified mass of elaidic acid (EA) was added to the reaction mixture of 54 mL of liquid.

Mass EA (mg)	Concentration of EA in Reactor Solution (M)	Rate (mmol EA consumed /s /surface Pd)
126	0.0083	0.13
356	0.023	2.2
831	0.055	4.8

3.3.4 Rate calculations: The rates of reaction reported in Figure 3-5 (b) are calculated based on the moles of reactant consumed per second per surface moles of exposed palladium. This was done using a linear approximation of the slope of consumption of reactant as was

discussed in Chapter 1.4.4. Note that the number of double bonds available for reaction varies for the mono-, di-, and tri-unsaturated acids, and the reaction probability may vary accordingly. The dispersion of 15.6% determined from chemisorption of the uncoated Pd/Al<sub>2</sub>O<sub>3</sub> catalyst was used to relate the amount of catalyst used to the amount of exposed palladium. The dispersion of the uncoated catalyst was used for all of the rate calculations, even for a coated catalyst as is done in the other chapters of this thesis. As a refresher, this calculation is made because it is undetermined whether alkanethiol SAMs cover active catalyst sites or which type of site is active in the reaction, with or without a SAM coating, so we find the most consistency by reporting all rates as the moles of reactant consumed per time per exposed surface moles of metal.

3.3.5 Contact angle measurements: Macroscopic interactions of fatty acids with a thiol coated surface were explored in an effort to describe the interaction between the fatty acid and the thiol SAM coating by measuring the contact angle of each fatty acid on thiol coated thin film palladium surface. Palladium thin films were prepared by thermal evaporation onto a  $\gamma$ -silica support. A 2 nm chromium layer was first deposited as an adhesive layer followed by 150 nm of palladium. The prepared thin film slides were cleaned with acetone and deposited in alkanethiol SAM solutions of the same concentration used to prepare SAM coated catalysts. After deposition, the thin films were blown dry with nitrogen gas. Contact angle measurements were performed with a First Ten Angstroms Inc. FTA32 video 2.0 apparatus. Contact angle measurements shown include linoleic acid, oleic acid, linolenic acid, 9-decenoic acid, and dodecane (for comparison).

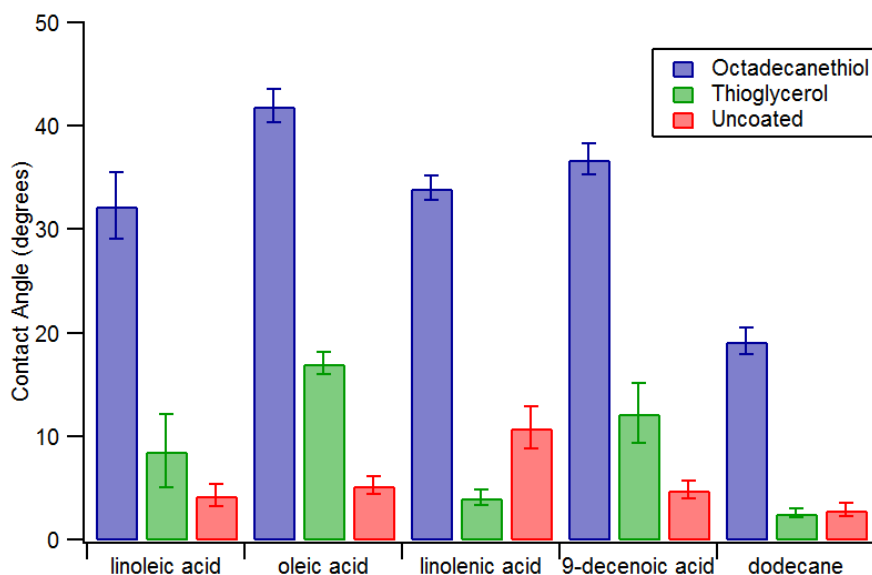


Figure 3-2: Contact angle measurements for linoleic acid, oleic acid, linolenic acid, 9-decenoic acid, dodecane, and water on thin film surfaces of octadecanethiol coated palladium, thioglycerol coated palladium, and uncoated palladium.

The highest contact angle was observed for oleic acid on an octadecanethiol-coated palladium thin film indicating the least favorable interaction in that case. Thioglycerol-coated Pd/Al<sub>2</sub>O<sub>3</sub> reduced the rate of hydrogenation of fatty acids below detection levels, but here indicates that the surface exhibited a more favorable interaction with the fatty acids. This analysis does not address any specific hypotheses of this chapter, but does suggest that there are significant differences between the interaction effects of fatty acids with different types of coatings.

### 3.4 Results

3.4.1 Hydrogenation of linoleic acid: The hydrogenation of linoleic acid was performed for 90 min; data from a typical experimental run are shown in Figure 3-3 for uncoated Pd/Al<sub>2</sub>O<sub>3</sub> and for dodecanethiol-coated Pd/Al<sub>2</sub>O<sub>3</sub>. Similar data were obtained for each of the alkanethiol-coated catalyst systems with each of the fatty acid reactants.

As illustrated in Figure 3-3 (a), the hydrogenation of linoleic acid using an uncoated palladium catalyst quickly passed through monounsaturated intermediates to the fully saturated product stearic acid, with the maximum selectivity being recorded before 10% conversion. The yield to oleic acid reached a maximum of 64% after which the series reaction resulted in a continuous decrease in selectivity. As shown in Figure 3-3 (b), application of an alkanethiol SAM coating to the Pd/Al<sub>2</sub>O<sub>3</sub> catalyst dramatically increased the selectivity of linoleic acid hydrogenation to monounsaturated products. With an alkanethiol coating, the yield to monounsaturated products was >80%, and remarkably this selectivity remained high to >80% conversion.

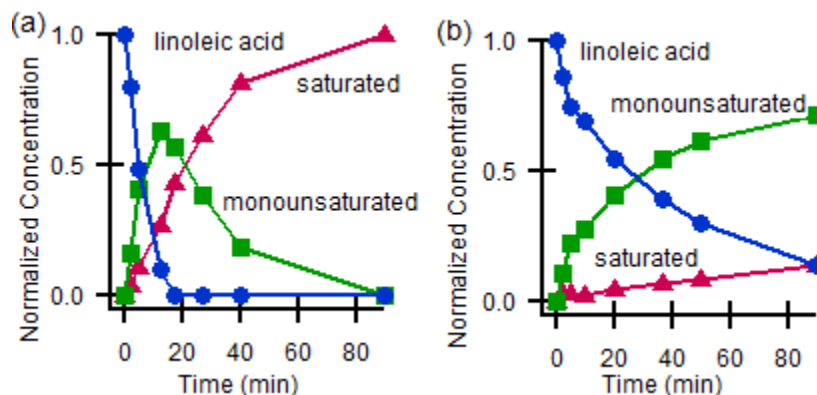


Figure 3-3: Kinetic data for linoleic acid hydrogenation over Pd/Al<sub>2</sub>O<sub>3</sub> at 30 °C and 6 bar H<sub>2</sub>. Reaction concentrations were normalized to one for clarity (a) uncoated Pd/Al<sub>2</sub>O<sub>3</sub> (b) dodecanethiol coated Pd/Al<sub>2</sub>O<sub>3</sub>

Reaction data for various SAM-coated catalysts are shown in Figure 3-4 (a). Each of the alkanethiol coatings achieved a greater selectivity to monounsaturated products than the uncoated catalyst. The initial variation in selectivity shown at low conversions in Figure 3-4 (a) may be due to limited GC sensitivity to the products at low conversions. The addition of alkanethiol SAMs to the Pd/Al<sub>2</sub>O<sub>3</sub> catalyst was also responsible for a decrease in the overall reaction activity, consistent with previous SAM catalysis studies<sup>22,25</sup>. As discussed in Chapter 1.4.4, an alkanethiol SAM may block some surface sites, but the extent of this effect is unclear, and which is why rates are again reported as the moles of reactant consumed per mole of exposed surface metal per second using the dispersion of the catalyst metal.

Experiments measuring the hydrogenation rates of different unsaturated fatty acids (Figure 3-4 (b)) show that SAM coatings reduce the hydrogenation rate much more for C<sub>18:1</sub> fatty acids, resulting in an enhanced yield of the intermediate (monounsaturated) product. That is, whereas the rate of hydrogenation on uncoated catalysts was fairly uniform (0.1–0.3 mol/s/mol surface Pd) for all reactants tested, the hydrogenation rate on coated catalysts decreased by an order of magnitude for C<sub>18:1</sub> fatty acids. Because each of the different alkanethiol tail lengths affected selectivity and rate in approximately the same way, activities for the reaction of each fatty acid over the C3, C6, C12, and C18 coated catalysts were averaged in Figure 3-4 (b) as ‘coated’.

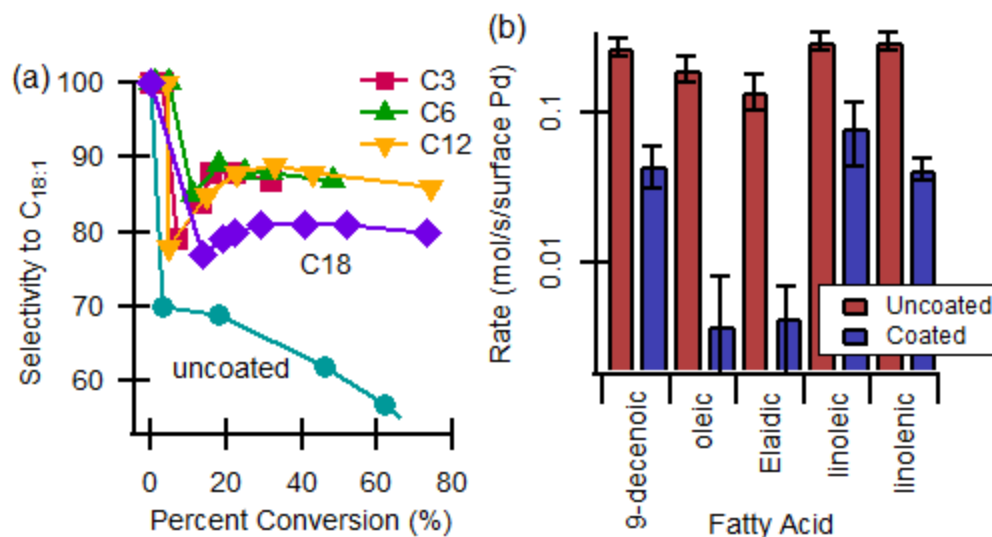


Figure 3-4: (a) Selectivity of linoleic acid hydrogenation to monounsaturated products over increasing conversion. C3, C6, C12 and C18 correspond to propanethiol, hexanethiol, dodecanethiol and octadecanethiol coated Pd/Al<sub>2</sub>O<sub>3</sub> (b) turnover frequency (1/s) for the hydrogenation of oleic acid (cis-9-octadecenoic acid), elaidic acid (trans-9-octadecenoic acid), linoleic acid (cis,cis 9-12-octadecadienoic acid), and linolenic acid (cis,cis,cis 9-12-15-octadecatrienoic acid) over alkanethiol coated (average rate of C3, C6, C12, and C18 coatings) and uncoated catalysts. Reaction rate measured as the moles of reactant consumed per mole of exposed surface Pd per second.

These data show that by coating the catalyst with a SAM, the selectivity to monounsaturated fatty acid products can be dramatically increased over the uncoated catalyst system. In addition, that increase in selectivity is exhibited to 80% conversion, so although there is a loss of rate over alkanethiol coated catalysts, a reaction system can be run at a greater overall production rate of monounsaturated fatty acid than a system with uncoated catalyst which must run at less than 10% conversion to maintain the same selectivity to monounsaturated products.

3.4.2 Hydrogenation of linolenic acid: The hydrogenation of linolenic acid  $C_{18:3}$  was also investigated and showed results consistent with the hydrogenation of linoleic acid. Again, the uncoated catalyst resulted in completely saturated products with low selectivity to partial hydrogenation. As shown in Figure 3-5 (b), the addition of an alkanethiol coating shifted the selectivity to unsaturated products, shown as 80% at 80 min, by reducing the production of saturated fatty acid. Figure 3-5 (b) is shown to highlight the trends of linolenic fatty acid hydrogenation, but when more catalyst was used, 80% selectivity was specifically achieved to monounsaturated fatty acid, in a kinetic result resembling Figure 3-3 (b). Supported by Figure 3-4 (b), the rate of consumption of linolenic acid  $C_{18:3}$  was similar to the rate of linoleic acid  $C_{18:2}$  consumption over both coated and uncoated catalysts. These results indicate that regardless of the position or the degree of unsaturation, alkanethiol monolayers can be used to direct hydrogenation to products with one degree of unsaturation.

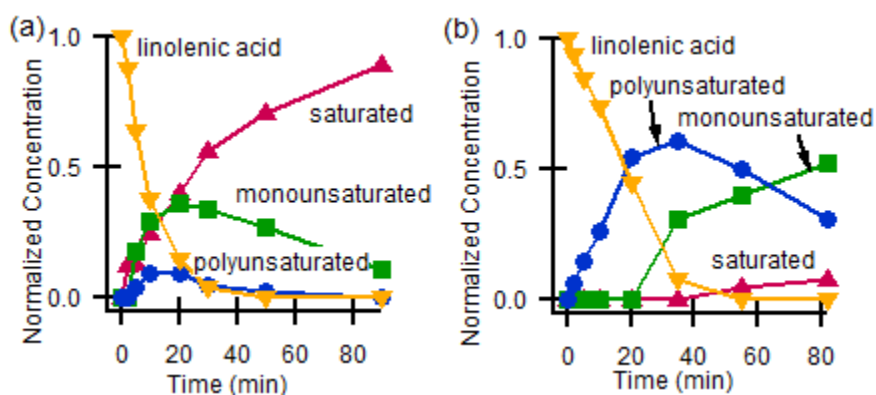


Figure 3-5: Kinetic data of linolenic acid hydrogenation over Pd/Al<sub>2</sub>O<sub>3</sub> (a) uncoated (b) dodecanethiol coated

Included in Figure 3-4 (b), kinetic data were also obtained for the hydrogenation of 9-decenoic acid to compare with the rates of hydrogenation of 18-carbon monounsaturated fatty acids. 9-Decenoic acid was chosen because it contains a double bond at the same position with respect to the fatty acid head group as both elaidic acid and oleic acid, with 9-decenoic acid lacking the eight-carbon terminal alkyl chain. Though the rates of oleic and elaidic acid hydrogenation were much lower on alkanethiol-coated catalysts, the rate of 9-decenoic acid hydrogenation was not as dramatically affected by the presence of an alkanethiol coating on the catalyst surface. This suggests that hydrogenation of the targeted double bond may depend more on its position from the terminal end of the fatty acid rather than its position relative to the fatty acid head.

2.4.3 Discussion of ligand effects: The mechanism for these effects is still not entirely clear. Previous studies have suggested that the position of a double bond within a fatty acid molecule should not strongly affect its reactivity toward hydrogenation over an uncoated Pd/C catalyst<sup>18</sup>. With respect to SAM-coated Pd catalysts, the effects of SAMs on reaction selectivity were previously attributed to poisoning effects of sulfur on the catalyst surface<sup>22,25</sup>. In the case of gas-phase ethylene hydrogenation, application of linear alkanethiol SAMs decreases the reaction rate by a factor of 100 (compared to uncoated catalyst), far greater than the effect observed here for hydrogenation of single olefin group of polyunsaturated fatty acids<sup>29</sup>. We hypothesize that the difference is smaller for the liquid-phase hydrogenation of fatty acids due to high coverage of unreactive species on an uncoated catalyst. Here, the site-blocking effects of SAMs are relatively less important when the surface is likely to contain higher coverage of competitively adsorbed, unreactive species such as the (much heavier) reactant or solvent. Such a view is consistent with the observation that alkanethiol SAMs also decrease olefin

hydrogenation rates by less than an order of magnitude for 1-epoxy-3-butene, which is known to form strongly-adsorbed spectator species on the surface during reaction<sup>22,25,30,31</sup>. Thus, it appears that the creation of high-coverage structures with SAMs decreases olefin hydrogenation rates to a smaller extent in “stickier” reaction environments.

Our prior studies have indicated that adsorbed alkanethiols do not strongly affect activation barriers for gas-phase olefin hydrogenation, but primarily alter the site densities<sup>25</sup>. It is furthermore not clear how electronic modification of the surface by sulfur would decrease the rate of hydrogenation of olefin functions in particular positions on a fatty acid molecule. Rather than an electronic mechanism, we therefore propose a geometric mechanism, whereby C<sub>18:1</sub> fatty acids have more difficulty interacting with an alkanethiol coated surface than polyunsaturated fatty acids. We hypothesize that when a fatty acid chain contains more than one degree of unsaturation, such as linoleic acid shown in Scheme 3, it has the appropriate shape to reach that catalyst surface and react within an alkanethiol monolayer; in contrast, a C<sub>18:1</sub> fatty acid (which has only a single “kink”) does not. As demonstrated in Figure 3-4 (b) and illustrated in Figure 3-6 for the hydrogenation of 9-decenoic acid, monounsaturated fatty acids can better react on a coated surface when the double bond is at the terminal end of the molecule.

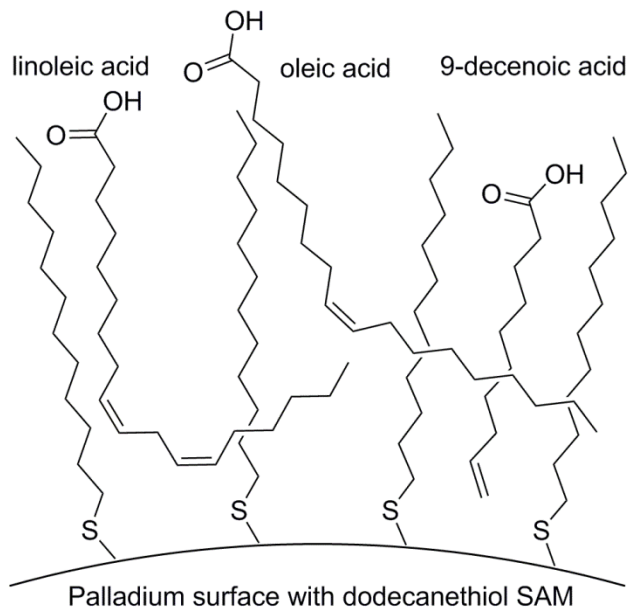


Figure 3-6: Proposed interaction mechanism of fatty acids with an alkanethiol coated palladium catalyst. Monounsaturated fatty acids are excluded from interacting with the surface.

Unfortunately, a direct measurement of how thiolate SAMs affect orientation or uptake of different fatty acids on the catalyst is lacking. Previous researchers successfully measured the adsorption of fatty acids onto montmorillonite surfaces via solution depletion acid-base titration<sup>32</sup>. Attempts to use such a technique in our case did not yield statistically significant results, due to relatively low active surface area per mass of material compared to the prior studies. For the same reason, GC analysis of supernatant liquid was not effective for characterizing adsorption of different fatty acids.

In addition to alkanethiol monolayers, a polar thioglycerol monolayer was deposited on the palladium catalyst surface, which reduced the activity of this catalyst beyond system sensitivity. The reaction rate over these thioglycerol coatings was at least four orders of

magnitude smaller than the rate of reaction over alkanethiol coated catalysts, consistent with repulsion of the oily regions of the fatty acid tails from the near surface environment. This contrasts strongly with previous studies of 1-epoxy-3-butene hydrogenation and nitrostyrene hydrogenation, where selectivity and activity differences between hydrophobic and hydrophilic coatings were minor, and implicates interactions between SAM tails and fatty acid reactants (as opposed to modification by the sulfur head group) in the selectivity-promotion mechanism<sup>25,33</sup>.

### 3.5 Conclusion

Chapter 3 has demonstrated that the application of thiol SAMs to a Pd/Al<sub>2</sub>O<sub>3</sub> catalyst can increase the hydrogenation selectivity of polyunsaturated fatty acids to their monounsaturated products. Here, we demonstrated that the force for this selectivity improvement was the ability to decrease the rate of monounsaturated fatty acid hydrogenation while keeping the rate of hydrogenation of di- and tri- polyunsaturated fatty acids an order of magnitude greater. The mechanism by which alkanethiol SAMs increase hydrogenation selectivity of polyunsaturated C<sub>18</sub> fatty acids to monounsaturated C<sub>18:1</sub> fatty acids requires further study, but as a result of this effect, any feedstock mixture of 18-carbon fatty acids with differing degrees of unsaturation such as sunflower or rapeseed oil can be reacted selectively to monounsaturated products. The fatty acid compositions of sunflower oil and rapeseed oil, two important biorenewable feedstocks, have naturally less than 30% C<sub>18:1</sub> fatty acids with the makeup consisting of various degrees of polyunsaturated fatty acids, so the application of thiol SAMs to hydrogenation catalysts could be a valuable method for improving selectivity to monounsaturated products<sup>3,6</sup>.

### 3.6 References

- (1) Torborg, C.; Beller, M. *Adv. Synth. Catal.* **2009**, *351*, 3027.
- (2) Behrens, M. *Angewandte Chemie International Edition* **2010**, *49*, 2095.
- (3) Nohair, B.; Especel, C.; Lafaye, G.; Marécot, P.; Hoang, L. C.; Barbier, J. *Journal of Molecular Catalysis A: Chemical* **2005**, *229*, 117.
- (4) Gill, I.; Valivety, R. *Trends in Biotechnology* **1997**, *15*, 401.
- (5) Steen, E. J.; Kang, Y.; Bokinsky, G.; Hu, Z.; Schirmer, A.; McClure, A.; del Cardayre, S. B.; Keasling, J. D. *Nature* **2010**, *463*, 559.
- (6) Ravasio, N.; Zaccheria, F.; Gargano, M.; Recchia, S.; Fusi, A.; Poli, N.; Psaro, R. *Applied Catalysis A: General* **2002**, *233*, 1.
- (7) Jurg, J. W.; Eisma, E. *Science* **1964**, *144*, 1451.
- (8) Ramos, M. J.; Fernández, C. M.; Casas, A.; Rodríguez, L.; Pérez, Á. *Bioresource Technology* **2009**, *100*, 261.
- (9) Verziu, M.; Cojocaru, B.; Hu, J.; Richards, R.; Ciuculescu, C.; Filip, P.; Parvulescu, V. I. *Green Chem.* **2007**, *10*, 373.
- (10) Kim, H.-J.; Kang, B.-S.; Kim, M.-J.; Park, Y. M.; Kim, D.-K.; Lee, J.-S.; Lee, K.-Y. *Catalysis Today* **2004**, *93–95*, 315.
- (11) Carvalho, M. S.; Lacerda, R. A.; Leao, J. P. B.; Scholten, J. D.; Neto, B. A. D.; Suarez, P. A. Z. *Catalysis Science & Technology* **2011**, *1*, 480.
- (12) Knothe, G. *Fuel Processing Technology* **2007**, *88*, 669.
- (13) Mittelbach, M.; Gangl, S. *Journal of the American Oil Chemists' Society* **2001**, *78*, 573.

- (14) Moser, B. R.; Haas, M. J.; Winkler, J. K.; Jackson, M. A.; Erhan, S. Z.; List, G. R. *European Journal of Lipid Science and Technology* **2007**, *109*, 17.
- (15) Dunn, R. O. *Fuel Processing Technology* **2005**, *86*, 1071.
- (16) Karavalakis, G.; Stournas, S.; Karonis, D. *Fuel* **2010**, *89*, 2483.
- (17) Veldsink, J. W.; Bouma, M. J.; Schoon, N. H.; Beenackers, A. *Catal. Rev.-Sci. Eng.* **1997**, *39*, 253.
- (18) Bernas, A.; Myllyoja, J.; Salmi, T.; Murzin, D. Y. *Applied Catalysis A: General* **2009**, *353*, 166.
- (19) Yang, R.; Su, M.; Li, M.; Zhang, J.; Hao, X.; Zhang, H. *Bioresource Technology* **2010**, *101*, 5903.
- (20) Sadeghmoghadam, E.; Gaieb, K.; Shon, Y. S. *Applied Catalysis a-General* **2011**, *405*, 137.
- (21) Snelders, D. J. M.; Yan, N.; Gan, W.; Laurency, G.; Dyson, P. J. *ACS Catalysis* **2011**, *2*, 201.
- (22) Kahsar, K. R.; Schwartz, D. K.; Medlin, J. W. *Applied Catalysis A: General* **2012**.
- (23) Taguchi, T.; Isozaki, K.; Miki, K. *Adv. Mater.* **2012**, *24*, 6462.
- (24) Kwon, S. G.; Krylova, G.; Sumer, A.; Schwartz, M. M.; Bunel, E. E.; Marshall, C. L.; Chattopadhyay, S.; Lee, B.; Jellinek, J.; Shevchenko, E. V. *Nano Lett.* **2012**, *12*, 5382.
- (25) Marshall, S. T.; O'Brien, M.; Oetter, B.; Corpuz, A.; Richards, R. M.; Schwartz, D. K.; Medlin, J. W. *Nat. Mater.* **2010**, *9*, 853.
- (26) Ulman, A.; Eilers, J. E.; Tillman, N. *Langmuir* **1989**, *5*, 1147.
- (27) Love, J. C.; Wolfe, D. B.; Haasch, R.; Chabinyk, M. L.; Paul, K. E.; Whitesides, G. M.; Nuzzo, R. G. *Journal of the American Chemical Society* **2003**, *125*, 2597.

- (28) Schlenoff, J. B.; Li, M.; Ly, H. *Journal of the American Chemical Society* **1995**, *117*, 12528.
- (29) Schoenbaum, C. A.; Schwartz, D. K.; Medlin, J. W. *Journal of Catalysis* **2013**, *303*, 92.
- (30) Marshall, S. T.; Horiuchi, C. M.; Zhang, W. Y.; Medlin, J. W. *Journal of Physical Chemistry C* **2008**, *112*, 20406.
- (31) Marshall, S. T.; Schwartz, D. K.; Medlin, J. W. *Langmuir* **2011**, *27*, 6731.
- (32) Bayrak, Y. *Microporous and Mesoporous Materials* **2006**, *87*, 203.
- (33) Makosch, M.; Lin, W.-I.; Bumbálek, V.; Sá, J.; Medlin, J. W.; Hungerbühler, K.; van Bokhoven, J. A. *ACS Catalysis* **2012**, *2*, 2079.

## CHAPTER 4

### Control of Metal Catalyst Selectivity through Specific Non-Covalent Molecular Interactions

#### 4.1 Abstract

The specificity of chemical reactions conducted over solid catalysts can potentially be improved by utilizing non-covalent interactions to direct reactant binding geometry. In this chapter, we apply thiolate self-assembled monolayers (SAMs) with an appropriate structure to Pt/Al<sub>2</sub>O<sub>3</sub> catalysts to selectively orient the reactant molecule cinnamaldehyde in a configuration associated with hydrogenation to the desired product cinnamyl alcohol. While non-specific effects on the surface active site were shown to generally enhance selectivity, specific aromatic stacking interactions between the phenyl ring of cinnamaldehyde and phenylated SAMs allowed tuning of reaction selectivity without compromising the rate of desired product formation. Infrared spectroscopy showed that increased selectivity was a result of favorable orientation of the reactant on the catalyst surface. In contrast, hydrogenation of an unsaturated aldehyde without a phenyl ring showed a non-tunable improvement in selectivity indicating that thiol SAMs can improve reaction selectivity through a combination of non-specific surface effects and ligand-specific near-surface effects.

#### 4.2 Introduction

As discussed in Chapter 1, heterogeneous catalysts, such as supported transition metals, are widely used in industrial applications due to their recoverability, but they are generally far less selective toward forming desired products compared to organometallic or enzyme catalysts<sup>1</sup>. Enzyme catalysts have evolved an advantage for improving selectivity: the active site is often contained within a binding pocket, and non-covalent interactions between the reactant and binding pocket cause reactant molecules to bind in a specific orientation to the active site<sup>2</sup>. Similar interactions have been successfully exploited to produce branched chain alcohols as biofuels<sup>3</sup>, and alcohol dehydrogenase enzymes achieve selective hydrogenation of  $\alpha,\beta$ -unsaturated aldehydes through alignment of the reactant molecules in a hydrophobic barrel within the catalyst structure<sup>4</sup>. Previous attempts to improve the chemoselectivity of heterogeneous catalysts have not generally focused on controlling non-covalent interactions, and instead have focused on changing the size, shape, or composition of the surface layer<sup>5-8</sup>. While these methods represent powerful tools for improving selectivity through (for example) control of the electronic properties of the active site, the engineering of non-covalent interactions above the active surface may provide an additional lever for approaching optimal selectivity.

In this chapter, we move to this additional level of selectivity control by depositing thiolate self-assembled monolayers (SAMs) on conventional heterogeneous catalysts to control the selectivity of an important model reaction, the hydrogenation of cinnamaldehyde (Figure 4-1). By changing the functional groups of the hydrocarbon “tail” of the thiolate modifier, it is possible to adjust non-covalent interactions in the near-surface environment in a manner analogous to changing functional groups in an enzyme binding pocket<sup>9</sup>. Previous work has shown that self-assembled monolayers can change the properties of the active catalyst surface *non-specifically* through the interaction of the sulfur head group with the surface<sup>10</sup>, but here we

show that it is possible to control selectivity *specifically* by precise placement of functional groups in the organic tail that (de)stabilize particular geometries of adsorbed reacting species. Interestingly, fifteen years ago, Gallezot and Richard<sup>6</sup> speculated that such an approach might be possible, but it has not been successfully demonstrated previously.

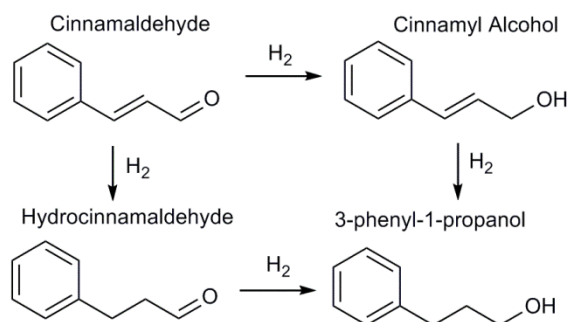


Figure 4-1: Hydrogenation pathway of cinnamaldehyde

The hydrogenation of  $\alpha,\beta$ -unsaturated aldehydes, such as cinnamaldehyde, to their respective unsaturated alcohols is among the most widely studied classes of model reactions for understanding methods to promote chemoselectivity<sup>5,6,11-15</sup>. In addition, the production of unsaturated alcohols is a less favorable yet more industrially valuable pathway for the fragrance and pharmaceutical industries<sup>6</sup>. The selectivity of this reaction has been shown to be highly dependent on the precious metal used, and since platinum is among the most selective for producing the desired cinnamyl alcohol product, it was chosen as a starting point for this study<sup>5</sup>.

### 4.3 Materials and methods

4.3.1 Materials: The 5 wt% Pt/Al<sub>2</sub>O<sub>3</sub> catalyst was purchased from Sigma Aldrich; its characterization is discussed in Chapter 1. 1-Propanethiol (C<sub>3</sub>SH), 1-hexanethiol (C<sub>6</sub>SH), 1-dodecanethiol (C<sub>12</sub>SH), 1-octadecanethiol (C<sub>18</sub>SH), thiophenol, thiophene, benzyl mercaptan,

and 2-phenyl-ethanethiol were all obtained from Sigma Aldrich. The 3-phenyl-1-propanethiol (>95%) was obtained from MolPort. Ethanol (>99.5%) used as a solvent during SAM deposition and in the reactor was from Sigma Aldrich. Tetrahydrofuran (>99.5%) internal standard, and reactants cinnamaldehyde and prenal were also obtained from Sigma Aldrich. All gases (H<sub>2</sub>, O<sub>2</sub>, and He) used for catalyst preparation and reaction were Airgas ultra-high purity.

4.3.2 Surface area and preparation of catalysts. Characterization of the commercial uncoated 5wt% Pt/Al<sub>2</sub>O<sub>3</sub> is discussed in Chapter 1 as is the deposition procedure of the thiol coatings. All thiol coated catalysts were used the same day they were prepared unless specified otherwise.

Phenylated SAM coatings used for the hydrogenation of cinnamaldehyde were susceptible to subtle changes of the deposition procedure, including aging in air. Aging of the thiol coating in air (ambient laboratory conditions) significantly altered the selectivity of the 3-phenyl-1-propanethiol coating, reducing the selectivity from 90% to near 15% for times longer than 1 week and is hypothesized to be due to degradation of the SAM layer. Numerous effects can contribute to the degradation of an alkanethiol SAM including ozone oxidation in air enhanced by time and light<sup>16</sup>. In addition, SAM coated surfaces degrade under solvated conditions, though this degradation is minor up to 25 hours<sup>17</sup>. To minimize degradation in this study, all reactions were run for 1 hour minimizing any degradation of the SAM surface in situ. Aging was achieved by leaving a dry catalyst exposed to ambient laboratory conditions for the desired time.

4.3.3 Reaction System. Reactions were run in the 100mL Parr semi-batch reactor at 50°C pressurized to 40 bar with hydrogen gas. Reactor contents were prepared as 48mL solvent, 5mL THF internal standard for the GC analysis, and 1mL of cinnamaldehyde or prenal reactant giving

the system a reactant concentration of approximately 0.15 M. Solvent choice has been shown not to significantly influence the selectivity of  $\alpha,\beta$ -unsaturated aldehyde reactions, and light alcohols such as alcohol have been shown previously to give the highest rates<sup>6</sup>. The effect of solvent on SAM coated systems will be further discussed here as well. For reactions of uncoated catalysts between 10 and 50mg of catalyst were used, and for coated catalysts, up to 300mg catalyst were used. All reactions were run for 60 minutes during which eight 1.5 mL liquid samples were taken. All samples were taken using the reactor procedure described in Chapter 1. The column used for these reactions was the Agilent HP-5 capillary column.

4.3.4 Thin film PM-RAIRS: Thin films of platinum were prepared by electron beam evaporation onto soda lime glass slides. The slides were cleaned with a nanostrip solution (sulfuric acid/peroxide/buffer) for 10 minutes at 95°C, rinsed in DI water for 10 minutes and then cleaned in a UV ozone plasma machine at 150W for 3 minutes, rinsed in DI water and blown dry. An adhesion layer of 30nm Ti followed by 150nm Pt was deposited onto the cleaned slides. Thiol coatings were deposited to the platinum thin films at the same concentration used to prepare thiol coated catalysts. When removed from solution, platinum thin films were blown dry with nitrogen rather than under a vacuum desiccator as had been done for the catalysts.

PM-RAIRS (Polarization Modulation-Reflection Absorption Infrared Spectroscopy) data was taken using a Thermo Scientific Nicolet 6700 spectrometer with a Thermo Scientific TOM (tabletop optical module) PM-RAIRS attachment. The PEM (photoelastic modulator) was made by Hinds Instruments and the synchronous sampling demodulator by GWC Technologies. The signal was received by a Thermo Scientific MCT-A (mercury cadmium telluride) detector cooled with liquid nitrogen. In order to hold the cinnamaldehyde or prenal liquid in place to take the IR scan, an Edmund Optics (1mm x 50mm) zinc selenide cover slip was used. Zinc selenide is IR

inactive and therefore served as a way to maintain a uniform thin film of cinnamaldehyde or prenal while not disrupting the infrared signal on the surface. Some incident light was reflected from the surface of the zinc selenide cover slip before reaching the platinum surface but this light was not focused at the detector and so could not interfere with the measured signal. The cover slip had an anti-reflective coating rated from 3-12 $\mu\text{m}$  to allow as much light to pass through as possible. The cover slip was clipped in place over top of the liquid sample so as not to interfere with the signal. Error bars of the  $\eta^1/\eta^2$  ratio were calculated from repeat measurements on freshly prepared slides.

#### 4.4 Results and discussion

4.4.1 Non-covalent control of selectivity: Over an uncoated Pt/Al<sub>2</sub>O<sub>3</sub> catalyst (Figure 4-2 (a)), cinnamyl alcohol was produced at much lower levels than hydrocinnamaldehyde at all times and conversions. In fact, the selectivity to cinnamyl alcohol was constant at 25% (Figure 4-5) over a broad range of conversions (20%-90%), in agreement with previous reports<sup>5,6</sup>.

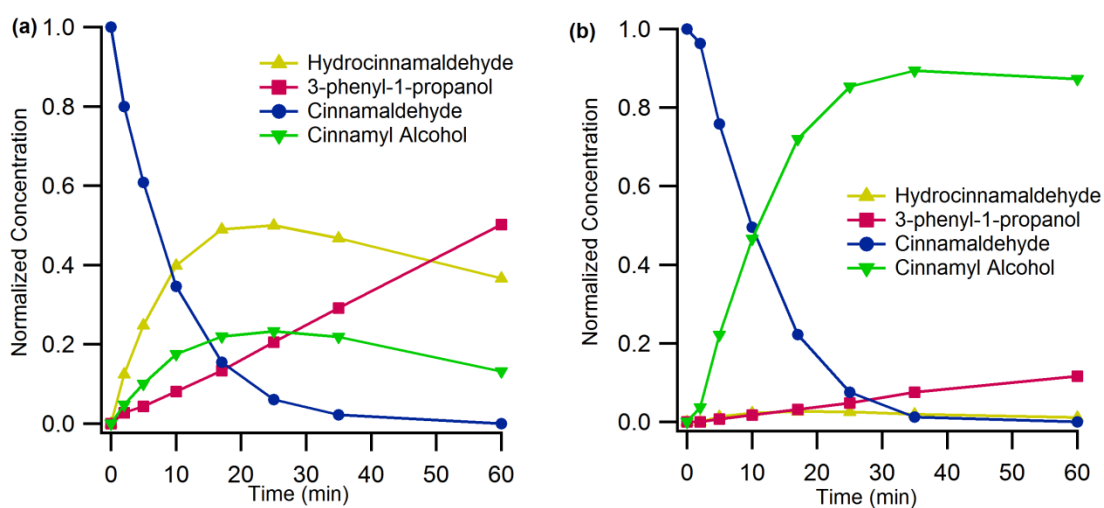


Figure 4-2: Kinetic plots for the hydrogenation of cinnamaldehyde. (a) Hydrogenation over an uncoated 5wt% Pt/Al<sub>2</sub>O<sub>3</sub> catalyst. (b) Hydrogenation over a 3-phenyl-1-propanethiol coated 5wt% Pt/Al<sub>2</sub>O<sub>3</sub> catalyst.

To tune non-covalent interactions in the near-surface environment, SAMs comprised of a number of organic ligands (Figure 4-3) were employed. Prenal, a branched non-aromatic  $\alpha,\beta$ -unsaturated aldehyde, was used as a reactant for control experiments. Because  $\alpha,\beta$ -unsaturated aldehydes contain the same reactive double bond and aldehyde at their terminal end, they can be expected to respond similarly to changes in the electronic properties of the catalyst surface; however, cinnamaldehyde contains a phenyl group resulting in additional spatial constraints within the crowded surface region<sup>6</sup> as well as the potential for additional non-covalent aromatic stacking interactions.

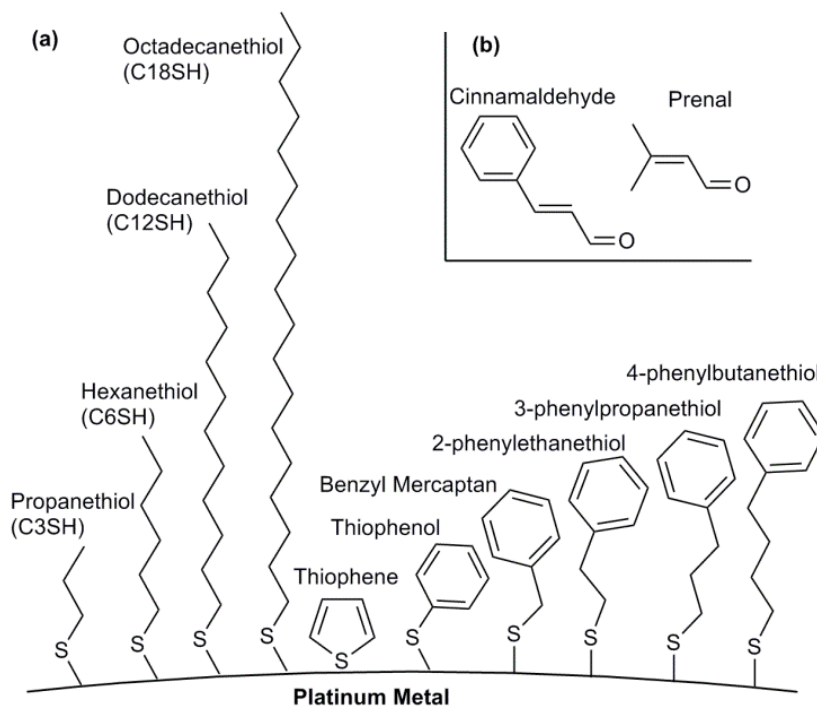


Figure 4-3: Molecules used in the hydrogenation system. (a) Thiol SAMs used to coat the Pt/Al<sub>2</sub>O<sub>3</sub> surface. (b) Cinnamaldehyde and prenal reactants

Whereas linear alkyl ligands are not expected to interact preferentially with a particular region of the cinnamaldehyde reactant, phenylated ligands can interact with cinnamaldehyde's phenyl group through aromatic pi-pi stacking<sup>18</sup>. For example, the contact angle of cinnamaldehyde can be measured on phenylated and non-phenylated surfaces to show macroscopic differences in wetting behavior. Shown in Figure 4-4, cinnamaldehyde contact angle on phenylated SAMs was consistently measured as less than 10° indicating a strong wetting effect for the phenylated thiols, consistent with attractive interactions between the phenylated SAMs and cinnamaldehyde. In contrast, cinnamaldehyde showed a much higher contact angle on the uncoated surface and on alkanethiol coated surfaces. Water exhibited a high contact angle on each SAM coated surface as expected for each of the hydrophobic coatings.

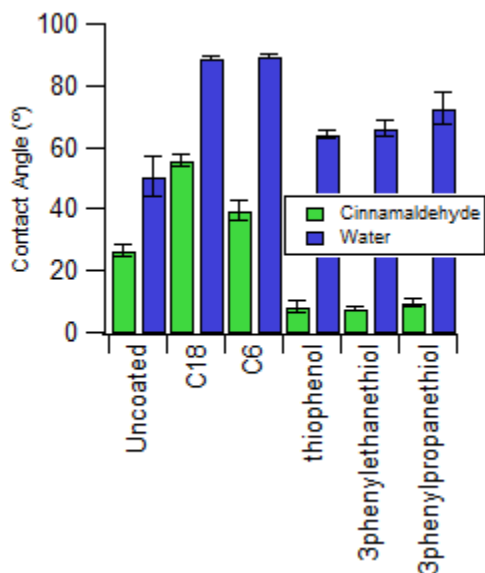


Figure 4-4: Contact angle measurements of water and cinnamaldehyde on different thiol coated surfaces. Water showed a high contact angle for each hydrophobic coating while cinnamaldehyde showed a low contact angle for phenylated thiol coatings.

By changing the vertical position of the modifying phenyl group within the SAM layer, it is hypothetically possible to control the orientation of the cinnamaldehyde with respect to the active surface via these pi-pi stacking interactions. Prenal, which lacks an aromatic moiety, exhibits no such specific interaction with phenylated SAMs.

Using a catalyst coated with a 3-phenyl-1-propanethiol SAM (Figure 4-2 (b) and Figure 4-5) increased the hydrogenation selectivity of cinnamaldehyde to greater than 90% indicating a highly-favorable specific interaction between the properly spaced phenyl ring from the SAM and the phenyl ring of the cinnamaldehyde. 2-phenylethanethiol and benzylmercaptan modifiers improved selectivity to a lesser extent, while catalyst modification with thiophene and thiophenol decreased selectivity. In other words, the highest selectivity was associated with a three-methylene spacer between the S atom and the phenyl ring, a structure that approximately matches that of cinnamaldehyde. Over long time intervals, at 100% conversion, the series reaction to produce 3-phenyl-1-propanol occurred; however, high selectivity was observed even at conversions of 90%.

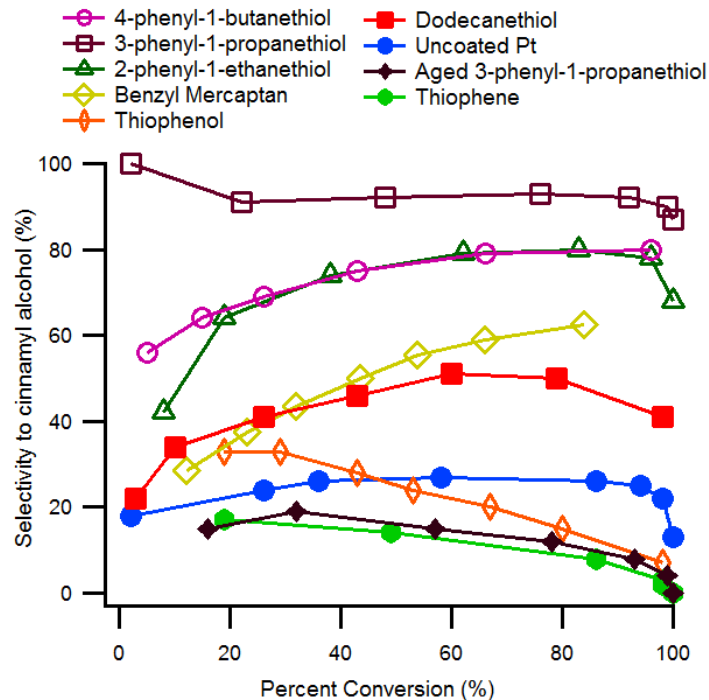


Figure 4-5: Selectivity to cinnamyl alcohol for the hydrogenation of cinnamaldehyde over Pt/Al<sub>2</sub>O<sub>3</sub> catalysts. All reactions were carried out at 40 bar hydrogen pressure, 0.15 M initial cinnamaldehyde concentration in ethanol solvent. Alkanethiol SAMs (shown separately in Figure 4-7) non-specifically increased the selectivity to cinnamyl alcohol over the uncoated case, but phenylated SAMs showed the ability to dramatically increase or decrease the selectivity depending on the location of the phenyl ring with respect to the surface.

A longer 4-phenylbutanethiol coating showed an increase in selectivity similar to that of the 2-phenylethanethiol coating, but not as good as the 3-phenylpropanethiol coating, indicating a peak in selectivity at the proper spacing length of the cinnamaldehyde molecule. The longer spacer also decreased the rate of reaction by a factor of 2 over the shorter phenylated SAM cases. An even larger rate decrease was seen for the hydrogenation of benzaldehyde (C<sub>6</sub>H<sub>5</sub>CHO) on

uncoated and 3-phenyl-1-propanethiol coated catalysts (Table 4-1). That is, in cases where the spacer length in the modifier is greater than the distance between the phenyl ring and the carbonyl function in the reactant, the reaction rate is suppressed. This result suggests that if aromatic stacking interactions occur too far above the surface, the carbonyl function is hindered from reaching the surface.

Table 4-1: Rates of benzaldehyde hydrogenation over coated and 3-phenyl-1-propanethiol coated Pt/Al<sub>2</sub>O<sub>3</sub> reported as moles converted per surface metal atom per second

Reactant:	Uncoated Pt/Al <sub>2</sub> O <sub>3</sub>	3-phenyl-1-propanethiol coated Pt/Al <sub>2</sub> O <sub>3</sub>
Cinnamaldehyde	0.35	0.38
Benzaldehyde	1.96	0.17

Molecular order of the phenylated SAMs for these hydrogenation experiments was critical to their efficacy. Well-ordered SAMs contain few surface vacancies and exhibit a standing-up adsorption geometry, while poorly ordered SAMs adopt a lying-down structure and are prone to C-S bond scission due to greater tail disorder on the catalytic surface<sup>19,20</sup>. For the hydrogenation of cinnamaldehyde, the quality of the SAM was shown to have a dramatic impact on the selectivity of the reaction. A 3-phenyl-1-propanethiol SAM that had been aged for 1-3 weeks in air decreased the selectivity to cinnamyl alcohol to lower than the uncoated case (Figure 4-5), similar to the effect caused by shorter phenylated SAMs, consistent with a strong dependence on the position of the SAM phenyl ring relative to the catalyst surface. The 2-phenylethanethiol SAM was even more sensitive to aging showing a decrease in selectivity after

less than a day. Degradation of SAMs in air and in the reaction solution is further addressed in Chapter 6.

Metal particle size has been shown previously to significantly affect the selectivity of cinnamaldehyde hydrogenation, where large particles, with larger flat facets, favor selective hydrogenation and small particles with large curvature have low selectivity to cinnamyl alcohol<sup>6</sup>. The 5 wt% Pt/Al<sub>2</sub>O<sub>3</sub> catalyst used here had a measured average particle size of 3.9 ± 1.1 nm, but we also studied a 0.5wt% Pt/Al<sub>2</sub>O<sub>3</sub> catalyst particle size of 0.8 nm ± 0.3 nm prepared with one cycle of atomic layer deposition. The catalyst was characterized by hydrogen chemisorption to have an active surface area of 1.8 m<sup>2</sup>/g and >100% dispersion. The mass loading was determined by ICP. For these smaller particles, as shown in Figure 4-6, the selectivity was improved for thiol-coated catalysts as compared to the uncoated case, but the increase in selectivity did not depend on the functionality of the coating. This loss of ligand-specific selectivity control suggests that for small particles with high curvature, the ligand specific control is difficult to maintain. Low weight loading also made it difficult to measure high conversion and led to poor mass balances.

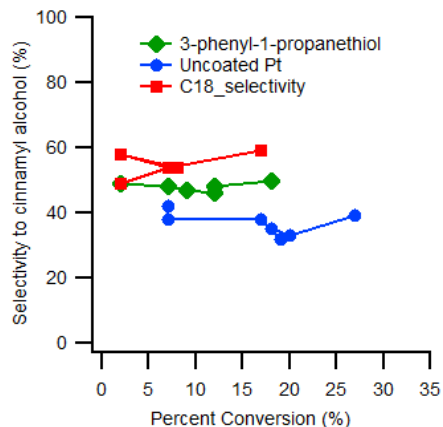


Figure 4-6: Hydrogenation of cinnamaldehyde over coated and uncoated 0.5wt% Pt/Al<sub>2</sub>O<sub>3</sub> ALD catalysts.

Alkanethiol SAMs formed from propanethiol, hexanethiol, dodecanethiol, and octadecanethiol were all shown to increase the selectivity of the reaction (Figure 4-5, and Figure 4-7) to up to 60% selectivity. These selectivity values were improved over the uncoated case, but they were not specific to the length of the thiol tail, similar to the nonspecific effect typically seen from sulfur poisoning.

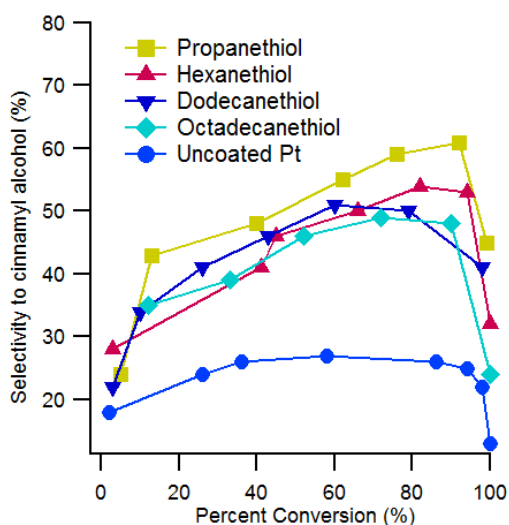


Figure 4-7: Selectivity to cinnamyl alcohol for the hydrogenation of cinnamaldehyde over alkanethiol coated Pt/Al<sub>2</sub>O<sub>3</sub> catalysts. All reactions were carried out at 40bar hydrogen pressure, 0.15 M initial cinnamaldehyde concentration in ethanol solvent.

This result suggests that a non-specific selectivity improvement may be realized through modification by inorganic sulfur sources, as has been observed previously in the hydrogenation of 1-epoxy-3-butene on alkanethiol- and H<sub>2</sub>S-modified Pd catalysts<sup>10</sup>. Studies of H<sub>2</sub>S-modified Pt for cinnamaldehyde hydrogenation showed a decrease in rate with no improvement in selectivity. However, we cannot rule out the possibility that exposure to H<sub>2</sub>S or another

inorganic sulfur source can improve selectivity; as reported elsewhere, sulfur deposition for selectivity modification is notoriously difficult to control<sup>15,21-24</sup>.

Whereas the phenylated SAMs exerted specific control based on their tail lengths, the alkanethiol modifiers non-specifically enhanced the reaction selectivity. Previous studies have shown that unsaturated alcohol selectivity is increased by weakening the binding strength of the desired product to the catalyst surface<sup>25,26</sup>, and the same adsorption weakening effect is hypothesized to be responsible for the non-specific increase in selectivity over alkanethiol coated catalysts.

4.4.2 Hydrogenation of prenal: To test this hypothesis, we also investigated the hydrogenation of a non-aromatic  $\alpha,\beta$ -unsaturated aldehyde, prenal, which contains the same reactive groups as cinnamaldehyde without a phenyl moiety. Whereas cinnamaldehyde showed specific control of selectivity via phenylated thiols, prenal hydrogenation selectivity was insensitive to the presence of a phenyl group in the SAM. Prenal hydrogenation selectivity (Figure 4-8) increased similarly for each of the alkanethiol-coated catalysts as well as the 2-phenylethanethiol and the 3-phenyl-1-propanethiol coated platinum catalysts. This suggested a lack of specific interaction effects between the thiol coating and the reactant; the general increase in selectivity was consistent with previous hydrogenation studies of small molecules over thiol-coated catalysts due to changes in the electronic properties of the catalyst surface<sup>10</sup>. These results indicate that although non-specific electronic effects can increase the selectivity of the reaction, the position of the phenyl ring from the surface provides the extra functional handle with which to direct selectivity still higher, or lower from there. The low selectivity observed for catalysts modified with thiophene and thiophenol was likely due to the close proximity of the aromatic functional group to the surface.

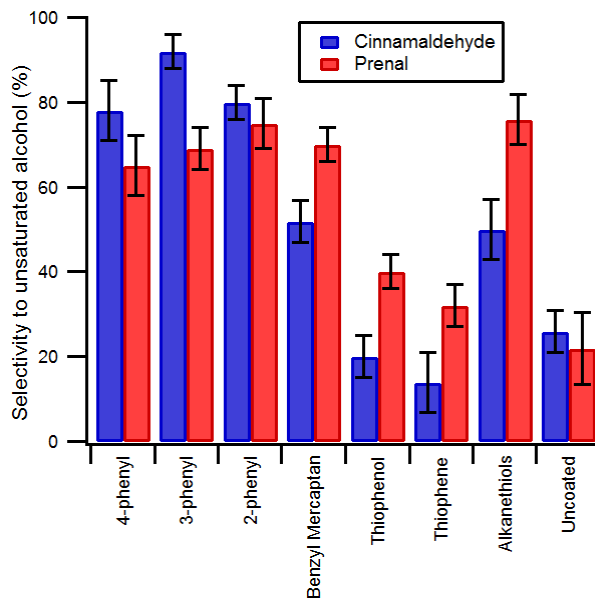


Figure 4-8: Selectivity of cinnamaldehyde and prenal hydrogenation to its respective unsaturated alcohol. The alkanethiols C3SH, C6SH, C12SH, and C18SH were averaged for one data point. Reactions were run at 40bar H<sub>2</sub> and 50°C, and 0.01M reactant solvated in ethanol. Selectivity reported at 50% conversion.

An additional factor is that thiophene is known to undergo extensive C-S bond-breaking reactions on noble metal surfaces<sup>27</sup>, consistent with a greater deposition of surface sulfur. This effect was observed experimentally in Figure 4-9 by ICP-AES analysis which was used to measure the metal loading and sulfur loading of the thiol deposited catalysts.

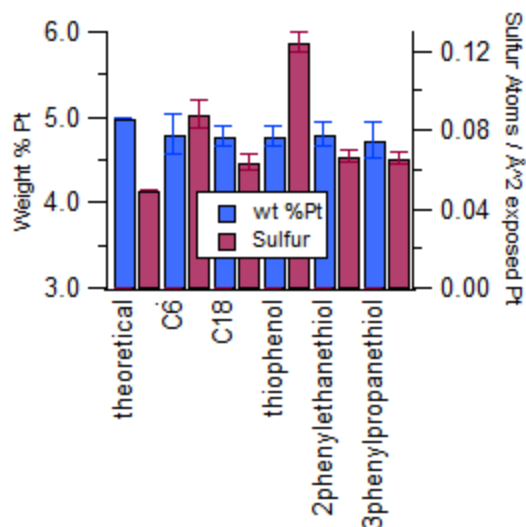


Figure 4-9: ICP-AES data. Metal loading of platinum and sulfur coverage of the surface metal. Theoretical metal loading is 5 wt% as provided by the manufacturer. Theoretical sulfur coverage is calculated as a 1/3 SAM monolayer on a Pt(111) surface using the surface area obtained from CO chemisorption on an uncoated Pt/Al<sub>2</sub>O<sub>3</sub> catalyst.

Theoretically, the weight loading of each catalyst should be the same since each is from the same batch of 5 wt% platinum catalyst (as specified by Sigma Aldrich) and each of the thiols is expected to assemble in the same  $\sqrt{3}\sqrt{3}R30^\circ$  structure on the Pt(111) surface. Here, the theoretical sulfur loading was calculated as: theoretical sulfur atoms of a SAM forming a  $\sqrt{3}\sqrt{3}R30^\circ$  structure on Pt(111) / Å<sup>2</sup> exposed Pt determined by chemisorption. Each of the catalysts was rinsed in ethanol to remove any potentially physisorbed thiols and the ICP-AES analysis showed no measurable sulfur on the blank alumina control which had been deposited in octadecanethiol and then rinsed as if metal were present. In addition, an uncoated platinum catalyst was analyzed and no trace of sulfur was detected.

4.4.3 PM-RAIRS study of reactant binding geometry: We hypothesize that the direction of selectivity change (i.e., increase or decrease) for the hydrogenation of cinnamaldehyde is controlled in part by the orientation of adsorbed cinnamaldehyde in relation to the surface (Figure 4-10) via the interaction of its phenyl moiety with the phenyl ring of the SAM. For the 3-phenyl-1-propanethiol SAM, the distance between the phenyl ring and surface is such that cinnamaldehyde is directed to a standing-up orientation in which only the aldehyde group interacts with the surface.

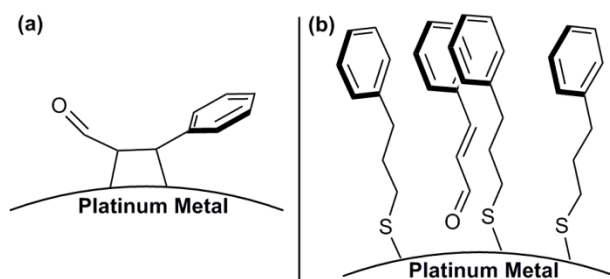


Figure 4-10: SAM enhanced orientation of cinnamaldehyde with the catalyst surface. (a) cinnamaldehyde interacting with an uncoated platinum surface through the C=C double bond. (b) 3-phenyl-1-propanethiol SAMs favor aldehyde hydrogenation by creating an upright molecular orientation

It has been shown previously that binding in a horizontal configuration favors C=C hydrogenation while binding in a vertical orientation favors C=O hydrogenation<sup>28</sup>. In order to probe binding geometries, polarization modulation reflection-absorption infrared spectroscopy (PM-RAIRS) was used to examine how the adsorption of cinnamaldehyde varies in the presence of different thiol coatings. The advantage of this technique is the ability to isolate the spectra of adsorbed molecules in the presence of an isotropic solution phase. Because PM-RAIRS requires

an optically-reflective surface, the study was performed on a thin film of platinum (150 nm) deposited on a silica glass wafer. Thiol SAM-coated surfaces were prepared in ethanolic solutions identical to the solutions used to prepare catalysts. Each spectrum was normalized to its background and adjusted to a zero baseline between 2500-2600  $\text{cm}^{-1}$ .

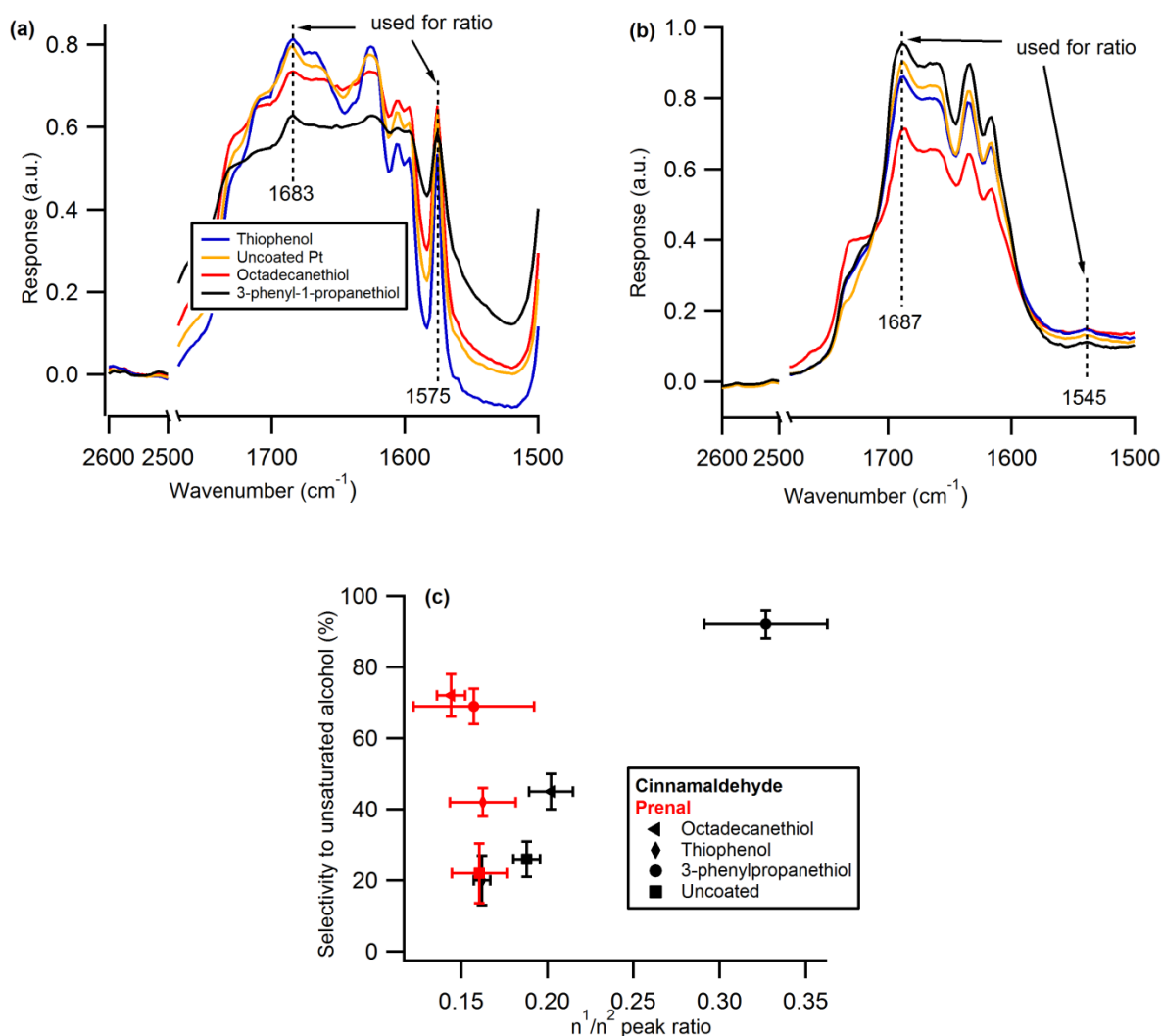


Figure 4-11: PM-RAIRS analysis of reactant adsorption geometry. (a) Cinnamaldehyde and (b) prenal adsorbed on thiophenol coated platinum, uncoated platinum, octadecanethiol coated platinum, and 3-phenyl-1-propanethiol coated platinum thin film surfaces. (c) The spectra were deconvoluted to obtain the ratio of  $\eta^1/\eta^2$  C=O peaks and

are shown with selectivity data for cinnamaldehyde and prenal hydrogenation. Error bars were calculated from replicate measurements.

There are distinct differences between the spectra collected after adsorption of cinnamaldehyde on each of the four surfaces (Figure 4-11 (a)). Peaks in the frequency range 1500-1750  $\text{cm}^{-1}$  correspond to the vibrational modes of C=C double bonds as well as C=O aldehyde stretches. The large qualitative differences in peak structure in this region suggested that the various coatings had a strong effect on the cinnamaldehyde adsorption geometry. In contrast, the general structure of the prenal spectra was insensitive to the various coatings (Figure 4-11 (b)). Previous studies have used a combination of experimental vibrational spectroscopy and density functional theory (DFT) to identify the stretching modes in this region associated with binding configurations of prenal and crotonaldehyde (2-butenal) on platinum and tin-doped platinum surfaces<sup>13,25</sup>. The DFT studies identified numerous binding configurations of which two are especially prominent in high coverage conditions: the  $\eta^1$  configuration (associated with C=O hydrogenation) where the molecule is bound through the carbonyl oxygen lone pair electrons in an upright geometry similar to Figure 4-10 (b), and the  $\eta^2$  configuration (associated with C=C hydrogenation) where the molecule is bound in a di- $\sigma_{\text{cc}}$  configuration through its C=C double bond parallel to the surface similar to the position shown in Figure 4-10(a)<sup>13,29</sup>. Peak assignments from prior studies using DFT and vibrational spectroscopy (Table 4-2) were used together with spectra of related molecules such as hydrocinnamaldehyde (Figure 4-12) to assign peaks for the adsorption of cinnamaldehyde and prenal on platinum thin films<sup>13,14,25</sup>.

Table 4-2: Peak assignments for C=C and C=O stretches of  $\alpha,\beta$ -unsaturated aldehydes. Prenal and crotonaldehyde were assigned by Haubrich<sup>13,25</sup> et al for a 1/9 monolayer coverage of aldehyde on a Pt(111) surface. These assignments were used to identify PM-RAIRS data for prenal and crotonaldehyde performed in this study. All values reported as ( $\text{cm}^{-1}$ ).

Pt (111)	Data from Haubrich <sup>13,25</sup> et al for 1/9 monolayer coverage		Stretching modes identified from PM-RAIRS data	
	$\nu(\text{C}=\text{O})$	$\nu(\text{C}=\text{C})$	$\nu(\text{C}=\text{O})$	$\nu(\text{C}=\text{C})$
Crotonaldehyde:				
$\eta^1$ -top-E-(s)-trans	1562	1633		
$\eta^2$ - $\pi(\text{CC})$ -E-(s)-trans	1671	1446		
$\eta^2$ - $\text{di}\sigma(\text{CC})$ -E-(s)-trans	1686	1115		
Prenal:				
$\eta^1$ -top-E-(s)-trans	1545	1618	1545	1616
$\eta^2$ - $\pi(\text{CC})$ -E-(s)-trans	1660	1379	1664	1378
$\eta^2$ - $\text{di}\sigma(\text{CC})$ -E-(s)-trans	1666	1189	1687	1197
Cinnamaldehyde:				
$\eta^1$ -top-E-(s)-trans			1575	1625
$\eta^2$ - $\pi(\text{CC})$ -E-(s)-trans			1683	1392
$\eta^2$ - $\text{di}\sigma(\text{CC})$ -E-(s)-trans			1666	1203
Hydrocinnamaldehyde:				
$\eta^1$ -top-E-(s)-trans			1602	-
Unbound C=O ( $\eta^2$ config)			1718	-

Adsorbed hydrocinnamaldehyde was also studied with PM-RAIRS and included in Table 4-2 in order to confirm vibrational modes. Hydrocinnamaldehyde has the same molecular structure as cinnamaldehyde but with a saturated double bond. This allowed the aldehyde related stretches to be observed in the absence of C=C stretches, and furthermore eliminated the possibility of  $\eta^2$  adsorption through an olefin function. The C=O stretching features consistent with unbound hydrocinnamaldehyde ( $1718 \text{ cm}^{-1}$ ) and the aldehyde adsorbed in an  $\eta^1$

configuration ( $1602\text{ cm}^{-1}$ ) were observed and the difference in stretching frequency between these two states were nearly identical to the difference seen for cinnamaldehyde at  $\sim 100\text{ cm}^{-1}$ . The uniformly higher aldehyde stretching frequencies for hydrocinnamaldehyde are a result of the lack of conjugation with an adjacent  $\text{C}=\text{C}$  bond, which is present for cinnamaldehyde<sup>30</sup>. The absence of features in the  $1620\text{-}1680\text{ cm}^{-1}$  range for hydrocinnamaldehyde is consistent with assignment of peaks in that region to  $\eta^2$  adsorbed species for cinnamaldehyde.

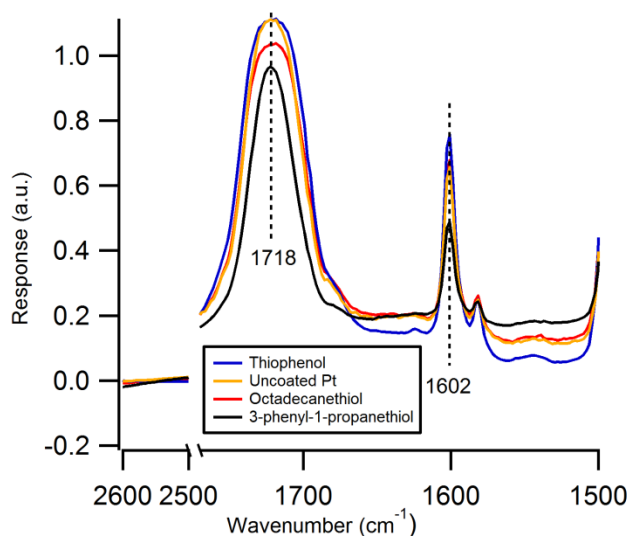


Figure 4-12: Hydrocinnamaldehyde PM-RAIRS spectra. Hydrocinnamaldehyde is shown to exhibit a strong unbound aldehyde stretch at  $1718$  and an  $\eta^1$  aldehyde stretch at  $1602$

Using these assignments, we can look at the data from Figure 4-11 and interpret the observed IR peaks. The peaks at  $1683\text{ cm}^{-1}$  and  $1687\text{ cm}^{-1}$  corresponded to the aldehyde stretch of an  $\eta^2$  binding configuration for cinnamaldehyde and prenal, respectively, and the peaks at  $1575\text{ cm}^{-1}$  and  $1545\text{ cm}^{-1}$  corresponded to an aldehyde stretch of the  $\eta^1$  binding configuration respectively. The spectra in Figure 4-11 (a) show a relative increase in the prominence of  $\eta^2$

binding configuration compared to  $\eta^1$  binding configuration for thiophenol SAMs, which exhibit low selectivity to the unsaturated alcohol. Conversely, the highly-selective 3-phenyl-1-propanethiol SAM shows a stronger signal from the  $\eta^1$  binding configuration. Since the  $\eta^1$  binding configuration is associated with C=O hydrogenation while the  $\eta^2$  binding configuration is associated with C=C hydrogenation, the effect observed for cinnamaldehyde orientation on these surfaces is consistent with the selectivity data for the hydrogenation of cinnamaldehyde. This effect was quantified in Figure 4-11 (c) where peaks identified in Figure 4-11 (a,b) were integrated and a ratio of the  $\eta^1/\eta^2$  peak area for cinnamaldehyde and for prenal was each compared to its reaction selectivity for each SAM coating. Cinnamaldehyde reaction selectivity was shown to trend directly with this ratio while the adsorbed states of prenal were uncorrelated with the ratio of peak intensities. Consistent with previous studies, this suggests a different mode of selectivity enhancement for prenal which is non-specific to the organic function of the SAM, and has been previously attributed to a weakened adsorption state of prenal on the catalyst surface<sup>13</sup>.

As electronic properties of a catalyst are altered, the selectivity typically improves at the expense of reactivity, consistent with the weakening of reactant adsorption to a catalyst surface<sup>13,15</sup>. Generally the catalysts investigated here showed a tradeoff between activity and selectivity as would be expected for a modified catalytic system, but the 3-phenyl-1-propanethiol SAM did not compromise activity (Figure 4-12) due to its different mode of selectivity improvement with cinnamaldehyde. Although the rate of cinnamaldehyde consumption decreased by a factor of three, the rate of cinnamyl alcohol production was indistinguishable, within experimental error, on the uncoated and 3-phenyl-1-propanethiol coated catalysts (Table

4-1). Also shown in Table 4-1, the effect of a phenylated SAM with a longer alkyl spacer is hypothesized to further decrease the rate of reaction.

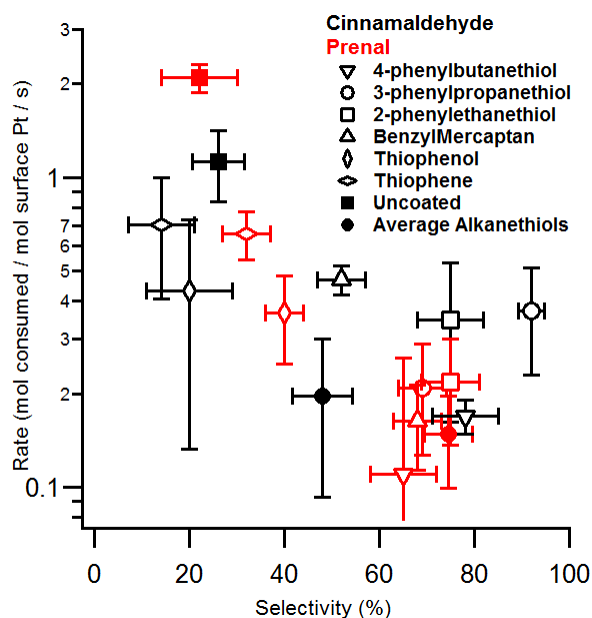


Figure 4-12: Rate versus selectivity to unsaturated alcohol for both uncoated and SAM coated Pt/Al<sub>2</sub>O<sub>3</sub> catalysts. Rates are shown as the moles of reactant consumed per moles of surface platinum per second. Alkanethiols C<sub>3</sub>SH, C<sub>6</sub>SH, C<sub>12</sub>SH, and C<sub>18</sub>SH were averaged for one data point.

4.4.4 Rates of intermediate consumption: Because the selective hydrogenation of  $\alpha,\beta$ -unsaturated aldehydes to their respective unsaturated alcohol can be increased by either inhibiting the hydrogenation of the C=C bond or activating the hydrogenation of the C=O bond, it is useful to know the respective hydrogenation rates of these intermediates. Previous studies of  $\alpha,\beta$ -unsaturated aldehydes have focused on impairing the binding affinity of the C=C double bond or stabilizing the aldehyde on the catalyst surface to increase its hydrogenation rate. Shown in Figure 4-13, over an uncoated catalyst, the rate of rate of cinnamyl alcohol

hydrogenation is approximately 10 times higher than the rate of hydrocinnamaldehyde hydrogenation, consistent with former work which has shown olefin hydrogenation to be kinetically favorable over the hydrogenation of the aldehyde<sup>31</sup>. For the hydrogenation of cinnamaldehyde over an unmodified platinum catalyst, this difference results in low apparent selectivity since cinnamyl alcohol is quickly consumed to produce the series product, the fully saturated alcohol 3-phenyl-1-propanol.

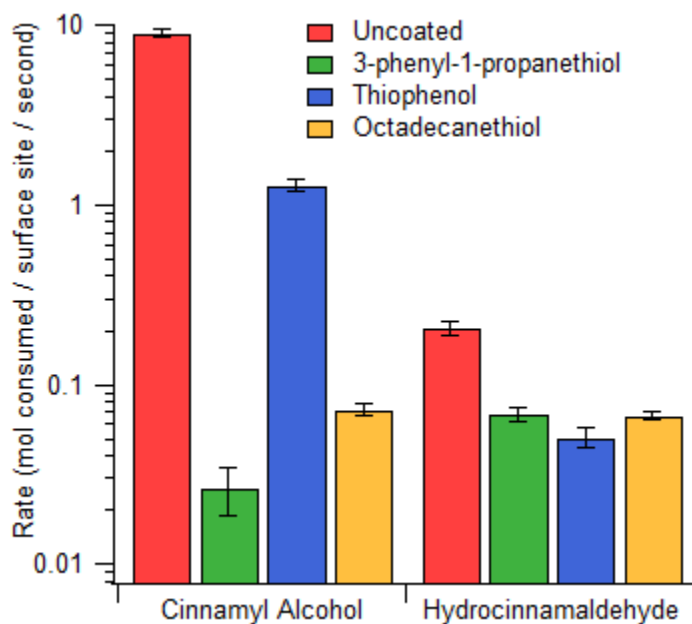


Figure 4-13: Hydrogenation of cinnamyl alcohol and hydrocinnamaldehyde solvated by ethanol. Reaction activity, displayed as the moles of reactant consumed per mole of surface metal sites per second.

When a thiol coating is deposited on the platinum catalyst, the rate of consumption of cinnamyl alcohol decreased differently for each of the different functionalized coatings. The octadecanethiol coating decreases rate of hydrogenation for both cinnamyl alcohol and

hydrocinnamaldehyde to where they are approximately the same. This results in a selectivity improvement on the octadecanethiol catalyst due to a relatively large decrease in the rate of cinnamyl alcohol consumption. The most significant effect is the decrease in cinnamyl alcohol hydrogenation over the 3-phenyl-1-propanethiol coated catalyst, making it the only coating that resulted in a lower hydrogenation rate for cinnamyl alcohol than hydrocinnamaldehyde. This further confirms the high selectivity observed for cinnamaldehyde hydrogenation that attributed the high selectivity of the 3-phenyl-1-propanethiol coated catalyst to its ability to favor hydrocinnamaldehyde hydrogenation over cinnamyl alcohol hydrogenation<sup>32</sup>. In contrast, hydrogenation over a thiophenol-coated catalyst showed the opposite effect, where hydrogenation of hydrocinnamaldehyde was slower than the hydrogenation of cinnamyl alcohol, consistent with a ligand specific interaction which favors C=C double bond hydrogenation. Finally, Figure 4-13 suggests that the most important handle for controlling cinnamaldehyde selectivity is by changing the rate of cinnamyl alcohol hydrogenation. The rate of hydrocinnamaldehyde hydrogenation is less responsive to thiol ligand tuning effects.

4.4.5 Solvent effects on ligand specific interactions: In this chapter, studies of the effects of different thiol SAMs on the hydrogenation selectivity of cinnamaldehyde were performed in ethanol in order to provide a consistent procedure for comparing the efficacy of different coating interactions<sup>32</sup>. While this allows for a constant comparison of catalysts, the polarity and aromaticity of solvent were hypothesized to play a role in the selectivity and activity observed for the hydrogenation of cinnamaldehyde via their competing interactions with the SAM coating. In addition, it has been shown previously that solvent can play some role in the selectivity of the hydrogenation of  $\alpha,\beta$ -unsaturated aldehydes<sup>33</sup>. Here, we hypothesize that ligand specific interactions can be influenced by solvent choice. First, the ligand specific interaction proposed to

induce an upright binding structure which resulted in the increase in selectivity for the 3-phenyl-1-propanethiol coated catalyst could potentially be susceptible to a solvent which would weaken this interaction, such as benzene. Second, different solvent polarities might better solvate certain families of thiols, resulting in a decreased efficacy in those systems.

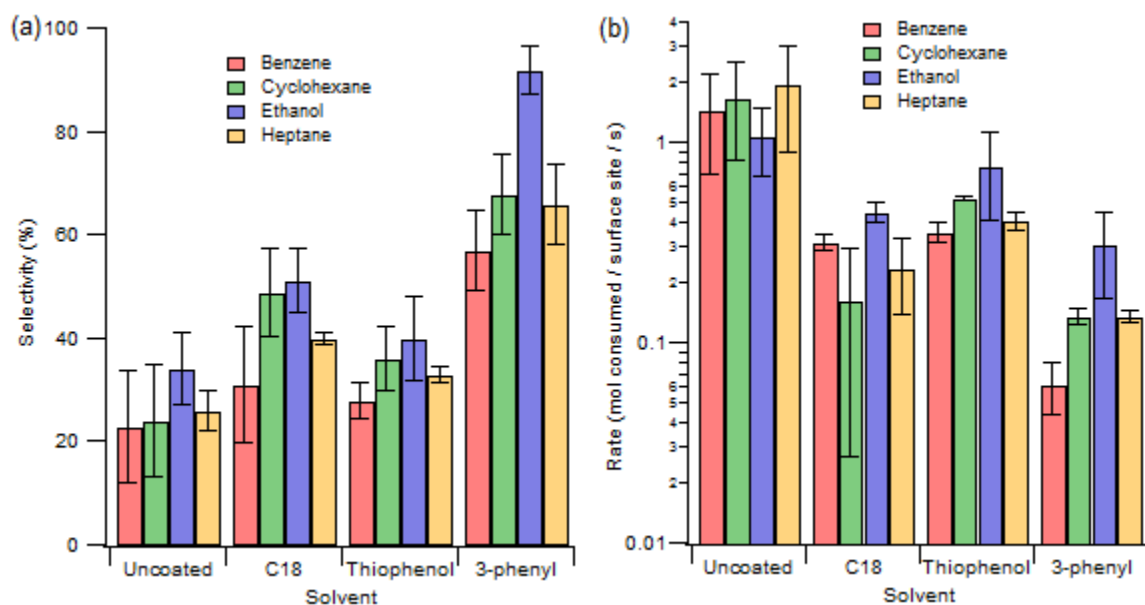


Figure 4-14: Hydrogenation of cinnamaldehyde solvated by benzene, cyclohexane, ethanol, and heptane. (a) Reaction selectivity taken at 50% conversion. (b) Reaction activity, displayed as the moles of cinnamaldehyde consumed per mole of surface metal sites per second.

For example, as shown in Figure 4-14, the selectivity of the hydrogenation of cinnamaldehyde to cinnamyl alcohol was observed as approximately 90% on the 3-phenyl-1-propanethiol coated catalyst but fell approximately 55% under benzene solvated conditions. This wide swing in coating efficacy was much larger than the difference between these different solvents for hydrogenation over an uncoated catalyst. If such a difference is due to the aromatic

benzene solvent weakening the pi-pi stacking interaction between the cinnamaldehyde reactant and the 3-phenyl-1-propanethiol SAM coating, we would expect a similar weakening of the interaction between the thiophenol coating and cinnamaldehyde thereby increasing the selectivity of the reaction in benzene for thiophenol. This trend of selectivity however was consistent between each of the different solvents where ethanol-solvated reactions were consistently the most selective and benzene-solvated reactions were the least selective.

Similarly, the rates of reaction were typically highest for ethanol-solvated reactions, but solvent effects were different among different coatings. For the uncoated catalysts, all of the hydrogenation rates were within experimental error suggesting that solvent does not play a significant role in the reaction in this case. However, when thiol coatings were deposited on the catalyst surfaces, the rates of reaction differed as predicted within aromatic classes. Over the octadecanethiol-coated catalyst, the rate of consumption for benzene-solvated and ethanol-solvated reactions was within experimental error, but for the two phenylated thiols, thiophenol and 3-phenyl-1-propanethiol, the rate of hydrogenation when solvated in benzene was significantly lower than the rate in ethanol. This decrease suggests that when phenylated thiols are deposited on the surface of a catalyst, aromatic solvent can compete with the reactant for access to the near surface environment. This result is supported by contact angle experiments using a sessile drop of cinnamaldehyde on phenylated surfaces that showed greater surface wetting than cinnamaldehyde on alkanethiol coated surfaces<sup>32</sup>.

#### **4.5 Conclusions**

Here we demonstrate that thiol modifiers can improve selectivity in hydrogenation of  $\alpha,\beta$ -unsaturated aldehydes by a combination of electronic effects and specific non-covalent

interactions of the reactant in the near-surface environment. The selective hydrogenation of both prenal and cinnamaldehyde to the desired unsaturated alcohols was enhanced with a thiol-coated catalyst surface, but the selective hydrogenation of cinnamaldehyde was further controlled through interactions of its phenyl ring with aromatic ligands within the SAM-coating layer. The selective hydrogenation of  $\alpha,\beta$ -unsaturated aldehydes is commonly achieved through active site modification<sup>6,11</sup>, but here we demonstrate that ligand-specific control exhibited by phenylated SAMs can create a reaction environment that functions in analogy to biological catalysts. This ability to exercise control over the selective hydrogenation of cinnamaldehyde by ligand-specific interactions provides a promising new method for controlling a reactive system beyond modifying the active site of heterogeneous catalysts.

#### 4.6 References

- (1) de Jong, K. P. *Synthesis of solid catalysts*; Wiley-VCH: Darmstadt, 2009.
- (2) Siegel, J. B.; Zanghellini, A.; Lovick, H. M.; Kiss, G.; Lambert, A. R.; St.Clair, J. L.; Gallaher, J. L.; Hilvert, D.; Gelb, M. H.; Stoddard, B. L.; Houk, K. N.; Michael, F. E.; Baker, D. *Science* **2010**, 329, 309.
- (3) Atsumi, S.; Hanai, T.; Liao, J. C. *Nature* **2008**, 451, 86.
- (4) Fersht, A. *Structure and mechanism in protein sciences: a guide to enzyme catalysis and protein folding* W. H Freeman and Company, 1999.
- (5) da Silva, A. B.; Jordão, E.; Mendes, M. J.; Fouilloux, P. *Applied Catalysis A: General* **1997**, 148, 253.
- (6) Gallezot, P.; Richard, D. *Catalysis Reviews* **1998**, 40, 81.

- (7) Marimuthu, A.; Zhang, J.; Linic, S. *Science* **2013**, 339, 1590.
- (8) Lee, I.; Delbecq, F.; Morales, R.; Albiter, M. A.; Zaera, F. *Nat Mater* **2009**, 8, 132.
- (9) Pecsí, I.; Leveles, I.; Harmat, V.; Vertessy, B. G.; Toth, J. *Nucleic Acids Research* **2010**, 38, 7179.
- (10) Marshall, S. T.; O'Brien, M.; Oetter, B.; Corpuz, A.; Richards, R. M.; Schwartz, D. K.; Medlin, J. W. *Nat. Mater.* **2010**, 9, 853.
- (11) Delbecq, F.; Sautet, P. *Journal of Catalysis* **2003**, 220, 115.
- (12) Pradier, C. M.; Birchem, T.; Berthier, Y.; Cordier, G. *Catal Lett* **1994**, 29, 371.
- (13) Haubrich, J.; Loffreda, D.; Delbecq, F.; Sautet, P.; Jugnet, Y.; Becker, C.; Wandelt, K. *The Journal of Physical Chemistry C* **2009**, 114, 1073.
- (14) de Jesús, J. C.; Zaera, F. *Surface science* **1999**, 430, 99.
- (15) Hutchings, G. J.; King, F.; Okoye, I. P.; Padley, M. B.; Rochester, C. H. *Journal of Catalysis* **1994**, 148, 453.
- (16) Schoenfish, M. H.; Pemberton, J. E. *Journal of the American Chemical Society* **1998**, 120, 4502.
- (17) Schlenoff, J. B.; Li, M.; Ly, H. *Journal of the American Chemical Society* **1995**, 117, 12528.
- (18) Dou, R.-F.; Ma, X.-C.; Xi, L.; Yip, H. L.; Wong, K. Y.; Lau, W. M.; Jia, J.-F.; Xue, Q.-K.; Yang, W.-S.; Ma, H.; Jen, A. K. Y. *Langmuir* **2006**, 22, 3049.
- (19) Floridia Addato, M. a. A.; Rubert, A. A.; Benítez, G. A.; Fonticelli, M. H.; Carrasco, J.; Carro, P.; Salvarezza, R. C. *The Journal of Physical Chemistry C* **2011**, 115, 17788.
- (20) Kahsar, K. R.; Schwartz, D. K.; Medlin, J. W. *Applied Catalysis A: General* **2012**, 445–446, 102.

- (21) Baldyga, L. M.; Blavo, S. O.; Kuo, C.-H.; Tsung, C.-K.; Kuhn, J. N. *ACS Catalysis* **2012**, *2*, 2626.
- (22) Hutchings, G. J.; King, F.; Okoye, I. P.; Rochester, C. H. *Applied Catalysis A: General* **1992**, *83*, L7.
- (23) Oudar, J. *Catalysis Reviews* **1980**, *22*, 171.
- (24) Marinelli, T. B. L. W.; Ponc, V. *Journal of Catalysis* **1995**, *156*, 51.
- (25) Haubrich, J.; Loffreda, D.; Delbecq, F.; Sautet, P.; Jugnet, Y.; Krupski, A.; Becker, C.; Wandelt, K. *The Journal of Physical Chemistry C* **2008**, *112*, 3701.
- (26) Delbecq, F.; Sautet, P. *Journal of Catalysis* **2002**, *211*, 398.
- (27) Lang, J. F.; Masel, R. I. *Surface science* **1987**, *183*, 44.
- (28) Medlin, J. W. *ACS Catalysis* **2011**, *1*, 1284.
- (29) Neurock, M.; Pallassana, V.; van Santen, R. A. *Journal of the American Chemical Society* **2000**, *122*, 1150.
- (30) Nishiyama, S.; Hara, T.; Tsuruya, S.; Masai, M. *The Journal of Physical Chemistry B* **1999**, *103*, 4431.
- (31) Kliewer, C. J.; Bieri, M.; Somorjai, G. A. *Journal of the American Chemical Society* **2009**, *131*, 9958.
- (32) Kahsar, K. R.; Schwartz, D. K.; Medlin, J. W. *Journal of the American Chemical Society* **2013**, *136*, 520.
- (33) Ulman, A. *Chem. Rev.* **1996**, *96*, 1533.

## CHAPTER 5

### Hydrogenation of cinnamaldehyde over Pd/Al<sub>2</sub>O<sub>3</sub> catalysts modified with thiol monolayers

#### 5.1 Abstract

Modification of supported Pt catalysts with thiols was shown in Chapter 4 to improve the hydrogenation selectivity of  $\alpha,\beta$ -unsaturated aldehydes to unsaturated alcohols. Here, we apply a variety of organic thiol coatings to Pd/Al<sub>2</sub>O<sub>3</sub> catalysts that typically have a much lower intrinsic selectivity for desired product formation. Thiol monolayers were found to increase hydrogenation selectivity to cinnamyl alcohol; however, unlike with Pt catalysts, the increase was independent of the identity of the organic tail.

#### 5.2 Introduction

One of the major themes of this thesis is the ability to direct reactions as efficiently as possible to the desired product of a reaction pathway. Catalytic efficiency requires a high rate of reaction accompanied by high selectivity to the desired product, so it is not surprising that these characteristics are the main focus of much catalysis research as well<sup>1,2</sup>. Methods for improving selectivity include choosing different metals, bimetallics, or catalyst promoters<sup>3-5</sup>, changing the catalyst support<sup>6</sup>, and throughout this thesis, modifying the near-surface environment of the catalyst with self-assembled monolayers (SAMs)<sup>7-13</sup>.

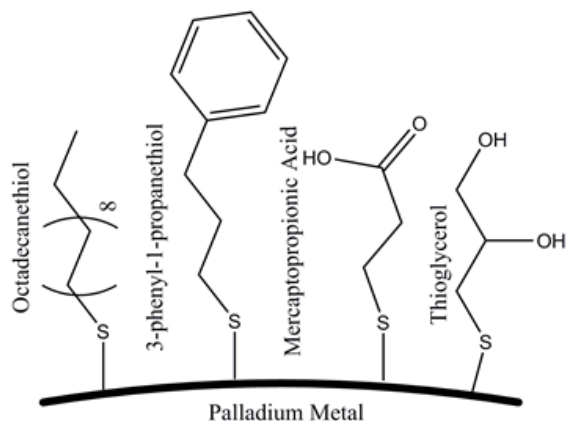


Figure 5-1: Thiol SAMs used in Chapter 5

While several reactants have been used to study the effects of SAM modifiers<sup>7,10-12,14</sup>, one of the most interesting applications was the selective hydrogenation of  $\alpha,\beta$ -unsaturated aldehydes such as cinnamaldehyde studied in Chapter 4. As review, cinnamaldehyde contains two reactive moieties, a double bond and an aldehyde, both of which can be reduced under hydrogenation conditions over a noble metal catalyst, shown in Figure 5-2 (a). The reaction of the double bond is thermodynamically more favorable than the aldehyde resulting in a naturally higher selectivity towards the saturated aldehyde over an uncoated catalyst<sup>15</sup>; therefore, it is useful to study how hydrogenation can be selectively directed down the less favorable hydrogenation pathway to produce an unsaturated alcohol<sup>3</sup>.

The study of cinnamaldehyde proved to be especially interesting because of its terminal phenyl ring which can serve as a functional “handle” for controlling its adsorbed orientation, and thus its selectivity. By designing the near-surface environment of a supported metal catalyst to control the orientation of the phenyl ring with respect to the surface, we demonstrated a

functional handle for controlling selectivity<sup>3,6</sup>. Most importantly, we demonstrated that modification of Pt/Al<sub>2</sub>O<sub>3</sub> catalysts with 3-phenyl-1-propanethiol can improve cinnamyl alcohol selectivity from <30% to >90% under equivalent reaction conditions<sup>16</sup>. Using vibrational spectroscopy and various control experiments, the selectivity improvement was traced to aromatic stacking interactions between adsorbed cinnamaldehyde and the thiol modifier similar to the scheme shown in Figure 5-2 (b). These non-covalent interactions were found to favor adsorption and reaction through the carbonyl function of cinnamaldehyde, thus producing cinnamyl alcohol at high selectivity and rate.

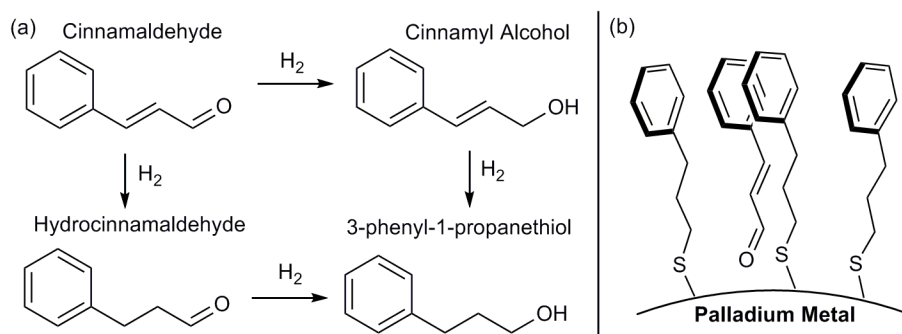


Figure 5-2: Hydrogenation of cinnamaldehyde (a) pathway (b) orientation effect exerted by a 3-phenyl-1-propanethiol modifier

In other non-related studies, the selectivity of cinnamaldehyde hydrogenation has shown a characteristic trend across noble metals where iridium is the most naturally selective, followed closely by platinum<sup>16</sup>, but palladium is known to be the least selective of all metals studied<sup>17</sup>. For this reason, previous work on improving the selectivity of cinnamaldehyde hydrogenation over SAM modified catalysts has focused on modifying platinum<sup>16</sup>, but an obvious question is whether SAM modification can result in dramatic selectivity improvements for other transition

metal catalysts such as Pd that are much less selective. Here we show that modification of palladium catalysts with thiol SAMs can also improve the selectivity of cinnamaldehyde hydrogenation to its unsaturated alcohol cinnamyl alcohol.

### 5.3 Methods

5.3.1 Materials: All reactions were run with the same commercial 5 wt% Pd/Al<sub>2</sub>O<sub>3</sub> catalyst discussed in Chapter 1 and used in other chapters. Mercaptopropionic acid (99%), thioglycerol (99%), and octadecanethiol (>99.5%) were purchased from Sigma Aldrich. The 3-phenyl-1-propanethiol was obtained from MolPort. The reaction solvent ethanol (>99.5% anhydrous) was obtained from Sigma Aldrich and was also used for making ethanolic solutions of thiols for SAM deposition. Also obtained from Sigma Aldrich were the reactant cinnamaldehyde and tetrahydrofuran (>99.5%) which was used as internal standard in the reactor. All gasses: hydrogen (used for the reactor and for catalyst preparation), oxygen, and helium (for catalyst preparation) were Airgas ultra-high purity.

5.3.2 Reaction system: SAM coated catalysts were prepared in an ethanolic deposition procedure identical to Chapter 4 and described in detail in Chapter 1. For the octadecanethiol coating, 40 mL of a 1 mM ethanolic solution was used for the deposition of up to 200 mg of catalyst. For the deposition of all other coatings (3-phenyl-1-propanethiol, thioglycerol, and mercaptopropionic acid) a deposition concentration of 10 mM was used. All reactions discussed were run in the 100 mL Parr batch reactor at 50°C solvated by ethanol. The procedure for running reactions and taking samples is described in detail in Chapter 1. The GC analysis was run with the Agilent HP-5 capillary column with dimensions of 30 m x 0.32 mm x 0.25 μm.

Active surface area of the uncoated 5 wt% Pd/Al<sub>2</sub>O<sub>3</sub> is described extensively in Chapter 1. It was determined by chemisorption with carbon monoxide on a Quantachrome Autosorb-1, and was measured to be 3.7 m<sup>2</sup>/g with a dispersion of 15.6%. This surface area and dispersion were used to calculate the rates of reaction that are reported here for both uncoated and thiol coated catalysts as the moles of cinnamaldehyde reactant consumed per surface site of uncoated catalyst per second. This is the same method of reporting rates used in previous Chapters and in other SAM catalysis papers<sup>7,11,13,14,16</sup>. The error in the rates was calculated from the error in estimation of the initial rate of reactant consumption, determined by assuming a linear consumption at initial times. All selectivities were calculated as the percent conversion to the specified product.

## 5.4 Results and discussion

The hydrogenation of cinnamaldehyde was carried out over Pd/Al<sub>2</sub>O<sub>3</sub> catalysts at both 6 bar H<sub>2</sub> and at 40 bar H<sub>2</sub>, and as expected<sup>17</sup>, the selectivity to cinnamyl alcohol was low. As shown in Figure 5-3 (a), the predominant hydrogenation products were hydrocinnamaldehyde and 3-phenyl-1-propanol. Modification of the Pd catalyst with a number of thiol coatings shown in Figure 5-1 did not change the major products, but did decrease the 3-phenyl-1-propanethiol yield and increase the cinnamyl alcohol yield, though the yield of the latter product was still low. In all cases, the series product 3-phenyl-1-propanol did not appear to be formed primarily from hydrocinnamaldehyde, since the rate of 3-phenyl-1-propanol formation was not closely related to hydrocinnamaldehyde concentration<sup>18</sup>. This suggests that the primary pathway for 3-phenyl-1-propanol formation is through rapid hydrogenation of the desired cinnamyl alcohol product. The

hydrogenation of cinnamyl alcohol was carried out here under the 40 bar reaction conditions and showed 98% selectivity to the saturated alcohol and 100% conversion within 2 min, consistent with these results. Previous studies with Pt catalysts have suggested that desorption of the unsaturated alcohol may be the selectivity-determining step in hydrogenation of  $\alpha,\beta$ -unsaturated aldehydes<sup>4,15,19,20</sup>, and over a Pd surface, this effect is exacerbated by the increased rate of cinnamyl alcohol hydrogenation.

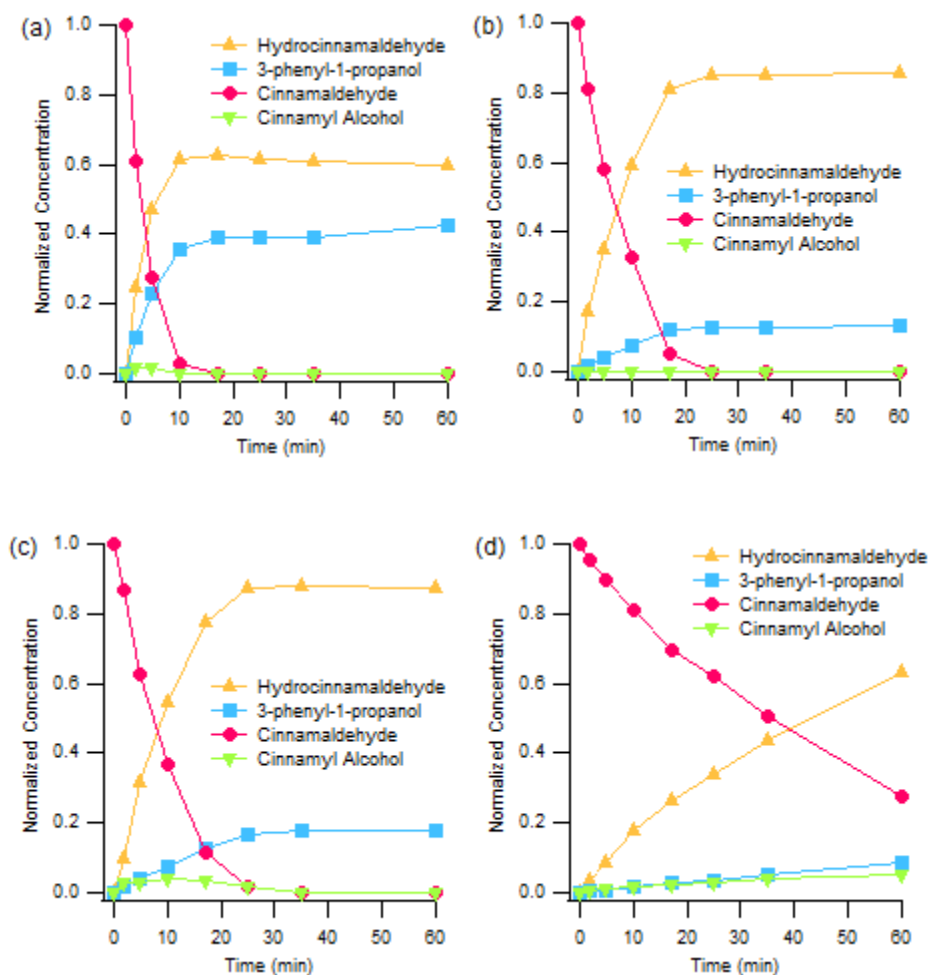


Figure 5-3: Kinetic plots for the hydrogenation of cinnamaldehyde over Pd/Al<sub>2</sub>O<sub>3</sub> catalysts: (a) uncoated Pd/Al<sub>2</sub>O<sub>3</sub> at 40 bar H<sub>2</sub> pressure; (b) uncoated Pd/Al<sub>2</sub>O<sub>3</sub> at 6 bar H<sub>2</sub>

pressure; (c) 3-phenyl-1-propanethiol coated Pd/Al<sub>2</sub>O<sub>3</sub> at 40 bar H<sub>2</sub> pressure; (d) 3-phenyl-1-propanethiol coated Pd/Al<sub>2</sub>O<sub>3</sub> at 6 bar H<sub>2</sub> pressure

As shown in Figure 5-3 (a,b), the difference in hydrogen pressure led to a significant difference in the production of hydrocinnamaldehyde over the uncoated Pd/Al<sub>2</sub>O<sub>3</sub> catalysts. This effect was not observed over 3-phenyl-1-propanethiol coated Pd/Al<sub>2</sub>O<sub>3</sub> catalysts, as shown in Figure 5-3 (c,d), which were both approximately 80% selective to hydrocinnamaldehyde. Shown in Figure 5-4, the selectivity to cinnamyl alcohol did improve for thiol coated catalysts, although that increase in selectivity was modest compared to the increase seen for the same reaction over a Pt/Al<sub>2</sub>O<sub>3</sub> catalyst<sup>16</sup>. The selectivity also declined much more rapidly with conversion on the Pd catalysts, again consistent with high rates for unsaturated alcohol hydrogenation on Pd catalysts.

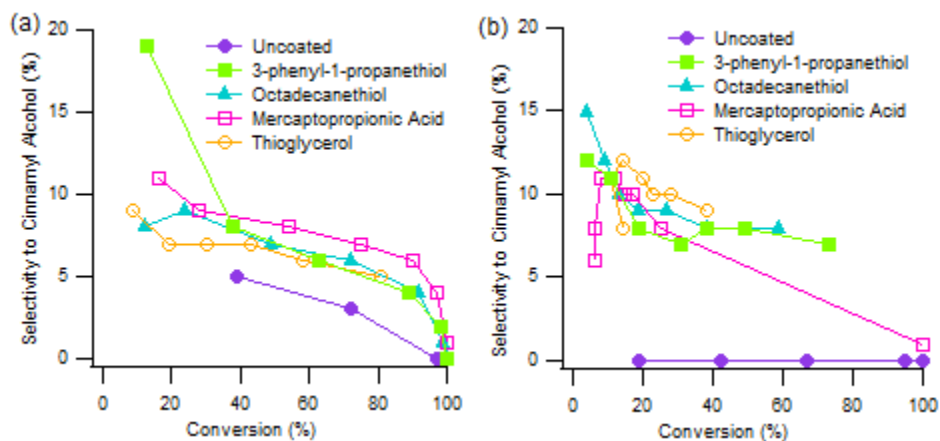


Figure 5-4: Selectivity v. conversion for the hydrogenation of cinnamaldehyde to the desired product cinnamyl alcohol at (a) 40 bar and (b) 6 bar hydrogen pressure

As shown in Figure 5-4 (a), for experiments conducted at 40-bar hydrogen pressure the selectivity was a few percentage points better than using an uncoated catalyst, with the largest increase occurring for the 3-phenyl-1-propanethiol coated catalyst at low conversions. In contrast, the selectivity in the 6-bar hydrogen system improved from 0% on the uncoated Pd/Al<sub>2</sub>O<sub>3</sub> catalyst to around 10% for each of the thiol coated catalysts.

Under all reaction conditions investigated, the thiol coated catalysts improved the selectivity of the reaction similarly, in a manner non-specific to their tails. Our previous work has shown that one effect of SAM catalyst modification is to increase selectivity via electronic or geometric effects of sulfur on the surface<sup>7</sup>. In this type of *surface* effect, selectivity is generally improved the same amount by all SAMs regardless of their tail structure. At such high hydrogen pressures the thiol tail appears to have little effect on the selectivity of the reaction and the increase in selectivity is due to a non-specific selectivity enhancement.

In addition to these non-specific electronic effects on the catalyst surface<sup>7,11</sup>, thiol SAMs have been shown to also exhibit ligand-specific effects via interactions with the reactant<sup>16</sup>. For the hydrogenation of cinnamaldehyde on Pt catalysts, the ligand specific effects were shown to control the orientation of cinnamaldehyde for directing hydrogenation selectivity. For example, the 3-phenyl-1-propanethiol coating was shown to direct selectivity to cinnamyl alcohol with >90% selectivity, whereas linear alkanethiol coatings (like octadecanethiol) produced cinnamyl alcohol with selectivities closer to 60%. This improved selectivity effect was found to be due to the orientation of cinnamaldehyde in an upright configuration, thereby excluding the double bond from interacting with the surface.

The absence of this ligand-dependent effect on Pd catalysts may be consistent with a change in the mechanism for the hydrogenation of  $\alpha,\beta$ -unsaturated aldehydes on Pd surfaces compared to Pt. Note that on Pd catalysts, our group and others have observed that the fully saturated alcohol is primarily generated through production of an intermediate unsaturated alcohol<sup>3,18,21</sup>. That is, the rate of carbonyl hydrogenation is competitive with olefin hydrogenation, but the desired reaction intermediate cinnamyl alcohol is rapidly converted to 3-phenyl-1-propanethiol. In contrast, the rate of cinnamyl alcohol hydrogenation is low on Pt-based catalysts<sup>22</sup>. Thus, whereas selectivity promotion of Pt relies on favoring the rate of formation of the unsaturated alcohol, selectivity promotion on Pd relies on reducing the rate of consumption of that intermediate. Interestingly, the thiol ligands do not appear to affect selectivity in the same way for the two different types of surfaces. Though reasons for this are not immediately clear, previous groups have found significantly different favored adsorption geometries for Pd compared to Pt surfaces, so that the nature of thiol-reactant interactions could be altered<sup>3,23</sup>.

Related to the effects described above, there was also a change in selectivity to hydrocinnamaldehyde, the alternative intermediate product to cinnamyl alcohol (Figure 5-2). As shown in Figure 5-5 (a), the selectivity to hydrocinnamaldehyde increased over thiol coated catalysts as compared to the uncoated Pd/Al<sub>2</sub>O<sub>3</sub> catalyst at 40-bar pressure, but decreased at 6-bar pressure as shown in Figure 5-5 (b).

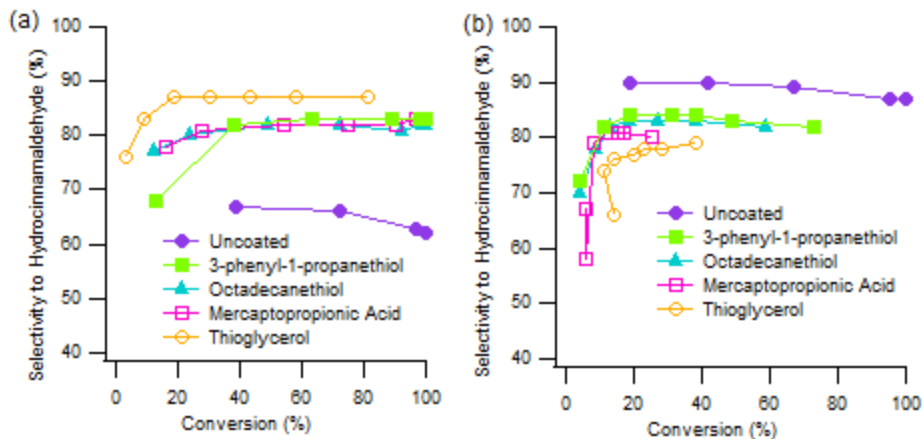


Figure 5-5: Selectivity for the hydrogenation of cinnamaldehyde to the intermediate product hydrocinnamaldehyde at (a) 40 bar and (b) 6 bar hydrogen pressure

As shown previously over Pt catalysts<sup>22</sup>, and in Figure 5-4 (a-b) for Pd catalysts, higher hydrogen pressure increased the reaction selectivity to cinnamyl alcohol. For the Pd system discussed here, these higher hydrogen pressures consequently resulted in the direction of more product through the cinnamyl alcohol intermediate pathway to the final saturated product 3-phenyl-1-propanol. The result was not apparent from Figure 5-4, where cinnamyl alcohol selectivity at different pressures is approximately the same. Figure 5-5 shows that in fact, at higher pressures, more product was directed away from hydrocinnamaldehyde, to cinnamyl alcohol and subsequently to the final series product. The application of a thiol monolayer thus serves two purposes. At high pressure, the dominant effect was to slow the conversion of cinnamyl alcohol to 3-phenyl-1-propanol rather than increase selectivity to cinnamyl alcohol. At low pressure, as indicated by the decrease in hydrocinnamaldehyde selectivity for the coated catalysts shown in Figure 5-5 (b), the effect was to crowd the surface in a manner similar to the effect of higher hydrogen pressure thus reducing the production of hydrocinnamaldehyde in

favor of production of cinnamyl alcohol. Whereas the focus of most studies of  $\alpha,\beta$ -unsaturated aldehydes was to increase reaction selectivity to the unsaturated alcohol, here the effect of the thiol coatings can serve to either increase or decrease the selectivity to hydrocinnamaldehyde based on a moderate or high pressure hydrogen system.

The increase in selectivity comes at the expense of the rate of reaction. Shown in Figure 5-6, the rate of hydrogenation over an uncoated Pd/Al<sub>2</sub>O<sub>3</sub> catalyst is approximately 1.0 (mol/surface site/s) and decreases most for the polar coatings of mercaptopropionic acid and thioglycerol.

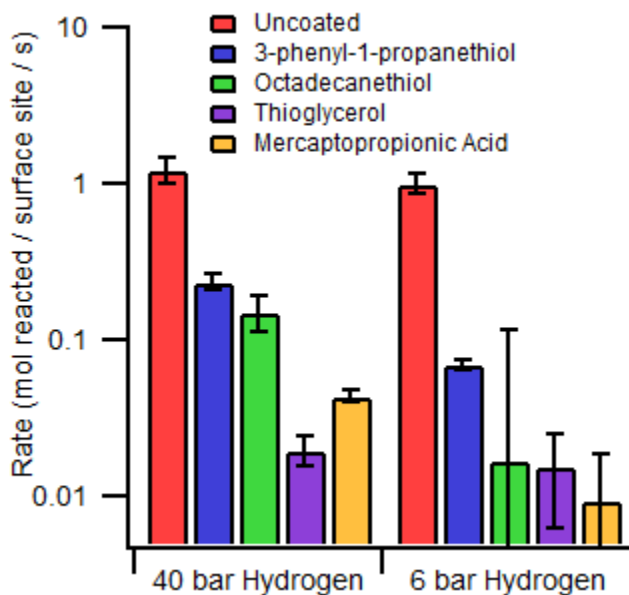


Figure 5-6: Rates of hydrogenation for the consumption of cinnamaldehyde. Rates were calculated as the moles consumed per surface site per second.

The hydrogenation rates of cinnamaldehyde over uncoated Pd/Al<sub>2</sub>O<sub>3</sub> catalyst at 40 bar and 6 bar were approximately equal indicating that the adsorption of hydrogen on the surface of

the catalyst was not likely to be limiting. The coated catalysts however show quite different rates at different pressures indicating that in these systems, the rate may be limited by the ability of hydrogen to adsorb on the crowded surface.

This loss of activity is consistent with improving selectivity through a general weakening of unsaturated oxygenate adsorption, as has been characterized extensively on supported Pt catalysts<sup>3,4</sup>. These rate data accompanied by the favorable increases in selectivity over a range of conversions indicate that the 3-phenyl-1-propanethiol coating was the most effective catalyst modifier studied here as it was for the hydrogenation of cinnamaldehyde over Pd/Al<sub>2</sub>O<sub>3</sub><sup>16</sup>. In this case, as in earlier studies of epoxybutene hydrogenation chemistry, the organic ligand of the thiol helps control the rate of reaction, but does not affect selectivity.

## 5.5 Conclusions

The addition of thiol self-assembled monolayers to the surface of palladium catalysts was shown to improve the selectivity of the hydrogenation of cinnamaldehyde to the unsaturated alcohol cinnamyl alcohol at both 6 bar and 40 bar hydrogen pressure in the liquid phase. The selectivity to the saturated aldehyde hydrocinnamaldehyde was improved for thiol coated catalysts at 40 bar hydrogen but was depressed for thiol coated catalysts at 6 bar hydrogen pressure. In contrast to platinum catalysts where selective hydrogenation of cinnamaldehyde to cinnamyl alcohol was dependent on the production of product, over palladium catalysts, increased selectivity was dependent on preventing its subsequent hydrogenation.

## 5.6 References

- (1) Besson, M.; Gallezot, P. *Catalysis Today* **2000**, *57*, 127.
- (2) de Jong, K. P. *Synthesis of solid catalysts*; Wiley-VCH: Darmstadt, 2009.
- (3) Gallezot, P.; Richard, D. *Catalysis Reviews* **1998**, *40*, 81.
- (4) Haubrich, J.; Loffreda, D.; Delbecq, F.; Sautet, P.; Jugnet, Y.; Krupski, A.; Becker, C.; Wandelt, K. *The Journal of Physical Chemistry C* **2008**, *112*, 3701.
- (5) Ponec, V. *Applied Catalysis A: General* **1997**, *149*, 27.
- (6) Pham-Huu, C.; Keller, N.; Ehret, G.; Charbonniere, L. c. J.; Ziessel, R.; Ledoux, M. J. *Journal of Molecular Catalysis A: Chemical* **2001**, *170*, 155.
- (7) Marshall, S. T.; O'Brien, M.; Oetter, B.; Corpuz, A.; Richards, R. M.; Schwartz, D. K.; Medlin, J. W. *Nat. Mater.* **2010**, *9*, 853.
- (8) Kwon, S. G.; Krylova, G.; Sumer, A.; Schwartz, M. M.; Bunel, E. E.; Marshall, C. L.; Chattopadhyay, S.; Lee, B.; Jellinek, J.; Shevchenko, E. V. *Nano Lett.* **2012**, *12*, 5382.
- (9) Torborg, C.; Beller, M. *Adv. Synth. Catal.* **2009**, *351*, 3027.
- (10) Wu, B.; Huang, H.; Yang, J.; Zheng, N.; Fu, G. *Angewandte Chemie International Edition* **2012**, *51*, 3440.
- (11) Kahsar, K. R.; Schwartz, D. K.; Medlin, J. W. *Applied Catalysis A: General* **2012**, *445–446*, 102.
- (12) Taguchi, T.; Isozaki, K.; Miki, K. *Adv. Mater.* **2012**, *24*, 6462.
- (13) Schoenbaum, C. A.; Schwartz, D. K.; Medlin, J. W. *Journal of Catalysis* **2013**, *303*, 92.
- (14) Kahsar, K. R.; Schwartz, D. K.; Medlin, J. W. *ACS Catalysis* **2013**, *3*, 2041.

- (15) Kliewer, C. J.; Bieri, M.; Somorjai, G. A. *Journal of the American Chemical Society* **2009**, *131*, 9958.
- (16) Kahsar, K. R.; Schwartz, D. K.; Medlin, J. W. *Journal of the American Chemical Society* **2013**, *136*, 520.
- (17) da Silva, A. B.; Jordão, E.; Mendes, M. J.; Fouilloux, P. *Applied Catalysis A: General* **1997**, *148*, 253.
- (18) Zhao, F.; Ikushima, Y.; Chatterjee, M.; Shirai, M.; Arai, M. *Green Chemistry* **2003**, *5*, 76.
- (19) Haubrich, J.; Loffreda, D.; Delbecq, F.; Sautet, P.; Jugnet, Y.; Becker, C.; Wandelt, K. *The Journal of Physical Chemistry C* **2009**, *114*, 1073.
- (20) Medlin, J. W. *ACS Catalysis* **2011**, *1*, 1284.
- (21) Marshall, S. T.; Horiuchi, C. M.; Zhang, W. Y.; Medlin, J. W. *Journal of Physical Chemistry C* **2008**, *112*, 20406.
- (22) Shirai, M.; Tanaka, T.; Arai, M. *Journal of Molecular Catalysis A: Chemical* **2001**, *168*, 99.
- (23) Delbecq, F.; Sautet, P. *Journal of Catalysis* **1995**, *152*, 217.

## CHAPTER 6

### Stability of Self-Assembled Monolayer Coated Pt/Al<sub>2</sub>O<sub>3</sub> Catalysts for Liquid Phase

#### Hydrogenation of Cinnamaldehyde

##### 6.1 Abstract

Thiolate self-assembled monolayers have recently been demonstrated to be effective catalyst modifiers for selectivity control, but these studies have not extensively explored the long term stability of these modifiers or the effects of specific reaction conditions. Here we investigate how the performance of thiolate-modified Pt/Al<sub>2</sub>O<sub>3</sub> catalysts are affected by recycling and regeneration, using the selective hydrogenation of cinnamaldehyde to cinnamyl alcohol as a probe reaction. Desorption and degradation of thiols on the catalyst surface is particularly concerning as it could result in a loss of selectivity improvement for modified catalysts. Although modification of Pt catalysts with 3-phenyl-1-propanethiol results in high selectivity due to a ligand specific interaction between modifier and reactant during the first catalyst use, repeated recycling was shown to decrease the efficacy of this mechanism by causing disorder in the monolayer, identified by infrared spectroscopy. However, selectivity and order could be stabilized with a thiol regeneration step. Similarly, aging in air was shown to decrease the order of the thiol and reduced the selectivity improvement of both a 3-phenyl-1-propanethiol and an octadecanethiol (C18) modified Pt/Al<sub>2</sub>O<sub>3</sub> catalyst. These studies show that the pliable nature of thiol modifiers makes ligand specific interactions between the SAM and the reactant particularly sensitive to conditions which might degrade the monolayer.

##### 6.2 Introduction

The ability to exert control over the selectivity of a reaction with numerous competing pathways is of paramount concern in catalysis for chemicals production<sup>1</sup>. Catalyst design plays a fundamental role in determining selectivity, where selection of the metal composition, metal loading, support, and particle shape can all influence the selectivity and reactivity<sup>2-5</sup>. It is equally important to consider the long-term stability of the catalyst; as design becomes more complicated, deterioration of the catalyst under reaction conditions becomes a growing concern. For example, the use of organic coatings in Chapters 2-5 was shown to be a successful method of catalyst modification, but these organic modifiers are a good example of a potentially fragile modifier<sup>6-8</sup>. Thiol self-assembled monolayers (SAMs) have been used as selectivity modifiers for their ability to covalently bind to a metal catalyst surface and enhance reaction selectivity through a combination of surface and near-surface effects<sup>9-13</sup>. Especially for ligand specific interactions such as those shown in Chapters 4 and 5, these modifications to the catalyst surface raise questions about durability over long reaction times or reuse in subsequent reactions. Moreover, studies of catalyst performance over time and under different environmental conditions can provide fundamental information about how interactions of reacting species with the near-surface environment influence selectivity.

As brief review, alkanethiols bind to a metal surface, such as that of a Pt catalyst, in a multistep process to form a self-assembled monolayer. The substrate metal is immersed in a dilute solution of typically 1-100mM of the intended thiol precursor, and a bulk diffusion process quickly saturates the surface followed by a slow reordering step which results in the SAM<sup>14,15</sup>. The thiols bind to the surface through a covalent bond between the sulfur atom and the metal constituting a strong bond, but one that is susceptible to degradation under harsh liquid phase

conditions, especially in the presence of H<sub>2</sub> as is the case in these liquid phase reaction studies<sup>16</sup>. A complete description of the formation of alkanethiols is provided in Chapter 1.2.2.

In Chapters 4 and 5, we showed that thiolate SAMs can be used to dramatically improve selectivity for the hydrogenation of cinnamaldehyde through a combination of ligand specific and ligand non-specific interactions<sup>13</sup>. High selectivity to the desired product cinnamyl alcohol was achieved by modifying the catalyst with a thiol (3-phenyl-1-propanethiol) which exhibited aromatic stacking interactions with the phenyl head group of cinnamaldehyde. It was shown that the 3-phenyl-1-propanethiol SAM is of the proper spacing such that non-covalent aromatic stacking interactions favor an adsorbate orientation that leads to carbonyl hydrogenation to form the desired product, cinnamyl alcohol. In addition to this ligand-specific effect, selectivity was also influenced by a non-specific surface effect induced by attachment of the thiolate sulfur atom to the metal surface.

Preliminary characterization of the cinnamaldehyde system showed that the selectivity changed upon re-use of the catalyst in subsequent reactions, aging of the prepared catalyst in air, and choice of solvent. Organic modifiers such as thiols are naturally susceptible to degradation, especially under harsh reaction conditions. For example, under hydrogenation reaction conditions in the liquid phase, it is expected that thiolates can undergo the reverse of the deposition reaction, i.e. that they will gradually desorb from the catalyst as thiols<sup>17</sup>. Despite the growing use of SAMs as catalyst modifiers for liquid phase reactions<sup>9,12,18,19</sup>, a systematic study of the effects of this phenomenon and its effect on catalysis has not yet been presented. Here we use the hydrogenation of cinnamaldehyde as a probe reaction to study how environmental conditions affect influence the structure and catalytic performance of SAM coated catalysts, and to identify methods can be used to moderate these effects.

## 6.3 Materials and Methods

6.3.1 Materials: A commercial 5 wt% Pt/Al<sub>2</sub>O<sub>3</sub> catalyst was purchased from Sigma Aldrich. 1-octadecanethiol (>99.5%) was purchased from Sigma Aldrich. 3-phenyl-1-propanethiol was purchased from MolPort (>95%). Ethanol (>99.5% anhydrous), used as solvent in reactions as well as for making ethanolic solutions of thiols for SAM deposition, tetrahydrofuran (>99.5%) used as internal standard, and the reactant cinnamaldehyde was also obtained from Sigma Aldrich. Gasses (hydrogen, oxygen, and helium) used for catalyst preparation and reaction were Airgas ultra-high purity.

6.3.2 Catalyst Preparation: SAM-coated catalysts were prepared from the as-purchased commercial 5wt% Pt/Al<sub>2</sub>O<sub>3</sub> catalyst using the methods described in Chapter 1.4.1 and used in Chapters 4 and 5. The catalyst (250 mg or less) was added to 40 mL of 10 mM thiophenol and 3-phenyl-1-propanethiol and 1 mM for octadecanethiol, deposited at a lower concentration due to reduced solubility of octadecanethiol in ethanol. Using the maximum amount of catalyst, the 1 mM concentration corresponds to a deposition of thiol at 10x the theoretical monolayer coverage assuming a packing structure of  $\sqrt{3}\sqrt{3}$  R30° on the active surface area of the catalyst. Active surface area was determined by chemisorption with carbon monoxide on a Quantachrome Autosorb-1and was determined to be 2.9 m<sup>2</sup>/g for uncoated 5 wt% Pt/Al<sub>2</sub>O<sub>3</sub>. As will be highlighted in this chapter, degradation of the catalysts was achieved by placing the catalyst uncovered in ambient laboratory conditions for the desired incubation time.

In some of the results described below, the catalyst was regenerated between reactions. In this regeneration procedure, the catalyst was deposited in an ethanolic solution of the thiol precursor under the same incubation time as was performed for the initial deposition. The concentration was reduced by half for the 3-phenyl-1-propanethiol coated catalyst and by a

factor of 10 for the octadecanethiol coated catalyst. Less thiol deposition was required since the surface still contained some thiols from the initial deposition, and to help stymie leaching of metal from the alumina support. In addition, using full thiol deposition concentrations rendered the rinse step less effective in removing physisorbed thiols, a condition easily noted by a significant decrease in the reaction rate. Due to the low solubility of octadecanethiol in ethanol, the rinse-removal of physisorbed thiols was paramount to preventing the accidental addition of thiol to the reaction solution.

6.3.3 Materials: All reactions shown were run in the 100 mL Parr batch reactor at 50°C and were pressurized to 40 bar with hydrogen gas. The reactor was prepared as done previously with 48 mL solvent, 5 mL THF internal standard, and 1 mL of cinnamaldehyde<sup>13</sup>. These proportions give an initial reactant concentration of approximately 0.15 M. For reactions of uncoated catalysts between 10 and 100 mg of catalyst were used, and for coated catalysts, up to 300 mg catalyst were used. For the catalysts submitted for ICP analysis, an initial loading of up to 500 mg of catalyst was used so that there would be enough catalyst to submit for quantification. These reactions were not used for kinetic data.

For recycle studies where thiol precursor was added to the reaction mixture, a dilute concentration of the thiol was added to the solvent/THF/reactant solution prior to the start of the reaction and was assumed to be a well-mixed additive to the reaction mixture.

6.3.4 Diffuse Reflectance Infrared Fourier Transform Spectroscopy (DRIFTS) Fourier Transform Infrared Spectroscopy analysis was performed with a Thermo Scientific Nicolet 6700 FT-IR. A Harrick closed cell Diffuse Reflectance Infrared Fourier Transform Spectroscopy (DRIFTS) attachment was used to take IR measurements. For each sample, 50 scans at 4 cm<sup>-1</sup> resolution were taken to compile the spectra. Approximately 50 mg of catalyst was used for

each measurement. Measurements of CO DRIFTS were taken using a vacuum cell at an initial pressure of <0.10 Torr. Carbon monoxide was dosed incrementally to the sample and allowed to equilibrate for 10 min before taking measurements. Multiple measurements were taken at increasing CO partial pressure to monitor the CO saturation of the surface. CO-DRIFTS spectra are reported at the last measurement before CO was observed in the gas phase.

6.3.5 Inductively Coupled Plasma/Optical Emission Spectroscopy (ICP/OES) Inductively Coupled Plasma experiments were performed to analyze the sulfur content and platinum content of catalysts after deposition. Samples were analyzed with an ARL 3410+ inductively coupled optical emission spectrometer (ICP-OES). A blank and three standards were used for calibration. Catalyst samples were dissolved by adding 5 ml of a 7:3 mixture of hydrochloric acid and hydrofluoric acid followed by 2 ml of nitric acid to the digestion tubes. The samples were then heated to 95° C in a digestion block (HotBlock by Environmental Express) for 2 hours. The samples were then cooled and brought up to 50 ml with a 1.5 wt% boric acid solution. Finally, the samples were reheated to 95° C for 15 min, and then cooled for analysis.

6.3.6 CO chemisorption of recycled catalysts Additional chemisorption experiments were carried out to determine how the active surface area, the dispersion, and Pt particle size were changing upon multiple recycle reactions. A Micrometrics Chemisorb 2720 was used with 20% CO in 80% Ar. Catalysts were prepared by degassing in 20 sccm Ar overnight at 150°C. Analysis of the surface area was performed at 40°C by dosing volumetric amounts of the CO/Ar mixture. Non-adsorbed CO was measured by a thermal conductivity detector until saturation was reached.

## 6.4 Results and Discussion

6.4.1 Recyclability of thiol SAM coated catalysts: The effects of recycling were investigated for three types of catalysts: an uncoated Pt/A<sub>2</sub>O<sub>3</sub>, an octadecanethiol (C18) coated Pt/A<sub>2</sub>O<sub>3</sub> catalyst, and a 3-phenyl-1-propanethiol coated Pt/A<sub>2</sub>O<sub>3</sub> catalyst. As discussed in the introduction, the C18 modifier has been associated with non-specific effects on selectivity in cinnamaldehyde hydrogenation, while the 3-phenyl-1-propanethiol coating exhibits enhancements in selectivity specific to the organic ligand. Post-reaction, the used catalysts were recovered by allowing them to settle out of solution, decanting the solution, and then drying the catalyst in air. In the most basic method of catalyst recycling, the catalyst was recycled in a fresh reaction mixture immediately following the drying step. Cinnamyl alcohol selectivity versus conversion plots for these catalysts are shown in Figure 6-1.

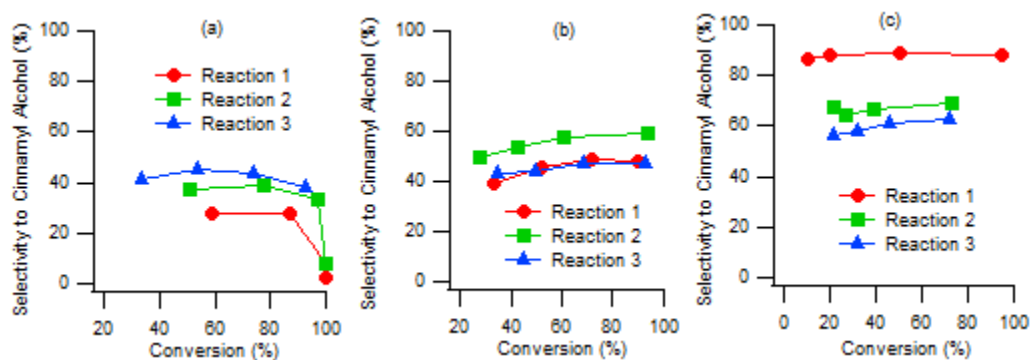


Figure 6-1: Recycle reactions for catalysts which were reused without any regeneration procedure. (a) uncoated catalyst (b) C18 coated catalyst (c) 3-phenyl-1-propanethiol coated catalyst. Error in selectivity is  $\pm 6\%$

Shown in Figure 6-1 (a), the uncoated Pt/Al<sub>2</sub>O<sub>3</sub> catalyst selectivity at 50% conversion improved after recycling from 28% to 45%, potentially due to coking of the catalyst surface. Partial coverage of the catalyst surface by spectator species may reduce the number of binding

sites and/or the binding affinity of the double bond in  $\alpha,\beta$ -unsaturated aldehydes<sup>2,20-23</sup>. The C18 coated catalyst selectivity showed little dependence on recycling, with selectivity remaining within experimental error during the three recycle reactions. The most dramatic effect of recycle was the decrease in selectivity for the 3-phenyl-1-propanethiol coated catalyst (Figure 6-1 (c)). Such a decrease in selectivity is consistent with the hypothesis that a ligand specific interaction is necessary to achieve high selectivity, and that this interaction effect is sensitive to subtle changes in the monolayer<sup>13</sup>. As the specific interaction effect of the thiol is compromised, the selectivity will decrease to parity with the non-specific selectivity improvement of the C18 coating. As seen in Figure 6-1, over the course of sequential recycle reactions, the selectivity of each catalyst do in fact converge towards 50% selectivity. This is consistent with the hypothesis that there is degradation of the ligand specific 3-phenyl-1-propanethiol interaction, but also that the selective poisoning of sulfur on the surface still results in selectivity improvement over that of the uncoated catalyst.

Table 6-1: Recycle procedures used for regenerating catalysts between reactions. For the recycle method of adding thiols to the reaction solution, the “Recycle with no regeneration” technique was used with thiol added to the reaction mixture.

<b>Recycle with no regeneration</b>	<b>Recycle with catalyst regeneration</b>
1 Run reaction	1 Run reaction
2 Allow catalyst to settle	2 Allow catalyst to settle
3 Decant reactant supernatant solution	3 Decant reactant supernatant solution
4 Dry in desiccator under vacuum	4 Dry in desiccator under vacuum
5 Run subsequent reaction	5 Deposit catalyst overnight in thiol solution
	6 Decant and rinse for 4 hours in ethanol
	7 Decant and dry catalyst in desiccator under vacuum
	8 Run subsequent reaction

We hypothesize that a critical factor to maintaining the performance of thiol-coated catalysts in solution is maintaining an adequate surface coverage of the thiolate under reaction conditions. Therefore, we used an alternative recycle method of regenerating the SAM coated catalysts before reusing them in a subsequent reaction, referred to as the “recycle-regeneration” procedure. Here, the catalysts were dried and decanted post-reaction and then immersed in a thiol solution similar to that used for initial deposition, but at a lower concentration (Chapter 6 methods section) to limit physisorption of thiols on the catalyst surface. This procedure was expected to replenish the thiols that had desorbed into the solution during reaction. In the case of the uncoated catalyst, pure ethanol containing no thiols was used for the immersion step.

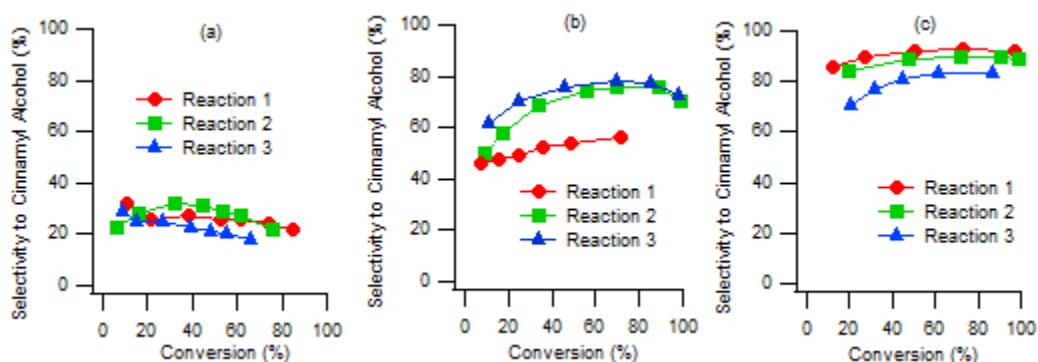


Figure 6-2: Recycle reactions for catalysts which were regenerated by re-depositing them in the thiol precursor. (a) uncoated catalyst, deposited and rinsed in pure ethanol (b) octadecanethiol coated catalyst (c) 3-phenyl-1-propanethiol coated catalyst

Shown in Figure 6-2 (a), rinsing of the uncoated catalyst with ethanol after recycle resulted in a near-constant selectivity at ca. 30% for all runs, in contrast to the procedure of simply re-using the catalyst without an ethanol rinse (Figure 6-1). This result suggests that the ethanol rinse served to remove carbonaceous species that had a beneficial effect on selectivity. The C18 coated catalyst was greatly influenced by this recycle-regeneration procedure, which

saw the selectivity increase from 50% to 79% selectivity during the 3<sup>rd</sup> reaction. The selectivity of the 3-phenyl-1-propanethiol coated catalyst at 50% conversion fell somewhat from 93% in the first reaction to 82% by the third reaction, but the decrease was not as large as the decrease seen for the original recycle discussed in Figure 6-1.

Another method of maintaining the thiolate surface coverage, and thus the efficacy, of a thiol coated catalyst was to add thiol to the reaction solution at a dilute concentration. This recycle technique has already been described in ref.<sup>13</sup> but is treated in further detail here with rate data and surface characterization to complement the discussion of recycle techniques. The technique of adding thiols to the reaction solution has been used for the hydrogenation of epoxybutene in ethanol<sup>18</sup>, a system where addition of thiol was hypothesized to maintain a critical equilibrium coverage of thiol in the reaction solvent. One of the key effects observed in this method was a sharp decrease in the rate, likely due to thiol outcompeting reactant for surface sites. Shown in Figure 6-3, very dilute concentrations of thiols, 0.005 mM C18 and 0.3 mM 3-phenyl-1-propanethiol, were used in the reaction mixture to minimize the decrease in reaction rate while still allowing the study of reaction selectivity.

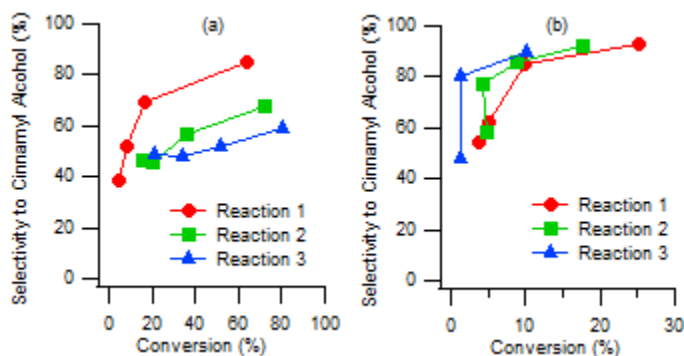


Figure 6-3: Recycle reactions where thiol was added to the reaction mixture (a) C18 coated Pt/Al<sub>2</sub>O<sub>3</sub> with 0.005 mM C18 added to the reaction solution (b) 3-phenyl-1-

propanethiol coated Pt/Al<sub>2</sub>O<sub>3</sub> with 0.3 mM 3-phenyl-1-propanethiol added to the reaction solution. Adapted from ref.<sup>13</sup>

Here, the C18-coated catalyst showed a higher selectivity for the first reaction than a C18 coated catalyst run in a pure solvent, although this increase was observed only for the first reaction after which it returned to the range of 50% which had been seen for a fresh C18 coated catalyst in a pure reaction mixture.

The 3-phenyl-1-propanthiol coated catalyst retained high selectivity when thiols were added to the reaction mixture, as shown in shown in Figure 6-3 (b). In contrast to a pure recycle, this method of introducing thiols to the reaction mixture shows that selectivity can be maintained, potentially as a method of compensating for desorption of thiols into reaction solution. However, this method of improving selectivity can potentially decrease the rate of reaction, an undesirable effect discussed next.

By coating a catalyst surface, thiol SAMs naturally reduce the rate of reaction as compared to an uncoated catalyst<sup>10</sup> similar to other methods of blocking surface sites, such as coking<sup>24</sup>. This simple effect is shown in Figure 6-4 (a) where, for the first reaction, the rate of reaction for the coated catalysts are approximately 1/3 of the rate of the uncoated catalyst. In subsequent reactions, the hydrogenation rate over the uncoated catalyst decreases, so that by the third reaction its rate is within experimental error of the octadecanethiol coated catalyst, and approaching that of the 3-phenyl-1-propanethiol coated catalyst. This trend was consistent with the convergence of the selectivities of the uncoated, octadecanethiol coated, and 3-phenyl-1-propanethiol coated catalysts shown in Figure 6-1, for the basic recycle procedure. This shows

that both uncoated and SAM coated catalysts converge on similar reaction rates and selectivities upon multiple recycles.

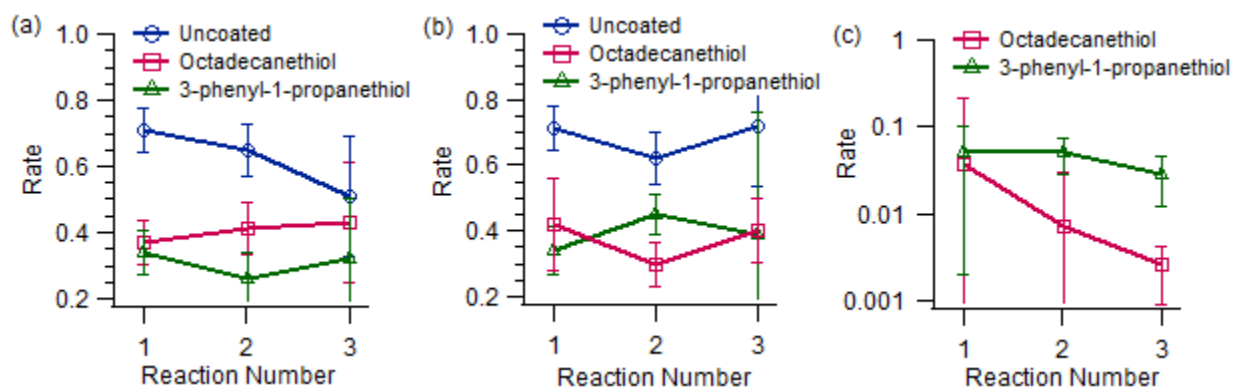


Figure 6-4: Rate data for each of the recycle procedures. (a) Recycle without regeneration (b) recycle with catalyst regeneration (c) recycle with thiols added to the reaction mixture. All rates were calculated as the moles of reactant (cinnamaldehyde) consumed per surface site of an uncoated Pt/Al<sub>2</sub>O<sub>3</sub> catalyst per second.

For the recycle-regeneration procedure, shown in Figure 6-4 (b), catalyst activity was stabilized, an effect particularly telling for the uncoated catalyst. The regeneration for the uncoated catalyst (methods section), which consisted of a rinse in pure ethanol, stabilized the rate and the selectivity, shown in Figure 6-2 (a), indicating that carbonaceous deposits left on the catalyst surface could be eliminated with the ethanol wash. The rates for the coated catalysts, shown in Figure 6-4 (b), were also stabilized with the recycle-regeneration procedure. The lack of change in the rate for the octadecanethiol coated catalyst is surprising when considering that the recycle regeneration procedure increased the selectivity of this reaction from 50% to 79%. Typically for an increase in selectivity over a thiol-coated catalyst, there would be an accompanying decrease in the rate of the reaction due to termination of an undesirable pathway.

Possible explanations for this behavior are discussed below. The rate of the 3-phenyl-1-propanethiol-coated catalyst was also stabilized for the regeneration-recycle procedure, but with a slight decrease in selectivity. This decrease might be due to degradation of the ligand specific interaction between the SAM and cinnamaldehyde as well as buildup of carbonaceous material on the surface of the catalyst, discussed in section 6.4.2.

Finally, the procedure of adding thiols to the reaction mixture was shown to have a significantly deleterious effect on the rate of reaction. Shown in Figure 6-4 (c), C18 was added to the reactor at the lowest consistently measurable dose of 0.005 mM. Here, the rate of the first reaction was within experimental error of the C18 catalyst case; however, subsequent dosing resulted in a dramatic decrease in the rate to nearly immeasurable values. High concentrations, not shown, completely suppressed the reaction yielding no conversion over a 60 min reaction. The 3-phenyl-1-propanethiol rate was relatively stable with 0.3 mM thiol in the reaction solution, decreasing by a factor of 3. Such decreases in rate for this procedure were consistent with previous studies where thiols have highly competitive affinity for the near surface region<sup>18</sup>. Thus, the method of including thiols in the reaction mixture appears to offer promise for maintaining high selectivity, but the concentration must be finely tuned to prevent significant loss of activity.

6.4.2 Characterization of recycled catalysts In order to measure the coverage of thiols on the catalyst surface and monitor potential coking, diffuse reflectance infrared Fourier transform spectroscopy (DRIFTS) was used to study two infrared regions of interest, the carbonyl C=O stretching region from 1550-1750  $\text{cm}^{-1}$  and the hydrocarbon C-H stretching region from 2850-3150  $\text{cm}^{-1}$ . These regions were used to characterize the order of the SAM layer, to identify the presence of remaining carbonyl species from the reaction and to measure carbonaceous species

left over from decomposed solvent or reactants. As shown in Figure 6-5 (a), the pre-reaction uncoated catalyst, as expected, showed no significant peaks in either the C-H stretching region or the C=O stretching region, with only a small hump at  $1650\text{ cm}^{-1}$  from the beginning of the platinum fingerprint region. Recycling the catalyst without regeneration led to organic deposits in both of these regions. Post reaction spectra showed the presence of an aldehyde stretch at  $1675\text{ cm}^{-1}$  indicating some remaining aldehyde, as well as C-H stretches between  $3000\text{ cm}^{-1}$  and  $3100\text{ cm}^{-1}$  indicating the presence of hydrocarbons deposited in the reaction mixture.

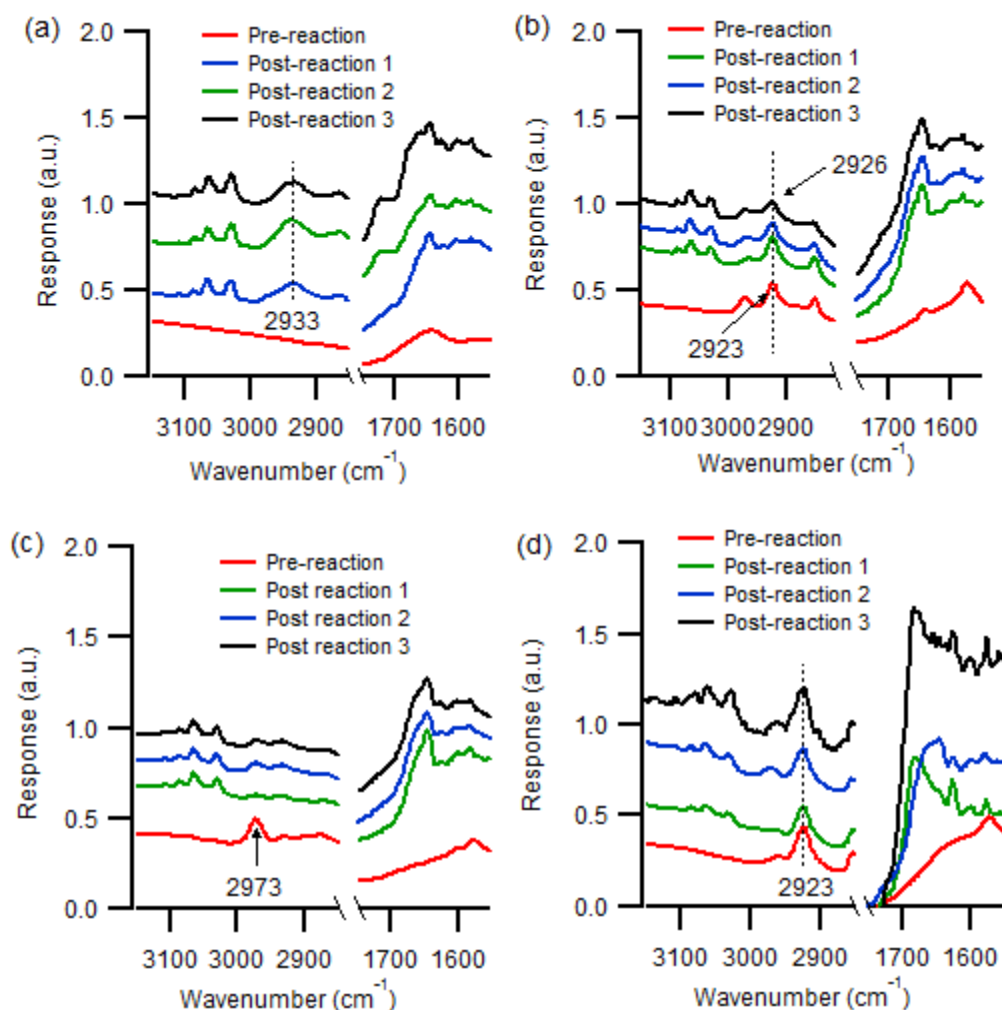


Figure 6-5: DRIFTS spectra of catalysts before reaction 1 and after reactions 1, 2, and 3 for catalyst recycle with no regeneration or thiol added to the reaction solution.

Reactions run with ethanol solvent over (a) uncoated Pt/Al<sub>2</sub>O<sub>3</sub>, (b) C18 coated Pt/Al<sub>2</sub>O<sub>3</sub>, (c) 3-phenyl-1-propanethiol coated Pt/Al<sub>2</sub>O<sub>3</sub>, (d) C18 coated Pt/Al<sub>2</sub>O<sub>3</sub> with added 0.005M thiol added to the reaction mixture. The peak at 1670 cm<sup>-1</sup> indicates the presence of aldehyde on the recycled catalyst surface. The peaks between 3000 cm<sup>-1</sup> and 3100 cm<sup>-1</sup> indicate the presence of hydrocarbons on the catalyst surface.

For the C18-coated catalysts, the C-H stretching region is particularly valuable for characterizing the ordering of the SAM. The peak position of the asymmetric methylene stretch ( $\nu_a$ ) is related to the intrinsic order within an alkanethiol SAM, where a lower frequency indicates higher crystallinity and greater order within the monolayer<sup>15,25-28</sup>. In Figure 6-5 (b) for the non-regeneration recycle, the asymmetric methylene stretch was observed on the pre-reaction catalyst at 2923 cm<sup>-1</sup> and increased to 2926 cm<sup>-1</sup> after reaction 3, indicating a decrease in the order of the alkanethiol monolayer, though the intensity was relatively constant<sup>25</sup>. The 3-phenyl-1-propanethiol monolayer, shown in Figure 6-5 (c), exhibited an alkyl CH stretch at 2973 cm<sup>-1</sup> that decreased significantly in magnitude after the first reaction. Such a change in the IR spectrum is indicative of a change in the structure of the 3-phenyl-1-propanethiol coating, and is correlated to a decrease in efficacy. Interestingly, as shown in Figure 6-5 (d), the procedure of adding octadecanethiol to the reaction mixture was able to maintain the  $\nu_a$  peak position at 2923 cm<sup>-1</sup> even though this case resulted in a dramatic reduction in the rate of reaction.

The recycle regeneration procedure showed the ability to stabilize the selectivity of the uncoated and 3-phenyl-1-propanethiol coated catalyst and to increase the selectivity of the octadecanethiol coated catalyst. The DRIFT spectra shown in Figure 6-6 were collected for the

catalyst before the first reaction, after the second reaction, after the second reaction regeneration (pre-run 3), and after the third reaction. As discussed above, the “regeneration” of an uncoated catalyst involved immersion of the catalyst in an ethanol solution prior to re-use, followed by an ethanol rinse of the catalyst. This recycle procedure was shown to decrease the intensity of peaks in the hydrocarbon region and the aldehyde region, for example comparing the post-reaction 2 spectra of Figure 6-6 (a) to the pre-reaction 3 spectra. Considering this in conjunction with the stabilization of the rate and selectivity data, this indicates that ethanol was likely effective in removing some of the hydrocarbons deposited from the previous reaction and restoring the surface of the uncoated catalyst.

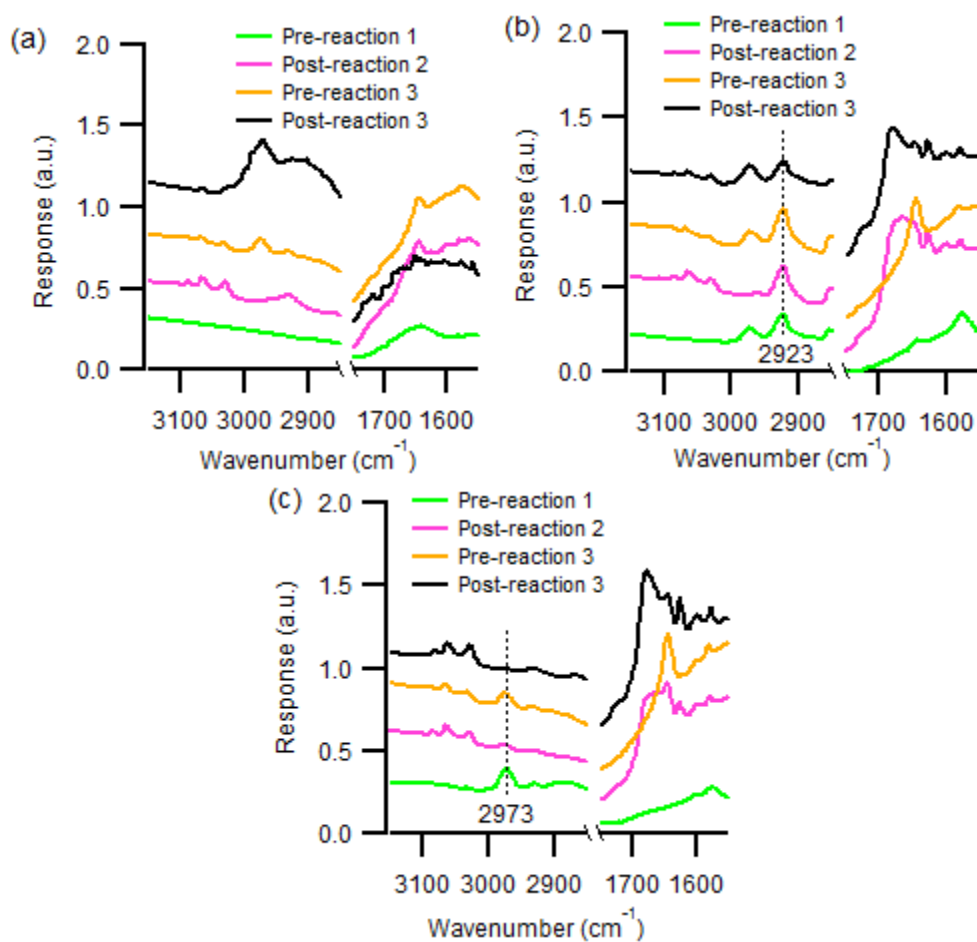


Figure 6-6: DRIFTS spectra of catalysts having undergone a recycle-regeneration procedure. (a) uncoated Pt/Al<sub>2</sub>O<sub>3</sub> (b) octadecanethiol coated Pt/Al<sub>2</sub>O<sub>3</sub> (c) 3-phenyl-1-propanethiol coated Pt/Al<sub>2</sub>O<sub>3</sub>

One of the key points of interest in section 6.4.1 was the recycle regeneration procedure for octadecanethiol which was shown to result in an increase in the selectivity of the reaction to cinnamyl alcohol. The DRIFT spectra in Figure 6-6 (b) show some removal of organic species from the catalyst during the regeneration procedure after reaction 2 and before reaction 3, as indicated by the decrease in the C-H peaks between 3000 cm<sup>-1</sup> and 3100 cm<sup>-1</sup> and the decrease of the aldehyde stretch at 1685cm<sup>-1</sup>. The asymmetric methylene stretch stayed constant at 2923 cm<sup>-1</sup> for all four spectra indicating that the initial order of the monolayer is maintained. Thus, the increase in selectivity observed for this catalyst system is not obviously related to changes in the DRIFT spectra. Attempts were made to understand the increase in selectivity of the recycle regenerated octadecanethiol coated catalyst by targeting potentially specific causes of the increase. For example, cinnamaldehyde was co-deposited with a C18 catalyst to test for imprinting of the catalyst surface as might occur under reaction conditions. C18-coated catalysts were also deposited at the reaction temperature of 50°C to mimic the potential ordering that might occur during reaction, which is at 50°C. None of these procedures increased the selectivity of the C18 catalyst to more than 50%, the same value seen for a standard C18 deposit.

Finally, the 3-phenyl-1-propanethiol coated catalyst, having shown a loss of its signature methylene stretch at 2973 cm<sup>-1</sup> post reaction was restored with the recycle regeneration procedure, although some coking was still observable on the catalyst surface. This indicated that

the redeposit procedure could mostly restore the ligand specific properties of the initial 3-phenyl-1-propanethiol coated catalyst (also shown by the selectivity data in Figure 6-2 (c)), but was slightly inhibited by some remaining organic material on the catalyst surface.

The catalyst surface was explored further by studying the effect of regeneration recycle reactions on available surface sites using a CO-DRIFTS technique<sup>29,30</sup>. With this technique, CO is adsorbed on the catalyst surface to characterize the accessible surface sites. Here, lower frequencies are indicative of stronger CO-surface binding. As seen in Figure 6-7 (a), the CO stretch at 1805  $\text{cm}^{-1}$  is associated with the most stable CO binding configuration on the uncoated catalyst, the threefold hollow site, which shifts to higher wavenumber, 1846  $\text{cm}^{-1}$ , after reaction.

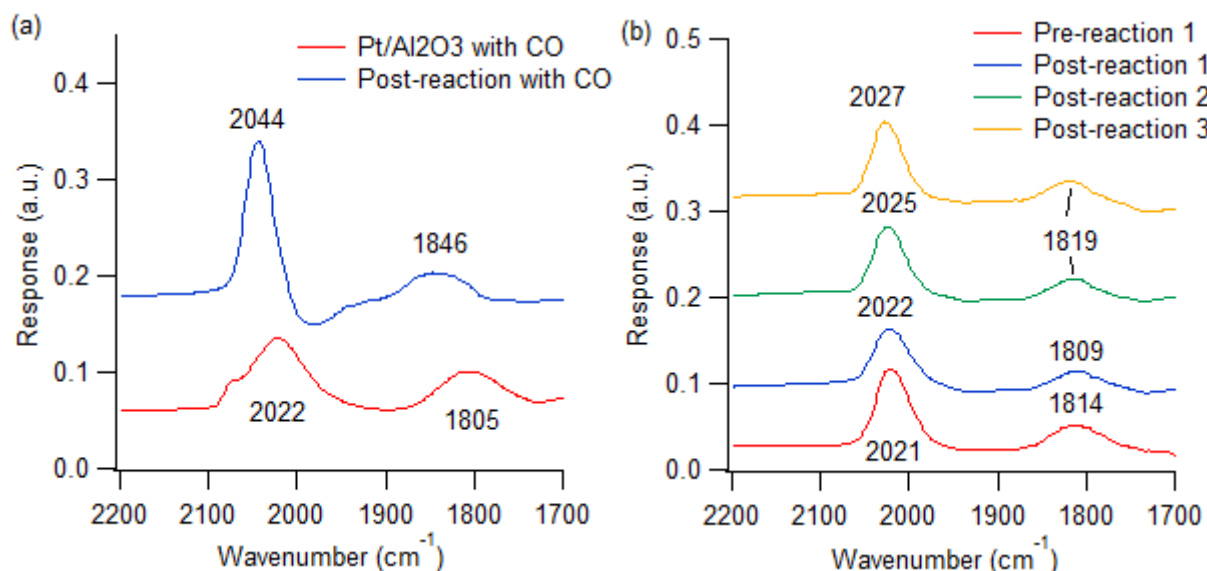


Figure 6-7: CO-DRIFTS of an (a) uncoated catalyst and (b) C18 coated catalyst before and after reaction of cinnamaldehyde solvated in ethanol. All dosings shown are at 500 mtorr CO

In contrast to the destabilized binding on the uncoated catalyst, the CO stretching frequency on the C18 catalyst is largely unaffected; as shown in Figure 6-7 (b), that frequency remains at  $1814 \pm 5 \text{ cm}^{-1}$ . The change observed for the uncoated catalyst suggests a coking of stable sites whereas the stabilization of this peak on the C18 coated catalyst indicates that such sites are preserved across reactions. Similarly, the binding of CO to edge sites, indicated by the peaks at  $\sim 2022 \text{ cm}^{-1}$  shift to higher wavenumber,  $2044 \text{ cm}^{-1}$  on the uncoated catalyst, but remain at  $2022 \text{ cm}^{-1}$  on the C18 coated catalyst, again indicating the preservation of more stable binding configurations on the C18 coated catalyst. These data indicate that the addition of a thiol monolayer creates surface sites that are more stable against changes during reaction.

To further characterize the recycle system, inductively coupled plasma optical emission spectroscopy (ICP-OES) was carried out on the C18 coated catalyst for the recycle regeneration procedure to measure the change in the weight loading of Pt and the loading of sulfur on the catalyst surface. Figure 6-8 displays these data as compared to the theoretical weight loading and theoretical sulfur coverage. Theoretical calculations were based on the as purchased 5wt% Pt/ $\text{Al}_2\text{O}_3$  and the theoretical coverage of 1/3 of a monolayer of sulfur on the surface, 0.05 sulfur atoms per  $\text{\AA}^2$  or a weight loading of  $7 \times 10^{-4}$  wt%.

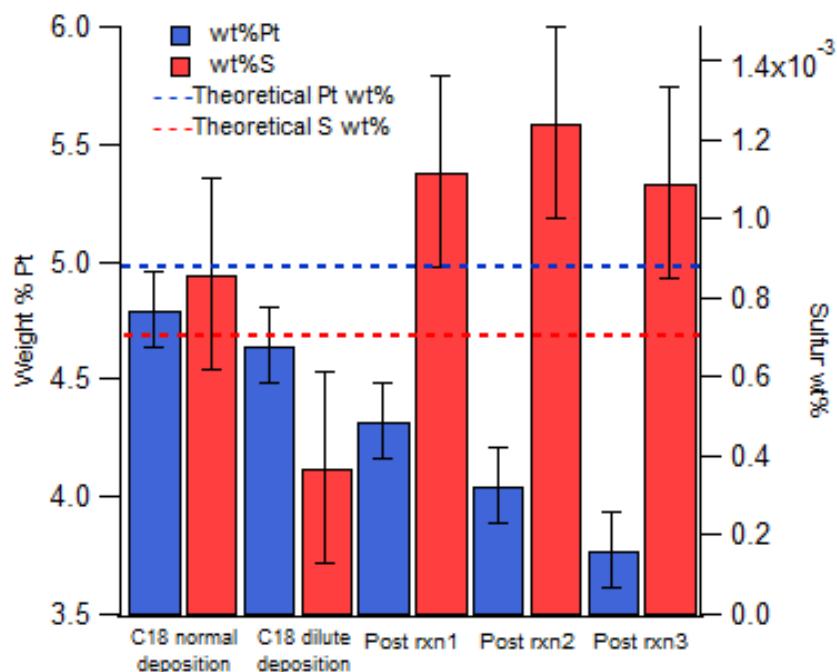


Figure 6-8: ICP-AES analysis of C18 coated catalysts. “C18 normal deposition” is the standard deposit procedure used for the catalysts throughout this study corresponding to thiol deposition concentration ca. 10x the theoretical coverage of thiol. C18 dilute deposit is the same deposition procedure but using ca. 1x theoretical coverage of thiol. Post reaction C18 catalysts were analyzed after the decanting step.

As shown in Figure 6-8, the C18 coated catalyst was analyzed after the standard deposition procedure and was then run and recycled with the regeneration procedure to generate the catalysts which were analyzed following reactions 1, 2, and 3.

The most striking trend from the ICP analysis is the decrease in metal loading of the catalysts across subsequent reactions. As a catalyst proceeds through numerous reactions, decanting steps and recycle procedures while in the presence of a thiol ligand, there is a strong

driving force for some of the metal to be detached from the alumina support and decanted with supernatant liquid. Thiols are particularly good at stabilizing nanoparticles in solution, often being used for just this purpose<sup>31</sup>, and likely contribute to the dissolution of Pt from the alumina support<sup>32</sup>. For example, such catalyst leaching to create monolayer protected clusters (MPCs) has been shown before for a 3-mercaptopropyl-functionalized silica support which self-quenched soluble palladium<sup>33</sup>. This effect may provide an explanation for the increase in selectivity observed for the regeneration recycle procedure since smaller nanoparticles are more likely to be leached from the alumina support<sup>34</sup>. CO chemisorption results (Table 6-2) indicate that the recycle regeneration procedure decreases the dispersion and surface area of the C18 catalyst, consistent with the hypothesis that smaller particles are preferentially removed.

Table 6-2: CO chemisorption of C18 coated and recycled catalysts. Metal loading determined from ICP. The final catalyst was oxidized in 80:20 He:O<sub>2</sub> for 3 hours at 300°C and then reduced in 80:20 He:H<sub>2</sub> for 2 hours at 200°C.

<b>Catalyst</b>	<b>wt%Pt</b>	<b>Dispersion (%)</b>	<b>SA (m<sup>2</sup>/g Pt)</b>
C18 coated Pt	4.93	6.6	16.2
C18 recycle regen 3x	3.77	1.4	3.5
C18 recycle regen 3x re/ox	3.77	25.4	62.8
Uncoated Pt	5.00	40.8	100.7

Here, the C18-coated catalyst shows that the surface area and dispersion decrease after 3 recycle reactions even when taking into account the loss of metal content. As further verification, the recycle regenerated catalyst was oxidized and reduced to return it to a clean surface where it could be compared with a fresh uncoated Pt/Al<sub>2</sub>O<sub>3</sub> catalyst. These data also

showed a significant decrease in active surface area and dispersion when taking into account loss of metal content. A simple factor such as coking of the catalyst surface could result in the decrease in surface area, but when considering each of these cases, both with thiol and cleaned, the data suggest that there is a loss of small metal particles, leaving larger particles behind which have less surface area per mass. Crucially, smaller Pt particles have been shown to have the lowest selectivity for  $\alpha,\beta$ -unsaturated aldehyde hydrogenation, whereas large particles with a higher percentage of flat surface, such as those potentially left behind, have naturally higher selectivity to unsaturated alcohols<sup>2,35</sup>. Overall, the chemisorption and ICP data combined with the reactivity results suggest that the recycle and regeneration procedure can facilitate the leaching of small metal nanoparticles into solution.

In this and our other studies, the initial deposition concentration of thiol used for preparation of the coated catalysts is typically 10x the thiol necessary to generate one theoretical monolayer of coverage. This seemingly high concentration, though potentially responsible for some leaching of platinum from the alumina, is necessary to ensure a complete monolayer of coverage. For comparison, a “dilute deposit” of C18 on a Pt/Al<sub>2</sub>O<sub>3</sub> catalyst was prepared using a concentration of thiol necessary to generate only 1x the theoretical monolayer. Shown in Figure 6-8, this deposition procedure, labeled “C18 dilute deposition”, shows that too little thiol in the initial deposition procedure can result in insufficient thiol adsorption, as indicated by the sulfur coverage being significantly less than what would be required to form one monolayer of theoretical sulfur coverage. In order to temper the effect of oversaturating the surface with thiol during the regeneration-recycle procedure, a lower concentration of thiol was used for regeneration depositions (methods section) but the ICP analysis indicated that this still resulted in significant leaching of metal from the alumina support.

The full effect of metal leaching during deposition was measured by making catalyst and then subsequently re-depositing it without running it in a reaction. This experiment was performed to identify how each of the subsequent recycle steps was affecting the leaching of metal. Shown in Figure 6-9, ICP analysis from a series of sequential depositions show a decrease in metal content for each of the catalyst systems.

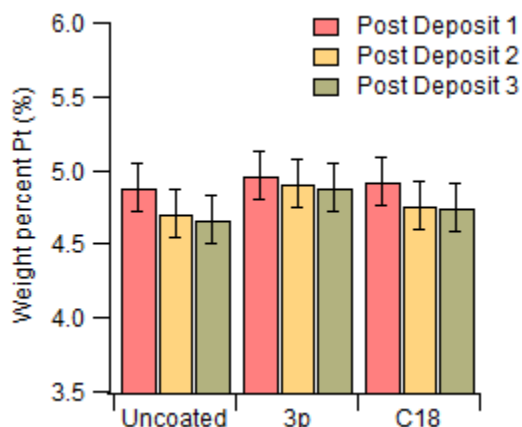


Figure 6-9: ICP-AES analysis for uncoated, 3-phenyl-1-propanethiol coated and C18 coated catalysts which were re-deposited without running reactions.

Here, simply re-depositing a coating contributes to a loss of metal content. In fact, even the uncoated catalyst, where deposition was merely rinsing of the catalyst in ethanol, resulted in a decreased weight loading. In order to test how different thiols have different effects on leaching of metal, the recycle regeneration procedure was completed for each of the catalysts. Shown in Figure 6-10, the regeneration recycle procedure resulted in the greatest loss of metal content for the C18 catalyst, but the recycle of the 3-phenyl-1-propanethiol and the uncoated catalysts also saw loss of metal content during recycle regeneration reactions, greater than the loss for a simple redeposit.

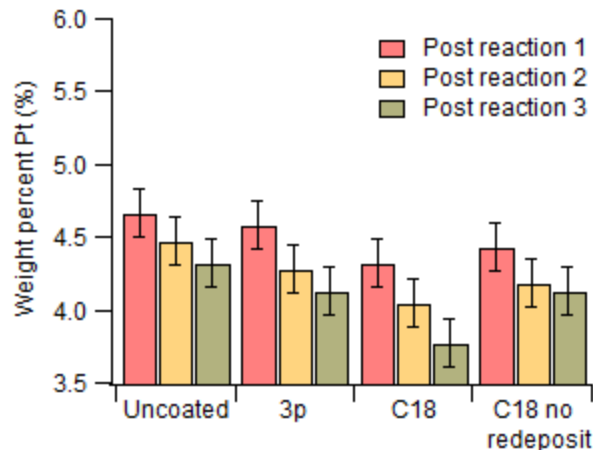


Figure 6-10: ICP-AES analysis recycle regeneration reactions for uncoated, 3-phenyl-1-propanethiol coated and C18 coated catalysts. For comparison, a recycle of the C18 catalyst with no regeneration/redeposit step is included.

This ICP data combined with the CO chemisorption experiments show that each of the steps involved in recycle result in loss of metal content and when combined, the loss is exacerbated. This effect is greatest for the C18 catalyst, but all of the catalysts are affected by such losses of metal content which are likely to be responsible for changes in the performance of the catalyst during subsequent recycle reactions. In the case of the C18 catalyst, the loss of metal content is through the leaching of small Pt particles.

A less pronounced effect was the increase in sulfur content for recycled reactions, shown in Figure 6-8. The three recycled catalysts each show sulfur content higher than the theoretical coverage of sulfur and higher than the initial deposition coverage indicating that the recycle-redeposit procedure is increasing the total amount of sulfur relative to total metal. Physisorbed thiols, those not bound to the metal surface, could explain the increased measurement of sulfur;

however, a control was performed by depositing octadecanethiol on a blank alumina support which showed no sulfur in subsequent ICP analysis. In addition, the sulfur content of each of the regenerated catalysts was shown to be constant indicating that there was no significant change in sulfur loading between different recycle procedures, regeneration procedures, or iterations of these procedures. This effect is especially important when considering the ICP and CO chemisorption data that indicate a decreasing surface area across recycled catalysts. For the surface area to be decreasing but the sulfur loading to stay the same, the sulfur must be going somewhere other than the surface.

This excess sulfur content could be described by sulfur breaking from its alkane ligand and diffusing into the bulk Pt metal<sup>36</sup>. If, as hypothesized, leaching of small metal nanoparticles is responsible for the loss of metal loading and increase in reaction selectivity, then the larger nanoparticles left behind would have less surface area per mass to hold sulfur atoms. The only way the remaining Pt could then hold the extra sulfur would be if it were to allow sulfur in the bulk.

Taken as a whole, the recycle procedures can be effective means of stabilizing a thiol coated catalyst, but can result in various changes to the morphology of the catalyst including the metal loading, the size distribution of particles, and the relative sulfur content.

6.4.3 Effects of SAM aging in air: The recyclability of thiol SAM coated catalysts lends insight into the sensitivity of reaction selectivity on the detailed structure of the catalytic interface. Another possible way in which that interface can be perturbed is through SAM degradation in air between or before reaction<sup>37</sup>. It was previously shown<sup>13</sup> that aging a 3-phenyl-

1-propanethiol coated catalyst in air decreased its selectivity to cinnamyl alcohol. A detailed investigation of this effect is reported in Figure 6-11 (a).

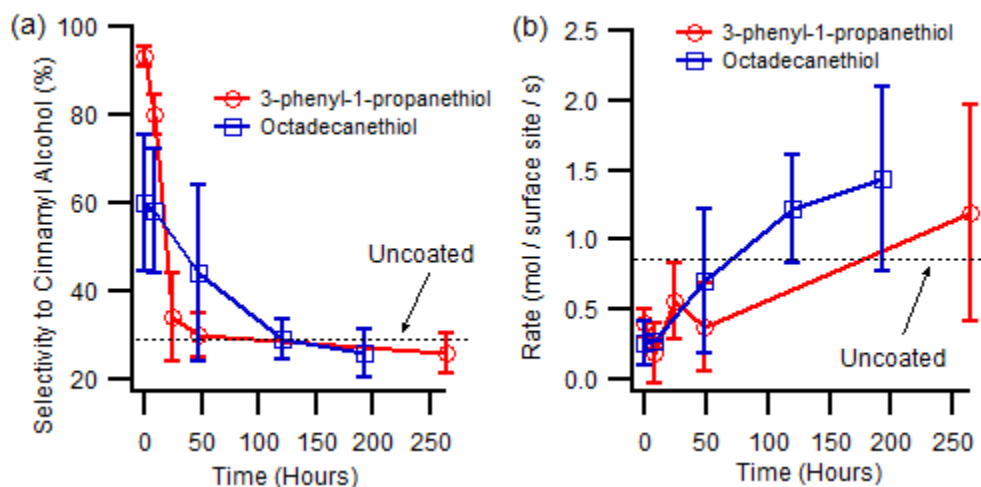


Figure 6-11: Effect of aging in air of 3-phenyl-1-propanethiol coated and C18 coated Pt/Al<sub>2</sub>O<sub>3</sub> catalysts on the (a) reaction selectivity and (b) reaction activity

The cinnamyl alcohol selectivity for the 3-phenyl-1-propanethiol coated catalyst decreased sharply from 94% to 38% in only 24 hr of air exposure and continued to decrease below the selectivity of an uncoated catalyst. The C18-coated catalyst also showed a susceptibility to aging in air, but the change in selectivity was more gradual with aging time. The differing selectivity decline for these two catalysts can be explained by their differing modes of selectivity enhancement. The 3-phenyl-1-propanethiol coated catalyst was shown to have an inherently high selectivity due to the ligand specific interaction exhibited between the phenyl ring of the thiol and the phenyl ring of the cinnamaldehyde. Only a slight decrease in the order of the thiol monolayer would have a significant impact on the selectivity of the catalyst, since the spacing of the phenyl ring from the surface was shown to be paramount to the ligand specific interaction. In contrast, the C18-coated catalyst, which was shown to non-specifically improve

the selectivity to cinnamyl alcohol, largely through the presence of the sulfur head group, was not as immediately susceptible to aging. Still, over time, both showed a decrease in selectivity suggesting that thiol-coated catalysts stored in the presence of oxygen or light should be used within a relatively short time period after preparation, and exposure to these oxidative species should be limited. In addition, over long time periods, the rates for both the C18 coated and the 3-phenyl-1-propanethiol coated catalysts increased, indicating greater cinnamaldehyde access to the surface. These results might also explain some of the losses in selectivity between recycle reactions as the catalysts were exposed to air during the catalyst-recycle procedure. Alkanethiols on flat Pd surfaces have been shown to be stable in air for 2-5 days<sup>25</sup>, and largely unchanged on flat Pt surfaces for 7 days<sup>15</sup>, but when used to modify supported metal catalysts, they appear to degrade more quickly.

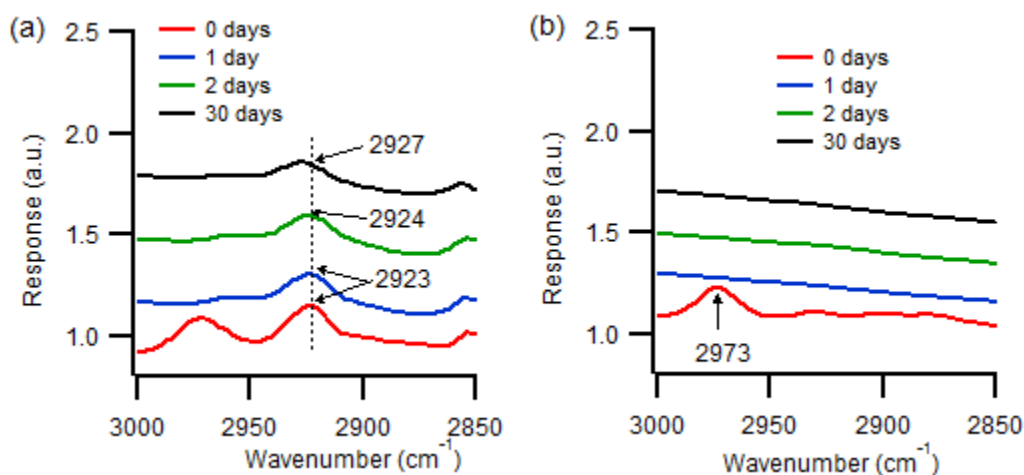


Figure 6-12: DRIFTS of an (a) C18 coated catalyst and (b) a 3-phenyl-1-propanethiol coated catalyst aged in ambient laboratory conditions

Shown in Figure 6-12 (a), DRIFTS analysis of the aged C18 catalyst over a month shows a shift in the asymmetric methylene stretch from the initial value of 2923 cm<sup>-1</sup> to 2927 cm<sup>-1</sup>,

indicative of deterioration in the order of the monolayer<sup>10,25</sup>. Aging of the 3-phenyl-1-propanethiol catalyst for just one day results in total loss of the C-H peak at 2973 cm<sup>-1</sup>. Unlike C18, the C-H stretching region for the 3-phenyl-1-propanethiol shown in Figure 6-12 (b) is not related to the order of the SAM, but still suggests a change in the monolayer.

## 6.5 Conclusions

The modification of Pt/Al<sub>2</sub>O<sub>3</sub> with thiol SAMs for controlling cinnamaldehyde hydrogenation has been further characterized. Recycling of spent catalysts showed a decrease in efficacy for ligand specific thiols, but selectivity could be largely regenerated by depositing the spent catalyst in a fresh thiol deposition. In contrast, the C18-coated catalyst did not show a decrease in selectivity upon ordinary recycle, but with the regeneration procedure showed an increase in reaction selectivity. It was shown that over multiple recycles, this procedure led to a decrease of metal loading and an increase in sulfur loading as indicated by ICP-OES analysis. CO chemisorption of these recycle regenerated C18-coated catalysts revealed a loss of surface area suggesting leaching of small Pt particles across recycle reactions. Aging of catalyst in air was shown to be an important effect for both selectivity and activity as the selectivity of a freshly prepared 3-phenyl-1-propanethiol coated Pt/Al<sub>2</sub>O<sub>3</sub> decreased from greater than 90% to less than 20% when aged for more than 2 days. C18 coated catalysts also showed a decrease in selectivity with aging in air but not as rapid of a decrease.

## 6.6 References

(1) de Jong, K. P. *Synthesis of solid catalysts*; Wiley-VCH: Darmstadt, 2009.

- (2) Gallezot, P.; Richard, D. *Catalysis Reviews* **1998**, *40*, 81.
- (3) da Silva, A. B.; Jordão, E.; Mendes, M. J.; Fouilloux, P. *Applied Catalysis A: General* **1997**, *148*, 253.
- (4) Lee, I.; Delbecq, F.; Morales, R.; Albiter, M. A.; Zaera, F. *Nat Mater* **2009**, *8*, 132.
- (5) Rajadhyaksha, R. A.; Karwa, S. L. *Chemical Engineering Science* **1986**, *41*, 1765.
- (6) Wu, B.; Huang, H.; Yang, J.; Zheng, N.; Fu, G. *Angewandte Chemie International Edition* **2012**, *51*, 3440.
- (7) Kwon, S. G.; Krylova, G.; Sumer, A.; Schwartz, M. M.; Bunel, E. E.; Marshall, C. L.; Chattopadhyay, S.; Lee, B.; Jellinek, J.; Shevchenko, E. V. *Nano Lett.* **2012**, *12*, 5382.
- (8) Snelders, D. J. M.; Yan, N.; Gan, W.; Laurency, G.; Dyson, P. J. *ACS Catalysis* **2011**, *2*, 201.
- (9) Taguchi, T.; Isozaki, K.; Miki, K. *Adv. Mater.* **2012**, *24*, 6462.
- (10) Marshall, S. T.; O'Brien, M.; Oetter, B.; Corpuz, A.; Richards, R. M.; Schwartz, D. K.; Medlin, J. W. *Nat. Mater.* **2010**, *9*, 853.
- (11) Kahsar, K. R.; Schwartz, D. K.; Medlin, J. W. *Applied Catalysis A: General* **2012**.
- (12) Makosch, M.; Lin, W.-I.; Bumbálek, V.; Sá, J.; Medlin, J. W.; Hungerbühler, K.; van Bokhoven, J. A. *ACS Catalysis* **2012**, *2*, 2079.
- (13) Kahsar, K. R.; Schwartz, D. K.; Medlin, J. W. *Journal of the American Chemical Society* **2013**, *136*, 520.
- (14) Schwartz, D. K. *Annual Review of Physical Chemistry* **2001**, *52*, 107.
- (15) Petrovykh, D. Y.; Kimura-Suda, H.; Opdahl, A.; Richter, L. J.; Tarlov, M. J.; Whitman, L. J. *Langmuir* **2006**, *22*, 2578.

- (16) Kodama, C.; Hayashi, T.; Nozoye, H. *Applied Surface Science* **2001**, *169–170*, 264.
- (17) Schlenoff, J. B.; Li, M.; Ly, H. *Journal of the American Chemical Society* **1995**, *117*, 12528.
- (18) Kahsar, K. R.; Schwartz, D. K.; Medlin, J. W. *Applied Catalysis A: General* **2012**, *445–446*, 102.
- (19) Kahsar, K. R.; Schwartz, D. K.; Medlin, J. W. *ACS Catalysis* **2013**, *3*, 2041.
- (20) Haubrich, J.; Loffreda, D.; Delbecq, F.; Sautet, P.; Jugnet, Y.; Becker, C.; Wandelt, K. *The Journal of Physical Chemistry C* **2009**, *114*, 1073.
- (21) Haubrich, J.; Loffreda, D.; Delbecq, F.; Sautet, P.; Jugnet, Y.; Krupski, A.; Becker, C.; Wandelt, K. *The Journal of Physical Chemistry C* **2008**, *112*, 3701.
- (22) Chen, B.; Dingerdissen, U.; Krauter, J. G. E.; Lansink Rotgerink, H. G. J.; Möbus, K.; Ostgard, D. J.; Panster, P.; Riermeier, T. H.; Seebald, S.; Tacke, T.; Trauthwein, H. *Applied Catalysis A: General* **2005**, *280*, 17.
- (23) Ponec, V. *Applied Catalysis A: General* **1997**, *149*, 27.
- (24) Barbier, J.; Churin, E.; Marecot, P.; Menezo, J. C. *Applied Catalysis* **1988**, *36*, 277.
- (25) Love, J. C.; Wolfe, D. B.; Haasch, R.; Chabinye, M. L.; Paul, K. E.; Whitesides, G. M.; Nuzzo, R. G. *Journal of the American Chemical Society* **2003**, *125*, 2597.
- (26) Ulman, A. *Chem. Rev.* **1996**, *96*, 1533.
- (27) Laibinis, P. E.; Whitesides, G. M.; Allara, D. L.; Tao, Y. T.; Parikh, A. N.; Nuzzo, R. G. *Journal of the American Chemical Society* **1991**, *113*, 7152.
- (28) Addato, M. A. F.; Rubert, A. A.; Benitez, G. A.; Fonticelli, M. H.; Carrasco, J.; Carro, P.; Salvarezza, R. C. *Journal of Physical Chemistry C* **2011**, *115*, 17788.
- (29) Pang, S. H.; Schoenbaum, C. A.; Schwartz, D. K.; Medlin, J. W. *Nature communications* **2013**, *4*.

- (30) Schoenbaum, C. A.; Schwartz, D. K.; Medlin, J. W. *Journal of Catalysis* **2013**, *303*, 92.
- (31) Jana, N. R.; Gearheart, L.; Murphy, C. J. *Langmuir* **2001**, *17*, 6782.
- (32) Yee, C.; Scotti, M.; Ulman, A.; White, H.; Rafailovich, M.; Sokolov, J. *Langmuir* **1999**, *15*, 4314.
- (33) Richardson, J. M.; Jones, C. W. *Journal of Catalysis* **2007**, *251*, 80.
- (34) Eklund, S. E.; Cliffler, D. E. *Langmuir* **2004**, *20*, 6012.
- (35) Coq, B.; Kumbhar, P. S.; Moreau, C.; Moreau, P.; Warawdekar, M. G. *Journal of Molecular Catalysis* **1993**, *85*, 215.
- (36) Vericat, C.; Vela, M.; Benitez, G.; Carro, P.; Salvarezza, R. *Chemical Society Reviews* **2010**, *39*, 1805.
- (37) Schoenfisch, M. H.; Pemberton, J. E. *Journal of the American Chemical Society* **1998**, *120*, 4502.

## CHAPTER 7

### Conclusions and Future Directions

#### 7.1 Introduction

The work conducted in this thesis has explored the potential of thiol SAMs for coating catalyst surfaces, expanding on a nascent branch of catalysis which was pioneered by S. Marshall only shortly before I began working on the project<sup>1,2</sup>. This previous work had shown that the addition of thiol SAMs to the surface of a Pd/Al<sub>2</sub>O<sub>3</sub> catalyst could improve the selectivity of epoxybutene hydrogenation in the gas phase, and that the improvement was largely due to the presence of sulfur on the surface. But as a whole, thiol SAM catalysis was an interesting new phenomenon with little known about its potential.

The work in this thesis has expanded the use of thiol-modified catalysts to the liquid phase providing new insight as to how a SAM coating affects a hydrogenation catalyst. Definitive conclusions and observations have been made and presented in Chapters 2-6, but in many ways, these results have opened up even more questions as to how SAMs affect a catalyst surface and in what ways they can be used to rationally design the near-surface environment. In this Chapter, I will provide a summary of some of the most important themes of this thesis, identify some of the outstanding questions, and propose experiments to further expand on this work.

#### 7.2 Thesis Conclusions

First and foremost, the work in this thesis demonstrates that thiol SAMs can be effectively used to modify catalysts for a variety of reactions in the liquid and gas phase. The interesting and novel results of epoxybutene hydrogenation were expanded to the hydrogenation of fatty acids,  $\alpha,\beta$ -unsaturated aldehydes and other small molecular probe reactants demonstrating the broader applicability of SAM modifiers.

Arguably the most important result from the work presented in this thesis is that thiol SAMs can exhibit two distinct modes of selectivity enhancement on a reaction environment, a ligand non-specific and a ligand specific interaction<sup>3-6</sup>. First, as demonstrated by the hydrogenation of epoxybutene in both the gas and liquid phase, ligand non-specific interactions can improve the selectivity of a reaction. In this case, the specific functionality of the tail is unimportant to the selectivity of the reaction—the selectivity improvement is largely attributed to the 1/3 monolayer coverage of sulfur on the surface of the catalyst<sup>1,2,4</sup>.

The second mechanism of selectivity improvement, discussed extensively in Chapters 4-6 are ligand specific interactions—modes of selectivity improvement which rely on the interaction effects between the functionality of a thiol tail ligand and a reactant molecule. In the case of cinnamaldehyde, it was shown that ligand specific interactions, exerted through a pi-pi stacking interaction between phenylated thiols and the phenyl ring of cinnamaldehyde were responsible for functionally orienting cinnamaldehyde in a specific conformation with the surface such that selectivity could be directed down one of two competing reaction pathways<sup>6</sup>. What's more, it was shown that ligand-specific interactions can compound upon ligand non-specific interactions such that selectivity can be improved a uniform amount by a ligand non-specific interaction due to the presence of sulfur on a catalyst surface and then tuned further by ligand specific interactions with the tail of the SAM modifier.

The rate of reaction for these specific types of interactions was not of top concern but important trends supported the initial work from epoxybutene hydrogenation in the gas phase. For ligand non-specific interactions, the rate of the reaction was dependent on the order of the thiol monolayer where a more ordered SAM had a greater rate of reaction. This result was demonstrated in both the gas and liquid phases<sup>1,4</sup>.

An important consideration which always raises questions at conferences and with peer reviewers is the durability of the SAM coatings both during and between reactions. Chapter 6 attempts to address some of these concerns, and importantly shows that a simple catalyst regeneration step can be used to stabilize the selectivity improvement of a ligand specific interaction. Additionally, ligand non-specific interactions appear to be relatively robust across recycle reactions, even showing indications that a non-specific SAM coating might be similar to a controlled coking of a catalyst surface.

Out of all of this work, Chapter 3 is likely the most overlooked, but potentially one of the most interesting. What this chapter illustrates is that for reactant molecules much larger than the spacing of thiols on the catalyst surface, extensive interaction with the monolayer is necessary. Many of the smaller reactants studied here are on the same size scale as the 5 Å spacing of the thiol monolayer. Using reactants such as fatty acids which are closer to 20 Å allows for greatly increased control of reaction by either excluding the reactant from the surface with a molecule like thioglycerol, or restricting it from lying down on the surface as was shown for polyunsaturated fatty acids<sup>5</sup>. Such systems will be considered in the discussion of Chapter 7.3.

### **7.3 Future Paths**

The field of catalysis is concerned with a wide range of reactions and systems, potentially all of which could exhibit interesting results when conducted over a thiol SAM modified catalyst. Here, I will briefly consider some of the questions that came up most often and discuss some experiments which might build on this thesis.

As discussed in Chapter 7.2, one of the most important results from this thesis is the discovery of ligand specific and ligand non-specific interactions between the SAM and the reactant. When looking at the results from the ligand specific studies presented in Chapters 4-6, it seems particularly enticing to look for molecules similar to cinnamaldehyde that could be functionally oriented in conformations affecting reaction selectivity. But, after considering numerous options for similar systems, it is my belief that such a discovery is limited in the number and types of molecules to which it can apply. My hypothesis is that types of molecules able to interact in the ligand specific interaction mechanism are limited to a small range of sizes. For example, larger molecules with more functionality would be more prone to be restricted access to the surface, similar to the study of fatty acids<sup>5</sup>, and smaller molecules would be able to skirt interaction mechanisms on catalyst defect sites and around the monolayer as was shown for epoxybutene and even prenal<sup>4,6</sup>.

In addition to the small range of sizes that appear to be controllable, the ligand specific-interaction is extremely sensitive to subtle changes in the near surface environment. For example, in Chapter 5, it was shown that extending the ligand specific coatings used in Chapter 4 from a Pt surface to a Pd surface did not result in the same control of selectivity. As discussed in Chapter 1.2.2, thiols form at an angle normal to the surface on Pt whereas they form at 14-18° on Pd<sup>7-9</sup>. Aging in air was shown to significantly deteriorate the ligand specific interaction of the 3-phenyl-1-propanethiol monolayer in only 1 day of aging. When considering the results of the

recycle studies presented in Chapter 6, the ligand specific interactions alone present numerous challenges for wide ranging use in catalysis. Of course, the concept of designing an active site on the surface of a metal catalyst is particularly compelling and worthy of further thought<sup>10,11</sup>.

7.3.1 Competitive reaction: One idea for using the ligand specific interaction is to design a near-surface environment that favors adsorption of one reactant over another. This concept is essentially to create a competitive reaction system where each reactant has an identical reactive group and in the absence of a SAM coating, would equally compete for the surface. Control could be exerted by coating the surface with a thiol that preferentially favors adsorption of one of the reactants. Such a concept is illustrated in Figure 7-1 for a coating with increased affinity for phenylated reactants.

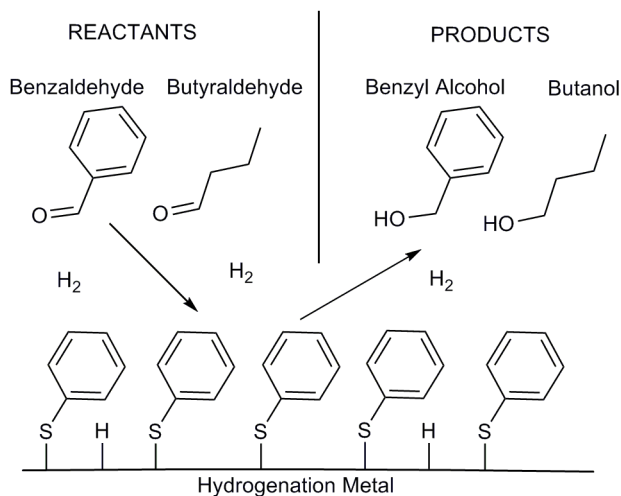


Figure 7-1: Competitive reaction scheme. Here benzaldehyde and butyraldehyde have the same reactive groups, but different structures. A surface coating such as thiophenol (shown) might preferentially attract benzaldehyde over butyraldehyde thus increasing its relative rate

In practice, this idea is similar to the competitive reaction that was shown to occur between hydrocinnamaldehyde and cinnamyl alcohol at the end of Chapter 4. Here, we merely would start with equal amounts of the reactants in question, and the reactive groups would be identical, instead of comparing hydrogenation of an olefin and an aldehyde. Already this technique has been attempted for the competitive hydrogenation of benzaldehyde and butyraldehyde and the results are shown in Figure 7-2.

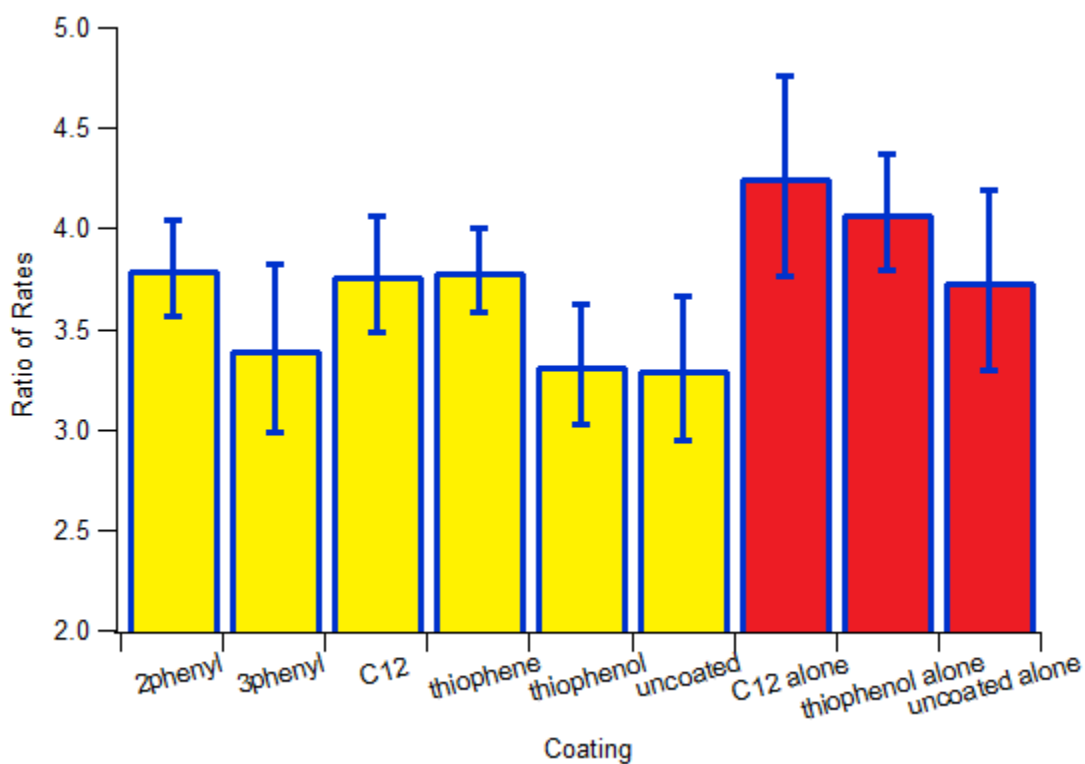


Figure 7-2: Competitive reaction of benzaldehyde and butyraldehyde. Ratio of rates is reported as the rate of benzaldehyde consumption divided by the rate of butyraldehyde consumption. The yellow bars are for reactions where benzaldehyde and butyraldehyde were reacted simultaneously to the reactor. The red bars are for reactions where benzaldehyde and butyraldehyde were run individually in the reactor. C12 refers to dodecanethiol.

As these data show, the competitive reaction did not show a statistically significant increase in selectivity when the surface was coated with a short phenylated molecule like thiophenol. In contrast, the rate of benzaldehyde consumption may have increased more for the other types of coatings shown. Still, none of the results presented illustrated a statistically significant improvement over the competitive reaction on an uncoated catalyst.

One explanation for the lack of selectivity enhancement is that even after reaction, the phenyl ring responsible for the attractive mechanism remains in active. Therefore, the near-surface environment could in fact be creating a favorable environment for benzaldehyde but also for the product benzyl alcohol thus equalizing the favorable adsorption environment for benzaldehyde by mitigating the increased on-rate with a decreased off-rate<sup>12,13</sup>. It is also important to remember that the ease of adsorption of a reactant does not necessarily parallel relative rates of reaction<sup>14</sup>.

Although this particular system did not work, it is possible to think of systems where the targeted reactant molecule might have an initial affinity for the near surface environment which is destroyed by the reaction. For example, a near surface environment that attracts olefins but then reacts these groups might be effective in increasing the relative rate of their reaction by only increasing the affinity of the reactant for the surface.

7.3.2 Imprinting: One of the problems with using thiol SAMs is that their coverage density (1/3 monolayer) has an interatomic spacing of approximately 5Å. This spacing is on the order of many small reactants and is potentially one of the limiting factors for designing a catalyst surface which can exert ligand specific interactions on small molecules—they simply slip through the spaces in the monolayer.

Therefore, in order to exploit and design active sites on metal catalysts, an alternative method might be to look at the selective hydrogenation of larger reactants, molecules such as the fatty acids studied in Chapter 3 which necessarily must interact with the thiol monolayer due to their large size. As shown in Chapter 3 for the hydrogenation of fatty acids, a full monolayer can dramatically restrict access of the reactant to the surface<sup>5</sup>. Using this restriction as an advantage, it might be possible to create an active site for a large reactant by imprinting with a template molecule in a SAM monolayer.

The idea of monolayer templating on gold and glass substrates has been discussed extensively for large biomolecules<sup>15-17</sup> after being pioneered by Sagiv et. al in 1979 in a report that described an insertion imprinting step to form holes in an n-octadecyltrichlorosilane SAM<sup>18</sup>. The underlying concept is to imprint the monolayer surface with the reactant molecule, leaving a binding pocket where only similar sized molecules can fit and react. Termed “Molecularly Imprinted Materials” or MIMs, these surfaces have been especially important for measuring the adsorption of large macromolecules on a surface.

Here we are interested in imprinting a surface for adsorption but also reaction on a surface. One promising system is trans-stilbene, a conjugated planar molecule with large bulky phenyl rings and a double bond in the center. Due to its planar configuration, trans-stilbene must lie flat on a catalyst surface to react, and at a length of ca. 12 Å it must have ample space on the surface to be able to lie down. Therefore imprinting, or a method designed to preserve access to the catalyst surface in the presence of a SAM is necessary to allow trans-stilbene to react. This general idea is presented in Figure 7-3 where imprinting is hypothesized with a thioglycerol SAM.

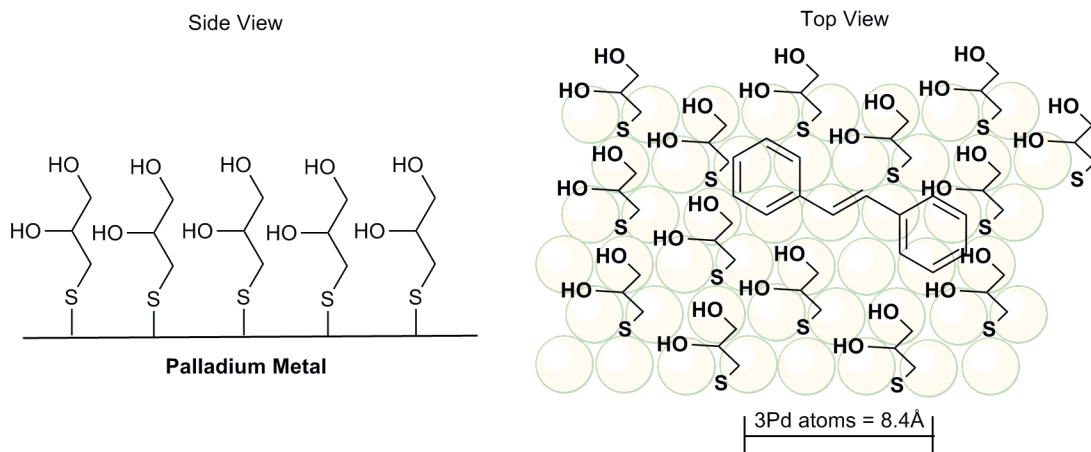


Figure 7-3: Imprinting a Pd surface with thioglycerol. Trans-stilbene or other large reactant molecules are large enough to exclude regions of the surface from thiol formation leaving behind a binding pocket properly spaced for the imprinted molecule.

Assuming imprinting is possible, one of the biggest hurdles is fixing the imprinted thiols in place on the catalyst surface. Potentially cross-linking the monolayer will be discussed as one option, but thioglycerol presents a compelling alternative. The hydroxyl groups present potential for non-covalent interactions which might stabilize the monolayer, and have already been shown in Chapters 3-4 to be effective at shutting down the reactivity of large reactants like fatty acids and cinnamaldehyde<sup>5,6</sup>. The idea presented in Figure 7-3 has undergone some preliminary testing to determine whether this path is worth pursuing and the results are shown in Figure 7-4.

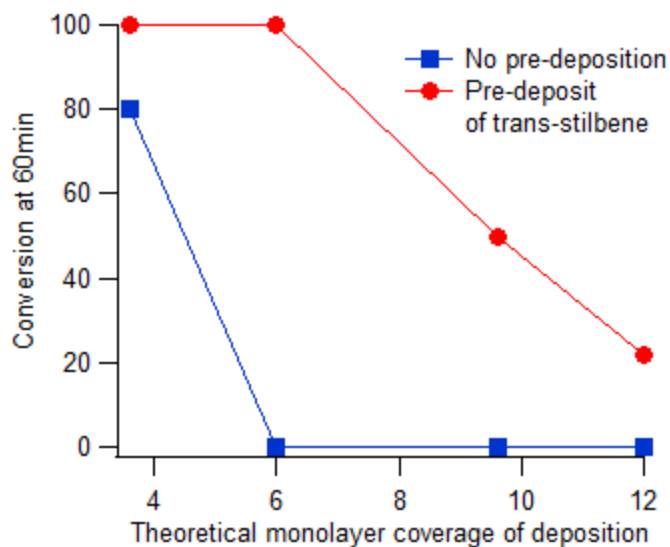


Figure 7-4: Reaction of trans-stilbene on imprinted Pd. For the reaction of trans-stilbene on a Pd catalyst that has been imprinted with trans-stilbene, conversion can be maintained to a higher deposition concentration than if no imprinting procedure is used

The results shown in Figure 7-4 indicate that for a thioglycerol coating of greater than 6 theoretical monolayers, the reaction of trans-stilbene achieves no conversion over a 60 minute reaction. In contrast, pre-depositing 250 mg of catalyst with 300 mg of trans-stilbene in 10 mL of THF before depositing the intended dose of thioglycerol in 40 mL of ethanol, the reaction still achieved 100% conversion over the course of a 60 minute reaction. These results are promising, but will require much additional testing to determine whether imprinting of trans-stilbene is occurring or whether stilbene is merely preventing the formation of a complete monolayer. The key studies that will be necessary to test this hypothesis are the use of different sized reactants which could theoretically fit or be excluded from an imprinted binding pocket on the catalyst surface.

Unfortunately, one of the biggest hurdles to testing this hypothesis is the availability of molecules capable of probing this system. Larger molecules tend to be insoluble in organic solvents, whereas smaller molecules such as styrene have the ability to react on a thioglycerol coated surface. As discussed previously, styrene and other small reactants are on the same order of size as the monolayer and are not as easy to control by coating the catalyst surface. Olefin hydrogenation is extremely favorable on Pd catalysts and styrene is small enough that it can potentially “cheat” by avoiding the imprinted surface and reacting exclusively on defect sites. With such a fast rate, controlling the reactivity in an on/off fashion is challenging, but potentially highly valuable. As alluded to earlier in this section, larger reactant molecules such as those derived from biomass are promising for their necessary interactions with a thiol coated surface.

If the concept of imprinting can be made to work, a variety of reaction systems could be designed. For example, size specific holes in a monolayer could be filled with a subsequent deposit of a different type of thiol. This could be used to exploit the interface of two thiols similar to the idea of exploiting the interface of two dissimilar liquids or phases.

Another future goal might be to imprint with crosslinking SAMs such that after imprinting, the SAMs can be locked in place by a crosslinking step. Now, not only would there be limited mobility into the holes on the surface, but the holes could be stable to harsh reaction conditions. One perennially studied and seldom achieved reaction in the field of catalysis is decarboxylation of an unsaturated fatty acid while preserving double bonds in the alkane tail region<sup>19,20</sup>. On a standard hydrogenation catalyst, the conditions required for decarboxylation, 300°C and 40 bar H<sub>2</sub>, will immediately hydrogenate the double bonds, valuable functional groups in downstream processing. By imprinting the catalyst surface with a small molecule such as styrene, depositing a crosslinking SAM such as (3-Mercaptopropyl)triethoxysilane,

crosslinking the silane groups, and then running operating conditions for the decarboxylation of linoleic acid, it may be possible to decarboxylate the react the head group while maintaining the hydrocarbon tail. Such a system would test the durability of a thiol modifier as well as the theory of creating an artificial enzyme.

7.3.3 Solvent effects: Catalyst and reaction experts have explored the idea of biphasic catalysis for years looking at ways to exploit the interface between two incompatible phases<sup>21-24</sup>. The same kind of effect could potentially be exhibited by the difference in polarity between a polar solvent and a non-polar thiol coating or vice versa. This concept, proposed in my preliminary exam, but never fully explored might provide an elegant method for orienting a large reactant between the near surface of the catalyst and the bulk reaction solution. Chapter 2 shows that such solvent and monolayer interactions are important for controlling the selectivity of the hydrogenation of epoxybutene, possibly due to the ability of a non-polar solvent like heptane to stabilize a polar coating like thioglycerol. Similarly, the results of solvent studies in Chapter 4 show that a polar solvent like ethanol is possibly the most effective solvent for stabilizing the non-polar thiol coatings. In general, consideration of the interaction between reaction solvent and monolayer is an important consideration for future reaction systems.

7.3.4 Desorption of thiols in solution: Building off of the discussion of solvent effect, one of the most pressing questions for the use of thiol modifiers in the liquid phase is their ability to maintain coverage in the presence of a solvent<sup>25</sup>. One simple experiment which would be interesting to carry out is a dynamic exchange of thiols from a metal surface. This procedure could best be accomplished with an ATR flow cell. ATR, discussed in Chapter 1.5.5 is particularly effective for looking at vibrational modes of molecules within 1 mm of the ATR crystal surface. A potential experiment would be to coat the ATR crystal with a thin film of Pd

and then deposit a labeled thiol on the surface. Using the flow cell to flow a distinctly different thiol through the chamber, it could be possible to measure the rate of replacement<sup>26,27</sup>. Similarly, a pure solvent could be flowed to measure the rate of dissolution from the metal surface.

**7.3.5 Active site characterization:** Finally, there are many additional lingering questions about the formation and effects of thiols on individual reactions. The suggestions presented throughout this thesis are engineering questions in nature, that is, they address functional concerns of the catalyst and measure macroscopic deliverables like activity and selectivity while largely overlooking the nuances of the microscopic origins of these deliverables. One constantly pressing question is the definition of an active site on a SAM coated catalyst. Currently, both coated and uncoated catalysts are treated the same where rate is reported as the moles of reactant consumed per second per site on an uncoated catalyst. This question is vital to truly understanding how the SAMs affect the rate of reaction.

Such characterization is difficult even on an uncoated catalyst<sup>28,29</sup>. Reactants come in many different sizes and conformations, so it is likely that there is no one definition of what an active site is on these catalysts. A small reactant such as acetylene might not experience a very different surface whether a catalyst is coated or not, while a large reactant such as cinnamaldehyde is clearly constrained on the surface such that some of the sites accessible to acetylene are inaccessible to cinnamaldehyde. Such subtle differences are scientific in nature and extremely difficult to quantify, but experiments which might shed light on the underlying nature would be valuable for understanding future systems. Already experiments with CO-DRIFTS have been carried out to measure the types of sites available on coated and uncoated catalysts<sup>30,31</sup>. The problem with these studies is exactly the problem described for the difference between a small reactant like acetylene and a large reactant like cinnamaldehyde—different sized

molecules might not have the same access to sites when spatially constrained by the monolayer. Careful isotherm measurements might similarly yield information on the availability of active sites but are also plagued by subtle confounding factors such as coking and defects.

In conclusion, I would like to say that this project has evolved greatly in the 4 years that I have worked on it. Starting off, little was known about the effects of thiol SAM catalyst modifiers, and in 4 years I have extended work to the liquid phase, opened experiment space to larger reactants, new conditions, and novel experiments. The project has been exciting and challenging at the same time, and I hope that future researchers can find as much joy and interest in the project as I have experienced. Good luck!

#### 7.4 References

- (1) Marshall, S. T.; O'Brien, M.; Oetter, B.; Corpuz, A.; Richards, R. M.; Schwartz, D. K.; Medlin, J. W. *Nat. Mater.* **2010**, *9*, 853.
- (2) Marshall, S. T.; Schwartz, D. K.; Medlin, J. W. *Langmuir* **2011**, *27*, 6731.
- (3) Briand, L. E.; Jehng, J.-M.; Cornaglia, L.; Hirt, A. M.; Wachs, I. E. *Catalysis Today* **2003**, *78*, 257.
- (4) Kahsar, K. R.; Schwartz, D. K.; Medlin, J. W. *Applied Catalysis A: General* **2012**, *445–446*, 102.
- (5) Kahsar, K. R.; Schwartz, D. K.; Medlin, J. W. *ACS Catalysis* **2013**, *3*, 2041.
- (6) Kahsar, K. R.; Schwartz, D. K.; Medlin, J. W. *Journal of the American Chemical Society* **2013**, *136*, 520.
- (7) Love, J. C.; Wolfe, D. B.; Chabynyc, M. L.; Paul, K. E.; Whitesides, G. M. *Journal of the American Chemical Society* **2002**, *124*, 1576.

- (8) Love, J. C.; Wolfe, D. B.; Haasch, R.; Chabinyc, M. L.; Paul, K. E.; Whitesides, G. M.; Nuzzo, R. G. *Journal of the American Chemical Society* **2003**, *125*, 2597.
- (9) Ulman, A. *Chem. Rev.* **1996**, *96*, 1533.
- (10) Pecsí, I.; Leveles, I.; Harmat, V.; Vertessy, B. G.; Toth, J. *Nucleic Acids Research* **2010**, *38*, 7179.
- (11) Siegel, J. B.; Zanghellini, A.; Lovick, H. M.; Kiss, G.; Lambert, A. R.; St.Clair, J. L.; Gallaher, J. L.; Hilvert, D.; Gelb, M. H.; Stoddard, B. L.; Houk, K. N.; Michael, F. E.; Baker, D. *Science* **2010**, *329*, 309.
- (12) Frennet, A.; Lienard, G.; Crucq, A.; Degols, L. *Journal of Catalysis* **1978**, *53*, 150.
- (13) Delbecq, F.; Sautet, P. *Journal of Catalysis* **1995**, *152*, 217.
- (14) Rader, C. P.; Smith, H. A. *Journal of the American Chemical Society* **1962**, *84*, 1443.
- (15) Balamurugan, S.; Spivak, D. A. *Journal of Molecular Recognition* **2011**, *24*, 915.
- (16) Turner, N. W.; Jeans, C. W.; Brain, K. R.; Allender, C. J.; Hlady, V.; Britt, D. W. *Biotechnology progress* **2006**, *22*, 1474.
- (17) Turner, N. W.; Wright, B. E.; Hlady, V.; Britt, D. W. *Journal of colloid and interface science* **2007**, *308*, 71.
- (18) Sagiv, J. *Israel Journal of Chemistry* **1979**, *18*, 346.
- (19) Mäki-Arvela, P.; Hajek, J.; Salmi, T.; Murzin, D. Y. *Applied Catalysis A: General* **2005**, *292*, 1.
- (20) Mäki-Arvela, P.; Kuusisto, J.; Sevilla, E. M.; Simakova, I.; Mikkola, J. P.; Myllyoja, J.; Salmi, T.; Murzin, D. Y. *Applied Catalysis A: General* **2008**, *345*, 201.
- (21) Cornils, B. *Journal of Molecular Catalysis A: Chemical* **1999**, *143*, 1.

- (22) Wachsen, O.; Himmler, K.; Cornils, B. *Catalysis Today* **1998**, *42*, 373.
- (23) Mercier, F.; Mathey, F. *Journal of organometallic chemistry* **1993**, *462*, 103.
- (24) Chheda, J. N.; Román-Leshkov, Y.; Dumesic, J. A. *Green Chemistry* **2007**, *9*, 342.
- (25) Schlenoff, J. B.; Li, M.; Ly, H. *Journal of the American Chemical Society* **1995**, *117*, 12528.
- (26) Heinen, M.; Jusys, Z.; Behm, R. *The Journal of Physical Chemistry C* **2010**, *114*, 9850.
- (27) Carter, C. F.; Lange, H.; Ley, S. V.; Baxendale, I. R.; Wittkamp, B.; Goode, J. G.; Gaunt, N. L. *Organic Process Research & Development* **2010**, *14*, 393.
- (28) Behrens, M.; Studt, F.; Kasatkin, I.; Kühl, S.; Hävecker, M.; Abild-Pedersen, F.; Zander, S.; Girgsdies, F.; Kurr, P.; Knief, B.-L. *Science* **2012**, *336*, 893.
- (29) Green, I. X.; Tang, W.; Neurock, M.; Yates, J. T. *Science* **2011**, *333*, 736.
- (30) Pang, S. H.; Schoenbaum, C. A.; Schwartz, D. K.; Medlin, J. W. *Nature communications* **2013**, *4*.
- (31) Schoenbaum, C. A.; Schwartz, D. K.; Medlin, J. W. *Journal of Catalysis* **2013**, *303*, 92.

## CHAPTER 8

### Bibliography

Abatzoglou, N.; Boivin, S. A review of biogas purification processes. *Biofuels, Bioproducts and Biorefining* **2009**, *3*, 42-71.

Addato, M. A. F.; Rubert, A. A.; Benitez, G. A.; Fonticelli, M. H.; Carrasco, J.; Carro, P.; Salvarezza, R. C. Alkanethiol Adsorption on Platinum: Chain Length Effects on the Quality of Self-Assembled Monolayers. *Journal of Physical Chemistry C* **2011**, *115*, 17788-17798.

Alcalá, R.; Greeley, J.; Mavrikakis, M.; Dumesic, J. A. Density-functional theory studies of acetone and propanal hydrogenation on Pt (111). *The Journal of chemical physics* **2002**, *116*, 8973-8980.

Aleksandrov, H. A.; Moskaleva, L. V.; Zhao, Z.-J.; Basaran, D.; Chen, Z.-X.; Mei, D.; Rösch, N. Ethylene conversion to ethylidyne on Pd (111) and Pt (111): A first-principles-based kinetic Monte Carlo study. *Journal of Catalysis* **2012**, *285*, 187-195.

Allara, D. L.; Nuzzo, R. G. Spontaneously organized molecular assemblies. 1. Formation, dynamics, and physical properties of n-alkanoic acids adsorbed from solution on an oxidized aluminum surface. *Langmuir* **1985**, *1*, 45-52.

Anderson, M. R.; Evaniak, M. N.; Zhang, M. Influence of Solvent on the Interfacial Structure of Self-Assembled Alkanethiol Monolayers. *Langmuir* **1996**, *12*, 2327-2331.

Armor, J. N. A history of industrial catalysis. *Catalysis Today* **2011**, *163*, 3-9.

Atsumi, S.; Hanai, T.; Liao, J. C. Non-fermentative pathways for synthesis of branched-chain higher alcohols as biofuels. *Nature* **2008**, *451*, 86-89.

Bain, C. D.; Whitesides, G. M. Modeling Organic Surfaces with Self-Assembled Monolayers. *Angewandte Chemie International Edition in English* **1989**, *28*, 506-512.

Balamurugan, S.; Spivak, D. A. Molecular imprinting in monolayer surfaces. *Journal of Molecular Recognition* **2011**, *24*, 915-929.

Baldyga, L. M.; Blavo, S. O.; Kuo, C.-H.; Tsung, C.-K.; Kuhn, J. N. Size-Dependent Sulfur Poisoning of Silica-Supported Monodisperse Pt Nanoparticle Hydrogenation Catalysts. *ACS Catalysis* **2012**, *2*, 2626-2629.

Barbier, J.; Churin, E.; Marecot, P.; Menezo, J. C. Deactivation by Coking of Platinum/Alumina Catalysts: Effects of Operating Temperature and Pressure. *Applied Catalysis* **1988**, *36*, 277-285.

Bayrak, Y. Application of Langmuir isotherm to saturated fatty acid adsorption. *Microporous and Mesoporous Materials* **2006**, *87*, 203-206.

Behrens, M. Synthesis of Solid Catalysts. Edited by Krijn P. de Jong. *Angewandte Chemie International Edition* **2010**, *49*, 2095.

Behrens, M.; Studt, F.; Kasatkin, I.; Kühl, S.; Hävecker, M.; Abild-Pedersen, F.; Zander, S.; Girgsdies, F.; Kurr, P.; Knief, B.-L. The active site of methanol synthesis over Cu/ZnO/Al<sub>2</sub>O<sub>3</sub> industrial catalysts. *Science* **2012**, *336*, 893-897.

Bernas, A.; Myllyoja, J.; Salmi, T.; Murzin, D. Y. Kinetics of linoleic acid hydrogenation on Pd/C catalyst. *Applied Catalysis A: General* **2009**, *353*, 166-180.

Besson, M.; Gallezot, P. Selective oxidation of alcohols and aldehydes on metal catalysts. *Catalysis Today* **2000**, *57*, 127-141.

Bigelow, W.; Pickett, D.; Zisman, W. Oleophobic monolayers: I. Films adsorbed from solution in non-polar liquids. *Journal of Colloid Science* **1946**, *1*, 513-538.

Bond, G.; Webb, G.; Wells, P.; Winterbottom, J. Patterns of behavior in catalysis by metals. *Journal of Catalysis* **1962**, *1*, 74-84.

Bratlie, K. M.; Lee, H.; Komvopoulos, K.; Yang, P.; Somorjai, G. A. Platinum Nanoparticle Shape Effects on Benzene Hydrogenation Selectivity. *Nano Letters* **2007**, *7*, 3097-3101.

Briand, L. E.; Jehng, J.-M.; Cornaglia, L.; Hirt, A. M.; Wachs, I. E. Quantitative determination of the number of surface active sites and the turnover frequency for methanol oxidation over bulk metal vanadates. *Catalysis Today* **2003**, *78*, 257-268.

Carter, C. F.; Lange, H.; Ley, S. V.; Baxendale, I. R.; Wittkamp, B.; Goode, J. G.; Gaunt, N. L. ReactIR flow cell: a new analytical tool for continuous flow chemical processing. *Organic Process Research & Development* **2010**, *14*, 393-404.

Carvalho, M. S.; Lacerda, R. A.; Leao, J. P. B.; Scholten, J. D.; Neto, B. A. D.; Suarez, P. A. Z. In situ generated palladium nanoparticles in imidazolium-based ionic liquids: a versatile medium for an efficient and selective partial biodiesel hydrogenation. *Catalysis Science & Technology* **2011**, *1*, 480-488.

Cervený, L. *Catalytic Hydrogenation*; Elsevier Science, 1986.

Chen, B.; Dingerdissen, U.; Krauter, J. G. E.; Lansink Rotgerink, H. G. J.; Möbus, K.; Ostgard, D. J.; Panster, P.; Riermeier, T. H.; Seebald, S.; Tacke, T.; Trauthwein, H. New developments in hydrogenation catalysis particularly in synthesis of fine and intermediate chemicals. *Applied Catalysis A: General* **2005**, *280*, 17-46.

Chheda, J. N.; Román-Leshkov, Y.; Dumesic, J. A. Production of 5-hydroxymethylfurfural and furfural by dehydration of biomass-derived mono- and poly-saccharides. *Green Chemistry* **2007**, *9*, 342-350.

Conder, J. R.; Young, C. L. *Physicochemical measurement by gas chromatography*; Wiley New York, 1979; Vol. 632.

Coq, B.; Kumbhar, P. S.; Moreau, C.; Moreau, P.; Warawdekar, M. G. Liquid phase hydrogenation of cinnamaldehyde over supported ruthenium catalysts: Influence of particle size, bimetallics and nature of support. *Journal of Molecular Catalysis* **1993**, *85*, 215-228.

Cornils, B. Bulk and fine chemicals via aqueous biphasic catalysis. *Journal of Molecular Catalysis A: Chemical* **1999**, *143*, 1-10.

da Silva, A. B.; Jordão, E.; Mendes, M. J.; Fouilloux, P. Effect of metal-support interaction during selective hydrogenation of cinnamaldehyde to cinnamyl alcohol on platinum based bimetallic catalysts. *Applied Catalysis A: General* **1997**, *148*, 253-264.

Dameron, A. A.; Charles, L. F.; Weiss, P. S. Structures and displacement of 1-adamantanethiol self-assembled monolayers on Au {111}. *Journal of the American Chemical Society* **2005**, *127*, 8697-8704.

Davis, M. E.; Davis, R. J. *Fundamentals of chemical reaction engineering*; Courier Dover Publications, 2012.

de Jesús, J. C.; Zaera, F. Adsorption and thermal chemistry of acrolein and crotonaldehyde on Pt (111) surfaces. *Surface science* **1999**, *430*, 99-115.

de Jong, K. P. *Synthesis of solid catalysts*; Wiley-VCH: Darmstadt, 2009.

Delbecq, F.; Sautet, P. Competitive CC and CO Adsorption of  $\alpha,\beta$ -Unsaturated Aldehydes on Pt and Pd Surfaces in Relation with the Selectivity of Hydrogenation Reactions: A Theoretical Approach. *Journal of Catalysis* **1995**, *152*, 217-236.

Delbecq, F.; Sautet, P. A Density Functional Study of Adsorption Structures of Unsaturated Aldehydes on Pt(111): A Key Factor for Hydrogenation Selectivity. *Journal of Catalysis* **2002**, *211*, 398-406.

Delbecq, F.; Sautet, P. Influence of Sn additives on the selectivity of hydrogenation of  $\alpha,\beta$ -unsaturated aldehydes with Pt catalysts: a density functional study of molecular adsorption. *Journal of Catalysis* **2003**, *220*, 115-126.

Deutschmann, O.; Knözinger, H.; Kochloefl, K.; Turek, T. In *Ullmann's Encyclopedia of Industrial Chemistry*; Wiley-VCH Verlag GmbH & Co. KGaA: 2000.

Dick, A. R.; Hull, K. L.; Sanford, M. S. A highly selective catalytic method for the oxidative functionalization of CH bonds. *Journal of the American Chemical Society* **2004**, *126*, 2300-2301.

Dill, K. A.; Bromberg, S. *Molecular Driving Forces: Statistical Thermodynamics in Chemistry and Biology*; Garland Science, 2003.

Dobrushin, R. L.; Kotecký, R.; Shlosman, S. *Wulff Construction: A Global Shape from Local Interaction*; American Mathematical Society, 1992.

Donnay, J.; Harker, D. A new law of crystal morphology extending the law of Bravais. *Am. Mineral* **1937**, *22*, 446-467.

Dou, R.-F.; Ma, X.-C.; Xi, L.; Yip, H. L.; Wong, K. Y.; Lau, W. M.; Jia, J.-F.; Xue, Q.-K.; Yang, W.-S.; Ma, H.; Jen, A. K. Y. Self-Assembled Monolayers of Aromatic Thiols Stabilized by Parallel-Displaced  $\pi$ - $\pi$  Stacking Interactions. *Langmuir* **2006**, *22*, 3049-3056.

Dunn, R. O. Effect of antioxidants on the oxidative stability of methyl soyate (biodiesel). *Fuel Processing Technology* **2005**, *86*, 1071-1085.

Dziomkina, N. V.; Vancso, G. J. Colloidal crystal assembly on topologically patterned templates. *Soft Matter* **2005**, *1*, 265-279.

Eklund, S. E.; Cliffler, D. E. Synthesis and Catalytic Properties of Soluble Platinum Nanoparticles Protected by a Thiol Monolayer. *Langmuir* **2004**, *20*, 6012-6018.

Englisch, M.; Ranade, V. S.; Lercher, J. A. Liquid phase hydrogenation of crotonaldehyde over Pt/SiO<sub>2</sub> catalysts. *Applied Catalysis a-General* **1997**, *163*, 111-122.

Fahrenfort, J. Attenuated total reflection: A new principle for the production of useful infra-red reflection spectra of organic compounds. *Spectrochimica Acta* **1961**, *17*, 698-709.

Felder, R. M.; Rousseau, R. W. *Elementary Principles of Chemical Processes, Student Workbook*; Wiley, 2005.

Fersht, A. *Structure and mechanism in protein sciences: a guide to enzyme catalysis and protein folding* W. H Freeman and Company, 1999.

Florida Addato, M. a. A.; Rubert, A. A.; Benítez, G. A.; Fonticelli, M. H.; Carrasco, J.; Carro, P.; Salvarezza, R. C. Alkanethiol Adsorption on Platinum: Chain Length Effects on the Quality of Self-Assembled Monolayers. *The Journal of Physical Chemistry C* **2011**, *115*, 17788-17798.

Frennet, A.; Lienard, G.; Crucq, A.; Degols, L. Effect of multiple sites and competition in adsorption on the kinetics of reactions catalyzed by metals. *Journal of Catalysis* **1978**, *53*, 150-163.

Fuller, M. P.; Griffiths, P. R. Diffuse reflectance measurements by infrared Fourier transform spectrometry. *Analytical Chemistry* **1978**, *50*, 1906-1910.

Gallezot, P.; Richard, D. Selective Hydrogenation of  $\alpha,\beta$ -Unsaturated Aldehydes. *Catalysis Reviews* **1998**, *40*, 81-126.

Gardner, N. C.; Hansen, R. S. Concerted reaction mechanism for the hydrogenation of olefins on metals. *The Journal of Physical Chemistry* **1970**, *74*, 3298-3299.

GiBBS, J. W.; Longmans, New York: 1931.

Gibbs, J. W. *The collected works of J. Willard Gibbs*; Yale University Press, 1948; Vol. 1.

Gill, I.; Valivety, R. Polyunsaturated fatty acids, part 1: Occurrence, biological activities and applications. *Trends in Biotechnology* **1997**, *15*, 401-409.

Golden, W. G.; Saperstein, D. D.; Severson, M. W.; Overend, J. Infrared reflection-absorption spectroscopy of surface species: a comparison of Fourier transform and dispersion methods. *The Journal of Physical Chemistry* **1984**, *88*, 574-580.

Green, I. X.; Tang, W.; Neurock, M.; Yates, J. T. Spectroscopic observation of dual catalytic sites during oxidation of CO on a Au/TiO<sub>2</sub> catalyst. *Science* **2011**, *333*, 736-739.

Greenler, R. G. Infrared Study of Adsorbed Molecules on Metal Surfaces by Reflection Techniques. *The Journal of chemical physics* **1966**, *44*, 310-315.

Hackett, S. F.; Brydson, R. M.; Gass, M. H.; Harvey, I.; Newman, A. D.; Wilson, K.; Lee, A. F. High - Activity, Single - Site Mesoporous Pd/Al<sub>2</sub>O<sub>3</sub> Catalysts for Selective Aerobic Oxidation of Allylic Alcohols. *Angewandte Chemie* **2007**, *119*, 8747-8750.

Hair, M. L. *Infrared spectroscopy in surface chemistry*; M. Dekker New York, 1967.

Hammond, C.; Hammond, C. *Basics of crystallography and diffraction*; Oxford, 2001; Vol. 214.

Haubrich, J.; Loffreda, D.; Delbecq, F.; Sautet, P.; Jugnet, Y.; Krupski, A.; Becker, C.; Wandelt, K. Adsorption and Vibrations of  $\alpha,\beta$ -Unsaturated Aldehydes on Pure Pt and Pt-Sn Alloy (111) Surfaces I. Prenal. *The Journal of Physical Chemistry C* **2008**, *112*, 3701-3718.

Haubrich, J.; Loffreda, D.; Delbecq, F.; Sautet, P.; Jugnet, Y.; Becker, C.; Wandelt, K. Adsorption and Vibrations of  $\alpha,\beta$ -Unsaturated Aldehydes on Pt(111) and Pt-Sn Alloy (111) Surfaces. 3. Adsorption Energy vs Adsorption Strength. *The Journal of Physical Chemistry C* **2009**, *114*, 1073-1084.

Heinen, M.; Jusys, Z.; Behm, R. Ethanol, acetaldehyde and acetic acid adsorption/electrooxidation on a Pt thin film electrode under continuous electrolyte flow: an in situ ATR-FTIRS flow cell study. *The Journal of Physical Chemistry C* **2010**, *114*, 9850-9864.

Hoffert, M. I.; Caldeira, K.; Benford, G.; Criswell, D. R.; Green, C.; Herzog, H.; Jain, A. K.; Kheshgi, H. S.; Lackner, K. S.; Lewis, J. S.; Lightfoot, H. D.; Manheimer, W.; Mankins, J. C.; Mauel, M. E.; Perkins, L. J.; Schlesinger, M. E.; Volk, T.; Wigley, T. M. L. Advanced Technology Paths to Global Climate Stability: Energy for a Greenhouse Planet. *Science* **2002**, *298*, 981-987.

Holmes, F. L. *Lavoisier and the chemistry of life: an exploration of scientific creativity*; Univ of Wisconsin Press, 1987.

Houston, P. L. *Chemical Kinetics and Reaction Dynamics*; Dover Publications, 2012.

Hughes, M. D.; Xu, Y.-J.; Jenkins, P.; McMorn, P.; Landon, P.; Enache, D. I.; Carley, A. F.; Attard, G. A.; Hutchings, G. J.; King, F. Tunable gold catalysts for selective hydrocarbon oxidation under mild conditions. *Nature* **2005**, *437*, 1132-1135.

Hutchings, G. J.; King, F.; Okoye, I. P.; Rochester, C. H. Influence of sulphur poisoning of copper/alumina catalyst on the selective hydrogenation of crotonaldehyde. *Applied Catalysis A: General* **1992**, *83*, L7-L13.

Hutchings, G. J.; King, F.; Okoye, I. P.; Padley, M. B.; Rochester, C. H. Selectivity Enhancement in the Hydrogenation of  $\alpha$ ,  $\beta$ -Unsaturated Aldehydes and Ketones Using Thiophene-Modified Catalysts. *Journal of Catalysis* **1994**, *148*, 453-463.

Jana, N. R.; Gearheart, L.; Murphy, C. J. Seeding Growth for Size Control of 5–40 nm Diameter Gold Nanoparticles. *Langmuir* **2001**, *17*, 6782-6786.

Jenck, J.; Germain, J.-E. High-pressure competitive hydrogenation of aldehydes, ketones, and olefins on copper chromite catalyst. *Journal of Catalysis* **1980**, *65*, 141-149.

Jurg, J. W.; Eisma, E. Petroleum Hydrocarbons: Generation from Fatty Acid. *Science* **1964**, *144*, 1451-1452.

Kahsar, K. R.; Schwartz, D. K.; Medlin, J. W. Liquid- and vapor-phase hydrogenation of 1-epoxy-3-butene using self-assembled monolayer coated palladium and platinum catalysts. *Applied Catalysis A: General* **2012**.

Kahsar, K. R.; Schwartz, D. K.; Medlin, J. W. Liquid- and vapor-phase hydrogenation of 1-epoxy-3-butene using self-assembled monolayer coated palladium and platinum catalysts. *Applied Catalysis A: General* **2012**, *445–446*, 102-106.

- Kahsar, K. R.; Schwartz, D. K.; Medlin, J. W. Control of Metal Catalyst Selectivity through Specific Noncovalent Molecular Interactions. *Journal of the American Chemical Society* **2013**, *136*, 520-526.
- Kahsar, K. R.; Schwartz, D. K.; Medlin, J. W. Selective Hydrogenation of Polyunsaturated Fatty Acids Using Alkanethiol Self-Assembled Monolayer-Coated Pd/Al<sub>2</sub>O<sub>3</sub> Catalysts. *ACS Catalysis* **2013**, *3*, 2041-2044.
- Karavalakis, G.; Stournas, S.; Karonis, D. Evaluation of the oxidation stability of diesel/biodiesel blends. *Fuel* **2010**, *89*, 2483-2489.
- Kaufmann, T.; Kaldor, A.; Stuntz, G.; Kerby, M.; Ansell, L. Catalysis science and technology for cleaner transportation fuels. *Catalysis Today* **2000**, *62*, 77-90.
- Kieboom, A.; Moulijn, J.; Leeuwen, v. P.; Santen, v. R. History of catalysis. *Catalysis: an integrated approach/Ed. RA van Santen, PWNM van Leeuwen, JA Moulijn* **1999**, *123*, 3.
- Kim, H.-J.; Kang, B.-S.; Kim, M.-J.; Park, Y. M.; Kim, D.-K.; Lee, J.-S.; Lee, K.-Y. Transesterification of vegetable oil to biodiesel using heterogeneous base catalyst. *Catalysis Today* **2004**, *93-95*, 315-320.
- Kim, M.; Hohman, J. N.; Cao, Y.; Houk, K. N.; Ma, H.; Jen, A. K.-Y.; Weiss, P. S. Creating Favorable Geometries for Directing Organic Photoreactions in Alkanethiolate Monolayers. *Science* **2011**, *331*, 1312-1315.
- Kim, Y. T.; McCarley, R. L.; Bard, A. J. Observation of n-octadecanethiol multilayer formation from solution onto gold. *Langmuir* **1993**, *9*, 1941-1944.
- Kliwer, C. J.; Bieri, M.; Somorjai, G. A. Hydrogenation of the  $\alpha,\beta$ -Unsaturated Aldehydes Acrolein, Crotonaldehyde, and Prenal over Pt Single Crystals: A Kinetic and Sum-Frequency Generation Vibrational Spectroscopy Study. *Journal of the American Chemical Society* **2009**, *131*, 9958-9966.
- Knothe, G. Some aspects of biodiesel oxidative stability. *Fuel Processing Technology* **2007**, *88*, 669-677.
- Kodama, C.; Hayashi, T.; Nozoye, H. Decomposition of alkanethiols adsorbed on Au (1 1 1) at low temperature. *Applied Surface Science* **2001**, *169-170*, 264-267.

- Kung, H. H. *Transition metal oxides: surface chemistry and catalysis*; Elsevier, 1989.
- Kwon, S. G.; Krylova, G.; Sumer, A.; Schwartz, M. M.; Bunel, E. E.; Marshall, C. L.; Chattopadhyay, S.; Lee, B.; Jellinek, J.; Shevchenko, E. V. Capping Ligands as Selectivity Switchers in Hydrogenation Reactions. *Nano Letters* **2012**, *12*, 5382-5388.
- Laibinis, P. E.; Whitesides, G. M.; Allara, D. L.; Tao, Y. T.; Parikh, A. N.; Nuzzo, R. G. Comparison of the structures and wetting properties of self-assembled monolayers of n-alkanethiols on the coinage metal surfaces, copper, silver, and gold. *Journal of the American Chemical Society* **1991**, *113*, 7152-7167.
- Lang, J. F.; Masel, R. I. The adsorption of thiophene and tetrahydrothiophene on several faces of platinum. *Surface science* **1987**, *183*, 44-66.
- Lee, I.; Delbecq, F.; Morales, R.; Albiter, M. A.; Zaera, F. Tuning selectivity in catalysis by controlling particle shape. *Nat Mater* **2009**, *8*, 132-138.
- Lewis, M.; Tarlov, M.; Carron, K. Study of the Photooxidation Process of Self-Assembled Alkanethiol Monolayers. *Journal of the American Chemical Society* **1995**, *117*, 9574-9575.
- Loglio, F.; Schweizer, M.; Kolb, D. In situ characterization of self-assembled butanethiol monolayers on Au (100) electrodes. *Langmuir* **2003**, *19*, 830-834.
- Love, J. C.; Wolfe, D. B.; Chabinyc, M. L.; Paul, K. E.; Whitesides, G. M. Self-Assembled Monolayers of Alkanethiolates on Palladium Are Good Etch Resists. *Journal of the American Chemical Society* **2002**, *124*, 1576-1577.
- Love, J. C.; Wolfe, D. B.; Haasch, R.; Chabinyc, M. L.; Paul, K. E.; Whitesides, G. M.; Nuzzo, R. G. Formation and structure of self-assembled monolayers of alkanethiolates on palladium. *Journal of the American Chemical Society* **2003**, *125*, 2597-2609.
- Love, J. C.; Estroff, L. A.; Kriebel, J. K.; Nuzzo, R. G.; Whitesides, G. M. Self-assembled monolayers of thiolates on metals as a form of nanotechnology. *Chemical Reviews* **2005**, *105*, 1103-1170.
- MacMillan, D. W. The advent and development of organocatalysis. *Nature* **2008**, *455*, 304-308.

Mäki-Arvela, P.; Hajek, J.; Salmi, T.; Murzin, D. Y. Chemoselective hydrogenation of carbonyl compounds over heterogeneous catalysts. *Applied Catalysis A: General* **2005**, *292*, 1-49.

Mäki-Arvela, P.; Kuusisto, J.; Sevilla, E. M.; Simakova, I.; Mikkola, J. P.; Myllyoja, J.; Salmi, T.; Murzin, D. Y. Catalytic hydrogenation of linoleic acid to stearic acid over different Pd- and Ru-supported catalysts. *Applied Catalysis A: General* **2008**, *345*, 201-212.

Makosch, M.; Lin, W.-I.; Bumbálek, V.; Sá, J.; Medlin, J. W.; Hungerbühler, K.; van Bokhoven, J. A. Organic Thiol Modified Pt/TiO<sub>2</sub> Catalysts to Control Chemoselective Hydrogenation of Substituted Nitroarenes. *ACS Catalysis* **2012**, *2*, 2079-2081.

Marimuthu, A.; Zhang, J.; Linic, S. Tuning Selectivity in Propylene Epoxidation by Plasmon Mediated Photo-Switching of Cu Oxidation State. *Science* **2013**, *339*, 1590-1593.

Marinelli, T. B. L. W.; Ponc, V. A Study on the Selectivity in Acrolein Hydrogenation on Platinum Catalysts: A Model for Hydrogenation of  $\alpha,\beta$ -Unsaturated Aldehydes. *Journal of Catalysis* **1995**, *156*, 51-59.

Marshall, S. T.; Horiuchi, C. M.; Zhang, W. Y.; Medlin, J. W. Common Decomposition Pathways of 1-Epoxy-3-butene and 2-Butenal on Pd(111). *Journal of Physical Chemistry C* **2008**, *112*, 20406-20412.

Marshall, S. T.; O'Brien, M.; Oetter, B.; Corpuz, A.; Richards, R. M.; Schwartz, D. K.; Medlin, J. W. Controlled selectivity for palladium catalysts using self-assembled monolayers. *Nature Materials* **2010**, *9*, 853-858.

Marshall, S. T.; Schwartz, D. K.; Medlin, J. W. Adsorption of Oxygenates on Alkanethiol-Functionalized Pd(111) Surfaces: Mechanistic Insights into the Role of Self-Assembled Monolayers on Catalysis. *Langmuir* **2011**, *27*, 6731-6737.

Masel, R. I. *Chemical kinetics and catalysis*; Wiley-Interscience New York, 2001.

Medlin, J. W. Understanding and Controlling Reactivity of Unsaturated Oxygenates and Polyols on Metal Catalysts. *ACS Catalysis* **2011**, *1*, 1284-1297.

Mercier, F.; Mathey, F. A new type of water-soluble phosphine for biphasic catalysis. *Journal of organometallic chemistry* **1993**, *462*, 103-106.

Mittelbach, M.; Gangl, S. Long storage stability of biodiesel made from rapeseed and used frying oil. *Journal of the American Oil Chemists' Society* **2001**, *78*, 573-577.

Monnier, J. R. The direct epoxidation of higher olefins using molecular oxygen. *Applied Catalysis a-General* **2001**, *221*, 73-91.

Moser, B. R.; Haas, M. J.; Winkler, J. K.; Jackson, M. A.; Erhan, S. Z.; List, G. R. Evaluation of partially hydrogenated methyl esters of soybean oil as biodiesel. *European Journal of Lipid Science and Technology* **2007**, *109*, 17-24.

Mukherjee, S.; Vannice, M. A. Solvent effects in liquid-phase reactions - I. Activity and selectivity during citral hydrogenation on Pt/SiO<sub>2</sub> and evaluation of mass transfer effects. *Journal of Catalysis* **2006**, *243*, 108-130.

Neurock, M.; Pallassana, V.; van Santen, R. A. The Importance of Transient States at Higher Coverages in Catalytic Reactions. *Journal of the American Chemical Society* **2000**, *122*, 1150-1153.

Nishimura, S. *Handbook of heterogeneous catalytic hydrogenation for organic synthesis*; J. Wiley, 2001.

Nishiyama, S.; Hara, T.; Tsuruya, S.; Masai, M. Infrared Spectroscopy Study of Aldehydes Adsorbed on Rh-Sn Bimetallic Systems: Selective Activation of Aldehydes by Tin. *The Journal of Physical Chemistry B* **1999**, *103*, 4431-4439.

Nohair, B.; Especel, C.; Lafaye, G.; Marécot, P.; Hoang, L. C.; Barbier, J. Palladium supported catalysts for the selective hydrogenation of sunflower oil. *Journal of Molecular Catalysis A: Chemical* **2005**, *229*, 117-126.

Nuzzo, R. G.; Allara, D. L. Adsorption of bifunctional organic disulfides on gold surfaces. *Journal of the American Chemical Society* **1983**, *105*, 4481-4483.

Oudar, J. Sulfur Adsorption and Poisoning of Metallic Catalysts. *Catalysis Reviews* **1980**, *22*, 171-195.

Oura, K.; Zotov, A.; Lifshits, V.; Saranin, A.; Katayama, M. *Surface science*; Springer, 2003.

Pang, S. H.; Schoenbaum, C. A.; Schwartz, D. K.; Medlin, J. W. Directing reaction pathways by catalyst active-site selection using self-assembled monolayers. *Nature communications* **2013**, *4*.

Parker, J. F.; Kacprzak, K. A.; Lopez-Acevedo, O.; Häkkinen, H.; Murray, R. W. Experimental and Density Functional Theory Analysis of Serial Introductions of Electron-Withdrawing Ligands into the Ligand Shell of a Thiolate-Protected Au<sub>25</sub> Nanoparticle. *The Journal of Physical Chemistry C* **2010**, *114*, 8276-8281.

Patel, A. U. *Environmentally Benign Catalysts: For Clean Organic Reactions*; Springer London, Limited, 2013.

Pecsi, I.; Leveles, I.; Harmat, V.; Vertessy, B. G.; Toth, J. Aromatic stacking between nucleobase and enzyme promotes phosphate ester hydrolysis in dUTPase. *Nucleic Acids Research* **2010**, *38*, 7179-7186.

Petrovykh, D. Y.; Kimura-Suda, H.; Opdahl, A.; Richter, L. J.; Tarlov, M. J.; Whitman, L. J. Alkanethiols on Platinum: Multicomponent Self-Assembled Monolayers. *Langmuir* **2006**, *22*, 2578-2587.

Pham-Huu, C.; Keller, N.; Ehret, G.; Charbonniere, L. c. J.; Ziessel, R.; Ledoux, M. J. Carbon nanofiber supported palladium catalyst for liquid-phase reactions: An active and selective catalyst for hydrogenation of cinnamaldehyde into hydrocinnamaldehyde. *Journal of Molecular Catalysis A: Chemical* **2001**, *170*, 155-163.

Ponec, V. On the role of promoters in hydrogenations on metals;  $\alpha,\beta$ -unsaturated aldehydes and ketones. *Applied Catalysis A: General* **1997**, *149*, 27-48.

Pradier, C.-M.; Margot, E.; Berthier, Y.; Oudar, J. Hydrogenation of 1, 3-butadiene on Pt (111): Comparison with results on Pt (110) and Pt (100). *Applied Catalysis* **1988**, *43*, 177-192.

Pradier, C. M.; Birchem, T.; Berthier, Y.; Cordier, G. Hydrogenation of 3-methyl-butenal on Pt(110); comparison with Pt(111). *Catalysis Letters* **1994**, *29*, 371-378.

Rader, C. P.; Smith, H. A. Competitive Catalytic Hydrogenation of Benzene, Toluene and the Polymethylbenzenes on Platinum. *Journal of the American Chemical Society* **1962**, *84*, 1443-1449.

Rajadhyaksha, R. A.; Karwa, S. L. SOLVENT EFFECTS IN CATALYTIC-HYDROGENATION. *Chemical Engineering Science* **1986**, *41*, 1765-1770.

Ramos, M. J.; Fernández, C. M.; Casas, A.; Rodríguez, L.; Pérez, Á. Influence of fatty acid composition of raw materials on biodiesel properties. *Bioresource Technology* **2009**, *100*, 261-268.

Rao, C. N. R. Chemical applications of infrared spectroscopy. **1963**.

Ravasio, N.; Zaccheria, F.; Gargano, M.; Recchia, S.; Fusi, A.; Poli, N.; Psaro, R. Environmental friendly lubricants through selective hydrogenation of rapeseed oil over supported copper catalysts. *Applied Catalysis A: General* **2002**, *233*, 1-6.

Richardson, J. M.; Jones, C. W. Strong evidence of solution-phase catalysis associated with palladium leaching from immobilized thiols during Heck and Suzuki coupling of aryl iodides, bromides, and chlorides. *Journal of Catalysis* **2007**, *251*, 80-93.

Robertson, A. The early history of catalysis. *Platinum Metals Rev* **1975**, *19*, 64-69.

Rothenberg, G. The basics of catalysis. *Catalysis: Concepts and Green Applications* **2008**, 39-75.

Ruban, A. V.; Skriver, H. L. Calculated surface segregation in transition metal alloys. *Computational Materials Science* **1999**, *15*, 119-143.

Rylander, P. *Catalytic Hydrogenation over Platinum Metals*; Elsevier Science, 2012.

Sadeghmoghaddam, E.; Gaieb, K.; Shon, Y. S. Catalytic isomerization of allyl alcohols to carbonyl compounds using poisoned Pd nanoparticles. *Applied Catalysis a-General* **2011**, *405*, 137-141.

Sagiv, J. Organized monolayers by adsorption. III. Irreversible adsorption and memory effects in skeletonized silane monolayers. *Israel Journal of Chemistry* **1979**, *18*, 346-353.

Schaal, M. T.; Pickerell, A. C.; Williams, C. T.; Monnier, J. R. Characterization and evaluation of Ag-Pt/SiO<sub>2</sub> catalysts prepared by electroless deposition. *Journal of Catalysis* **2008**, *254*, 131-143.

Scherer, J.; Vogt, M.; Magnussen, O.; Behm, R. Corrosion of alkanethiol-covered Cu (100) surfaces in hydrochloric acid solution studied by in-situ scanning tunneling microscopy. *Langmuir* **1997**, *13*, 7045-7051.

Schlenoff, J. B.; Li, M.; Ly, H. Stability and self-exchange in alkanethiol monolayers. *Journal of the American Chemical Society* **1995**, *117*, 12528-12536.

Schoenbaum, C. A.; Schwartz, D. K.; Medlin, J. W. Controlling surface crowding on a Pd catalyst with thiolate self-assembled monolayers. *Journal of Catalysis* **2013**, *303*, 92-99.

Schoenfisch, M. H.; Pemberton, J. E. Air Stability of Alkanethiol Self-Assembled Monolayers on Silver and Gold Surfaces. *Journal of the American Chemical Society* **1998**, *120*, 4502-4513.

Schwartz, D. K. Mechanisms and Kinetics of Self-Assembled Monolayer Formation. *Annual Review of Physical Chemistry* **2001**, *52*, 107-137.

Seader, J. D.; Henley, E. J.; Roper, D. K. *Separation Process Principles, 3rd Edition*; John Wiley & Sons, 2010.

Seddon, D. *Petrochemical Economics: Technology Selection in a Carbon Constrained World*; Imperial College Press, 2010.

Sharma, Y. C.; Singh, B.; Korstad, J. Latest developments on application of heterogenous basic catalysts for an efficient and eco friendly synthesis of biodiesel: A review. *Fuel* **2011**, *90*, 1309-1324.

Sheen, C. W.; Shi, J. X.; Maartensson, J.; Parikh, A. N.; Allara, D. L. A new class of organized self-assembled monolayers: alkane thiols on gallium arsenide(100). *Journal of the American Chemical Society* **1992**, *114*, 1514-1515.

Shekhar, R.; Barteau, M. A. Decarbonylation and hydrogenation reactions of allyl alcohol and acrolein on Pd (110). *Surface science* **1994**, *319*, 298-314.

Shirai, M.; Tanaka, T.; Arai, M. Selective hydrogenation of  $\alpha$ -,  $\beta$ -unsaturated aldehyde to unsaturated alcohol with supported platinum catalysts at high pressures of hydrogen. *Journal of Molecular Catalysis A: Chemical* **2001**, *168*, 99-103.

Siegel, J. B.; Zanghellini, A.; Lovick, H. M.; Kiss, G.; Lambert, A. R.; St.Clair, J. L.; Gallaher, J. L.; Hilvert, D.; Gelb, M. H.; Stoddard, B. L.; Houk, K. N.; Michael, F. E.; Baker, D. Computational Design of an Enzyme Catalyst for a Stereoselective Bimolecular Diels-Alder Reaction. *Science* **2010**, *329*, 309-313.

Singh, U. K.; Vannice, M. A. Liquid-phase hydrogenation of citral over Pt/SiO<sub>2</sub> catalysts 1. Temperature effects on activity and selectivity. *Journal of Catalysis* **2000**, *191*, 165-180.

Singh, U. K.; Vannice, M. A. Kinetics of liquid-phase hydrogenation reactions over supported metal catalysts—a review. *Applied Catalysis A: General* **2001**, *213*, 1-24.

Smil, V. *Enriching the earth: Fritz Haber, Carl Bosch, and the transformation of world food production*; MIT press, 2004.

Snelders, D. J. M.; Yan, N.; Gan, W.; Laurency, G.; Dyson, P. J. Tuning the Chemoselectivity of Rh Nanoparticle Catalysts by Site-Selective Poisoning with Phosphine Ligands: The Hydrogenation of Functionalized Aromatic Compounds. *ACS Catalysis* **2011**, *2*, 201-207.

Spek, A. L. Structure validation in chemical crystallography. *Acta Crystallographica Section D: Biological Crystallography* **2009**, *65*, 148-155.

Spivey, J. J.; Dooley, K. M. *Catalysis*; Royal Society of Chemistry, 2011.

Steen, E. J.; Kang, Y.; Bokinsky, G.; Hu, Z.; Schirmer, A.; McClure, A.; del Cardayre, S. B.; Keasling, J. D. Microbial production of fatty-acid-derived fuels and chemicals from plant biomass. *Nature* **2010**, *463*, 559-562.

Stuart, B. *Infrared spectroscopy*; Wiley Online Library, 2004.

Taguchi, T.; Isozaki, K.; Miki, K. Enhanced Catalytic Activity of Self-Assembled-Monolayer-Capped Gold Nanoparticles. *Advanced Materials* **2012**, *24*, 6462-6467.

Taylor, C. D.; Neurock, M. Theoretical insights into the structure and reactivity of the aqueous/metal interface. *Current Opinion in Solid State and Materials Science* **2005**, *9*, 49-65.

Thomson, S. J.; Webb, G. Catalytic hydrogenation of olefins on metals: a new interpretation. *Journal of the Chemical Society, Chemical Communications* **1976**, 526-527.

Tilekaratne, A.; Simonovis, J. P.; López Fagúndez, M. F.; Ebrahimi, M.; Zaera, F. Operando Studies of the Catalytic Hydrogenation of Ethylene on Pt (111) Single Crystal Surfaces. *ACS Catalysis* **2012**, *2*, 2259-2268.

Torborg, C.; Beller, M. Recent Applications of Palladium-Catalyzed Coupling Reactions in the Pharmaceutical, Agrochemical, and Fine Chemical Industries. *Advanced Synthesis & Catalysis* **2009**, *351*, 3027-3043.

Toukoniitty, E.; Maki-Arvela, P.; Kuzma, M.; Villela, A.; Neyestanaki, A. K.; Salmi, T.; Sjöholm, R.; Leino, R.; Laine, E.; Murzin, D. Y. Enantioselective hydrogenation of 1-phenyl-1,2-propanedione. *Journal of Catalysis* **2001**, *204*, 281-291.

Trewavas, A. Malthus foiled again and again. *Nature* **2002**, *418*, 668-670.

Turner, N. W.; Jeans, C. W.; Brain, K. R.; Allender, C. J.; Hlady, V.; Britt, D. W. From 3D to 2D: a review of the molecular imprinting of proteins. *Biotechnology progress* **2006**, *22*, 1474-1489.

Turner, N. W.; Wright, B. E.; Hlady, V.; Britt, D. W. Formation of protein molecular imprints within Langmuir monolayers: a quartz crystal microbalance study. *Journal of colloid and interface science* **2007**, *308*, 71-80.

Ulman, A.; Eilers, J. E.; Tillman, N. Packing and molecular orientation of alkanethiol monolayers on gold surfaces. *Langmuir* **1989**, *5*, 1147-1152.

Ulman, A. Formation and structure of self-assembled monolayers. *Chemical Reviews* **1996**, *96*, 1533-1554.

Van Druten, G.; Ponec, V. Hydrogenation of carbonylic compounds: Part I: Competitive hydrogenation of propanal and acetone over noble metal catalysts. *Applied Catalysis A: General* **2000**, *191*, 153-162.

Van Druten, G.; Ponec, V. Hydrogenation of carbonylic compounds: Part II: The influence of alcohols on the hydrogenation of carbonyl compounds. *Applied Catalysis A: General* **2000**, *191*, 163-176.

Vannice, M. A.; Sen, B. Metal-support effects on the intramolecular selectivity of crotonaldehyde hydrogenation over platinum. *Journal of Catalysis* **1989**, *115*, 65-78.

Vargas, A.; Ferri, D.; Bonalumi, N.; Mallat, T.; Baiker, A. Controlling the sense of enantioselection on surfaces by conformational changes of adsorbed modifiers. *Angewandte Chemie-International Edition* **2007**, *46*, 3905-3908.

Veldsink, J. W.; Bouma, M. J.; Schoon, N. H.; Beenackers, A. Heterogeneous hydrogenation of vegetable oils: A literature review. *Catalysis Reviews-Science and Engineering* **1997**, *39*, 253-318.

Vericat, C.; Vela, M. E.; Salvarezza, R. C. Self-assembled monolayers of alkanethiols on Au(111): surface structures, defects and dynamics. *Physical Chemistry Chemical Physics* **2005**, *7*, 3258-3268.

Vericat, C.; Vela, M.; Benitez, G.; Carro, P.; Salvarezza, R. Self-assembled monolayers of thiols and dithiols on gold: new challenges for a well-known system. *Chemical Society Reviews* **2010**, *39*, 1805-1834.

Verziu, M.; Cojocaru, B.; Hu, J.; Richards, R.; Ciuculescu, C.; Filip, P.; Parvulescu, V. I. Sunflower and rapeseed oil transesterification to biodiesel over different nanocrystalline MgO catalysts. *Green Chem.* **2007**, *10*, 373-381.

Wachs, I. E. Recent conceptual advances in the catalysis science of mixed metal oxide catalytic materials. *Catalysis Today* **2005**, *100*, 79-94.

Wachsen, O.; Himmler, K.; Cornils, B. Aqueous biphasic catalysis: Where the reaction takes place. *Catalysis Today* **1998**, *42*, 373-379.

Wankat, P. C. *Separation Process Engineering*; Pearson Education, 2006.

Widegren, J. A.; Finke, R. G. A review of the problem of distinguishing true homogeneous catalysis from soluble or other metal-particle heterogeneous catalysis under reducing conditions. *Journal of Molecular Catalysis A: Chemical* **2003**, *198*, 317-341.

Wu, B.; Huang, H.; Yang, J.; Zheng, N.; Fu, G. Selective Hydrogenation of  $\alpha,\beta$ -Unsaturated Aldehydes Catalyzed by Amine-Capped Platinum-Cobalt Nanocrystals. *Angewandte Chemie International Edition* **2012**, *51*, 3440-3443.

Wulff, G. Zur frage der geschwindigkeit des wachstums und der auflösung der kristallflächen. *Z. kristallogr* **1901**, *34*, 449-530.

Xin, H.; Holewinski, A.; Linic, S. Predictive Structure-Reactivity Models for Rapid Screening of Pt-Based Multimetallic Electrocatalysts for the Oxygen Reduction Reaction. *ACS Catalysis* **2011**, *2*, 12-16.

Yang, R.; Su, M.; Li, M.; Zhang, J.; Hao, X.; Zhang, H. One-pot process combining transesterification and selective hydrogenation for biodiesel production from starting material of high degree of unsaturation. *Bioresource Technology* **2010**, *101*, 5903-5909.

Yee, C.; Scotti, M.; Ulman, A.; White, H.; Rafailovich, M.; Sokolov, J. One-Phase Synthesis of Thiol-Functionalized Platinum Nanoparticles. *Langmuir* **1999**, *15*, 4314-4316.

Yergin, D. *The prize: The epic quest for oil, money & power*; Simon and Schuster, 2011.

Zaera, F.; Somorjai, G. Hydrogenation of ethylene over platinum (111) single-crystal surfaces. *Journal of the American Chemical Society* **1984**, *106*, 2288-2293.

Zaera, F. On the Mechanism for the Hydrogenation of Olefins on Transition-Metal Surfaces: The Chemistry of Ethylene on Pt(111)†. *Langmuir* **1996**, *12*, 88-94.

Zaera, F. Key unanswered questions about the mechanism of olefin hydrogenation catalysis by transition-metal surfaces: a surface-science perspective. *Physical Chemistry Chemical Physics* **2013**, *15*, 11988-12003.

Zapf, A.; Beller, M. Fine chemical synthesis with homogeneous palladium catalysts: examples, status and trends. *Topics in Catalysis* **2002**, *19*, 101-109.

Zhang, G.; Wang, D.; Gu, Z.-Z.; Möhwald, H. Fabrication of superhydrophobic surfaces from binary colloidal assembly. *Langmuir* **2005**, *21*, 9143-9148.

Zhao, F.; Ikushima, Y.; Chatterjee, M.; Shirai, M.; Arai, M. An effective and recyclable catalyst for hydrogenation of  $\alpha$ ,  $\beta$ -unsaturated aldehydes into saturated aldehydes in supercritical carbon dioxide. *Green Chemistry* **2003**, *5*, 76-79.

Ziman, J. M. *Principles of the Theory of Solids*; Cambridge University Press, 1972.

Zope, B. N.; Hibbitts, D. D.; Neurock, M.; Davis, R. J. Reactivity of the Gold/Water Interface During Selective Oxidation Catalysis. *Science* **2010**, *330*, 74-78.